INFORMATION TO USERS

This manuscript has been reproduced from the microfilm master. UMI films the text directly from the original or copy submitted. Thus, some thesis and dissertation copies are in typewriter face, while others may be from any type of computer printer.

The quality of this reproduction is dependent upon the quality of the copy submitted. Broken or indistinct print, colored or poor quality illustrations and photographs, print bleedthrough, substandard margins, and improper alignment can adversely affect reproduction.

In the unlikely event that the author did not send UMI a complete manuscript and there are missing pages, these will be noted. Also, if unauthorized copyright material had to be removed, a note will indicate the deletion.

Oversize materials (e.g., maps, drawings, charts) are reproduced by sectioning the original, beginning at the upper left-hand corner and continuing from left to right in equal sections with small overlaps. Each original is also photographed in one exposure and is included in reduced form at the back of the book.

Photographs included in the original manuscript have been reproduced xerographically in this copy. Higher quality 6" x 9" black and white photographic prints are available for any photographs or illustrations appearing in this copy for an additional charge. Contact UMI directly to order.

UMI

Oxidizing side of the photosystem I

by

Jun Sun

A dissertation submitted to the graduate faculty

in partial fulfillment of the requirements for the degree of

DOCTOR OF PHILOSOPHY

Major: Biochemistry

Major Professor: Parag R. Chitnis

Iowa State University

Ames, Iowa

1999

Graduate College

Iowa State University

This is to certify that the Doctoral dissertation of

Jun Sun

has met the dissertation requirements of Iowa State University

Major Professor

For the Major Program

For the Graduate College

TABLE OF CONTENTS

ABSTRACT

Photosynthesis converts solar energy into the biological sources of energy for the life on our planet. Photosystem I (PSI) is one of the two reaction centers of oxygenic photosynthesis. PSI is a multiheteromeric membrane-protein complex that catalyzes light-driven electron transfer from plastocyanin or cytochrome c_6 to ferredoxin. The PsaA and PsaB subunits form the heterodimeric core that harbors the primary electron donor P700. On the oxidizing side of the PSI complex, plastocyanin or cytochrome c_6 donates electrons to the P700 reaction center. The objective of this dissertation is to identify elements of molecular recognition on the oxidizing side of PSI.

To identify PSI regions that are exposed on the luminal oxidizing side, the topography of the PSI complex from *Synechocystis* sp. PCC 6803 was examined by biochemical analyses. These studies indicated that the H and J luminal loops of the core proteins were the most logical candidates for hydrophobic interactions with the donor proteins. To test this hypothesis, site-directed mutations were generated in these loops. Biochemical characteristics of these mutants provided evidence for interactions between the electron donor proteins and a luminal surface helix in the J loop of the PsaB protein. Sections of the H loop of PsaB plays an important role in the structural integrity of the PsaB protein. The N-terminal lysine-rich region of PsaF in eukaryotic PSI complex has been proposed to provide a binding site for plastocyanin and cytochrome c_6 through electrostatic interactions. Chimeric PsaF proteins containing the lysine-rich region of spinach PsaF were produced in *Synechocystis* sp. PCC 6803 cells through mutagenesis. Cross-linking and functional studies showed that the lysine-rich region of spinach PsaF protein is sufficient for binding of donor proteins, but not for the electron transfer within the intermolecular complex. The results in this dissertation revealed the structural basis for the molecular recognition on the oxidizing side of PSI.

CHAPTER 1. GENERAL INTRODUCTION

Photosynthesis is one of the most important biological processes on the Earth. By converting the solar energy into the chemical energy, photosynthesis nourishes the living world directly or indirectly. In oxygenic photosynthesis, cyanobacteria and the chloroplasts of plants and algae harvest the light energy to release oxygen from water and to make carbohydrates by reducing carbon dioxide. During the light-driven reactions of photosynthesis, photosystem I and II (PSI and PSII) capture photons and utilize the energy to transfer electrons from water to $NADP^+$ through three membrane-bound complexes: PSII, cytochrome b_6f and PSI. The photosynthetic electron transfer produces NADPH and a proton gradient across the thylakoid membranes, which is used for ATP synthesis by ATP synthase. NADPH and ATP are used to reduce carbon dioxide and to produce carbohydrates.

PSI is a multisubunit membrane-protein complex that catalyzes light-driven electron transfer from the reduced plastocyanin in the thylakoid lumen to the oxidized ferredoxin in the chloroplast stroma or cyanobacterial cytoplasm (Chitnis, 1996; Fromme, 1996). Purified cyanobacterial PSI complex contains at least eleven subunits and approximately 12-16 β-carotenes, two phylloquinones, and three [4Fe-4S] clusters. The cyanobacterial PSI complex also binds 89 chlorophyll a molecules, 83 of which constitute a core antenna system (Krauß et al., 1996; Schubert et al., 1997). The PsaA and PsaB subunits form the heterodimeric core that harbors most of the cofactors including the P700 reaction center, which is a dimer of chlorophyll a molecules. The PsaC, PsaD, and PsaE subunits are peripheral proteins constituting the reducing side of the PSI complex. The PsaF, PsaI, PsaJ, PsaK, PsaL, and PsaM subunits are integral membrane proteins. Among them, the PsaF protein contains a large N-terminal luminal domain.

In the photosynthetic electron transfer chain, electrons are transferred from the cytochrome b_6f complex to the PSI complex via the soluble electron carrier proteins. In the chloroplasts of higher plants, plastocyanin is the only electron carrier protein whereas some cyanobacteria and green algae contain cytochrome c_6 as an alternative electron carrier protein depending on the relative availability of copper and iron in the culture medium (Hatanaka et al., 1993; Ho and Krogman, 1984; Kerfeld and Krogmann, 1998; Wood, 1978). The electron carrier proteins in the lumen are oxidized by the $P700^+$ reaction center. Thus, the donor proteins interact with PSI on the oxidizing side of the PSI complex.

The interactions between the donor proteins and PS I have been studied by monitoring the P700 rereduction kinetics with transient absorption spectroscopy. The interaction of

plastocyanin with plant PSI shows a fast kinetic step, indicating the first-order electron transfer within a complex of plastocyanin and PSI, and a slow phase attributed to the bimolecular reaction between plastocyanin and PSI (Bottin and Mathis, 1985; Haehnel et al., 1980; Ratajczak et al., 1988). The PSI-mediated oxidation of algal plastocyanin or cytochrome c_6 also takes place with a multi-step kinetic mechanism (Diaz et al., 1994; Hervás et al., 1992; Hervás et al., 1995). In contrast, kinetic analysis of cytochrome c_6 and plastocyanin oxidation by PSI of some cyanobacteria shows the absence of a fast phase, suggesting a one-step bimolecular collision mechanism (Hervás et al., 1994; Hippler et al., 1996; Xu et al., 1994b).

The interactions between donor proteins and PSI are highly specific. The specificity is because of precise molecular recognition elements in the interacting proteins. The molecular recognition sites in the donor proteins have been identified. Examination of the structures of plastocyanin and cytochrome c_6 reveals the presence of a conserved hydrophobic surface and a conserved negative region (Frazao et al., 1995; Navarro et al., 1997). The hydrophobic surface and its flat structure are required for the association and electron transfer to PSI (Haehnel et al., 1994; Nordling et al., 1991). The negative region has a significant role in the binding of plastocyanin to PSI (Hippler et al., 1996; Lee et al., 1995). Thus, the interactions between donor proteins and eukaryotic PSI involve the electrostatic interaction for the complex formation and the hydrophobic interaction that is crucial for the electron transfer.

On the oxidizing side of PSI, the luminal extramembrane loops of the core proteins and the large N-terminal domain of the PsaF subunit may interact with the donor proteins. A lysine-rich region is well conserved among plant and algal PsaF, but not found in cyanobacterial PsaF (Chitnis et al., 1991). Mutagenesis (Farah et al., 1995) and cross-linking (Hippler et al., 1996) studies have suggested that the N-terminal lysine-rich region of the chloroplast PsaF may interact with the negative region of plastocyanin through electrostatic interaction. However, the cyanobacterial PsaF is not required in the interaction of PSI with plastocyanin or cytochrome c_6 (Chitnis et al., 1991; Xu et al., 1994a; Xu et al., 1994b; Hatanaka et al., 1993). Therefore, plastocyanin and cytochrome c_6 contact the PsaA and PsaB core proteins directly. The luminal extramembrane loops of PsaA and PsaB are likely candidates to provide the hydrophobic interaction with donor proteins for the electron transfer. The molecular recognition sites in the PSI complex need to be further identified.

Based on our current understanding of electron transfer to PSI, we propose the following recognition elements in the interactions on the oxidizing side of PSI:

i.* The luminal loops of PsaA and PsaB provide surfaces for hydrophobic interactions with the donor proteins for the electron transfer.

ii.✦The N-terminal luminal domain of the chloroplast PsaF provides residues for electrostatic interactions with the eukaryotic donor proteins for the initial complex formation.

To test these hypotheses, common approaches include computational modeling, co-crystallization, and mutagenesis. Because of the lack of high-resolution structure for PSI complex and the extreme difficulties in membrane protein crystallization, mutagenesis provides a good tool to study the structural basis for the interactions on the oxidizing side of PSI. In this dissertation, site-directed mutagenesis and biochemical analyses in the model system *Synechocystis* sp. PCC 6803 were used to examine the roles of the luminal loops of PsaB and the N-terminal domain of PsaF in the molecular recognition with the donor proteins. These studies will benefit our understanding of the interactions on the oxidizing side of PSI.

Organization of Dissertation

The dissertation includes five manuscripts. It starts with the "General Introduction" followed by a literature review entitled "Photosystem I", which is a book chapter in *Plant Physiology, Biochemistry and Molecular Biology* edited by A. Hemantaranjan and published by Scientific Publishers, Jodhpur. To identify which of the luminal loops of PsaA and PsaB are the best candidates for interactions with the donor proteins, topography of the PSI core proteins was examined. This work was published as the paper "Topography of the photosystem I core proteins of the cyanobacterium *Synechocystis* sp. PCC 6803" in the *Journal of Biological Chemistry*, 272, 21793-21802, (1997). With the structural and topographic information, the H and J luminal loops of the PsaB protein were selected for mutagenesis studies. Mutational studies on the J loop of PsaB were summarized in the paper "Oxidizing side of cyanobacterial photosystem I: Evidence for interaction between the electron donor and the luminal J loop of the PsaB protein" published in the *Journal of Biological Chemistry*, 274, 19048-19054, (1999). Mutational studies on the H loop of PsaB resulted in another manuscript "Oxidizing side of cyanobacterial photosystem I: Mutational analysis of the luminal H loop of the PsaB subunit" that has been submitted for publication. Studies on the role of the N-terminal domain of plant PsaF are described in the manuscript "Oxidizing side of photosystem I: The lysine-rich region of plant PsaF is sufficient for binding of the donor proteins, but not for the electron transfer within the intermolecular complex". This manuscript has been prepared for submission to a professional journal.

In addition, several other studies are also included as appendices in this dissertation. The biochemical methods used in these studies were summarized as the paper "Isolation and functional study of photosystem I subunits in the cyanobacterium *Synechocystis* sp. PCC

6803" that was published in *Methods in Enzymology*, 297, 124-139, (1998). Appendix B contains summary of the paper "Structural features and assembly of the soluble overexpressed PsaD subunit of photosystem I" that was published in *Biochimica et Biophysica Acta*, 1410, 7-18, (1999). Appendix C contains the summary of the manuscript "The accumulation of the photosystem I complex in transformant *Synechocystis* sp. PCC 6803", which will be submitted to a professional journal.

References

Bottin, H. and Mathis, P. (1985) Interaction of plastocyanin with the photosystem I reaction center: a kinetic study by flash spectroscopy. *Biochemistry*, 24, 6453-6460.

Chitnis, P.R. (1996) Photosystem I. *Plant Physiol.*, 111, 661-669.

Chitnis, P.R., Purvis, D. and Nelson, N. (1991) Molecular cloning and targeted mutagenesis of the gene psaF encoding subunit III of photosystem I from the cyanobacterium *Synechocystis* sp. PCC 6803. *J. Biol. Chem.*, 266, 20146-20151.

Diaz, A., Hervas, M., Navarro, J.A., De La Rosa, M.A. and Tollin, G. (1994) A thermodynamic study by laser-flash photolysis of plastocyanin and cytochrome c_6 oxidation by photosystem I from the green alga *Monoraphidium braunii*. *Eur. J. Biochem.*, 222, 1001-1007.

Farah, J., Rappaport, F., Choquet, Y., Joliot, P. and Rochaix, J.D. (1995) Isolation of a *psaF*-deficient mutant of *Chlamydomonas reinhardtii*: efficient interaction of plastocyanin with the photosystem I reaction center is mediated by the PsaF subunit. *EMBO J.*, 14, 4976-4984.

Frazao, C., Soares, C.M., Carrondo, M.A., Pohl, E., Dauter, Z., Wilson, K.S., Hervas, M., Navarroo, J.A., De la Rosa, M.A. and Sheldrick, G.M. (1995) *Ab initio* determination of the crystal strucutre of cytochrome c_6 and compariosn with plastocyanin. *Structure*, 3, 1159-1169.

Fromme, P. (1996) Structure and function of photosystem I. *Curr. Opin. Struct. Biol.*, 6, 473-484.

Haehnel, W., Jansen, T., Gause, K., Klosgen, R.B., Stahl, B., Michl, D., Huvermann, B., Karas, M. and Herrmann, R.G. (1994) Electron transfer from plastocyanin to photosystem I. *EMBO J.*, 13, 1028-1038.

Haehnel, W., Propper, A. and Krause, H. (1980) Evidence for complexed plastocyanin as the immediate electron donor of P-700. *Biochim. Biophys. Acta*, 593, 384-399.

Hatanaka, H., Sonoike, K., Hirano, M. and Katoh, S. (1993) Small subunits of photosystem I reaction center complexes from *Synechococcus elongatus*. II. Is the *psaF* gene productrequired for oxidation of cytochrome c_{553}? *Biochim. Biophys. Acta*, **1141**, 45-51.

Hervás, M., De la Rosa, M.A. and Tollin, G. (1992) A comparative laser-flash absorption spectroscopy study of algal plastocyanin and cytochrome c_{552} photooxidation by photosystem I particles from spinach. *Eur. J. Biochem.*, **203**, 115-120.

Hervás, M., Navarro, J.A., Diaz, A., Bottin, H. and De la Rosa, M.A. (1995) Laser-flash kinetic analysis of the fast electron transfer from plastocyanin and cytochrome c_6 to photosystem I. Experimental evidence on the evolution of the reaction mechanism. *Biochemistry*, **34**, 11321-11326.

Hervás, M., Ortega, J.M., Navarro, J.A., de la Rosa, M.A. and Bottin, H. (1994) Laser flash kinetic analysis of *Synechocystis* sp. PCC 6803 cytochrome c6 and plastocyanin oxidation by photosystem I. *Biochim. Biophys. Acta*, **1184**, 235-241.

Hippler, M., Reichert, J., Sutter, M., Zak, E., Altschmied, L., Schröer, U., Herrmann, R.G. and Haehnel, W. (1996) The plastocyanin binding domain of photosystem I. *EMBO J.*, **15**, 6374-6384.

Ho, K.K. and Krogman, D.W. (1984) Electron donors to P700 in cyanobacteria and alga: an instance of unusual genetic variability. *Biochim. Biophys. Acta*, **766**, 310-316.

Kerfeld, C.A. and Krogmann, D.W. (1998) Photosynthetic cytochromes *c* in cyanobacteria, algae, and plants. *Annual Rev. Plant Physiol. Plant Mol. Biol.*, **49**, 397-425.

Krauß, N., Schubert, W.-D., Klukas, O., Fromme, P., Witt, H.T. and Saenger, W. (1996) Photosystem I at 4 Å resolution represents the first structural model of a joint photosynthetic reaction centre and core antenna system. *Nature Struct. Biol.*, **3**, 965-973.

Lee, B.H., Hibino, T., Takabe, T., Weisbeek, P.J. and Takabe, T. (1995) Site-directed mutagenetic study on the role of negative patches on Silene plastocyanin in the interactions with cytochrome *f* and photosystem I. *J. Biochem.*, **117**, 1209-1217.

Navarro, J.A., Hervas, M. and De la Rosa, M.A. (1997) Co-evolution of cytochrome c_6 and plastocyanin, mobile proteins transferring electrons from cytochrome $b_6 f$ to photosystem I. *J. Biol. Inorg. Chem.*, **2**, 11-12.

Nordling, M., Sigfridsson, K., Young, S., Lundberg, L.G. and Hansson, O. (1991) Flash-photolysis studies of the electron transfer from genetically modified spinach plastocyanin to photosystem I. *FEBS Lett.*, **291**, 327-330.

Ratajczak, R., Mitchell, R. and Haehnel, W. (1988) Properties of the oxidizing site of photosystem I. *Biochim. Biophys. Acta*, **933**, 306-318.

Schubert, W.-D., Klukas, O., Krauß, N., Saenger, W., Fromme, P. and Witt, H.T. (1997) Photosystem I of *Synechococcus elongarus* at 4 Å Resolution: Comprehensice Structure Analysis. *J. Mol. Biol.*, **272**, 741-769.

Wood, P.M. (1978) Interchangeable copper and iron proteins in algal photosynthesis. Studies on plastocyanin and cytochrome c-552 in *Chlamydomonas. Eur. J. Biochem.*, **87**, 9-19.

Xu, Q., Jung, Y.S., Chitnis, V.P., Guikema, J.A., Golbeck, J.H. and Chitnis, P.R. (1994a) Mutational analysis of photosystem I polypeptides in *Synechocystis* sp. PCC 6803. Subunit requirements for reduction of NADP$^+$ mediated by ferredoxin and flavodoxin. *J. Biol. Chem.*, **269**, 21512-21518.

Xu, Q., Yu, L., Chitnis, V.P. and Chitnis, P.R. (1994b) Function and organization of photosystem I in a cyanobacterial mutant strain that lacks PsaF and PsaJ subunits. *J. Biol. Chem.*, **269**, 3205-3211.

CHAPTER 2. PHOTOSYSTEM I

A book chapter published in Plant Physiology, Biochemistry and Molecular Biology
edited by A. Hemantaranjan, published by Scientific Publishers, Jodhpur

Jun Sun and Parag R. Chitnis

1. Introduction

All living systems require energy and the Sun is the ultimate source of energy for life on the Earth. By converting the solar energy into the chemical energy, photosynthesis is undoubtedly one of the most important biological processes. In oxygenic photosynthesis, cyanobacteria and the chloroplasts of plants and algae harvest the light energy to release oxygen from water and make carbohydrates by reducing carbon dioxide. Oxygenic photosynthesis nourishes almost all living world directly or indirectly. During the light reactions of oxygenic photosynthesis, the energy of photons is captured by photosystem I and II (PSI and PSII) and the energy is used for the photosynthetic electron transfer to yield strong reductants and a proton gradient across the thylakoid membranes. Electrons are transferred from water, the primary electron source, to ferredoxin and then the final electron acceptor $NADP^+$ through the electron transfer chain which contains three membrane-protein complexes, PSII, cytochrome b_6f complex, and PSI. In addition to the strong reductant, the electron transfer generates a proton gradient across the membrane. ATP synthase, which is located in the thylakoid membranes, utilizes the proton gradient to synthesize ATP. NADPH and ATP are used to reduce carbon dioxide and to produce carbohydrates by enzymes of the dark reactions of photosynthesis.

PSI is a multisubunit membrane-protein complex that catalyzes electron transfer from the reduced plastocyanin in the thylakoid lumen to the oxidized ferredoxin in the chloroplast stroma or cyanobacterial cytoplasm (Chitnis, 1996; Chitnis et al., 1995b; Fromme, 1996; Golbeck, 1994). In cyanobacteria, plastocyanin and ferredoxin can be replaced by cytochrome c_6 and flavodoxin, respectively, depending on the nutritional conditions. Purified cyanobacterial PSI complex contains at least eleven different proteins: the core proteins (PsaA and PsaB), three peripheral proteins (PsaC, PsaD, and PsaE) on the stromal side and six integral membrane proteins (PsaF, PsaI, PsaJ, PsaK, PsaL, and PsaM). Chloroplast PSI contains three additional proteins: one stromal peripheral protein (PsaH), one lumenal peripheral protein (PsaN), and one integral membrane protein (PsaG). These PSI proteins, their characteristics and their functions are listed in Table 2-1. The PsaA and PsaB proteins form the heterodimeric core around which other proteins are organized to form the complex (Fig. 2-1). The PSI complex

also contains approximately 100 chlorophyll a molecules, 12-16 β-carotenes, two phylloquinones, and three [4Fe-4S] clusters. These cofactors are bound to the PsaA, PsaB, and PsaC proteins. During the photosynthetic electron transfer across the thylakoid membrane, electrons are transported from the electron donor plastocyanin to the P700 reaction center, which is a dimer of chlorophyll a molecules, then through a chain of electron acceptors: a chlorophyll a monomer A_0, a phylloquinone A_1, [4Fe-4S] cluster F_X, F_A, and F_B, finally to the electron acceptor ferredoxin (Fig. 2-2). The energy for the excitation of the P700 reaction center is provided by the photons absorbed by the antenna chlorophyll a molecules of PSI as antenna and by the associated membrane-embedded light-harvesting complexes (LHCI). PSI converts the energy of photons into chemical energy with a remarkable quantum efficiency of 39 to 44%.

In the past 10 years, multidisciplinary research efforts have led to characterization of the components, the electron transfer reactions, and the structure of PSI complex. In this chapter, we will discuss recent progress in the understanding of the function and structure of PSI complex. Detailed discussion of LHCs proteins, the electron transfer and redox cofactors in PSI, the structure of PSI, and the regulation of PSI genes can be found in the recent reviews (Brettel, 1997; Chitnis, 1996; Chitnis, 1997; Fromme, 1996; Green and Durnford, 1996; Ort and Yocum, 1996).

2. Function of Photosystem I

PSI is a unique light-driven generator of the reducing power. PSI functions with PSII in a linear electron transport pathway to generate strong reductants, the reduced ferredoxin and NADPH. The products of PSI are among the most electronegative reductants in a biological system. These reductants are used in diverse biochemical processes, including Calvin cycle, nitrite reduction to ammonia, fatty acid desaturation, pyruvate decarboxylation, glutamate synthesis, sulfite reduction, and enzyme regulation through reduced thioredoxin. Thus, PSI plays a vital role in cyanobacteria and chloroplast metabolism. PSI also participates in the PSII-independent cyclic electron transport pathway which results in proton pumping and ATP synthesis.

2.1. Linear electron transfer

In the linear electron transfer, PSI and PSII function according to the Z-scheme. The PSII and PSI reaction centers form the light-driven uphill sections where the energy of a photon is used to increase the reducing ability. The electron transport between the two photosystems involves cytochrome b_6f complex. Among these three integral-membrane complexes, the

electron transfer is linked by mobile electron carriers: plastoquinone transfers electrons from PSII to the cytochrome b_6f complex which, in turn, donates electrons to PSI via plastocyanin.

The distribution of the photosynthetic complexes in the thylakoid membranes has been revealed by freeze-fracture electron microscopy. In chloroplasts, PSI is mainly located in the unstacked stroma lamellae, where contact with the stroma provides easy access to ferredoxin and $NADP^+$. PSII occurs almost exclusively in the closely stacked grana whereas cytochrome b_6f complex is uniformly distributed throughout the membrane (Staehelin and van der Staay, 1996). The mobile electron carriers plastoquinone and plastocyanin shuttle electrons between these membrane complexes. Similarly, PSI in cyanobacterial thylakoid membranes is spatially distributed in a radial asymmetric fashion, with higher concentration in the outermost thylakoids of a cyanobacterial cell (Sherman et al., 1994). The ATP synthase, utilizing the proton gradient to generate ATP, found only in unstacked regions. The physical separation of PSI and PSII eliminates the possibility that the higher excitation energy of PSII transfers to PSI (Trissl and Wilhelm, 1993).

To increase the effective absorption of the solar light for energy conversion, photosynthetic organisms have evolved various antenna systems. The PSI and PSII complexes contain integral core antenna systems with about 100 and 50 chlorophyll a molecules, respectively. The intrinsic antenna is complemented by light harvesting systems, such as the stromal extrinsic phycobilisomes mainly bound with PSII in cyanobacteria and the membrane-intrinsic LHCs in the chloroplasts of algae and higher plant. The physical separation of PSI and PSII also permits the chloroplast to respond to changes in illumination. The high illumination results in a predominant pool of reduced plastoquinone which, in turn, activates a protein kinase to phosphorylate specific threonine residues of the LHCs of PSII. The phosphorylated LHC II complexes migrate to the unstacked regions of the thylakoid membrane and transfer excitation energy to PSI. Under low illumination, the accumulation of oxidized plastoquinone results in the dephosphorylation of LHCs, which migrate to the stacked portions of the thylakoid membrane where they bind to PSII (Staehelin and Arntzen, 1983; Staehelin and van der Staay, 1996).

In the linear electron transfer, PSI is involved in three steps of electron transfer: (1) from plastocyanin to the oxidizing side of PSI, (2) within the PSI complex, (3) from the reducing side of PSI to ferredoxin.

2.1.1. Interactions on the oxidizing side

On the lumenal side of thylakoid membranes, PSI accepts electrons from plastocyanin. In cyanobacteria and algae, cytochrome c_6 can serve as an alternative electron donor to the P700 reaction center.

The interaction of plastocyanin with PSI has been studied by using transient absorption spectroscopy which can monitor the P700 rereduction kinetics *in vivo* or *in vitro*. The time course of P700$^+$ reduction using the plant PSI complexes shows two dominant kinetic components. A fast phase with $t_{1/2}$ of 12-14 μs and a second slower phase with variable $t_{1/2}$ of 100 - 200 μs, depending on the concentration of PC (Bottin and Mathis, 1985; Haehnel *et al.*, 1980). The fast rate can be attributed to the first-order electron transfer within a complex between plastocyanin and PSI. The slower phase may represent a distant plastocyanin population (Ratajczak *et al.*, 1988). The half-life of the slow component decreases with the increasing concentration of plastocyanin and is attributed to the bimolecular reaction between PSI and plastocyanin. The PSI-mediated oxidation of algal plastocyanin or cytochrome c_6 also takes place with a two-step kinetic mechanism (Diaz *et al.*, 1994; Hervas *et al.*, 1992a). In contrast, laser flash kinetic analysis of cytochrome c_6 and plastocyanin oxidation by PSI of *Synechocystis* shows the absence of the fast reduction phase, suggesting an apparent one-step bimolecular collision mechanism (Hervas *et al.*, 1994; Hippler *et al.*, 1996; Xu *et al.*, 1994e). At physiological pH, cytochrome c_6 is more efficient than plastocyanin in donating electrons to the cyanobacterial PSI; the basis for this difference is not understood (Hervas *et al.*, 1994; Hippler *et al.*, 1996; Medina *et al.*, 1993). Extensive spectroscopic and thermodynamic analysis of interactions between PSI and plastocyanin/cytochrome c_6 from different sources demonstrated that the PSI of plants, algae and cyanobacteria interact differently with the soluble proteins obtained from these sources (Hervas *et al.*, 1995; Hervas *et al.*, 1996). This work indicates a multi-step reaction mechanism of electron transfer in plant and algal proteins while cyanobacteria have a simpler mechanism (Hervas *et al.*, 1995). The structural basis for these different electron transfer mechanisms still needs to be demonstrated. The binding of a new reduced plastocyanin with the PSI complex requires dissociation of the oxidized plastocyanin. The dissociation constant for oxidized plastocyanin is six times larger than that of 7 μM found for reduced plastocyanin. Similarly, E_m of PSI-bound plastocyanin is 50-60 mV higher than the E_m at +370 mV of the soluble plastocyanin (Drepper *et al.*, 1996). Therefore, the driving force for the intracomplex electron transfer is decreased in favor of an optimized turnover of PSI.

Plastocyanin is a type I copper protein containing about 99 amino acids (Gross, 1996). The *petE* gene for plastocyanin is located in nucleus of higher plants and green algae. The amino acid sequences of plastocyanin from a large number of organisms are known. A high sequence

homology is observed in plants and green algae whereas cyanobacterial plastocyanins show a lower amino acid conservation. The invariant residues include the four ligands to the copper atom, H37, H87, C84, and M92, as well as Y83. Plastocyanin is acidic in higher plants and green algae whereas it is neutral or basic in cyanobacteria (Navarro et al., 1997).

Both crystal and solution structures of plastocyanin from different sources have been solved. Plastocyanin possesses a global fold formed by β-barrel structure, with the copper center coordinated by H37, H87, C84, and M92 in the northern end of the molecule. Two conserved regions have been identified as recognition and binding sites at the surface of the molecule, a flat hydrophobic region including the copper ligand H87 and a negative region of two parches adjacent to Y83. While Y83 is involved in the electron transfer from cytochrome f (He et al., 1991), the electrons are transferred to P700$^+$ via H87 (Haehnel et al., 1994; Nordling et al., 1991). Site-directed mutagenesis has shown that the hydrophobic region containing L12 on the surface of the spinach plastocyanin is crucial for the association and for electron transfer to PSI (Nordling et al., 1991). When G10 or A90 in the flat hydrophobic surface around the copper ligand H87 of spinach plastocyanin were replaced by leucine, a bulky hydrophobic residue, the formation of the plastocyanin-PSI complex was abolished. Therefore, these two residues are part of the flat structures required for the docking of plastocyanin on PSI and for the efficient electron transfer from plastocyanin to P700$^+$ (Haehnel et al., 1994). In contrast, Y83 mutations in plastocyanin affect electron transfer from cytochrome f (He et al., 1991) or from cytochrome c (Modi et al., 1992), but not to PSI (Sigfridsson et al., 1995). Site-directed mutations in two highly conserved negative patches on the surface of plant plastocyanin suggests that the 42-45 patch has a significant role in determining the electron transfer rate to P700, while mutations in the 59-61 patch changed the redox potential of plastocyanin (Hippler et al., 1996; Lee et al., 1995). Therefore the binding of plastocyanin to PSI involves both electrostatic and hydrophobic interactions. The former may be involved in initial docking whereas the latter may be more crucial during electron transfer.

Cyanobacteria and algae have cytochrome c_6 as an alternative electron donor to P700 depending on the availability of copper in the culture medium (Morand et al., 1994). Cytochrome c_6 is a heme-containing protein of 83 - 89 amino acids with a redox potential of +350 mV. The petJ gene coding for cytochrome c_6 is also present in nucleus of green algae. Like plastocyanin, cytochrome c_6 is acidic in green algae and can be either acidic, neutral, or basic in cyanobacteria. Examination of cytochrome c_6 structure reveals the presence of a hydrophobic surface and a negative patch (Beissinger et al., 1998; Frazao et al., 1995; Kerfeld et al., 1995). The negative region is conserved in eukaryotic but not in prokaryotic organisms.

Therefore, plastocyanin and cytochrome c_6 proceeded a convergent evolution in which different proteins have adapted to carry out the same physiological function. The evolution also led the substitution of the old heme protein by the recent copper protein.

Different reaction mechanisms of electron transfer from plastocyanin to PSI complexes of higher plants, algae and cyanobacteria corresponds with the requirement of PsaF in these interactions. The PsaF-less mutant of *Chlamydomonas reinhardtii* shows dramatic reduction in the rate of electron transfer to $P700^+$ (Farah *et al.*, 1995). In contrast, the PsaF-deficient mutant strains of *Synechocystis* sp. PCC 6803 do not show any defect in their photoautotrophic growth, cytochrome c_6-dependent $NADP^+$ photoreduction activity or $P700^+$ rereduction kinetics (Chitnis *et al.*, 1991; Xu *et al.*, 1994c; Xu *et al.*, 1994e). Cross-linking studies indicated that plastocyanin can be cross-linked to the N-terminal lysine-rich region of chloroplast PsaF, which is not found in the cyanobacterial PsaF (Hippler *et al.*, 1996). Thus, the interactions between the plant PSI and plastocyanin includes initial electrostatic interactions between the N-terminal domain of PsaF and the conserved negative patches of plastocyanin followed by accurate docking of plastocyanin through hydrophobic interaction with the PSI core proteins. Therefore, some luminal extramembrane loops of PsaA and PsaB may provide the plastocyanin-docking site.

Crystallographic studies show that the lumenal side of PSI is flat with 10 Å protrusion beyond the membrane boundary. There is a 3 nm deep indentation in the center, perhaps caused by a partial separation between PsaA and PsaB where plastocyanin can dock during electron transfer (Boekema *et al.*, 1994; Fromme *et al.*, 1994). Two α-helices lie parallel to the membrane plane near P700 chlorophyll dimer. These helices are analogous to similar helices seen in the purple bacterial reaction center (Deisenhofer and Michel, 1991; Fromme *et al.*, 1994). These helices may provide a hydrophobic docking region interacting with the hydrophobic surface of plastocyanin.

2.1.2. Electron carriers of the PSI complex

The electron transfer within the PSI complex involves a series of electron carriers with increasing electronegative redox potentials E_m from -1290 to -530 mV. Here we describe characteristics of the redox centers in the PSI complex.

2.1.2.1. P700

P700 is a dimer of chlorophyll *a* molecules oriented perpendicular to the thylakoid membranes (Rutherford and Setif, 1990). Upon transfer of excitation energy from the core antenna system, the primary electron donor P700 undergoes charge separation, producing $P700^+$. The estimated -1290 mV midpoint potential of the excited P700* is the most

electronegative redox center detected so far in a biological system (Golbeck and Bryant, 1991). The reaction center of PSI exhibits a characteristic bleaching at approximately 430 and 700 nm after photochemical oxidation (Kok, 1957); hence it is termed as P700. The photooxidation of P700 occurs at high quantum yield (Setif and Mathis, 1986). The P700 chlorophyll molecules are liganded by histidyl residues (Mac *et al.*, 1996). The E_m of the P700 center is approximately +500 mV (Setif and Mathis, 1980). The electron lost by P700 is gained by oxidizing plastocyanin (see the section 2.1.1).

In the crystal structure of PSI, a pair of chlorophyll *a* molecules are assigned as the primary reaction center (Krauß *et al.*, 1996; Schubert *et al.*, 1997). They are parallel to the two-fold axis with a plane-to-plane distance of 3.8 ± 0.5 Å and a center-to-center distance of 7.5 ± 1.0 Å. These chlorophyll molecules are separated from the lumen by about 10 to 15 Å.

2.1.2.2. A_0

The charge separation of P700 is stabilized by spatial displacement of electrons through a series of low potential redox centers. The primary acceptor A_0 is reduced to the anion form upon transfer of an electron from the excited P700. The accumulated A_0^- in the light at physiological temperature was seen as bleaching at 692 nm (Nuijs *et al.*, 1986; Shuvalov *et al.*, 1979). Time resolved kinetic experiments have shown that the spectrum of reduced A_0 with a bleaching at 686-688 nm can be observed only when high intensity light flashes are used (Hastings *et al.*, 1994b; Holzwarth *et al.*, 1993). In the blue region of the spectrum, A_0 reduction leads to bleaching with two valleys at 412 and 438 nm (Warren *et al.*, 1993a). These optical experiments and electron paramagnetic resonance (EPR) measurements at cryogenic temperatures have indicated that A_0 is a chlorophyll *a* monomer (Brettel and Setif, 1987; Furrer and Thurnauer, 1983). An intrinsic time constant of 1-2 ps has been estimated for the radical pair formation (Hastings *et al.*, 1994a; Hecks *et al.*, 1994; Holzwarth *et al.*, 1993). Time-resolved kinetic measurements on A_0 have been done under conditions where the PSI electron acceptors are in the oxidized state prior to light activation (Hastings *et al.*, 1994a; Hastings *et al.*, 1994b). The spectroscopy experiments have supported identity of A_0 as a monomeric form of chlorophyll *a*.

In the 4 Å structure of PSI, there are four chlorophyll molecules arranged in two-fold symmetrical positions between P700 chlorophyll pair and the F_X Fe-S cluster (Krauß *et al.*, 1996; Schubert *et al.*, 1997). A pair of chlorophyll *a* molecules positioned 16 Å from P700 towards the stroma is approximately half-way between P700 and F_X. By analogy to the positions of bacteriopheophytins in the photoreaction center of the purple bacteria, at least one of them is assumed to be equivalent to the spectroscopically characterized primary acceptor A_0. Another pair of chlorophyll *a* monomers are located approximately half-way between P700 and

the A_0 equivalent chlorophyll molecules. They are assigned as accessory chlorophylls. Thus there are two possible branches of electron transfer pathway between P700 and F_X. It is not known if only one or both sides of possible electron transfer pathway are used during the PSI function. It is also not known what is the role of the accessory chlorophylls in the electron transfer.

2.1.2.3. A_1

During electron transfer in PSI, A_1 serves as an intermediate electron transfer center that oxidizes A_0 and reduces F_X. A_1 can be detected and characterized using different criteria. An electron spin polarized transient EPR signal is shown to arise from the radical pair $P700^+A_1^-$ (Rustandi et al., 1990; Snyder et al., 1991; Thurnauer and Gast, 1985). Flash induced optical transients can be assigned to the reoxidation of A_1^- (Brettel, 1988; Mathis and Setif, 1988; Setif and Brettel, 1993) or due to charge recombination between the $P700^+$ and A_1^- radicals (Setif et al., 1984). An asymmetric EPR signal at g-value of 2.00 photoaccumulates at low temperature under reducing conditions due to A_1^- radical (Heathcote et al., 1996). A_1 is proposed to be a phylloquinone (vitamin K1) molecule. The PSI complexes from different organisms contain 2 phylloquinone molecules per P700 (Biggins and Mathis, 1988; Malkin, 1986; Schoeder and Lockau, 1986). Extraction of phylloquinones from PSI abolishes the photoaccumulated spectrum attributed to A_1^- (Itoh et al., 1987; Mansfield et al., 1987), electron spin polarized signal arising from the $P700^+$- A_1^- radical pair (Rustandi et al., 1990), and the forward electron transfer at room temperature (Biggins and Mathis, 1988; Biggins et al., 1989). Furthermore, A_1 is doubly reduced at pH 10, consistent with it being a quinone and not a chlorophyll or an amino acid (Bottin and Setif, 1991). Therefore, it is now well accepted that a phylloquinone molecule is the A_1 redox center in PSI.

Using picosecond photovoltage and fluorescence measurements, kinetics of electron transfer from A_0 to A_1 has been estimated to have a rate constant of 20-35 ps by (Hastings et al., 1995; Hastings et al., 1994b; Kleinherenbrink et al., 1994; Kumazaki et al., 1994). At room temperature, forward electron transfer from A_1 to F_X results in A_1^- reoxidation with $t_{1/2}$ of ~200 ns (Brettel, 1988; Luneberg et al., 1994; Setif and Brettel, 1993; Sieckman et al., 1991; van der Est et al., 1994). The E_m of A_1 has been indirectly estimated to be ~755 to -785 mV, but the E_m of phylloquinone in dimethyl formamide is only about -380 mV (Iwaki and Itoh, 1994). Therefore, protein interactions with phylloquinone lowers the E_m by more than 300 mV.

The presence of two phylloquinones per P700 leads to the pseudo-symmetrical location. Also, pulsed EPR structure analysis of photosystem I single crystals has indicated two possible location of A_1 within the electron transfer chain of PSI, which are related to each other by the

pseudo C2 symmetry (Bittl *et al.*, 1997). However, it is difficult to identify the phylloquinone molecule from the large aromatic side chains at the 4 Å resolution of the current crystallographic analysis of PSI. A well-defined pocket of electron density is identified and is likely to bind a phylloquinone molecule (Schubert *et al.*, 1997). The distance from the center of P700 to the center of this structure is 25 ± 1 Å, in excellent agreement with the Å 25.4 ± 0.3 Å distance determined by EPR studies (Bittl and Zech, 1997; Dzuba *et al.*, 1997). Similarly, the center-to-center distances from the A_0 chlorophyll to phylloquinone or from phylloquinone to F_X are in good correlation (Schubert *et al.*, 1997). However, there is no pseudo-symmetrical position for the other phylloquinone molecule observed in the electron density map. Based on the binding affinities of quinones for phylloquinone-binding site during *in vitro* reconstitution, the phylloquinone environment has been predicted to contain $\pi-\pi$ interactions from aromatic residues, H-bonds, and an acidic residue. Of these, $\pi-\pi$ interactions may be more important than H-bonding for holding phylloquinone in PSI (van der Est *et al.*, 1995). When reconstituted naphthoquinone was bound to the native A_1 binding pocket, the distance between P700$^+$ and A_1^- was same as wild type. This implies that the function of A_1 as an electron acceptor does not depend on the orientation or hydrogen bonding of the quinone (Zech *et al.*, 1997).

2.1.2.4. F_X

The next intermediate acceptor in the electron transfer pathway within PSI is the [4Fe-4S] cluster F_X (Golbeck, 1992). The EPR signal from the reduced F_X has *g*-values of 2.04, 1.88 and 1.78. This signal is highly temperature sensitive, being only detectable at cryogenic temperatures. The linewidths and microwave power saturation properties of F_X are substantially different than the typical low potential Fe-S clusters. The E_m of F_X is the lowest for any Fe-S clusters characterized to date. The E_m of F_X has been estimated to be -705 mV (Chamorovsky and Cammack, 1982) in EPR experiments and -670 mV in the P700 backreaction measurements (Parrett *et al.*, 1989).

F_X is clearly identified in the crystal structure due to its high electron density. It is located near the stromal surface at the edge of membrane plane (Krauß *et al.*, 1996; Schubert *et al.*, 1997). The centroid position of F_X coincides with the two-fold axis. Thus, F_X is at the center of the PSI complex from the top view. F_X is 32 Å away from P700 along the membrane normal and 14 Å from the center of the phylloquinone binding pocket.

2.1.2.5. F_A and F_B

The F_A and F_B clusters were the first bound electron acceptors identified in the PSI complexes (Malkin and Bearden, 1971). They are bound to the PsaC subunit, unlike other

electron carriers which are bound to the core proteins. Like the F_X center, they are also [4Fe-4S] clusters. The F_A and F_B clusters have characteristic low temperature EPR spectra with g-values of 2.05, 1.94 and 1.86 for the reduced F_A and 2.05, 1.92 and 1.89 for the reduced F_B. They also have characteristic optical properties. Reduction of these centers leads to absorbance changes at 430 nm, which may also be due to the reduction of F_X (Hiyama and Ke, 1971). The E_m values for F_A and F_B have been determined to be approximately -530 and -560 mV respectively (Ke *et al.*, 1973). Kinetics of reduction of the terminal electron acceptors has been difficult to examine due to problems in obtaining kinetic data on electron transfer among three [4Fe-4S] clusters.

In the electron density map, two Fe-S centers are clearly identified in the region of PsaC. However, the two-fold ambiguity of the PsaC protein folding prevents the distinction between the F_A and F_B clusters at the current resolution. Thus, these two clusters are tentatively assigned as F_1 and F_2 based on their distances from the F_X cluster. The F_1 and F_2 clusters, together with F_X, define an obtuse triangle roughly coplanar with the crystallographic C_3 of the PSI trimer. The center-to-center distances are 12 Å between F_1 and F_2, 15 Å between F_X and F_1, and 22 Å between F_X and F_2.

The very close redox potentials of F_A and F_B bring a major unresolved question about the path of electrons from F_X via F_A/F_B to ferredoxin. There are two alternative paths for electron-transfer from F_X to the [2Fe-2S] center of ferredoxin. First, the electrons may travel in series from F_X to F_B to F_A (or to F_A to F_B) to ferredoxin. Alternatively, the electrons from F_X may be transferred to F_A or F_B and then one or both of these reduced centers can donate electrons to ferredoxin. An attractive corollary to the parallel pathway may include the use of F_A and F_B as an alternative shunt to direct electrons to cyclic or noncyclic electron flow. Information gathered from mutagenesis, biochemical, and biophysical studies indicates that both the F_A and F_B centers are involved in a sequential electron transfer *in vivo* and F_A is the proximal cluster to F_X whereas F_B is the distal cluster that donates electrons to ferredoxin (detailed discussion in section 3.2). The electron from F_A/F_B is accepted by an oxidized ferredoxin.

2.1.3. Interactions on the reducing side

On the reducing side of PSI, electrons are transferred from F_A/F_B clusters to ferredoxin. Under iron-deficient conditions, cyanobacteria contain flavodoxin as an additional electron acceptor of PSI (Morand *et al.*, 1994). The interprotein electron transfer on the reducing side of PSI is a complex process. It involves electron transfer in a series of Fe-S centers, and the interactions of ferredoxin with three PSI proteins, PsaC, PsaD, and PsaE. The electron transfer involves several different PSI-ferredoxin complexes and three different first-order components

with $t_{1/2}$ of ~500 ns, 13-20 μs, and 100-123 μs (Setif and Bottin, 1995). The 500 ns phase corresponds to electron transfer from F_A/F_B to ferredoxin. The structural requirements for efficient electron transfer in *Anabaena* ferredoxin and flavodoxin are dependent on the reaction partner (Navarro *et al.*, 1995).

The PSI-ferredoxin complex formation precedes electron transfer and the rate constants for complex formation depend on ionic concentration, suggesting electrostatic interactions between ferredoxin and PSI (Hervas *et al.*, 1992b; Setif and Bottin, 1994). Ferredoxin accepts electrons from F_A/F_B clusters of PsaC, implying that these proteins should contact each other. The major obstacle in the association between PsaC and ferredoxin is the unfavorable electrostatic interactions; both proteins have strong electronegative surfaces at the physiological pH. Therefore docking proteins are required to facilitate the interaction by providing amino acid clusters of opposite charges. The PsaD protein of PSI can be cross-linked chemically with ferredoxin (Lelong *et al.*, 1994; Zilber and Malkin, 1992). The docking role was demonstrated by the loss of ferredoxin-mediated $NADP^+$ reduction activity in the PsaD-deficient PSI complex (Xu *et al.*, 1994c). The lack of PsaE severely reduces rate of ferredoxin reduction. Therefore, PsaD, PsaE and PsaC are the essential components of the reducing side of PSI.

Structure of the reducing side of PSI is not understood at a fine resolution. The PSI reaction center has a ridge of 35 Å height projecting from one side of the membrane (Krauß *et al.*, 1993); this ridge has been proposed to be composed of the PsaC, PsaD and PsaE subunits. Computer modeling of ferredoxin docking has predicted that the docking site may be on the outside of the ridge, tilted towards the membrane plane (Fromme *et al.*, 1994). Electron microscopy studies on PSI complexes that have been cross-lined with flavodoxin have shown that flavodoxin docks in the ridge formed by the peripheral subunits, from the outside of a PSI trimer, and 7 nm from the center (Mühlenhoff *et al.*, 1996a). The surface-exposed domains of PsaC, PsaD, and PsaE that may be involved in interaction with ferredoxin have been identified (Xu *et al.*, 1994b).

2.2. Cyclic electron transfer

In addition to the PSII-dependent linear electron transfer, PSI also participates in the cyclic electron flow that results in proton pumping and ATP production without the participation of PSII. Cyclic electron flow is essential in the bundle sheath cells of C4 plants that predominantly contain PSI, but its contribution to ATP generation in C3 plants and in cyanobacteria is rather limited (Bendall and Manasse, 1995; Yu *et al.*, 1993b). Recently, cyclic electron transfer has been proposed be involved in photoprotection and in fine-tuning of the balance between ATP and NADPH production (Bendall and Manasse, 1995).

Although cyclic electron transfer has been studied for a long time, all components involved in this pathway have not been identified. There is a general agreement that cyclic and linear electron pathways share components from plastoquinone to PSI. The inhibitors of cytochrome b_6f complex also abolish the ferredoxin-mediated cyclic electron transfer, indicating the involvement of cytochrome b_6f complex in cyclic electron transfer (Cleland and Bendall, 1992). Transfer of electrons from PSI back to plastoquinone involves unique components or additional functions of some components that are involved in linear electron transport. The PsaE subunit of PSI has been implicated in cyclic electron flow. The *psaE* deletion mutant of *Synechococcus* sp. PCC 7002 grows slowly at low light intensity and low CO_2 concentration. Moreover, in the double deletion mutant *psaE⁻ ndhF⁻*, the physiological $P700^+$ photoreduction was impaired when the linear electron flow was inhibited, indicating the absence of cyclic electron flow in the PsaE-less mutant (Yu *et al.*, 1993b). Characterization of a PsaE-less strain of *Synechocystis* sp. PCC 6803 has corroborated the notion that PsaE is essential for cyclic electron flow around PSI (Chitnis *et al.*, 1995a). The exact nature of PsaE participation in the cyclic electron flow is not understood. PsaE may provide a docking site for the ferredoxin isoform that is involved in cyclic electron flow. Alternatively, it may provide quinone binding sites. Three-dimensional solution structure of PsaE shows that charged residues form a basic patch on the surface and there are several aromatic residues which could potentially bind quinone (Falzone *et al.*, 1994a; Falzone *et al.*, 1994b). Of the two phylloquinones present in the PSI reaction center, one (A_1) was shown to be involved in the electron transfer to F_X, whereas the function of the other one is not known. The possibility that the second phylloquinone functions in the cyclic electron transfer is yet to be examined.

The major proposed pathways of cyclic electron transfer involve ferredoxin, the terminal electron acceptor of PSI as the soluble redox factor. In vitro reconstitution of cyclic electron flow has demonstrated that it is necessary to add a soluble redox factor. Ferredoxin is a good cofactor in reconstitution experiments, thus supporting the role of ferredoxin as an essential physiological component of the cyclic electron pathway. Flavodoxin can also mediate cyclic electron flow (Scheller, 1996). It is likely that different isoforms of ferredoxins have overlapping roles in cyclic and linear electron transfer. Transfer of electrons from ferredoxin to plastoquinone has been a matter of debate. An indirect pathway may include ferredoxin-$NADP^+$ reductase, NADPH, and NADPH dehydrogenase. This pathway occurs in cyanobacteria (Yu *et al.*, 1993b), but NADPH dehydrogenase activity is not demonstrated in plant chloroplasts. There are two NADPH-independent pathways that use reduced ferredoxin to transfer electrons to plastoquinone. Recent experiments with barley thylakoid membranes suggest that two parallel pathways of cyclic electron transport operate under anaerobic conditions (Scheller,

1996). These pathways differ in their antimycin sensitivity, saturation characteristics and substrate specificity. Under physiological conditions, the antimycin-insensitive pathway is predicted to predominate the antimycin-sensitive pathway. The antimycin sensitive pathway was thought to involve cytochrome b, but direct effect of antimycin on electron transfer rate of cytochrome b_6f complex has not been demonstrated. This pathway does not include a possible quinone-reducing side of PSI (Scheller, 1996). The ferredoxin-plastoquinone reductases have been postulated to mediate transfer of electrons directly to plastoquinone (Cleland and Bendall, 1992). One of these enzymes is inhibited by antimycin. Disilfodisalicyclidenepropane-1,2-diamine, an inhibitor of ferredoxin-NADP$^+$ reductase, also inhibits cyclic electron flow (Shahak et al., 1981). It is likely that the membrane-associated ferredoxin-NADP$^+$ reductase might represent an integral part of ferredoxin-plastoquinone reductase (Bendall and Manasse, 1995). Therefore, one can speculate that the PsaE of PSI, ferredoxin-NADP$^+$ reductase associated with it, and an unknown quinone-binding protein could make ferredoxin-plastoquinone reductase. Therefore, many crucial components of cyclic electron flow have been proposed, but their exact roles and identities of ferredoxin-plastoquinone reductases need to be determined.

Overall, the PSI complex utilizes energy of the photons trapped by either its core antenna system or the associated LHCs to function in linear or cyclic pathway producing strong reductants and ATP, and plays an important role in nourishing the whole world.

3. The catalytic subunits

As a light-driven oxidoreductase, PSI catalyses the electron transfer from the reduced plastocyanin to the oxidized ferredoxin. The electron carriers participating the electron transportation are bound to the PsaA, PsaB, and PsaC proteins.

3.1. PsaA and PsaB

The PsaA and PsaB proteins form the hydrophobic core of PSI. In higher plants, the genes encoding PsaA and PsaB are present in the chloroplast. The deduced molecular masses of PsaA and PsaB are approximately 83 kDa and 82 kDa, respectively. Because of their similar sizes, the PsaA and PsaB proteins normally co-migrate to form a diffuse band in a polyacrylamide gel. PsaA and PsaB are highly conserved and homologous. The primary sequences of PsaA and PsaB proteins from various sources contain higher than 78% and 76% amino acid identities, respectively (Sun et al., 1998). Comparison of the PsaA and PsaB primary sequences reveals more than 42% amino acid identity and an additional 15% conservative replacements. Thus, the PsaA and PsaB proteins might have evolved by gene duplication and are thought to have similar structural features.

3.1.1. Structural features of the core proteins

The hydropathy analysis of PsaA and PsaB indicated that each protein contains 11 potential transmembrane domains (Fish et al., 1985). This proposal is in agreement with the X-ray crystallographic studies (Krauß et al., 1993; Krauß et al., 1996). In the structural model at 4 Å resolution, twenty-two transmembrane helices are arranged in an approximate symmetry and have been assigned to PsaA and PsaB. Five transmembrane helices from each core protein form a palisade-like arrangement surrounding the pseudo-2-fold symmetry axis. The cofactors of the electron transfer chain from the primary reaction center P700 to F_x are located in this central cage. The other six transmembrane helices are far from the axis. Within the well-defined inner core of PSI, some of the transmembrane helices and the interhelical connections are assigned to the amino acid sequences of PsaA and PsaB. The C-terminal regions of PsaA and PsaB contribute to the central cage and the N-terminal regions are believed to form the antenna part of PSI.

The interpretation of electron density maps is consistent with some biochemical observations. Investigations using limited proteolysis indicated that the N-terminal regions of PsaA and PsaB in the plant and cyanobacterial PSI are much more accessible to proteases than the very C-terminal regions (Sun et al., 1997; Xu and Chitnis, 1995; Zilber and Malkin, 1992). Also, limited proteolysis on the subunit-deficient mutant PSI complexes indicated that the C-terminal regions of PsaA and PsaB are involved in interactions with other subunits (Sun et al., 1997; Xu and Chitnis, 1995). As observed in the crystal structure, the PsaC, PsaD, and PsaE subunits are located along the interface of the two-fold symmetry with PsaC in the middle. In this two-region architecture of the PsaA and PsaB proteins, the C-terminal regions harbor the electron carriers and provide the environment for electron transfer. The N-terminal regions of PsaA and PsaB coordinate most of the chlorophyll molecules and form the intrinsic antenna of the PSI complex.

Orientation of the PsaA and PsaB proteins with respect to the membrane has been studied by biochemical and histoimmunological methods (Sun et al., 1997; Vallon and Bogorad, 1993; Xu and Chitnis, 1995). The eleven transmembrane helices of PsaA and PsaB span the thylakoid membrane completely with the N-termini of PsaA and PsaB located on the n-side (stromal side in chloroplasts and cytoplasmic side of cyanobacteria) of the photosynthetic membrane. Consequently, the C-termini of the core proteins are on the p-side (lumenal side) of thylakoid membrane (Fig. 2-3). Such orientation makes the six n-side extramembrane loops with a majority of positive residues, which agrees with the "positive inside" rule (von Heijne and Gavel, 1988).

At the present resolution of the PSI crystal structure, the symmetrical PsaA and PsaB proteins could not be distinguished. Studies using limited proteolysis and subunit-deficient mutant PSI complexes have established the interactions of the core proteins with other subunits, among which the N-terminal region of PsaA with PsaE and the N-terminal region of PsaB with PsaD are dominant (Sun *et al.*, 1997). Chemical crosslinking and electron microscopy studies have revealed that PsaD and PsaE are located in different sides of the pseudo-2-fold symmetry axis (Armbrust *et al.*, 1996; Kruip *et al.*, 1997; Xu *et al.*, 1995a). PsaD is located adjacent to PsaL which is close to the central connecting region of trimers, while PsaE is in contact with regions of PsaF which is at the outer edge of the PSI trimer. Thus, the primed helices in the 4 Å crystal structure map are assigned to PsaA and the unprimed helices are assigned to PsaB (Sun *et al.*, 1997).

3.1.2. Cofactor binding pockets of the core proteins

The electron carriers from P700 to F_X are bound to the C-terminal regions of the core proteins. Specifically, the chlorophyll *a* dimer of the primary electron donor P700 are proposed to be coordinated by two histidyl residues, A_H676 and B_H651, which are located in the X transmembrane helices of PsaA and PsaB (Fromme *et al.*, 1994; Webber *et al.*, 1996). There are two symmetrical chlorophyll monomers adjacent to P700. At least one of them is equivalent to the primary electron acceptor A_0. These chlorophylls could also be coordinated by histidines. The suitable residues for the positions are two conserved histidines of the transmembrane helices VIII: A_H543 and B_H525 (Schubert *et al.*, 1997). Between the P700 and A_0, a third pair of chlorophyll *a* molecules, namely the accessory chlorophylls, are identified in the structural studies (Krauß *et al.*, 1993; Krauß *et al.*, 1996; Schubert *et al.*, 1997). They are proposed to be coordinated by the conserved asparagyl residues in the transmembrane helices IX: A_N600 and B_N582 (Schubert *et al.*, 1997). The phylloquinones for the secondary electron acceptor A_1 are not well identified in the crystal structures. However, a pocket of electron density is well defined which the phylloquinone molecule could be hold. In the primary amino acid sequences of PsaA and PsaB, the highly conserved peptides A_[686]LFSGRGYWQELIE[698] and B_[686]LISWRGYWQELIE[698] in the connections between the transmembrane helices *m* and *m'* and the peripheral helices *n* and *n'* are proposed to bind the phylloquinones (Schubert *et al.*, 1997). This fragment LxSxRGYWQELIE is also partially conserved in PshA of the P800 reaction center of *Heliobacterium* and PscA of the P840 reaction center of green sulfur bacterium *Chlorobrium*. The electron spin echo envelope modulation (ESEEM) spectroscopy study with ^{14}N- and ^{15}N-labeled PSI indicated that there are two protein nitrogen nuclei coupled to the phyllosemiquinone radical A_1^- (Hanley *et al.*, 1997).

The first coupled nitrogen is assigned to the indole nitrogen of a tryptophan residue. The second coupled nitrogen can be described as an amino nitrogen of a histidine, or an amide nitrogen of asparagine or glutamine. Thus, the well-conserved amino acids A_W693/A_Q694 or B_W668/B_Q669 may bind the secondary electron acceptor A_1. The Fe-S cluster F_X is located on the pseudo-two-fold symmetrical axis near the n-side surface. It is coordinated by both PsaA and PsaB with the conserved cysteines in the extramembrane loops between the transmembrane helices VIII and IX: A_C574, A_C583, B_C556, and B_C565. Not only the cysteinyl residues, but also the whole extramembrane loops containing the cysteines are highly conserved among PsaA and PsaB from various sources, PshA of the P800 reaction center of *Heliobacterium* and PscA of the P840 reaction center of *Chlorobrium* (Buttner et al., 1992; Liebl et al., 1993).

The PSI complex carries its integral core antenna system consisting of about 100 chlorophyll *a* molecules. In the crystal structure of PSI at 4 Å resolution, 89 chlorophyll *a* molecules have been identified (Schubert et al., 1997). Six chlorophylls are the cofactors of the electron transfer chain. The remaining 83 chlorophylls constitute the core antenna system. Most of these antenna chlorophylls are coordinated to PsaA and PsaB by the conserved histidines of the transmembrane helices the core proteins. Some of the small subunits, presumably PsaL, PsaK, and PsaF, may also coordinate some antenna chlorophylls and/or provide a suitable hydrophobic environment to accommodate such molecules (Schubert et al., 1997). Among the 83 antenna chlorophylls, a symmetrical pair is positioned closely to the potential primary electron acceptor chlorophylls. They may play a special role in the energy transfer from the core antenna to the primary reaction center, thus are referred as the connecting chlorophylls. The amino acids that are possible coordinating the connecting chlorophylls are the conserved histidines in the transmembrane helices VII of the core proteins: A_H450 and B_H430 (Schubert et al., 1997). The antenna chlorophylls are tightly packed into four clusters comprising 21, 23, 17, and 20 chlorophylls, respectively, with linking chlorophyll molecules bridging the neighboring clusters. The clusters laterally surround the electron transfer chain to form a hollow, elliptical cylinder which narrows slightly toward the luminal side. The maximal center-to-center distance between the antenna chlorophylls is shorter than 16 Å, which allows the transfer of the excitation energy from one chlorophyll to its neighbor and formation of a continuous network. Fluorescence spectroscopy of the trimeric and monomeric PSI complexes from the cyanobacterium *Spirulina platensis* indicated that the most longwave chlorophyll form originates from an interaction among chlorophylls bound to monomeric PSI subunits forming a trimer (Karapetyan et al., 1997).

3.1.3. Mutagenesis studies on the core proteins

Interruptions or deletions of the *psaA* and *psaB* genes in cyanobacteria, green algae, and higher plants result in undetectable level of PSI proteins in the membrane (Boussiba and Vermaas, 1992; Shen *et al.*, 1993; Smart and McIntosh, 1993; Smart *et al.*, 1993). The mutant strains assemble the wild type levels of functional PSII complexes. None of these mutant strains is capable of photoautotrophic growth, which is consistent with the Z-scheme model of photosynthesis. However, it was reported that *C. reinhardtii* PSI-deficient mutant strains in which the trans-splicing of the *psaA* mRNA was blocked could achieve photoautotrophic growth and CO_2 fixation (Lee *et al.*, 1996). More recently, the same mutant strains were tested and found to contain small but significant amounts of PSI, thus supporting electron transport and CO_2 fixation (Cournac *et al.*, 1997). From another approach, a yellowish white plastome mutant of *Antirrhinum majus* L. was identified to have a point mutation in *psaB* gene, which introduces a new stop codon and leads to a truncated PsaB protein (Schaffner *et al.*, 1995). Thus, the deficiency of the PsaA or PsaB proteins prevents the accumulation of PSI complex and inhibits the photoautotrophic growth.

With the availability of mutants that are deficient in the core proteins, site-directed mutagenesis of the PsaA and PsaB proteins has been employed to identify the residues near the bound cofactors. Obviously, the conserved histidines coordinating the primary donor P700 have been attractive targets for mutagenesis. H656 in PsaB of *C. reinhardtii* was mutated to asparagine or serine (Webber *et al.*, 1996). The mutations alternated the P700+·environment and increased oxidation midpoint potential of P700/P700+ by 40 mV. The spectroscopic characteristics of the point mutations were also affected. The P700/P700+· optical difference spectra produced a new bleaching band at 667 nm and the electron nuclear double resonance spectroscopy indicated a significant increase in the hyperfine coupling corresponding to methyl protons at position 12 of the spin carrying chlorophyll *a* of P700+·. Therefore, the residue H656 was suggested to provide a hydrogen bond to a keto carbonyl group or an axial ligand to the central Mg atom of one of the chlorophyll *a* molecules in P700. Time-resolved absorption and fluorescence spectroscopy revealed that the mutation of histidine to asparagine also increased the trapping process two times while had no affect on the difference spectrum of the photoreduction of the primary acceptor (Melkozernov *et al.*, 1997). The conserved histidines in the last six transmembrane helices of the core proteins of PSI in *C. reinhardtii* were changed by site-directed mutagenesis. Changes in the characteristics of P700 were screened and only mutations of A_H676 and B_656 resulted in changes in spectroscopic properties of P700. Thus, these histidines are the axial ligands to the P700 chlorophylls (Redding *et al.*, 1998). The conserved histidines in the transmembrane helix VIII of PsaB were also replaced in *C.*

reinhardtii. The mutants were impaired in the assembly of the PSI reaction center in the post-translational step in PSI assembly. The spectroscopic characteristics of P700 in the mutants remained unchanged (Cui *et al.*, 1995).

The highly conserved motif PCDGPGRGGTC in the core proteins also draws attention. This motif contributes to the coordination of the [4Fe-4S] cluster F_X. The insert of this motif into a designed four α-helix model protein introduced a [4Fe-4S] type cluster into the holoprotein (Scott and Biggins, 1997). When C565 in PsaB of *Synechocystis* sp. PCC 6803 was mutated to serine, histidine or aspartic acid, the mutations greatly reduced accumulation of PSI and failed to grow autotrophically (Smart *et al.*, 1993). The C565S mutant accumulated reduced amount of PSI and displayed photoreduction of the [4Fe-4S] terminal electron acceptors F_A and F_B. The PSI complex from the C565S mutant assembled [3Fe-4S] and [4Fe-4S] clusters at F_X and the mixed-ligand [4Fe-4S] cluster of F_X was capable of electron transfer to F_A/F_B (Warren *et al.*, 1993b). Similarly, the substitution of C556 in PsaB of *Synechocystis* sp. PCC 6803 with serine also introduced a mixed-ligand [4Fe-4S] cluster at F_X (Vassiliev *et al.*, 1995). Therefore, both C556 and C565 coordinate the F_X cluster, which in turn is essential for stable assembly of the PSI complex. The mixed-ligand [4Fe-4S] F_X cluster is an inefficient electron carrier and leads to a decreased quantum efficiency of electron transfer in the C556S and C565S mutant PSI complexes (Vassiliev *et al.*, 1995). This may explain the inability of the mutant organisms to grow photoautotrophically. Mutation of C560 to histidine in *C. reinhardtii* also led to undetectable accumulation of PSI (Webber *et al.*, 1993).

Many other residues in this F_X binding motif have been mutated to study their role around the F_X cluster. Biochemical study has showed that R561 in the PsaB protein of *Synechocystis* sp. PCC 6803 may interact with PsaC (Rodday *et al.*, 1993). This hypothesis was tested by site-directed mutagenesis in *Synechocystis* sp. PCC 6803 (Rodday *et al.*, 1994) and in *C. reinhardtii* (Rodday *et al.*, 1995). The site-directed change R561E in PsaB destabilizes the subunit interaction in *Synechocystis* sp. PCC 6803 (Rodday *et al.*, 1994). The mutant reaction center was much less stable in urea and the functional reconstitution of the mutant core using PsaC was impaired. The presence of divalent cations increased the reconstitution of PsaC with the mutant core whereas inhibited with the wild type core. It was suggested that the electrostatic interaction in the association of PsaC with the core heterodimer is important. Interestingly, the site-directed change of the corresponding R566 in the *Chlamydomonas* PsaB to glutamate results in the complete lack of PSI in the thylakoids (Rodday *et al.*, 1995). Several other *Chlamydomonas* mutants were generated on the conserved prolines and aspartate in the motif of PsaB. The P560A, P560L, and P564L mutants accumulated functional reaction centers but showed an impaired interaction between the reaction center core complex and the PsaC subunit.

The D562N mutant did not accumulate PSI. It was suggested that P560 and D562 may contribute to the stability of the F_X cluster by providing essential hydrogen bonding to the C56i ligand while the intercysteinyl region in PsaB is a domain involved in the interaction between PsaC and the PSI core (Rodday et al., 1995).

PsaA and PsaB also contain leucine zipper motifs in two conserved homologous putative transmembrane helices (Webber and Malkin, 1990). Site-directed mutants L522V, L536M, and L522V/L536M in PsaB of Synechocystis sp. PCC 6803 exhibited wild type characteristics and grew autotrophically, whereas the L522P mutation prevented PSI accumulation. These results did not support a major structural role of the leucine zipper in dimerization of the core (Smart et al., 1993). However, the conservative substitution might not have perturbed the leucine zipper.

3.1.4. Similarity between PSII and PSI core proteins

The PsaA and PsaB proteins contain 11 transmembrane helices each. According to their structural role, they can be categorized into the five C-terminal helices, which contribute to the central cage surrounding the electron carriers, and the six N-terminal helices, which form the core antenna system. In PSII, the electron carriers are bound to the D1 and D2 proteins while the core antenna containing about 50 chlorophyll molecules is bound by the CP47 and CP43 proteins. The comparison of the topographies of PSI core proteins and these PSII proteins underlines a close relationship between PSI and PSII (Fig. 2-3). The D1 and D2 proteins are predicted to have five transmembrane domains with the N-termini on the stroma and the C-termini on the lumen, whereas the CP47 and CP43 proteins are predicted to posses six transmembrane helices with both the N- and C-termini on the stroma. Splitting of proteins in the G loops (between transmembrane helices VI and VII) of PsaA and PsaB, the N-terminal regions and C-terminal regions contain the exact same orientations as the PSII proteins. The C-terminal regions of PsaA and PsaB also share similarity with D1 and D2 proteins in coordinating cofactors.

Therefore, the CP43 and CP47 core antenna proteins of PSII and the N-terminal regions of PSI PsaA and PsaB proteins, the D1 and D2 core proteins of PSII and the C-terminal regions of the PsaA and PsaB proteins may have evolved from a common ancestor. Considering the homology among PsaA and PsaB, D1 and D2, CP43 and CP47, an ancestral homodimeric complex may be the common ancestor and the divergence of evolution yields all these proteins. If the common ancestor is an antenna/reaction center complex, the evolution may involve the splitting to yield the PSII proteins. If the common ancestor contains separate antenna and reaction center proteins, the PSI proteins may have evolved through a combination of the antenna and reaction center genes.

The P700 reaction center of PSI complex, the P800 reaction center of *Heliobacterium*, and the P840 reaction center of green sulfur bacteria *Chlorobrium* are Type I reaction centers. They share structural and functional similarities, indicating a common evolutionary origin. However, the reaction centers of the anoxygenic bacteria do not seem to have polypeptides corresponding to the accessory subunits of PSI. Thus, the addition of these proteins of PSI complex in cyanobacteria and chloroplasts may be a more recent addition to meet the protective and interactive demands of the oxygenic photosynthesis.

3.2. PsaC

PsaC is an acidic peripheral protein with 80 amino acids. It coordinates the terminal electron transfer centers F_A and F_B of PSI. In higher plants, the *psaC* gene is located in the chloroplast genome. PsaC is an extraordinarily conserved protein. A comparison of the deduced amino acid sequences of PsaC from cyanobacteria, algae, and plants shows that most residues are completely conserved during evolution while some conservative replacements are near the N-terminus and in the center of the protein. PsaC also shares homology with the bacterial-type 2[4Fe-4S] ferredoxins. The most notable feature of PsaC is the nine conserved cysteines, eight of which are in two [4Fe-4S]-cluster binding motif, CxxCxxCxxxCP, for coordinating the [4Fe-4S] F_A and F_B clusters Site-specific mutagenesis has revealed that the F_A cluster is liganded by cysteines C21, C48, C51, and C54, while cysteines C11, C14, C17, and C58 are ligated to the F_B cluster (Zhao *et al.*, 1992). The ninth cysteine C34 does not participate in ligating either F_A or F_B (Yu *et al.*, 1993a). PsaC in the PSI complex can be modified by maleimide biotin indicating that C34 is located on the surface of the PSI complex (V. P. Chitnis and P. R. Chitnis, unpublished results).

PsaC obviously interacts with the core proteins. Chemical cross-linking studies have demonstrated that PsaC can be cross-linked to PsaD and PsaE proteins. Genetic inactivation of the *psaC* gene by insertion of antibiotic resistance gene in *Synechocystis* sp. PCC 6803, *Anabaena variabilis* ATCC 29413, and *C. reinhardtii* resulted in photosynthesis-deficiency. Although all these mutants lack EPR signals that can be attributed to F_A/F_B, the lack of PsaC has different effects on the assembly of the complex in different organisms. The PsaC-less mutant of *C. reinhardtii* could not assemble PSI core and resulted in complete loss of any PSI proteins (Takahashi *et al.*, 1991). In cyanobacteria, the mutants were able to accumulate core proteins, but failed to incorporate the PsaD and PsaE proteins (Mannan *et al.*, 1994; Yu *et al.*, 1995a). PsaL is present in the PsaC-less thylakoids, but is lost during isolation of the PSI complexes. Thus, PsaC interacts with the PsaD and PsaE proteins and is necessary for stable

assembly of PsaD and PsaE into PSI complex. It is not needed for assembly of PsaA and PsaB core in cyanobacterial PSI.

Ferredoxin from *Peptostreptococcus asaccharolyticus* (PaFd, (Adman *et al.*, 1976)) has been used as the prototype in the structural studies of the proteins with the [4Fe-4S] binding motif. Compared to PaFd, PsaC contains an extra internal loop of 8 residues and a C-terminal extension of 15 residues. In the crystal structure of PSI, the distance between the [4Fe-4S] clusters is 12 Å, closely matching that observed in PaFd. Fitted into the electron density, PsaC structure is observed to be highly similar to this model ferredoxin. In the 4 Å crystal structure, PsaC occupies the central position of the n-side ridge of PSI, with a pseudo-two-fold axis related the two halves of the molecule each of which includes one [4Fe-4S] cluster and a short single-turn α-helix from the conserved cluster-binding motif. Due to the limitation of resolution, a two-fold ambiguity in the orientation of PsaC remains unresolved, which takes into account the assignment of the sequence of the clusters by mutagenesis work. In the case where the F_A cluster is closer to the F_X cluster than the F_B cluster, the C- and N- termini will face towards the PsaA and PsaB core and the loop connecting the two clusters is peripheral. In the opposite orientation where the F_A is the terminal [4Fe-4S] cluster, the loop will lie near PsaA/B and the C- and N-termini are located peripherally.

So far, many studies have been performed to describe the structure-function relationships in PsaC. However, two questions are still ambiguous: Are both [4Fe-4S] clusters both essential for electron transfer? Which cluster, F_A or F_B, is proximal to F_X?

Characterization of the unbound PsaC by UV/visible, EPR, and ^{1}H NMR spectroscopy suggested that the electron is transferred from F_X to one the [4Fe-4S] clusters of PsaC and within 100 μs both clusters F_A and F_B are partially reduced at room temperature due to fast intramolecular electron exchange (Bentrop *et al.*, 1997). Thus, a linear electron flow within PSI involved both F_A and F_B is indeed the scheme. Site-directed mutations of the cysteine ligands C14 and C51 to the F_A and F_B clusters, respectively, in *Synechocystis* sp. PCC 6803 resulted the deficient in photoautotrophic growth (Yu *et al.*, 1997). It seems clear that both the F_A and F_B centers are involved in a sequential electron transfer *in vivo*. However, similar modification in *Anabaena variabilis* ATCC 29413 supported the opposite argument (Mannan *et al.*, 1996). Low-temperature EPR studies demonstrated that the C50D mutant has a normal F_B cluster and a modified F_A center. In contrast, the C13D mutant has a normal F_A cluster and no F_B signal. Both mutants grow photoautotrophically. Thus, the F_B cluster is not essential for the assembly of the PsaC protein in PSI and the F_B cluster is not absolutely required for the electron transfer from the PSI reaction center to ferredoxin.

In the sequential electron transfer, the information is in favor of F_A as the proximal cluster to F_X. Biochemical analysis indicated that F_B is essential for reduction of $NADP^+$ (He and Malkin, 1994; Jung *et al.*, 1995). Targeted mutations of two positively charged residues, K53 and R53, near the F_A center of PsaC in *C. reinhardtii* led a preferential reduction of F_B and the normal electron transfer rate from PSI to ferredoxin (Fischer *et al.*, 1997). Therefore, F_B is the donating cluster to ferredoxin. Similarly, kinetic study using $HgCl_2$ treated PSI complex, in which F_B is selectively inactivated, indicated that the electron transfer to ferredoxin and flavodoxin was inhibited and concluded that F_A is the proximal cluster to F_X and F_B is the distal cluster that donates electrons to ferredoxin (Vassiliev *et al.*, 1998). Thus, it is in favor of the electron transfer pathway orientated as F_X to F_A to F_B. However, site-directed mutagenesis on D9 of PsaC suggested that this aspartate is participating the electrostatic interaction with the core, thus supported an orientation of PsaC on the core such that center F_B is proximal to F_X (Rodday *et al.*, 1996). The redox potentials of F_B and F_A, the inhibition of F_A photoreduction after selective diazonium inactivation of F_B (Malkin, 1984), and their proposed locations in the X-ray crystallographic structure (Fromme *et al.*, 1994; Krauß *et al.*, 1993) imply a serial flow of electrons from F_B to F_A. Thus, more experiments are needed to make accurate assignments.

In the *in vitro* assembly of Fe-S centers into mutated PsaC proteins, earlier it was reported a [3Fe-4S] center in the F_A site of C51D mutant and a unidentified cluster in the F_B site of C14D mutant (Zhao *et al.*, 1992). The midpoint potentials of the single [4Fe-4S] centers in these mutated PsaC proteins are identical to F_A and F_B in bound PsaC of PSI (Yu *et al.*, 1993a). When the mutant PsaC proteins were reconstituted with a core complex, the PSI complex shows that [4Fe-4S] cluster is presented in the mixed ligand 3Cys-1Asp site and no [3Fe-4S] cluster in the bound PsaC (Yu *et al.*, 1995b). Thus, the P700-F_X core selectively rebinds those free PsaC mutated proteins with two [4Fe-4S] clusters. In a comprehensive study, C14, C21, C34, C51, or C58 in PsaC were replaced with Asp, Ser, or Ala (Mehari *et al.*, 1995). Characterization of free and rebound mutant PsaC proteins revealed that PsaC requires two Fe-S centers to refold, one of which must be cubane. Furthermore, the presence of two cubane Fe-S clusters in the free PsaC is a necessary precondition for binding to P700-F_X cores. *In vivo* mutagenesis on the ligands of F_A and F_B also indicated that only those PsaC proteins that contain two [4Fe-4S] clusters are capable of assembling onto PSI cores (Jung *et al.*, 1998).

Interaction of PsaC with the PSI core have been studied by molecular genetic manipulations. *In vitro* reconstitution of PsaC isolated from mutants lacking internal loop and C-terminal extension with a barley P700-F_X core (that lacks PsaC, PsaD and PsaE subunits) showed that such mutant subunits can bind to P700-F_X core and retain 2 [4Fe-4S] clusters, but

F_A/F_B back-reaction back reaction was less efficiently restored when reconstituted in the presence of PsaD (Naver et al., 1996). Reconstitution of these mutant proteins in the presence or absence of PsaD implied that internal loop of PsaC interacts with PsaA/B heterodimer whereas C-terminus of PsaC interacts with PsaD subunit (Naver et al., 1996). Proper orientation of PsaC may also involve acidic residues of PsaC that have been proposed to be involved in electrostatic interactions with the PSI core (Rodday et al., 1993). Changing some of these acidic amino acids to basic residues not only results in reduced level of reconstitution of PsaC subunit to PSI core, but also decreases electron transfer efficiency. Among all acidic residues examined in this study, E9 was found to be the most important residue for electrostatic interaction (Rodday et al., 1993). Site-directed mutagenesis on K35 of PsaC in C. reinhardtii revealed that K35 is the main interaction site between PsaC and ferredoxin and that it plays a key role in the electrostatic interaction between PSI and ferredoxin (Fischer et al., 1998).

4. The docking subunits

PSI complex accepts electrons from plastocyanin in the thylakoid lumen and donates electrons to ferredoxin in the chloroplast stroma or cyanobacterial cytoplasm. PsaD and PsaE are involved in the docking of ferredoxin, whereas PsaF may interact with plant plastocyanin to form a complex for fast electron transfer.

4.1. PsaD

The PsaD subunit of PSI is a conserved peripheral protein on the reducing side of PSI. In higher plants, the PsaD protein is encoded by the nuclear gene psaD. In general, the cyanobacterial PsaD protein contains 139-144 amino acids while the plant PsaD has about 23 additional residues forming an extension at the N-terminus (Manna and Chitnis , 1998). This extension of eukaryotic PsaD is accessible to proteases (Lagoutte and Vallon, 1992; Zilber and Malkin, 1992). The insertional inactivation of the psaD gene of Synechocystis sp. PCC 6803 indicated that PsaD is essential for efficient function of the cyanobacterial PSI (Chitnis et al., 1989).

PsaD has several roles in the function and organization of PSI. First, it interacts with at least three proteins of PSI and stabilizes their organization within the complex. These interactions are specific and crucial for the organization and function of the PSI complex. Chemical crosslinking experiments have demonstrated the physical interactions of PsaD with PsaC and PsaL subunits (Armbrust et al., 1996; Xu et al., 1994a). Limited proteolysis experiments showed that PsaD shields extramembrane loops of PsaB (Sun et al., 1997; Xu and Chitnis, 1995). Second, PsaD is required for the stable binding of PsaC to the PSI core proteins (Chitnis et al., 1996; Li et al., 1991). When PsaC was reconstituted with the PSI core

in the absence of PsaD, ESR studies showed that F_B and F_A were photoreduced about equally at 19 K, and while the resonances were shifted upfield, they remained as broad as in the free PsaC holoprotein. In the presence of PsaD, the reconstituted complex showed nearly identical resonances as control PSI complex (Li *et al.*, 1991). In the PsaD-deficient ADC4 mutant, F_B, rather than F_A, became preferentially photoreduced and the EPR line shapes were relatively broad. PsaC and the F_A/F_B clusters were lost more readily from the ADC4 membrane after treatment with Triton X-100 or chaotropic agents (Chitnis *et al.*, 1996). PsaD is also required for the stable assembly of PsaE (Chitnis *et al.*, 1989). Third, PsaD provides an essential ferredoxin-docking site (Lelong *et al.*, 1994; Xu *et al.*, 1994c). The ferredoxin-mediated $NADP^+$ photoreduction was severely inhibited in the membrane of PsaD-less mutant (Xu *et al.*, 1994c). The first order reduction of ferredoxin cannot be observed in PsaD-less mutant (Hanley *et al.*, 1996). The docking involves electrostatic interactions between the basic PsaD protein and the electronegative surfaces of ferredoxin (Lelong *et al.*, 1994). Cross-linking study has shown that K106 of PsaD from *Synechocystis* sp. PCC 6803 can be cross-linked to E93 in ferredoxin (Lelong *et al.*, 1994). Site-directed mutagenesis study revealed that the K106 residue of PsaD from *Synechocystis* sp. PCC 6803 PSI is a dispensable component of the docking site (Chitnis *et al.*, 1996; Hanley *et al.*, 1996). These results suggest that binding of PsaD in correct orientation depends on multiple charge interactions.

Crystallographic studies at limited resolution have shown that PsaD contains a single, short α-helix located near the common interface with PsaC and the integral membrane core subunits which may be important for the stable association of both PsaC and PsaD with the PSI core (Krauß *et al.*, 1996). Analysis of the PsaD sequences indicated that an α-helix was predicted from L19 to T31 in the N-terminal region of PsaD. When viewed in a helical wheel diagram, this predicted α-helix forms faces with clustered hydrophilic and hydrophobic residues. The topography of PsaD protein has been also studied by biochemical and mutagenesis analyses. Limited proteolysis and chemical modification indicated that K106 and/or K117 of PsaD could react with N-hydroxysuccinimidobiotin (NHS-biotin) and E93 of PsaD was readily accessible to protease (Xu *et al.*, 1994b). The region around K106 is exposed on the surface of PsaD and interacts with ferredoxin. This region contains several basic residues which may be involved in the electrostatic interactions with the acidic residues of ferredoxin. The conserved H97 of PsaD is also present in this region. Various mutations of H97 showed that this amino acid is involved in the increased affinity of PSI for ferredoxin when the pH is lowered. This histidine could be central in regulation *in vivo* the rate of ferredoxin reduction as a precise sensor of the local proton concentration (Hanley *et al.*, 1996). However, other residues involved in this pH effect can not be ruled out. When up to 24 residues from the C-terminus of PsaD were deleted,

the mutant protein was able to assemble into PSI *in vivo* (Chitnis *et al.*, 1995a). However, the deletions impaired the reductase activity of Ps I in the ferredoxin-mediated $NADP^+$ photoreduction. Therefore, the C-terminus of PsaD is not essential for the assembly of PsaD into PSI complex but may be required for the proper orientation of ferredoxin binding region. Examination of the primary sequence of PsaD reveals a basic domain between R72 and R86 in the central region of the protein (Manna and Chitnis , 1998). The basic domain contains four conserved and one or two nonconserved basic residues. Mutagenesis study indicated that the basic residues in this domain of PsaD, especially R74, are crucial in the assembly of PsaD into the PSI complex (Chitnis *et al.*, 1997). The mutations in the basic domain disturbed the interaction between PsaD and PsaL. Thus the basic domain may interact with PsaL in the assembly of the PSI complex.

4.2. PsaE

PsaE is a moderately conserved peripheral subunit of PSI . Together with PsaC and PsaD, PsaE is a component of a curved ridge on the stromal surface of PSI (Schubert *et al.*, 1997). In higher plants, *psaE* gene is located in the nucleus. Cyanobacterial PsaE contains 70-75 amino acid residues whereas the plant and algal PsaE has an N-terminal extension. Similar to the plant PsaD, the extension of spinach PsaE is accessible to exogenous proteases (Lagoutte and Vallon, 1992).

The 3-dimensional solution structure of PsaE of *Synechococcus* sp. PCC 7002 has been proposed from NMR analysis. PsaE is comprised of an antiparallel five-stranded β-sheet with (+1, +1, +1, -4x) topology. There is no helical region except for a single turn of 3_{10} helix between two β-stands (Falzone *et al.*, 1994a; Falzone *et al.*, 1994b). Topological studies using limited proteolysis and chemical modification have shown that the E63, E67, and K74 of *Synechocystis* sp. PCC 6803 PsaE are exposed on the surface of PSI (Xu *et al.*, 1994b).

PsaE facilitates the interaction between PSI and ferredoxin. Membranes of the PsaE-less mutant were severely deficient in the reduction of ferredoxin (Xu *et al.*, 1994c). The reduction of flavodoxin by PSI in the PsaE-less mutant was impaired partially indicating that PsaE is required for correct formation of the complex between flavodoxin and PSI (Xu *et al.*, 1994c). However, the PsaE subunit cannot be directly cross-linked to flavodoxin (Mühlenhoff *et al.*, 1996b). It is suggested that PsaD and PsaE together generate a suitable docking site for the electron acceptors of PSI. Site-directed mutagenesis of R9 into glutamine in PsaE of *Synechocystis* sp. PCC 6803 dramatically affected the reduction of ferredoxin, indicating that this residue is involved in the ferredoxin interaction (Lagoutte *et al.*, 1995).

PsaE may also be required for the cyclic electron transport around PSI (Chitnis *et al.*, 1995a; Yu *et al.*, 1993b). The turnover of PSI was increased in the *Synechocystis* PsaE-less mutant (Chitnis and Nelson, 1992). Therefore, PsaE is important for the stable assembly of PSI. Site-directed mutagenesis study indicated that the C-terminal eight amino acids are necessary for precise anchoring of PsaC into PSI (Lagoutte *et al.*, 1995). PsaE in the PSI complex can be cross-linked chemically to ferredoxin:NADP$^+$ reductase (Andersen *et al.*, 1992), indicating an additional role for PsaE in interaction with ferredoxin:NADP$^+$ reductase. Moreover, the inhibition of electron transport to NADP$^+$ by an antibody raised against PsaE has been shown to result from the interference of binding of PsaE and ferredoxin:NADP$^+$ reductase (Strotmann and Weber, 1993). Therefore, PsaE is involved in docking ferredoxin and the cyclic electron transfer around PSI.

4.3. PsaF

PsaF is a membrane-integral protein with substantial N-terminal domain exposed on the luminal side of PSI. The crosslinking product of PsaE and PsaF demonstrated the transmembrane nature of PsaF (Armbrust *et al.*, 1996). Analysis of the amino acid sequences of PsaF reveals two moderately hydrophobic regions in this protein. In higher plant, PsaF is coded by a nuclear gene. PsaF is synthesized as a precursor protein with a transit sequence that is typical of proteins targeted to thylakoid lumen, suggesting the N-terminal bulk of the protein is exposed on the luminal side and the C-terminal hydrophobic domain serves as a stop-transfer sequence.

Electron microscopy study using wild type and PsaF-PsaJ-less mutant PSI has shown that PsaF and PsaJ form a structural unit, positioned at the periphery of the PSI-trimer diametrically opposite to the connection domain formed by PsaL and PsaI (Kruip *et al.*, 1997). In the electron density map, this region contains three transmembrane and a surface α-helices (Krauß *et al.*, 1996; Schubert *et al.*, 1997). PsaF is proposed to contain two of the three transmembrane helices and the surface α-helices and the surrounding region of electron density represent the N-terminal region of PsaF. Two to three extended β-strands may be presented in PsaF running parallel to the surface helix. Several chlorophyll *a* molecules are located in the PsaF-PsaJ region indicating that PsaF may indeed bind chlorophyll *a* molecules. Also, PsaF has been isolated as a chlorophyll-binding protein (Anandan *et al.*, 1989).

Based on biochemical depletion and chemical cross-linking experiments, PsaF has been proposed to function as the plastocyanin or cytochrome c_6 docking site on the oxidizing side of PSI (Bengis and Nelson, 1977; Hippler *et al.*, 1989; Wynn *et al.*, 1989; Wynn and Malkin, 1988). Inactivation of the *psaF* gene from the green alga *C. reinhardtii* resulted a mutant that

still assembles functional PSI complex and is capable of photoautotrophic growth. However, electron transfer from plastocyanin to the oxidized reaction center $P700^+$ is dramatically reduced in the mutant, thereby providing the evidence that PsaF plays an important role in docking plastocyanin to the PSI complex in chloroplasts (Farah *et al.*, 1995; Hippler *et al.*, 1997). In contrast, the PsaF-less mutant strains of *Synechocystis* sp. PCC 6803 do not show any defect in their photoautotrophic growth, cytochrome c_6-dependent $NADP^+$ photoreduction activity of PSI or $P700^+$ rereduction kinetics (Chitnis *et al.*, 1991; Hippler *et al.*, 1996; Xu *et al.*, 1994c; Xu *et al.*, 1994e). Also, the removal of PsaF from PSI complex of *Synechocystis elongatus* had no effect on electron transfer from cytochrome c_6 to P700 (Hatanaka *et al.*, 1993). This controversial function of PsaF is addressed by the peculiarities of molecular recognition between plastocyanin and PSI (Hippler *et al.*, 1996). Two conserved negative patched in plant plastocyanin were cross-linked with lysine residues of a domain near the N-terminus of the PsaF subunit of plant PSI. This lysine-rich domain of the plant PsaF protein is not found in cyanobacteria and is predicted to fold into amphipathic α-helix with six lysine residues on one side, which may guide a fast one-dimensional diffusion of plastocyanin and provide the electrostatic attraction at a binding site to increase the electron transfer rate by two orders of magnitude in plants as compared with cyanobacteria. The functions of plant PsaF and cyanobacterial PsaF are different indicating that selection pressure led to evolution of plastocyanin and plant PsaF toward fast electron transfer. It is likely that effective concentrations of plastocyanin and cytochrome c_6 in lumen are higher in cyanobacteria than in chloroplast. Alternatively, clear segregation of PSI in grana vs. stroma lamellae require greater diffusion of plastocyanin in chloroplasts, thus needing electrostatic attraction for initial interactions.

5. Other proteins of photosystem I

The other subunits of PSI do not bind electron carriers. They are not involved in docking of soluble electron carriers, either. However, some of these proteins provide essential structural roles in the organization of PSI complex. Also, these subunits contribute to a roughly continuous ring of transmembrane helices around the core antenna system of PSI. Thus, they may provide a partially enclosed framework to the antenna system, thereby providing protection and stability.

5.1. PsaI and PsaL

Comparison of deduced primary sequences indicates that the PsaL proteins contains a greater diversity than seen in other subunits (Chitnis *et al.*, 1995b). However, the protein contains several conserved regions of homology, most notably in the hydrophobic regions.

Hydropathy analysis of PsaL suggests the presence of a hydrophilic N-terminal domain followed by two potential transmembrane domains (Chitnis *et al.*, 1993). A relatively large N-terminal domain of PsaL in stacked spinach thylakoids resists proteolysis and is predicted to be located on the stromal side (Zilber and Malkin, 1992).

Function of PsaL was revealed by the inactivation of the *psaL* gene. Trimeric PSI complexes cannot be obtained from the PsaL-deficient mutants of *Synechocystis* sp. PCC 6803. Furthermore, PsaL is accessible to digestion by thermolysin in the monomers, but not in the PSI trimers from the wild type membranes. Therefore, PsaL is necessary for trimerization of PSI and located in the trimer-forming domain in the structure of PSI (Chitnis and Chitnis, 1993; Chitnis *et al.*, 1993). The requirement of PsaL for the formation of PSI trimers has been confirmed in a PsaL-less mutant of another cyanobacterium *Synechococcus* sp. PCC 7002 (Schluchter *et al.*, 1996). PsaL in *Synechocystis* sp. PCC 6803 binds calcium, which in turns may regulate the formation of PSI trimers (V. P. Chitnis, P. R. Chitnis, unpublished results).

The deduced amino acid sequences of PsaI from plants and cyanobacteria share high degree of conservation (Xu *et al.*, 1995b). The PsaI subunits contain a central hydrophobic domain flanked by hydrophilic N- and C-termini (Scheller *et al.*, 1989)). The hydrophobic region potentially could make a kinked transmembrane helix. The *psaI* gene from *Anabaena variabilis* ATCC 29413 contains a presequence before the mature polypeptide (Sonoike *et al.*, 1992). This presequence of the *Anabaena variabilis* PsaI is predicted to assist the thylakoid translocation and consequently the N-terminus of PsaI may be located in the lumen. PsaI in intact thylakoids is not accessible to external proteases (Zilber and Malkin, 1992) and is resistant to removal by chaotropic agents (Scheller *et al.*, 1989; Xu *et al.*, 1994a). Thus PsaI is an integral membrane protein with one transmembrane helix. The C-terminal hydrophilic domain of PsaI of plants contains several positively charged residues (Scheller *et al.*, 1989), whereas it contains several negatively charged residues in cyanobacteria. Significance of this difference is not understood.

Targeted inactivation of the *psaI* gene in *Synechocystis* sp. PCC 6803 has revealed the role of PsaI in normal organization of the PsaL subunit of PSI (Xu *et al.*, 1995b). The absence of PsaI results in a complete loss of PsaL from the PSI core upon detergent extraction. PsaL in the wild-type and PsaI-less membranes showed equal resistance to removal by chaotropic extraction, but exhibited an increased susceptibility to proteolysis in the mutant strain (Xu *et al.*, 1995b). Therefore, a structural interaction between PsaL and PsaI may stabilize association of PsaL with the PSI core. The growth rate of PsaI-less mutant was identical to that of wild type under low or high-intensity of white light but slower than wild type in green light (Schluchter *et al.*, 1996). Both PsaI-less and PsaL-less mutants showed a decreased growth

rate at higher temperature of 40°C, which suggests a possible function for the trimeric organization of PSI in cyanobacteria.

In the crystal structure, there are three full-length transmembrane α-helices near the C_3 axis (Krauß et al., 1996; Schubert et al., 1997). The two helices involved in the trimer contacts are assigned to PsaL while the third helix which lies between the core and the PsaL is assigned to PsaI. The assignment elucidates clearly the trimer formation function of PsaL and the stabilization function of PsaI. A short surface α-helix is observed near the stromal which matched the prediction of an surface helix in the N-terminus of PsaL. Thus, the N- and C-termini of PsaL are located at the stromal side. Since PsaL can be crosslinked to PsaD, these termini are the regions of the crosslinking site. At least three chlorophyll a molecules are positioned within the trimerization domain. Therefore, PsaL and/or PsaI may harbor chlorophyll a molecules.

5.2. PsaJ

PsaJ is a 4.4-kDa hydrophobic protein, which has been identified in PSI preparations from cyanobacteria and higher plants. Analysis of the deduced amino acid sequence reveals a highly conserved sequence of 22 amino acids which may span the membrane. The hydrophilic N-terminal domain of PsaJ is only 4-5 amino acids long while the C-terminal domain has overall negative charge and more than 15 amino acids. Analysis of a PsaJ-less mutant in *Synechocystis* sp. PCC 6803 has revealed that PsaJ is not required for the electron transfer function of PSI, but may interact with both PsaE and PsaF and stabilize PsaF (Xu et al., 1994d). Therefore, the relatively large C-terminal domain of PsaJ may be located on the stromal side and interact with PsaE. In the crystal structure, PsaJ is proposed to be located in the same region of PsaF. One transmembrane helix, which is slightly removed from the other two, is assigned to PsaJ.

PsaI, PsaJ and PsaM are small hydrophobic proteins in PSI complex, which usually contain one putative transmembrane helix flanked by short hydrophilic, charged domains. These proteins may function as nuts and bolt in the organization of PSI complex. They may assist in the correct organization of other subunits by anchoring peripheral proteins and stabilizing transmembrane helices in lipid bilayer (Xu et al., 1995b). The PsaJ-PsaF interaction may involve stabilization of the transmembrane helix of PsaF (Xu et al., 1994d). PsaI stabilize the association of PsaL with the PSI core (Xu et al., 1995b). Whether PsaM has the similar role in organization of other subunits has not been identified.

5.3. PsaK

PsaK is an integral membrane protein that is tightly associated with the PsaA-PsaB complex. It can be removed from this complex by treatment with thiol reagents, without affecting PSI charge separation (Wynn and Malkin, 1990). Deduced primary sequences of PsaK from higher plants and cyanobacteria do not show high degree of homology (Chitnis *et al.*, 1995b); however, they do contain two hydrophobic domains predicted to be membrane-spanning α-helices. From positive inside rule (Gavel *et al.*, 1991), the N-terminus of PsaK may be in the lumen of thylakoids. A central part of PsaK is exposed to external proteases and may be on the stromal side of the membranes (Zilber and Malkin, 1992). Detergent treatment removes PsaK from the PSI monomer, but not from PSI trimer. In the electron density map of PSI, two transmembrane α-helices which are linked luminally, in the interaction region of the adjoining monomer, are assigned to PsaK. In higher plants, PsaK can be crosslinked to Lhca3.

The complete sequence of *Synechocystis* sp. PCC 6803 genome reveals that two unlinked *psa*K genes are present in the genome. The *psaK*1 gene codes for the PsaK protein that is identified in the PSI complex whereas the larger *psaK*2 gene codes for a distinct PsaK protein which has not been identified in the PSI complex. The PsaK-less mutant in *Synechococcus* sp. PCC 7002 and PsaK1-less and PsaK2-less mutant in *Synechocystis* sp. PCC 6803 have been isolated and studied; the mutant strains do not show any defect in the function, assembly or organization of PSI.

5.4. PsaM

PsaM is a very small protein of about 29 amino acids. PsaM is detected only in cyanobacterial PSI (Ikeuchi *et al.*, 1993). However, an open reading frame coding for a PsaM-like peptide is present in the liverwort chloroplast genome (Ohyama *et al.*, 1986). PsaM contains a hydrophobic domain flanked by hydrophilic termini. The N-terminus of PsaM may be exposed on the *p*-side of thylakoids. PsaM-less mutants in cyanobacteria have defect in photoautotrophic growth under high light intensity (P. R. Chitnis, unpublished results). PsaM is assigned to a transmembrane α-helix in the interaction region of PSI monomers in the crystal structure. This assignment position PsaM to face the transmembrane helices of PsaK from the adjacent PSI monomer. Thus, PsaM could function in stabilizing the trimer in co-operation with PsaK, a similar 'nuts and bolt' function as PsaI and PsaJ.

5.5. PsaH, PsaG, and PsaN

PsaH, PsaG, and PsaN are the three eukaryote-specific subunits of PSI. The coding genes for these three polypeptide *psaH*, *psaG*, and *psaN* are all present in the nucleus.

PsaG is an integral-membrane protein with about 100 amino acids, which has been only found in eukaryotic PSI complex. The analysis of the primary sequence revealed that the moderately conserved PsaG may contain two putative transmembrane domains placed towards termini and a highly hydrophilic large extramembrane loop (Chitnis *et al.*, 1995b). From the positive inside rule (Gavel *et al.*, 1991), the N-terminus of PsaG is predicted to be in the lumen (Okkels *et al.*, 1992). The comparison of the deduced primary sequences of PsaK and PsaG shows significant similarity, suggesting that an ancestral gene has been duplicated in a chloroplast progenitor to evolve into *psaG* and *psaK*, but remained single in cyanobacteria (Kjærulff *et al.*, 1993). Crosslinking using higher plants PSI indicated that PsaG may interact with the Lhca2.

PsaH is another PSI subunit that has only been detected in algae (Franzen *et al.*, 1989) and plants (Hayashida *et al.*, 1992; Okkels *et al.*, 1989; Steppuhn *et al.*, 1989). It is ~ 95 amino acids in length and has conserved primary structure (Chitnis *et al.*, 1995b). The mature PsaH protein contains an N-terminal acidic domain, a central hydrophobic domain and a C-terminal basic region. PsaH is an extrinsic subunit on the stromal side of PSI (Tjus and Andersson, 1991; Zilber and Malkin, 1992). Like PsaG, PsaH may play a role that is specific for PSI from plant and algae. In higher plants, PsaH may be located close to PsaI and PsaL subunits.

PsaN is a 9 kDa extrinsic polypeptide of plant PSI located on the *p*-side of thylakoids (He and Malkin, 1992). It does not bind any cofactors and is not required for NADP$^+$ photoreduction. The cDNA clones encoding the PsaN subunits have been isolated from barley and maize (Heck and Chitnis, 1998; Knoetzel and Simpson, 1993). The mature PsaN is 85 amino acids in length, with no putative transmembrane domain. Its transit peptide routes this protein to thylakoid lumen by a *sec*-independent pathway (Mant *et al.*, 1995). In contrast, PsaF is routed by a *sec*-dependent pathway. It is likely that PsaN was added to PSI after the divergence of chloroplasts and cyanobacteria. Function of PsaN is not yet identified.

6. Epilogue

During the last ten years, information on PSI has increased exponentially due to advances in spectroscopy, crystallography and molecular genetics. Elegant combination of these techniques has unraveled details of structure and function of the PSI complex. Now we know how this complex is organized and what are the functions of its protein and cofactor components. Soon an atomic resolution structure of PSI will be available and will allow us to probe structure-function relations at finer resolution. These advances will enable use of sophisticated techniques of molecular genetics, such as directed evolution of the redox-center binding pockets, to engineer novel properties. Such studies are likely to lead us to design of

new herbicides and resistance genes. With a solid base in structural and functional knowledge, attention will also shift to understanding of dynamics of PSI in thylakoid membranes. How is the level of PSI regulated in the membranes? How are different PSI genes controlled to avoid wastage due to unassembled proteins? How does feed-back inhibition modulate PSI activity? Questions related to regulatory mechanisms can now be addressed through application of systems biology approaches in which global changes in the gene expression is studied at genomic level. Advances in functional genomics and proteomics are destined to be instrumental in understanding the essential and amazing processes in photosynthesis.

Acknowledgements

References

Adman, E.T., Sieker, L.C. and Jensen, L.H. (1976) The structure of *Peptococcus aerogenes* ferredoxin. Refinement at 2 Å resolution. *J. Biol. Chem.*, **251**, 3801-3806.

Anandan, S., Vainstein, A. and Thornber, P. (1989) Correlation of some published amino acid sequences for photosystem I polypeptides to a 17 kDa LHCI pigment-protein and to subunits III and IV of the core complex. *FEBS Lett.*, **256**, 150-154.

Andersen, B., Scheller, H. and Moller, B. (1992) The PSI-E subunit of photosystem I binds ferredoxin:NADP$^+$ oxidoreductase. *FEBS Lett.*, **311**, 169-173.

Armbrust, T.S., Chitnis, P.R. and Guikema, J.A. (1996) Organization of photosystem I polypeptides examined by chemical cross-linking. *Plant Physiol.*, **111**, 1307-1312.

Beissinger, M., Sticht, H., Sutter, M., Ejchart, A., Haehnel, W. and Rosch, P. (1998) Solution structure of cytochrome c_6 from the thermophilic cyanobacterium *Synechococcus elongatus*. *EMBO J.*, **17**, 27-36.

Bendall, D.S. and Manasse, R.S. (1995) Cyclic phosphorylation and electron transport. *Biochim. Biophys. Acta*, **1229**, 23-38.

Bengis, C. and Nelson, N. (1977) Subunit structure of chloroplast photosystem I reaction center. *J. Biol. Chem.*, **252**, 4564-4569.

Bentrop, D., Bertini, I., Luchinat, C., Nitschke, W. and Muhlenhoff, U. (1997) Characterization of the unbound 2[Fe4S4]-ferredoxin-like photosystem I subunit PsaC from the cyanobaterium *Synechococcus elongatus*. *Biochemistry*, **36**, 13629-13637.

Biggins, J. and Mathis, P. (1988) Functional role of vitamin K in photosystem I of the cyanobacterium *Synechocystis* 6803. *Biochemistry*, **27**, 1494-500.

Biggins, J., Tanguay, N.A. and Frank, H.A. (1989) Electron transfer reactions in photosystem I following vitamin K1 depletion by ultraviolet irradiation. *FEBS Lett.*, **250**, 271-4.

Bittl, R. and Zech, S.G. (1997) Pulsed EPR study of spin coupled radical pairs in photosynthetic reaction centers: measurement of the distance between $P_{700}^{+\cdot}$ and $A_1^{-\cdot}$ in Photosystem I and between $P_{865}^{+\cdot}$ and $Q_A^{-\cdot}$ in bacterial reaction center. *J. Phys. Chem.*, **B101**, 1429-1436.

Bittl, R., Zech, S.G., Fromme, P., Witt, H.T. and Lubitz, W. (1997) Pulsed EPR structure analysis of photosystem I single crystals: localization of the phylloquinone acceptor. *Biochemistry*, **36**, 12001-12004.

Boekema, E.J., Boonstra, A.F., Dekker, J.P. and Rögner, M. (1994) Electron microscopic structural analysis of photosystem I, photosystem II, and the cytochrome b_6/f complex from green plants and cyanobacteria. *J. Bioenerg. Biomemb.*, **26**, 17-29.

Bottin, H. and Mathis, P. (1985) Interaction of plastocyanin with the photosystem I reaction center: a kinetic study by flash spectroscopy. *Biochemistry*, **24**, 6453-6460.

Bottin, H. and Setif, P. (1991) Inhibition of electron transfer from A_0 to A_1 in photosystem I after treatment in darkness at low redox potential. *Biochim. Biophys. Acta*, **1057**, 331-36.

Boussiba, S. and Vermaas, W.F.J. (1992) Creation of a mutant with an enriched photosystem II/pigment ratio in the cyanobacterium *Synechocystis* sp. PCC 6803. In Murata, N. (ed.) *Research in Photosynthesis*, Dordrecht: Kluwer, Vol. III, pp. 429-432.

Brettel, K. (1988) Electron transfer from A_1^- to an iron-sulfur center with $t_{1/2} = 200$ ns at room temperature in photosystem I. Characterization by absorption spectroscopy. *FEBS Lett.*, **239**, 93-98.

Brettel, K. (1997) Electron transfer and arrangement of the redox cofactors in photosystem I. *Biochim. Biophys. Acta*, **1318**, 322-373.

Brettel, K. and Setif, P. (1987) Magentic-field effects on primary reaction in photosystem I. *Biochim. Biophys. Acta*, **893**, 109-14.

Buttner, M., Xie, D.L., Nelson, H., Pinther, W., Hauska, G. and Nelson, N. (1992) Photosynthetic reaction center genes in green sulfur bacteria and in photosystem 1 are related. *Proc. Natl. Acad. Sci. U S A*, **89**, 8135-9.

Chamorovsky, S.K. and Cammack, R. (1982) Direct determination of the mid-point potential of the acceptor X in chloroplast photosystem I by electrochemical reduction and ESR spectroscopy. *Photobiochem. Photobiophys.*, **4**, 195-200.

Chitnis, P.R. (1996) Photosystem I. *Plant Physiol.*, **111**, 661-669.

Chitnis, P.R. (1997) Targeting, assembly and degradation of chloroplast proteins. In Raghavendra, A.S. (ed.) *Photosynthesis: A comprehensive treatise,*. Cambridge University Press, Cambridge.

Chitnis, P.R., Chitnis, V.P., Xu, Q., Jung, Y.-S., Yu, L. and Golbeck, J.H. (1995a) Mutational analysis of photosystem I polypeptides. In Mathis, P. (ed.) *Photosynthesis: from Light to Biosphere*. Kluwer, Dodrecht, Vol. II, pp. 17-22.

Chitnis, P.R. and Nelson, N. (1992) Biogenesis of photosystem I : The subunit PsaE is important for the stability of PSI complex. In Argyroudi-Akoyunoglou, J. (ed.) *Chloroplast Biogenesis*. Plenum Press, New York, pp. 285-290.

Chitnis, P.R., Purvis, D. and Nelson, N. (1991) Molecular cloning and targeted mutagenesis of the gene *psaF* encoding subunit III of photosystem I from the cyanobacterium *Synechocystis* sp. PCC 6803. *J. Biol. Chem.*, **266**, 20146-20151.

Chitnis, P.R., Reilly, P.A. and Nelson, N. (1989) Insertional inactivation of the gene encoding subunit II of photosystem I from the cyanobacterium *Synechocystis* sp. PCC 6803. *J. Biol. Chem.*, **264**, 18381-18385.

Chitnis, P.R., Xu, Q., Chitnis, V.P. and Nechushtai, R. (1995b) Function and organization of photosystem I polypeptides. *Photosynth. Res.*, **44**, 23-40.

Chitnis, V.P., An, K. and Chitnis, P.R. (1997) The PsaD subunit of photosystem I: Mutations in the basic domain impair the assembly of PsaD into the complex. *Plant Physiol.*, **115**, 1699-1705.

Chitnis, V.P. and Chitnis, P.R. (1993) PsaL subunit is required for the formation of photosystem I trimers in the cyanobacterium *Synechocystis* sp. PCC 6803. *FEBS Lett.*, **336**, 330-334.

Chitnis, V.P., Jung, Y.-S., Albee, L., Golbeck, J.H. and Chitnis, P.R. (1996) Mutational analysis of photosystem I polypeptides: Role of PsaD and the lysyl 106 residue in the reductase activity of photosystem I. *J. Biol. Chem.*, **271**, 11772-11780.

Chitnis, V.P., Xu, Q., Yu, L., Golbeck, J.H., Nakamoto, H., Xie, D.L. and Chitnis, P.R. (1993) Targeted inactivation of the gene psaL encoding a subunit of photosystem I of the cyanobacterium *Synechocystis* sp. PCC 6803. *J. Biol. Chem.*, **268**, 11678-11684.

Cleland, R.E. and Bendall, D.S. (1992) Photosystem I cyclic electron transport: measurement of ferredoxin: plastoquinone reductase activity. *Photosynth. Res.*, **34**, 409-418.

Cournac, L., Redding, K., Bennoun, P. and Peltier, G. (1997) Limited photosynthetic electron flow but no CO_2 fixation in *Chlamydomonas* mutants lacking photosystem I. *FEBS Letters*, **416**, 65-68.

Cui, L., Bingham, S.E., Kuhn, M., Kass, H., Lubitz, W. and Webber, A.N. (1995) Site-directed mutagenesis of conserved histidines in the helix VIII domain of PsaB impairs assembly of the photosystem I reaction center without altering spectroscopic characteristics of P700. *Biochemistry*, **34**, 1549-1558.

Deisenhofer, J. and Michel, H. (1991) Structure of bacterial photosynthetic reaction centers. *Annual Review of Cell Biology*, **7**, 1-23.

Diaz, A., Hervas, M., Navarro, J.A., De La Rosa, M.A. and Tollin, G. (1994) A thermodynamic study by laser-flash photolysis of plastocyanin and cytochrome c_6 oxidation by photosystem I from the green alga *Monoraphidium braunii*. *Eur. J. Biochem.*, **222**, 1001-7.

Drepper, F., Hippler, M., Nitschke, W. and Haehnel, W. (1996) Binding dynamics and electron transfer between plastocyanin and photosystem I. *Biochemistry*, **35**, 1282-1295.

Dzuba, S.A., Hara, H., Karamori, A., Iwaki, M., Itoh, S. and Tsvetkoc, Y.D. (1997) Electron spin echo of spin-polarised radical pairs in the intact and quinone-reconstituted plant photosystem I reaction center. *Chem. Phys. Letters*, **264**, 238-244.

Falzone, C.J., Kao, Y.H., Zhao, J., Bryant, D.A. and Lecomte, J.T. (1994a) Three-dimensional solution structure of PsaE from the cyanobacterium *Synechococcus* sp. strain PCC 7002, a photosystem I protein that shows structural homology with SH3 domains. *Biochemistry*, **33**, 6052-62.

Falzone, C.J., Kao, Y.H., Zhao, J., MacLaughlin, K.L., Bryant, D.A. and Lecomte, J.T. (1994b) ^{1}H and ^{15}N NMR assignments of PsaE, a photosystem I subunit from the cyanobacterium *Synechococcus* sp. strain PCC 7002. *Biochemistry*, **33**, 6043-51.

Farah, J., Rappaport, F., Choquet, Y., Joliot, P. and Rochaix, J.D. (1995) Isolation of a psaF-deficient mutant of *Chlamydomonas reinhardtii*: efficient interaction of plastocyanin with the photosystem I reaction center is mediated by the PsaF subunit. *EMBO J.*, **14**, 4976-4984.

Fischer, N., Hippler, M., Setif, P., Jacquot, J.P. and Rochaix, J.D. (1998) The PsaC subunit of photosystem I provides an essential lysine residue for fast electron transfer to ferredoxin. *EMBO J.*, **17**, 849-858.

Fischer, N., Setif, P. and Rochaix, J.D. (1997) Targeted mutations in the psaC gene of *Chlamydomonas reinhardtii*: preferential reduction of F_B at low temperature is not accompanied by altered electron flow from photosystem I to ferredoxin. *Biochemistry*, **36**, 93-102.

Fish, L.E., Kuck, U. and Bogorad, L. (1985) Two partially homologous adjacent light-inducible maize chloroplast genes encoding polypeptides of the P700 chlorophyll *a*-protein complex of photosystem I. *J. Biol. Chem.*, **260**, 1413-21.

Franzen, L.-G., Frank, G., Zuber, H. and Rochaix, J.-D. (1989) Isolation and characterization of cDNA clones encoding photosystem I subunits with molecular masses 11.0, 10.0 and 8.4 kDa from *Chlamydomonas reinhardtii. Mol. Gen. Genet.*, **219**, 137–144.

Frazao, C., Soares, C.M., Carrondo, M.A., E, P., Z, D., Wilson, K.S., Hervas, M., Navarroo, J.A., De la Rosa, M.A. and Sheldrick, G.M. (1995) Ab initio determination of the crystal strucutre of cytochrome c_6 and compariosn with plastocyanin. *Current Biol.*, **3**, 1159-1169.

Fromme, P. (1996) Structure and function of photosystem I. *Curr. Opin. Struct. Biol.*, **6**, 473-484.

Fromme, P., Schubert, W.-D. and Krauss, N. (1994) Structure of photosystem I: Suggestions on the docking sites for plastocyanin, ferredoxin and the coordination of P700. *Biochim. Biophys. Acta*, **1187**, 99-105.

Furrer, R. and Thurnauer, M.C. (1983) Resolution of signals attributed to photosystem I primary reactants by time resolved EPR at K band. *FEBS Lett.*, **153**, 399-403.

Gavel, Y., Steppuhn, J., Herrmann, R. and von Heijne, G. (1991) The 'positive-inside rule' applies to thylakoid membrane proteins. *FEBS Lett.*, **282**, 41-46.

Golbeck, J.H. (1992) Structure and function of photosystem I. *Ann. Rev. Plant Physiol. Plant Mol. Biol.*, **43**, 293-324.

Golbeck, J.H. (1994) Photosystem I in Cyanobacteria. In Bryant, D.A. (ed.) *The Molecular Biology of Cyanobacteria*. Kluwer Academic Publishers, Dordrecht, The Netherlands, pp. 179-220.

Golbeck, J.H. and Bryant, D.A. (1991) Photosystem I. *Current Topics in Bioenergetics*, **16**, 83-177.

Green, B.R. and Durnford, D.G. (1996) The chlorophyll-carotenoid proteins of oxygenic photosysthesis. *Annu. Rev. Plant Physiol. Plant Mol. Biol.*, **47**, 685-714.

Gross, E.L. (1996) Plastocyanin: structure, location, diffusion, and electron transfer mechanisms. In Ort, D. and Yocum, C.F. (eds.), *Oxygenic Photosynthesis: The Light Reactions*. Kluwer Academic Publishers, Dodrecht, pp. 413-429.

Haehnel, W., Jansen, T., Gause, K., Klosgen, R.B., Stahl, B., Michl, D., Huvermann, B., Karas, M. and Herrmann, R.G. (1994) Electron transfer from plastocyanin to photosystem I. *EMBO J.*, **13**, 1028-1038.

Haehnel, W., Propper, A. and Krause, H. (1980) Evidence for complexed plastocyanin as the immediate electron donor of P-700. *Biochim. Biophys. Acta*, **593**, 384-399.

Hanley, J., Deligiannakis, Y., MacMillan, F., Bottin, H. and Rutherford, A.W. (1997) ESEEM study of the phyllosemiquinone redical A_1·· in ^{14}N-and ^{15}N-labeled photosystem I. *Biochemistry*, **36**, 11543-11549.

Hanley, J., Setif, P., Bottin, H. and Lagoutte, B. (1996) Mutagenesis of photosystem I in the region of the ferredoxin cross- linking site: modifications of positively charged amino acids. *Biochemistry*, **35**, 8563-8571.

Hastings, G., Hoshina, S., Webber, A.N. and Blankenship, R.E. (1995) Universality of energy and electron transfer processes in photosystem I. *Biochemistry*, **34**, 15512-15522.

Hastings, G., Kleinherenbrink, F.A., Lin, S. and Blankenship, R.E. (1994a) Time-resolved fluorescence and absorption spectroscopy of photosystem I. *Biochemistry*, **33**, 3185-92.

Hastings, G., Kleinherenbrink, F.A., Lin, S., McHugh, T.J. and Blankenship, R.E. (1994b) Observation of the reduction and reoxidation of the primary electron acceptor in photosystem I. *Biochemistry*, **33**, 3193-200.

Hatanaka, H., Sonoike, K., Hirano, M. and Katoh, S. (1993) Small subunits of photosystem I reaction center complexes from *Synechococcus elongatus*. II. Is the *psaF* gene productrequired for oxidation of cytochrome c_{553}? *Biochim. Biophys. Acta*, **1141**, 45-51.

Hayashida, N., Izuchi, S., Sugiura, M. and Obokata, J. (1992) Nucleotide sequence of cDNA clones encoding the PSI-H subunit of photosystem I in tobacco. *Plant Cell Physiol.*, **33**, 1031-1034.

He, S., Modi, S., Bendall, D.S. and Gray, J.C. (1991) The surface-exposed residue tyrosine Tyr-83 of pea plastocyanin is involved in both binding and electron transfer reactions with cytochrome *f*. *EMBO J.*, **10**, 4011-4016.

He, W.Z. and Malkin, R. (1992) Specific release of a 9-kDa extrinsic polypeptide of photosystem I from spinach chloroplasts by salt washing. *FEBS Lett.*, **308**, 298-300.

He, W.Z. and Malkin, R. (1994) Reconstitution of iron-sulphur center B of photosystem I damaged by mercuric chloride. *Photosynth. Res.*, **41**, 381-388.

Heathcote, P., Moenne-Loccoz, P., Rigby, S.E.J. and Evans, M.C.W. (1996) Photoaccumulation in photosystem I does produce a phylloquinone (A_1^-) radical. *Biochemistry*, **35**, 6644-6650.

Heck, D.A. and Chitnis, P.R. (1998) Nucleotide sequence of cDNAs encoding the PsaH and PsaN subunits of the Maize photosystem I complex (Accession Nos. AF052076 and AF052429) (PGR98-107). *Plant Physiol.*, **In press**.

Hecks, B., Wulf, K., Breton, J., Leibl, W. and Trissl, H.W. (1994) Primary charge separation in photosystem I: a two-step electrogenic charge separation connected with $P700^+A_0^-$ and $P700^+A_1^-$ formation. *Biochemistry*, **33**, 8619-24.

Hervas, M., De la Rosa, M.A. and Tollin, G. (1992a) A comparative laser-flash absorption spectroscopy study of algal plastocyanin and cytochrome c_{552} photooxidation by photosystem I particles from spinach. *Eur. J. Biochem.*, **203**, 115-20.

Hervas, M., Navarro, J. and Tollin, G. (1992b) A laser-flash spectroscopy study of the kinetics of electron transfer from spinach photosystem I to spinach and algal ferredoxins. *Photochem. Photobiol.*, **56**, 319-324.

Hervas, M., Navarro, J.A., Diaz, A., Bottin, H. and De la Rosa, M.A. (1995) Laser-flash kinetic analysis of the fast electron transfer from plastocyanin and cytochrome c_6 to photosystem I. Experimental evidence on the evolution of the reaction mechanism. *Biochemistry*, **34**, 11321-11326.

Hervas, M., Navarro, J.A., Diaz, A. and De la Rosa, M.A. (1996) A comparative thermodynamic analysis by laser-flash absorption spectroscopy of photosystem I reduction by plastocyanin and cytochrome c_6 in *Anabaena* PCC 7119, *Synechocystis* PCC 6803, and spinach. *Biochemistry*, **35**, 2693-2698.

Hervas, M., Ortega, J.M., Navarro, J.A., de la Rosa, M.A. and Bottin, H. (1994) Laser flash kinetic analysis of *Synechocystis* sp. PCC 6803 cytochrome c_6 and plastocyanin oxidation by photosystem I. *Biochim. Biophys. Acta*, **1184**, 235-241.

Hippler, M., Drepper, F., Farah, J. and Rochaix, J.D. (1997) Fast electron transfer from cytochrome c_6 and plastocyanin to photosystem I of *Chlamydomonas reinhardtii* requires PsaF. *Biochemistry*, **36**, 6343-6349.

Hippler, M., Ratajczak, R. and Haehnel, W. (1989) Identification of the plastocyanin binding subunit of photosystem I. *FEBS Lett.*, **250**, 280-284.

Hippler, M., Reichert, J., Sutter, M., Zak, E., Altschmied, L., Schröer, U., Herrmann, R.G. and Haehnel, W. (1996) The plastocyanin binding domain of photosystem I. *EMBO J.*, **15**, 6374-6384.

Hiyama, T. and Ke, B. (1971) A new photosynthetic pigment, "P430": its possible role as the priary electron acceptor of photosystem I. *Proc. Natl. Acad. Sci. USA*, **68**, 1010-1013.

Holzwarth, A.R., Schatz, G., Brock, H. and Bittersmann, E. (1993) Energy transfer and charge separation kinetics in photosystem I. Part 1: Picosecond transient absorption and fluorescence study of cyanobacterial photosystem I particles. *Biophys. J.*, **64**, 1813-1826.

Ikeuchi, M., Sonoike, K., Koike, H., Pakrasi, H. and Inoue, Y. (1993) A novel 3.5 kDa protein component of cyanobacterial photosystem I complexes. *Plant Cell Physiol.*, **33**, 1057-1063.

Itoh, S., Iwqaki, M. and Ikegami, I. (1987) Extraction of vitamin K-1 from photosystem I particles by treatment with diethyl ether and its effect on the A_1^- EPR signal and system I photochemistry. *Biochim. Biophys. Acta*, **893**, 508-516.

Iwaki, M. and Itoh, S. (1994) Reaction of reconstituted acceptor quinone and dynamic equilibration of electron transfer in the photosystem I reaction center. *Plant Cell Physiol.*, **35**, 983-993.

Jung, Y.S., Vassiliev, I.R., Yu, J., McIntosh, L. and Golbeck, J.H. (1998) Strains of Synechocystis sp. PCC 6803 with altered PsaC. II. EPR and optical spectroscopic properties of F_A and F_B in aspartate, serine, and alanine replacements of cysteines 14 and 51 . *J. Biol. Chem.*, **272**, 8040-8049.

Jung, Y.-S., Yu, L. and Golbeck, J.H. (1995) Reconstitution of iron-sulfur center F_B results in complete restoration of $NADP^+$ photoreduction in Hg-treated photosystem I complexes from Synechococcus sp. PCC 6301. *Photosynth. Res.*, **46**, 249-255.

Karapetyan, N.V., Dorra, d., Schweitzer, G., Bezsmertnaya, I.N. and R., H.A. (1997) Fluorescence spectroscopy of the longwave chlorophylls in trimeric and monomeric photosystem I core complexes from the cyanobacterium Spiruline platensis. *Biochemistry*, **36**, 13830-13837.

Ke, B., Hansen, R.E. and Beinert, H. (1973) Oxidation-reduction potentials of bound iron-sulfur proteins of photosystem I. *Proc. Natl. Acad. Sci. USA*, **70**, 2941-2945.

Kerfeld, C.A., Anwar, H.P., Interrante, R., Merchant, S. and Yeates, T.O. (1995) The structure of chloroplast cytochrome c_6 at 1.9 A resolution: evidence for functional oligomerization. *J. Mol. Biol.*, **250**, 627-647.

Kjærulff, S., Andersen, B., Nielsen, V.S., Møller, B.L. and Okkels, J.S. (1993) The PSI-K Subunit of Photosystem I from Barley (Hordeum vulgare L.): Evidence for a gene duplication of an ancestral PSI-G/K gene. *J. Biol. Chem.*, **268**, 18912-18916.

Kleinherenbrink, F.A., Hastings, G., Wittmerhaus, B.P. and Blankenship, R.E. (1994) Delayed fluorescence from Fe-S type photosynthetic reaction centers at low redox potential. *Biochemistry*, **33**, 3096-105.

Knoetzel, J. and Simpson, D.J. (1993) The primary structure of a cDNA for PsaN, encoding an extrinsic lumenal polypeptide of barley photosystem I. *Plant Mol. Biol.*, **22**, 337-345.

Kok, B. (1957) Absorption changes induced by the photochemical reaction of photosynthesis. *Nature*, **179**, 583-584.

Krauß, N., Hinrichs, W., Witt, I., Fromme, P., Pritzkow, W., Dauter, Z., Betzel, C., Wilson, K.S., Witt, H.T. and Saenger, W. (1993) Three-dimensional structure of system I of photosynthesis at 6 Å resolution. *Nature*, **361**, 326-331.

Krauß, N., Schubert, W.-D., Klukas, O., Fromme, P., Witt, H.T. and Saenger, W. (1996) Photosystem I at 4 Å resolution represents the first structural model of a joint photosynthetic reaction centre and core antenna system. *Nature Struct. Biol.*, **3**, 965-973.

Kruip, J., Chitnis, P.R., Lagoutte, B., Rogner, M. and Boekema, E.J. (1997) Structural Organization of subunits in cyanobacterial photosystem I: Localization of subunits PsaC, -D, -E, -F and -J. *J. Biol. Chem.*, **272**, 17061-17069.

Kumazaki, S., Iwaki, M., Ikegami, I., Kandori, H., Yoshihara, K. and Itoh, S. (1994) Rates of primary electron transfer reactions in the photosystem I reaction center reconstituted with different quinones as the secondary acceptor. *J. Phys. Chem.*, **98**, 11220-11225.

Lagoutte, B., Barth, P. and Setif, P. (1995) Photosystem I/ferredoxin interactio: Site directed mutagenesis of PSI-E. In Mathis, P. (ed.) *Photosynthesis: from Light to Biosphere*. Kluwer, Dodrecht, Vol. II, pp. 71-74.

Lagoutte, B. and Vallon, O. (1992) Purification and membrane topology of PSI-D and PSI-E, two subunits of the photosystem I reaction center. *Eur. J. Biochem.*, **205**, 1175-1185.

Lee, B.H., Hibino, T., Takabe, T., Weisbeek, P.J. and Takabe, T. (1995) Site-directed mutagenetic study on the role of negative patches on Silene plastocyanin in the interactions with cytochrome *f* and photosystem I. *J. Biochem.*, **117**, 1209-1217.

Lee, J.W., Tevault, C.V., Owens, T.G. and Greenbaum, E. (1996) Oxygenic Photoautotrophic Growth Without Photosytem I. *Science*, **273**, 364-367.

Lelong, C., Setif, P., Lagoutte, B. and Bottin, H. (1994) Identification of the amino acids involved in the functional interaction between photosystem I and ferredoxin from *Synechocystis* sp. PCC 6803 by chemical cross-linking. *J. Biol. Chem.*, **269**, 10034-10039.

Li, N., Zhao, J.D., Warren, P.V., Warden, J.T., Bryant, D.A. and Golbeck, J.H. (1991) PsaD is required for the stable binding of PsaC to the photosystem I core protein of *Synechococcus* sp. PCC 6301. *Biochemistry*, **30**, 7863-7872.

Liebl, U., Mockensturm-Wilson, M., Trost, J.T., Brune, D., Blankenship, R. and Vermaas, W.F.J. (1993) Single core polypeptide in the reaction ceter of the photosynthetic bacterium *Heliobacillus mobilis* - structural implications and relations to other photosystems. *Proc. Natl. Acad. Sci. USA*, **90**, 7124-7128.

Luneberg, J., Fromme, P., Jekow, P. and Schlodder, E. (1994) Spectroscopic characterization of PSI core complexes from thermophilic *Synechococcus* sp. Identical reoxidation kinetics of A$_1^-$ before and after removal of the iron-sulfur-clusters F$_A$ and F$_B$. *FEBS Lett.*, **338**, 197-202.

Mac, M., Tang, X.-S., Diner, B.A., McCracken, J. and Babcocl, G.T. (1996) Identification of histidine as an axial ligand to P700. *Biochemistry*, **35**, 13288-13293.

Malkin, R. (1984) Diazonium modification of photosystem I. A specific effect on iron-sulfur center B. *Biochim. Biophys. Acta*, **4**, 63-69.

Malkin, R. (1986) On the function of two vitamin K molecules in the PSI electron acceptor complex. *FEBS Lett.*, **208**, 343-346.

Malkin, R. and Bearden, A.J. (1971) Primary reactions of photosynthesis: photoreduction of a bound chloroplast ferredoxin at low temperature as detected by EPR spectroscopy. *Proc. Natl. Acad. Sci. U S A*, **68**, 16-9.

Manna, P. and Chitnis, P.R. (1998) Function and molecular genetics of photosystem I. In Singhal, G.S., Renger, G. and Sapory, S.K. (eds.), *Concepts in Photobiology: Photosynthesis and Photomorphogenesis*, Vol. In press.

Mannan, R.M., He, W.Z., Metzger, S.U., Whitmarsh, J., Malkin, R. and Pakrasi, H.B. (1996) Active photosynthesis in cyanobacterial mutants with directed modifications in the ligands for two iron-sulfur clusters on the PsaC protein of photosystem I. *EMBO J.*, **15**, 1826-1833.

Mannan, R.M., Pakrasi, H.B. and Sonoike, K. (1994) The PsaC protein is necessary for the stable association of the PsaD, PsaE, and PsaL proteins in the photosystem I complex: analysis of a cyanobacterial mutant strain. *Arch. Biochem. Biophys.*, **315**, 68-73.

Mansfield, R.W., Hubbard, J.A.M., Nugent, J.H.A. and Evans, M.C.W. (1987) Extraction of electron acceptor A$_1$ from pea photosystem I. *FEBS Lett.*, **220**, 74-78.

Mant, A., Schmidt, I., Herrmann, R.G., Robinson, C. and Klosgen, R.B. (1995) Sec-dependent thylakoid protein translocation. Delta pH requirement is dictated by passenger protein and ATP concentration. *J. Biol. Chem.*, **270**, 23275-23281.

Mathis, P. and Setif, P. (1988) Kinetic studies on the function of A$_1$ in the photosystem I reaction center. *FEBS Lett.*, **237**, 65-68.

Medina, M., Diaz, A., Hervas, M., Navarro, J.A., Gomez-Moreno, C., de la Rosa, M.A. and Tollin, G. (1993) A comparative laser-flash absorption spectroscopy study of *Anabaena* PCC 7119 plastocyanin and cytochrome c_6 photooxidation by photosystem I particles. *Eur. J. Biochem.*, **213**, 1133-8.

Mehari, T., Qiao, F., Scott, M.P., Nellis, D.F., Zhao, J., Bryant, D.A. and Golbeck, J.H. (1995) Modified ligands to FA and FB in photosystem I. I. Structural constraints for the formation of iron-sulfur clusters in free and rebound PsaC. *J. Biol. Chem.*, **270**, 28108-28117.

Melkozernov, A.N., Su, H., Lin, S., Bingham, S., Webber, A.N. and Blankenship, R.E. (1997) Specific mutation near the primary donor in photosystem I from Chlamydomonas reinhardtii alters the trapping time and spectroscopic properties of P700. *Biochemistry*, **36**, 2898-2907.

Modi, S., He, S., Gray, J.C. and Bendall, D.S. (1992) The role of surface-exposed Tyr-83 of plastocyanin in electron transfer from cytochrome c. *Biochim. Biophys. Acta*, **1101**, 64-68.

Morand, L.Z., Cheng, L., Krogmann, D.W. and Ho, K.K. (1994) Soluble electron transfer catalysts of cyanobacteia. In Bryant, D.A. (ed.) *The Molecular Biology of Cyanobacteria.* Kluwer, Amsterdam, pp. 381-407.

Mühlenhoff, U., Kruip, J., Bryant, D.A., Rögner, M., Setif, P. and Boekema, E. (1996a) Characterization of a redox-active cross-linked complex between cyanobacterial photosystem I and its physiological acceptor flavodoxin. *EMBO J.*, **15**, 488-497.

Mühlenhoff, U., Zhao, J. and Bryant, D.A. (1996b) Interaction between photosystem I and flavodoxin from the cyanobacterium *Synechococcus* sp. PCC 7002 as revealed by chemical cross- linking. *Eur. J. Biochem.*, **235**, 324-331.

Navarro, J.A., Hervas, M. and De la Rosa, M.A. (1997) Co-evolution of cytochrome c_6 and plastocyanin, mobile proteins transferring electrons from cytochrome b_6f to photosystem I. *J. Biol. Inorg. Chem*, **2**, 11-22.

Navarro, J.A., Hervas, M., Genzor, C.G., Cheddar, G., Fillat, M.F., de la Rosa, M.A., Gomez-Moreno, C., Cheng, H., Xia, B., Chae, Y.K. and et, a. (1995) Site-specific mutagenesis demonstrates that the structural requirements for efficient electron transfer in *Anabaena* ferredoxin and flavodoxin are highly dependent on the reaction partner: kinetic studies with photosystem I, ferredoxin:NADP$^+$ reductase, and cytochrome c. *Arch. Biochem. Biophys.*, **321**, 229-238.

Naver, H., Scott, M.P., Golbeck, J.H., Moller, B.L. and Scheller, H.V. (1996) Reconstitution of barley photosystem I with modified PSI-C allows identification of domains interacting with PSI-D and PSI-A/B. *J. Biol. Chem.*, **271**, 8996-9001.

Nordling, M., Sigfridsson, K., Young, S., Lundberg, L.G. and Hansson, O. (1991) Flash-photolysis studies of the electron transfer from genetically modified spinach plastocyanin to photosystem I. *FEBS Lett.*, **291**, 327-330.

Nuijs, A.M., Shuvalov, V.A., van Gorkom, H.J., Plijter, J.J. and Duysens, L.N.M. (1986) Picosecond absorbance difference spectroscopy on the primary reaction and the antenna-excited states in photosystem I particles. *Biochim. Biophys. Acta*, **850**, 310-318.

Ohyama, K., Fukuzawa, H., Kohchi, T., Shirai, H., Tohru, S., Sano, S., Umesono, K., Shiki, Y., Takeuchi, M., Chang, Z., Aota, S.I., Inokuchi, H. and Ozeki, H. (1986) Chloroplast gene organization deduced from complete sequence of liverwort *Marchantia polymorpha* chloroplast DNA. *Nature*, **322**, 572-574.

Okkels, J.S., Nielsen, S., Scheller, H.V. and Møller, B.L. (1992) A cDNA clone from barley encoding the precursor from the photosystem I polypeptide PSI-G: Sequence similarity to PSI-K. *Plant Mol. Biol.*, **18**, 989-994.

Okkels, J.S., Scheller, H.V., Jepsen, L.B. and Moller, B.L. (1989) A cDNA clone encoding the precursor for a 10.2 kDa photosystem I polypeptide of barley. *FEBS Lett.*, **250**, 575-579.

Ort, D.R. and Yocum, C.F. (eds.) (1996) *Oxygenic photosynthesis: the light reactions.* Kluwer Academic Publishers, Dordrecht, Netherlands.

Parrett, K.G., Mehari, T., Warren, P.G. and Golbeck, J.H. (1989) Purification and properties of the intact P-700 and Fx-containing Photosystem I core protein. *Biochim. Biophys. Acta*, **973**, 324-32.

Ratajczak, R., Mitchell, R. and Haehnel, W. (1988) Properties of the oxidizing site of photosystem I. *Biochim. Biophys. Acta*, **933**, 306-318.

Redding, K., MacMillan, f., Leibl, W., Brettel, K., Hanley, J., Rutherford, A.W., Breton, J. and Rochaix, J.D. (1998) A systematic survey of conserved histidines in the core subunits of Photosystem I by site-directed mutagenesis reveals the likely axial ligands of P700. *EMBO J.*, **17**, 50-60.

Rodday, S.M., Do, L.T., Chynwat, V., Frank, H.A. and Biggins, J. (1996) Site-directed mutagenesis of the subunit PsaC establishes a surface-exposed domain interacting with the photosystem I core binding site. *Biochemistry*, **35**, 11832-11838.

Rodday, S.M., Jun, S.-S. and Biggins, J. (1993) Interaction of the F_AF_B-containing subunit with the photosystem I core heterodimer. *Photosynth. Res.*, **36**, 1-9.

Rodday, S.M., Jun, S.-S. and Biggins, J. (1994) Structure-function studies on the interaction of PsaC with the photosystem I heterodimer. The site-directed change R561E in PsaB destabilizes the subunit interaction in *Synechocystis* sp. PCC 6803. *Photosynth. Res.*, **42**, 185-190.

Rodday, S.M., Webber, A.N., Bingham, S.E. and Biggins, J. (1995) Evidence that the F_X domain in photosystem I interacts with the subunit PsaC: site-directed changes in PsaB destabilize the subunit interaction in *Chlamydomonas reinhardtii. Biochemistry*, **340**, 6328-6334.

Rustandi, R.R., Snyder, S.W., Feezel, L.L., Michalski, T.J., Norris, J.R., Thurnauer, M.C. and Biggins, J. (1990) Contribution of vitamin K1 to the electron spin polarization in spinach photosystem I. *Biochemistry*, **29**, 8030-2.

Rutherford, A.W. and Setif, P. (1990) Orientation of P700, the primary electron donor of photosystem I. *Biochim. Biophys. Acta*, **1019**, 128-32.

Schaffner, C., Laasch, H. and Hagemann, R. (1995) Detection of point mutations in chloroplast genes of Antirrhinum majus L. I. Identification of a point mutation in the psaB gene of a photosystem I plastome mutant. *Mol Gen Genet*, **249**, 533-544.

Scheller. (1996) In vitro cyclic electron transport in barley thylakoids follows two independent pathways. *Plant Physiol.*, **110**, 187-194.

Scheller, H.V., Okkels, J.S., Høj, P.B., Svendsen, I., Roepstorff, P. and Møller, B.L. (1989) The primary structure of a 4.0-kDa photosystem I polypeptide encoded by the chloroplast *psaI* gene. *J. Biol. Chem.*, **264**, 18402-18406.

Schluchter, W.M., Shen, G., Zhao, J. and Bryant, D.A. (1996) Characterization of psaI and psaL mutants of Synechococcus sp. strain PCC 7002: a new model for state transitions in cyanobacteria. *Photochem. Photobiol.*, **64**, 53-66.

Schoeder, H.U. and Lockau, W. (1986) Phylloquinone copurifies with the large subunit of photosystem I. *FEBS Lett.*, **199**, 23-27.

Schubert, W.-D., Klukas, O., Krauß, N., Saenger, W., Fromme, P. and Witt, H.T. (1997) Photosystem I of Synechccoccus elongarus at 4 Å Resolution: Comprehensice Structure Analysis. *J. Mol. Biol.*, **272**, 741-769.

Scott, M.P. and Biggins, J. (1997) Introduction of a [4Fe-4S (S-cys)4]+1,+2 iron-sulfur center into a four-alpha helic protein using design parameters from the domain of the F_x cluster in the Photosystem I reaction center. *Protein Sci.*, **6**, 340-346.

Setif, P. and Brettel, K. (1993) Forward electron transfer from phylloquinone A_1 to iron-sulfur centers in spinach photosystem I. *Biochemistry*, **32**, 7846-54.

Setif, P. and Mathis, P. (1980) The oxidation-reduction potential of P-700 in chloroplast lamellae and subchloroplast particles. *Arch. Biochem. Biophys.*, **204**, 477-485.

Setif, P. and Mathis, P. (1986) Photosystem I reaction center and its primary electron transfer reactions. *Encyclopedia Plant Physiol.*, **19**, 476-486.

Setif, P., Mathis, P. and Vanngard, T. (1984) Photosystem I photochemistry at low temperature. Heterogeneity in pathways for electron transfer to thesecondary acceptors and for recombination processes. *Biochim. Biophys. Acta*, **767**, 404-414.

Setif, P.Q. and Bottin, H. (1994) Laser flash absorption spectroscopy study of ferredoxin reduction by photosystem I in *Synechocystis* sp. PCC 6803: evidence for submicrosecond and microsecond kinetics. *Biochemistry*, **33**, 8495-504.

Setif, P.Q. and Bottin, H. (1995) Laser flash absorption spectroscopy study of ferredoxin reduction by photosystem I: spectral and kinetic evidence for the existence of several photosystem I-ferredoxin complexes. *Biochemistry*, **34**, 9059-9070.

Shahak, Y., Crowther, D. and Hind, G. (1981) The involvement of ferredoxin-NADP+ reductase in cyclic electron transport. *Biochim. Biophys. Acta*, **636**, 234-243.

Shen, G., Boussiba, S. and Vermaas, W.F. (1993) *Synechocystis* sp PCC 6803 strains lacking photosystem I and phycobilisome function. *Plant Cell*, **5**, 1853-63.

Sherman, D.M., Troyan, T.A. and Sherman, L.A. (1994) Localization of membrane proteins in the cyanobacterium *Synechococcus* sp. PCC7942: Radial asymmetry in the photosynthetic complexes. *Plant Physiol.*, **106**, 251-262.

Shuvalov, V.A., Ke, B. and Dolan, E. (1979) Kinetic and spectral properties of the intermediary electron acceptor A1 in photosystem I. *FEBS Lett.*, **100**, 5-8.

Sieckman, I., van der Est, A., Bottin, H., Setif, P. and Stehlik, D. (1991) Nanosecond electron transfer kinetics in photosystem I following substitution of quinones for vitamin K1 as studied by time resolved EPR. *FEBS Lett.*, **284**, 98-102.

Sigfridsson, K., Hansson, O., Karlsson, B.G., Baltzer, L., Nordling, M. and Lundberg, L.G. (1995) Spectroscopic and kinetic characterization of the spinach plastocyanin mutant Tyr83-His: a histidine residue with a high pK value. *Biochim. Biophys. Acta*, **1228**, 28-36.

Smart, L.B. and McIntosh, L. (1993) Genetic inactivation of the *psaB* gene in *Synechocystis* sp. PCC 6803 disrupts assembly of photosystem I. *Plant Mol. Biol.*, **21**, 177-180.

Smart, L.B., Warren, P.V., Golbeck, J.H. and McIntosh, L. (1993) Mutational analysis of the structure and biogenesis of the photosystem I reaction center in the cyanobacterium *Synechocystis* sp. PCC 6803. *Proc. Natl. Acad. Sci. U. S. A.*, **90**, 1132-1136.

Snyder, S.W., Rustandi, R.R., Biggins, J., Norris, J.R. and Thurnauer, M.C. (1991) Direct assignment of vitamin K1 as the secondary acceptor A1 in photosystem I. *Proc. Natl. Acad. Sci. USA.*, **88**, 9895-9896.

Sonoike, K., Ikeuchi, M. and Pakrasi, H.B. (1992) Presence of an N-terminal presequence in the PsaI protein of the photosystem I complex in the filamentous cyanobacterium *Anabaena variabilis* ATCC 29413. *Plant Mol. Biol.*, **20**, 987-90.

Staehelin, L.A. and Arntzen, C.J. (1983) Regulation of chloroplast membrane function: protein phosphorylation changes the spatial organization of membrane components. *J Cell Biol*, **97**, 1327-37.

Staehelin, L.A. and van der Staay, G.W.M. (1996) Structure, composition, functional organization and dynamic properties of thylakoid membranes. In Ort, D.R. and Yocum,

C.F. (eds.), *Oxygenic photosynthesis: the light reactions.* Kluwer Academic Publishers, Dordrecht, Netherlands, pp. 11-30.

Steppuhn, J., Hermans, J., Nechushtai, R., Herrmann, G.S. and Herrmann, R.G. (1989) Nucleotide sequence of cDNA clones encoding the entire precursor polypeptide for subunit VI and of the plastome-encoded gene for subunit VII of photosystem I reaction center from spinach. *Curr. Genet.*, **15**, 99-108.

Strotmann, H. and Weber, N. (1993) On the function of PsaE in chloroplast photosystem I. *Biochim. Biophys. Acta*, **1143**, 204-210.

Sun, J., He, Z., Nechushtai, R. and Chitnis, P.R. (1998) Molecular cloning of the *psaA* and *psaB* genes for the core proteins of photosystem I from the thermophilic cyanobacterium *Mastigocladus laminosus* (Accession No. AF038558). *Plant Physiol.*, **116**, 1192.

Sun, J., Xu, Q., Chitnis, V.P., Jin, P. and Chitnis, P.R. (1997) Topography of the Photosystem I Core Proteins of the Cyanobacterium Synechocystis sp. PCC 6803. *J. Biol. Chem.*, **272**, 21793-21802.

Takahashi, Y., Goldschmidt-Clermont, M., Soen, S.-Y., Franzen, L.G. and Rochaix, J.-D. (1991) Directed chloroplast transformation in *Chlamydomonas reinhardtii* : Insertional inactivation of the *psaC* gene encoding the iron sulfur protein destabilizes photosystem I. *EMBO J.*, **10**, 2033-2040.

Thurnauer, M.C. and Gast, P. (1985) Q-band (35GHz) EPR results on the nature of A1 and the electron spin polarization in photosystem I particles. *Photobiochem. Photobiophys.*, **9**, 29-38.

Tjus, S.E. and Andersson, B. (1991) Extrinsic polypeptides of spinach photosystem I. *Photosynth. Res.*, **27**, 209-219.

Trissl, H.-W. and Wilhelm, C. (1993) Why do thylakoid membranes from higher plants form grana stacks? *Trends Biochem. Sci.*, **18**, 415-419.

Vallon, O. and Bogorad, L. (1993) Topological study of PSI-A and PSI-B, the large subunits of the photosystem-I reaction center. *Eur. J. Biochem.*, **214**, 907-915.

van der Est, A., Bock, C., Golbeck, J., Brettel, K., Setif, P. and Stehlik, D. (1994) Electron transfer from the acceptor A1 to the iron-sulfur centers in photosystem I as studied by transient EPR spectroscopy. *Biochemistry*, **33**, 11789-97.

van der Est, A., Sieckmann, I., Lubitz, W. and Stehlik, D. (1995) Differences in the binding of the primary quinone acceptor in photosystem I and reaction centres of *Rhodobacter sphaeroides* studied by transient EPR spectroscopy. *Chem. Physics*, **194**, 349-359.

Vassiliev, I.R., Jung, Y.S., Smart, L.B., Schulz, R., McIntosh, L. and Golbeck, J.H. (1995) A mixed-ligand iron-sulfur cluster (C556SPsaB or C565SPsaB) in the F_X- binding site leads to a decreased quantum efficiency of electron transfer in photosystem I. *Biophys. J.*, **69**, 1544-1553.

Vassiliev, I.R., Jung, Y.S., Yang, F. and Golbeck, J.H. (1998) PsaC subunit of photosystem I is oriented with iron-sulfur cluster F_B as the immediate electron donor to ferredoxin and flavodoxin. *Biophys. J.*, **74**, 2029-2035.

von Heijne, G. and Gavel, Y. (1988) Topogenic signals in integral membrane proteins. *Eur. J. Biochem.*, **174**, 671-674.

Warren, P.V., Golbeck, J.H. and Warden, J.T. (1993a) Charge recombination between P700+ and A1- occurs directly to the ground state of P700 in a photosystem I core devoid of FX, FB, and FA. *Biochemistry*, **32**, 849-57.

Warren, P.V., Smart, L.B., McIntosh, L. and Golbeck, J.H. (1993b) Site-directed conversion of cysteine-565 to serine in PsaB of photosystem I results in the assembly of [3Fe-4S] and [4Fe-4S] clusters in Fx. A mixed-ligand [4Fe-4S] cluster is capable of electron transfer to FA and FB. *Biochemistry*, **32**, 4411-4419.

Webber, A.N., Gibbs, P.B., Ward, J.B. and Bingham, S.E. (1993) Site-directed mutagenesis of the photosystem I reaction center in chloroplasts. The proline-cysteine motif. *J. Biol. Chem.*, **268**, 12990-5.

Webber, A.N. and Malkin, R. (1990) Photosystem I reaction-centre proteins contain leucine zipper motifs. A proposed role in dimer formation. *FEBS Lett.*, **264**, 1-4.

Webber, A.N., Su, H., Bingham, S.E., Kass, H., Krabben, L., Kuhn, M., Jordan, R., Schlodder, E. and Lubitz, W. (1996) Site-directed mutations affecting the spectroscopic characteristics and midpoint potential of the primary donor in photosystem I. *Biochemistry*, **35**, 12857-12863.

Wynn, R. and Malkin, R. (1990) The Photosystem I 5.5 kDa subunit (the *psaK* gene product). An intrinsic subunit of the PSI reaction center complex. *FEBS Lett.*, **262**, 45-48.

Wynn, R.M., Luong, C. and Malkin, R. (1989) Maize photosystem I. Identification of the subunit which binds plastocyanin. *Plant Physiol.*, **91**, 445-449.

Wynn, R.M. and Malkin, R. (1988) Interaction of plastocyanin with photosystem I: a chemical cross- linking study of the polypeptide that binds plastocyanin. *Biochemistry*, **27**, 5863-9.

Xu, Q., Armbrust, T.S., Guikema, J.A. and Chitnis, P.R. (1994a) Organization of photosystem I polypeptides: A structural interactions between PsaD and PsaL subunits. *Plant Physiol.*, **106**, 1057-1063.

Xu, Q. and Chitnis, P.R. (1995) Organization of photosystem I polypeptides. Identification of PsaB domains that may interact with PsaD. *Plant Physiol.*, **108**, 1067-1075.

Xu, Q., Chitnis, V.P., Ke, A. and Chitnis, P.R. (1995a) Structural Organization of Photosystem I. In Mathis, P. (ed.) *Photosynthesis: from Light to Biosphere*. Kluwer, Dodrecht, Vol. II, pp. 87-90.

Xu, Q., Guikema, J.A. and Chitnis, P.R. (1994b) Identification of surface-exposed domains on the reducing side of photosystem I. *Plant Physiol.*, **106**, 617-624.

Xu, Q., Hoppe, D., Chitnis, V.P., Odom, W.R., Guikema, J.A. and Chitnis, P.R. (1995b) Mutational analysis of photosystem I polypeptides in the cyanobacterium *Synechocystis* sp. PCC 6803. Targeted inactivation of *psaI* reveals the function of PsaI in the structural organization of PsaL. *J. Biol. Chem.*, **270**, 16243-16250.

Xu, Q., Jung, Y.S., Chitnis, V.P., Guikema, J.A., Golbeck, J.H. and Chitnis, P.R. (1994c) Mutational analysis of photosystem I polypeptides in *Synechocystis* sp. PCC 6803. Subunit requirements for reduction of NADP$^+$ mediated by ferredoxin and flavodoxin. *J. Biol. Chem.*, **269**, 21512-21518.

Xu, Q., Odom, W.R., Guikema, J.A., Chitnis, V.P. and Chitnis, P.R. (1994d) Targeted deletion of *psaJ* from the cyanobacterium *Synechocystis* sp. PCC 6803 indicates structural interactions between the PsaJ and PsaF subunits of photosystem I. *Plant Mol. Biol.*, **26**, 291-302.

Xu, Q., Yu, L., Chitnis, V.P. and Chitnis, P.R. (1994e) Function and organization of photosystem I in a cyanobacterial mutant strain that lacks PsaF and PsaJ subunits. *J. Biol. Chem.*, **269**, 3205-3211.

Yu, J., Smart, L.B., Jung, Y.S., Golbeck, J. and McIntosh, L. (1995a) Absence of PsaC subunit allows assembly of photosystem I core but prevents the binding of PsaD and PsaE in *Synechocystis* sp. PCC6803. *Plant Mol Biol*, **29**, 331-342.

Yu, J., Vassiliev, I.R., Jung, Y.S., Golbeck, J.H. and McIntosh, L. (1997) Strains of *Synechocystis* sp. PCC 6803 with altered PsaC. I. Mutations incorporated in the cysteine ligands of the two [4Fe-4S] clusters F_A and F_B of photosystem I. *J. Biol. Chem.*, **272**, 8032-8039.

Yu, L., Bryant, D.A. and Golbeck, J.H. (1995b) Evidence for a mixed-ligand [4Fe-4S] cluster in the C14D mutant of PsaC. Altered reduction potentials and EPR spectral properties of the F_A and F_B clusters on rebinding to the P700-F_X core. *Biochemistry*, **34**, 7861-7868.

Yu, L., Zhao, J., Lu, W., Bryant, D.A. and Golbeck, J.H. (1993a) Characterization of the [3Fe-4S] and [4Fe-4S] clusters in unbound PsaC mutants C14D and C51D. Midpoint potentials of the single [4Fe-4S] clusters are identical to F_A and F_B in bound PsaC of photosystem I. *Biochemistry*, **32**, 8251-8.

Yu, L., Zhao, J., Mühlenhoff, U., Bryant, D.A. and Golbeck, J.H. (1993b) PsaE is required for in vivo cyclic electron flow around photosystem I in the cyanobacterium *Synechococcus* sp. PCC 7002. *Plant Physiol.*, **103**, 171-180.

Zech, S.G., van der Est, A.J. and Bittl, R. (1997) Measurement of cofactor distances between $P700^{+\cdot}$ and $A_1^{-\cdot}$ in native and quinone-substituted photosystem I using pulsed electron paramagnetic resonance spectroscopy. *Biochemistry*, **36**, 9774-9779.

Zhao, J., Li, N., Warren, P.V., Golbeck, J.H. and Bryant, D.A. (1992) Site-directed conversion of a cysteine to aspartate leads to the assembly of a [3Fe-4S] cluster in PsaC of photosystem I. The photoreduction of FA is independent of FB. *Biochemistry*, **31**, 5093-9.

Zilber, A.L. and Malkin, R. (1992) Organization and topology of photosystem I subunits. *Plant Physiol.*, **99**, 901-911.

Figure Legends

Fig. 2-1. A model for the organization of PSI proteins. A side view of PSI proteins is presented. Details of interactions among the PSI proteins can be found in the text.

Fig. 2-2. Electron transfer in PSI. The electron carriers are arranged according to the electron flow on the scale of midpoint redox potentials (Em). Typical values for the half-time for the forward reactions are indicated.

Fig. 2-3. The topographic models of PSI and PSII core proteins. A, PsaA and PsaB form both the core antenna and the reaction center of PSI. The 11 transmembrane helices are shown as *dark boxes* for the N-terminal helices and *light boxes* for the C-terminal helices and are *numbered* as I-XI followed by *italic letters a-o* corresponding to the helices in the 4Å crystal structure. The surface helices are shown as *horizontal boxes*. The bound electron carriers P700, PhQ (phylloquinone), and F_X are also shown. **B**, CP43 and CP47 form the core antenna of PSII. The 6 transmembrane helices are shown as *dark boxes*. **C**, D1 and D2 proteins form the reaction center of PSII. The 5 transmembrane helices are shown as *light boxes*. The putative surface helices are shown as *horizontal boxes*. The bound cofactors P680, PQ (plastoquinone), and iron are shown.

Table 2-1. Polypeptide subunits of PSI.

The molecular mass predicted from the deduced primary sequences of *Synechocystis* sp. PCC 6803 PSI is given; the apparent mass observed during PAGE is parenthesized. For PsaG, PsaH, and PsaN, a range of molecular masses for the proteins from higher plants are given.

| Subunit	Gene	Mass	Properties	Functions
PsaA	*psaA*	82.9 (66)	11 transmembrane, 3 stromal and 1 lumenal surface helices each; together, they bind about 100 chlorophyll *a*, P700 chlorophyll *a* dimer, 12-16 ß-carotenes, 2 phylloquinones, and one [4Fe-4S] cluster (F_x)	Light-harvesting; charge separation; electron transfer; photoprotection; charge stabilization
PsaB	*psaB*	81.2 (66)		
PsaC	*psaC*	8.8 (8)	Peripheral on stromal (cytoplasmic) side; binds two [4Fe-4S] clusters (F_A, F_B) ; 2 single-turn α-helices	Terminal acceptors; donates electrons to ferredoxin
PsaD	*psaD*	15.6 (17.7)	Peripheral on stromal (cytoplasmic) side; 1 α-helix	Ferredoxin-docking; assembly of PsaC; normal EPR properties of F_A and F_B
PsaE	*psaE*	8.1 (8.8)	Peripheral on stromal (cytoplasmic) side; β-barrel structure	Facilitates interaction with ferredoxin; essential for cyclic electron transport
PsaF	*psaF*	15.7 (15.8)	2 transmembrane helices; large exposure on lumenal side; may bind 1-3 chlorophyll *a*	Plastocyanin-docking for fast electron transfer; stabilize core antenna?
PsaG	*psaG*	10-10.8	2 putative transmembrane helices; only in chloroplasts	Interaction with LHCI
PsaH	*psaH*	10.2-11	Peripheral on stromal side; only in chloroplasts	?
PsaI	*psaI*	4.4 (3.4)	1 transmembrane helix	Normal organization of PsaL
PsaJ	*psaJ*	4.5 (3.0)	1 transmembrane helix	Normal organization of PsaF
PsaK	*psaK*	8.6 (5.1)	2 transmembrane helices; may bind 1-2 chlorophyll *a*	Interaction with LHCI; stabilize core antenna?
PsaL	*psaL*	16.6 (14.3)	2 transmembrane helices; may bind 2-4 chlorophyll *a*	PSI trimerization; stabilize core antenna?
PsaM	*psaM*	3.4 (2.8)	1 transmembrane helix; not in chloroplasts	Stabilize trimer in cooperation with PsaK?
PsaN	*psaN*	9	Peripheral on lumenal side; only in chloroplasts	?
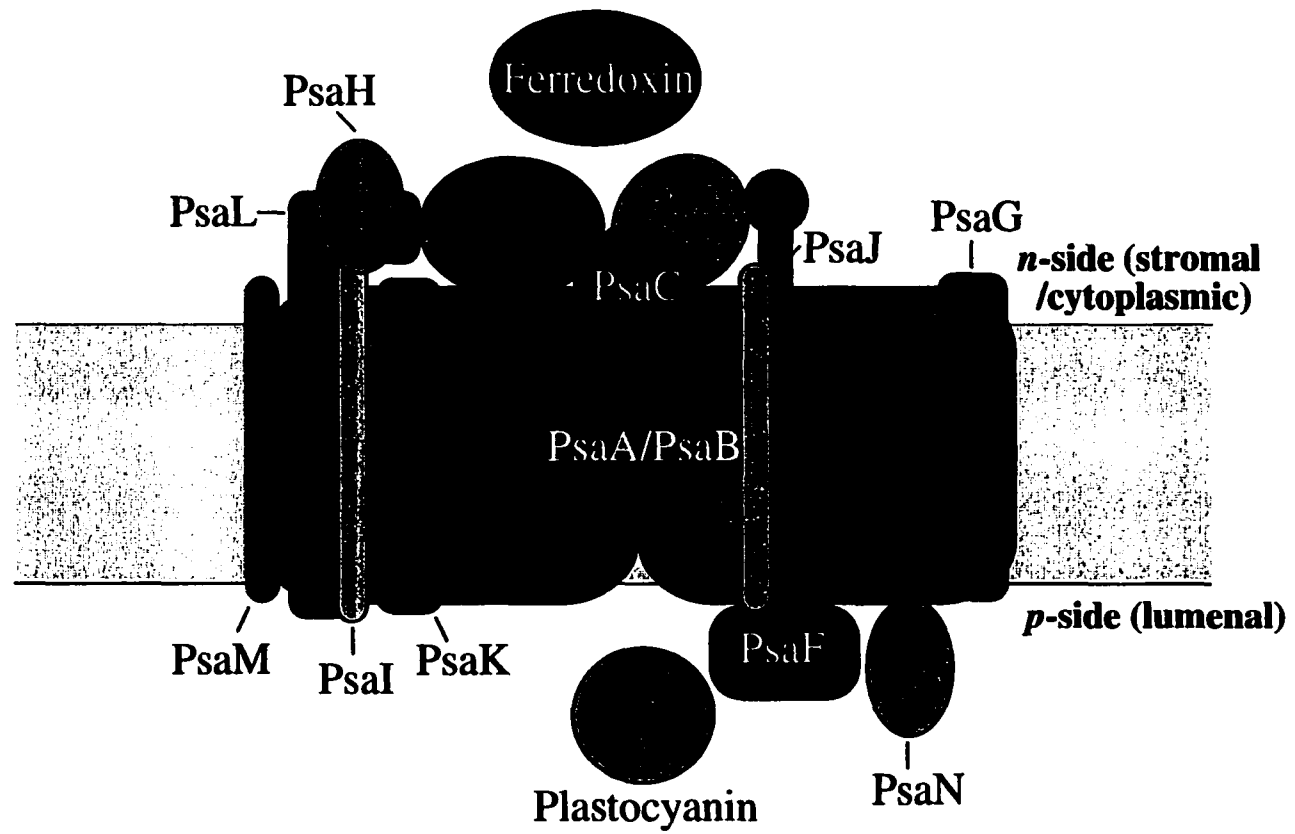
Fig. 2-1
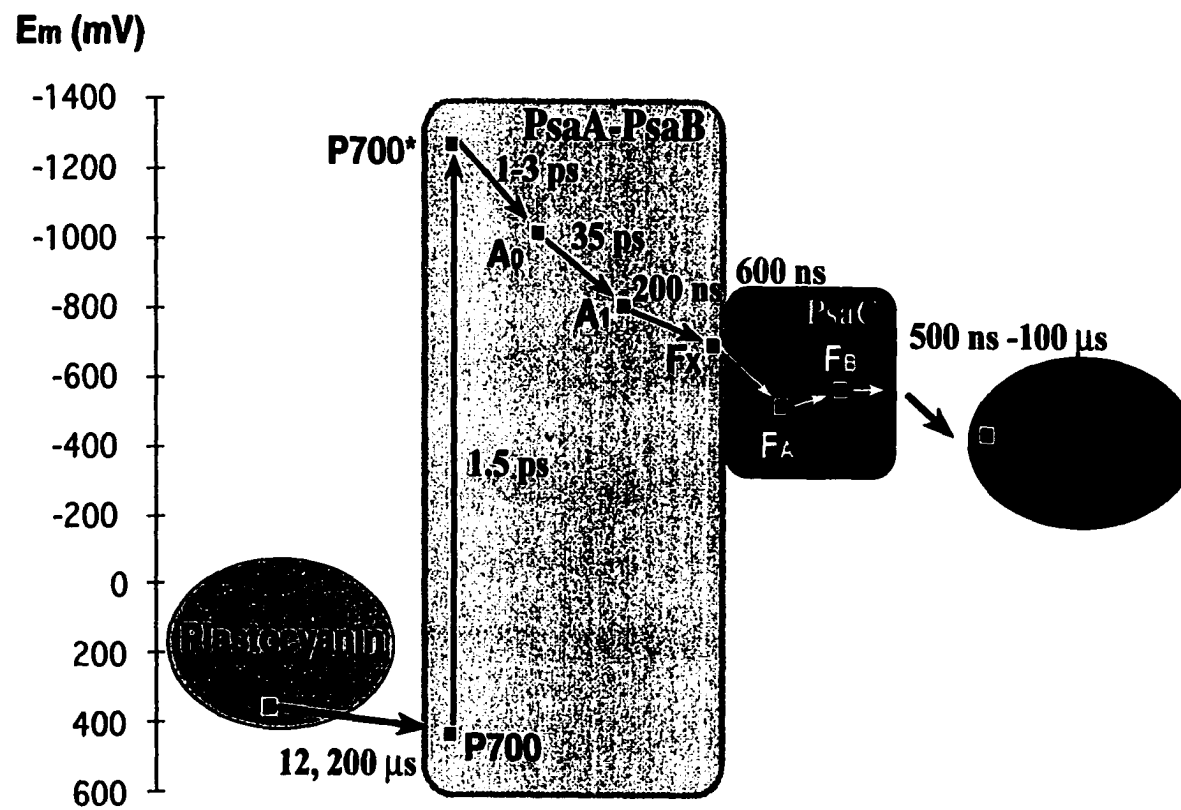
Fig. 2-2

A, PsaA/B
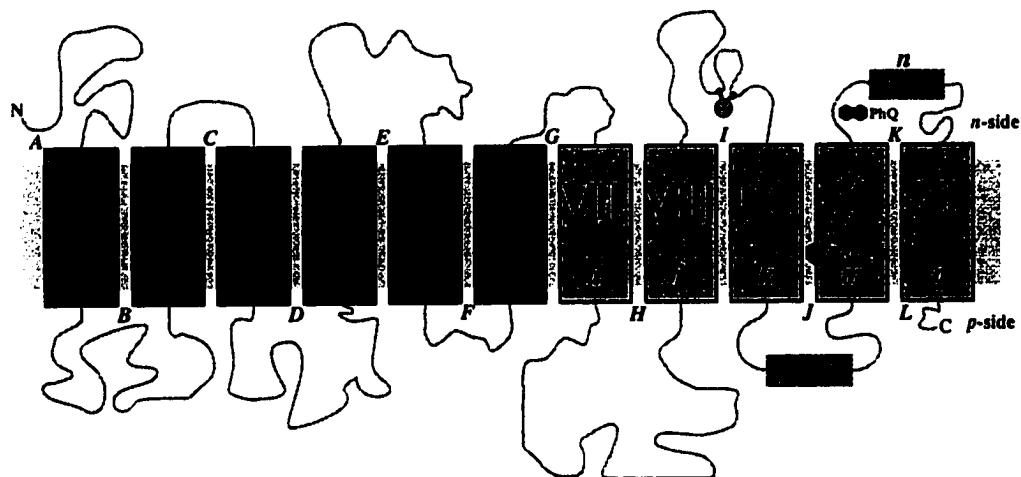
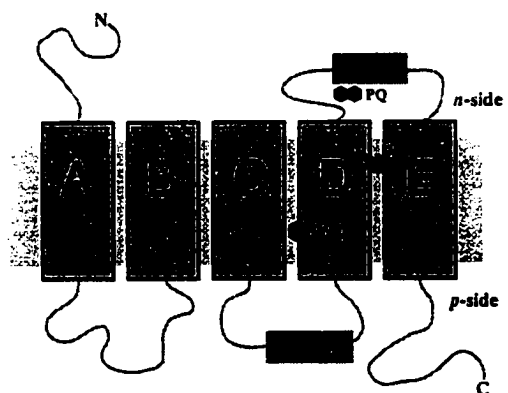## B, CP43/47
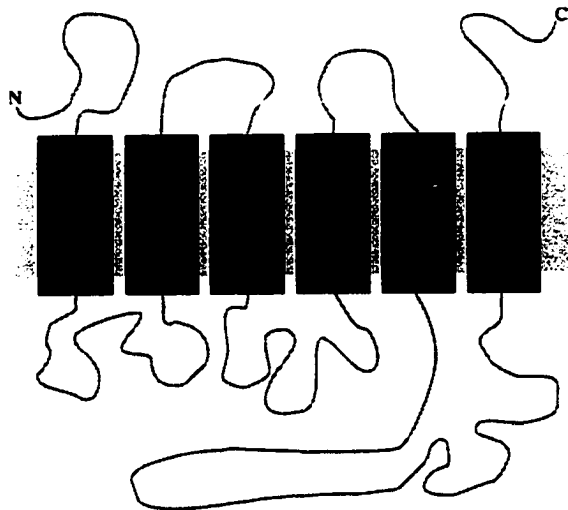
C, D1/D2

Fig. 2-3

CHAPTER 3. TOPOGRAPHY OF THE PHOTOSYSTEM I CORE PROTEINS OF THE CYANOBACTERIUM *SYNECHOCYSTIS* SP. PCC 6803[1]

A paper published in the Journal of Biological Chemsitry[2]

Jun Sun, Qiang Xu, Vaishali P. Chitnis, Ping Jin, Parag R. Chitnis

Summary

PsaA and PsaB are homologous integral membrane proteins that form the heterodimeric core of photosystem I. Domain-specific antibodies were generated to examine the topography of PsaA and PsaB. The purified photosystem I complexes from the wild type strain of Synechocystis sp. PCC 6803 were treated with eight proteases to study the accessibility of cleavage sites in PsaA and PsaB. Proteolytic fragments were identified using the information from N-terminal amino acid sequencing, reactivity to antibodies, apparent mass, and specificity of proteases. The extramembrane loops of PsaA and PsaB differed in their accessibility to proteases, which indicated the folded structure of the loops or their shielding by the small subunits of photosystem I. NaI-treated and mutant photosystem I complexes were used to identify the extramembrane loops that were exposed in the absence of specific small subunits. The absence of PsaD exposed additional proteolytic sites in PsaB while the absence of PsaE exposed sites in PsaA. These studies distinguish PsaA and PsaB in the structural model for photosystem I that has been proposed on the basis of X-ray diffraction studies (Krauβ, N., Schubert, W.-D., Klukas, O., Fromme, P., Witt, H. R., and Saenger, W., (1996) Nature Structural Biol., 3, 965). Using osmotically shocked cells for proteases treatments, N-terminus of PsaA was determined to be on the n-side of the photosynthetic membranes. Based on these data and available published information, we propose a topological model for PsaA and PsaB.

Introduction

Photosystem I (PS I)[3] from cyanobacteria and chloroplasts is a multisubunit membrane-protein complex that catalyzes electron transfer from reduced plastocyanin (or cytochrome c_6)

to oxidized ferredoxin (or flavodoxin) (1-4). The PsaA and PsaB subunits of PS I form the heterodimeric core of the complex which harbors approximately 100 antenna chlorophyll a molecules, 10-12 β carotenes, the primary electron donor P700, and a chain of electron acceptors (A_0, A_1 and F_X). PsaA and PsaB also interact directly with plastocyanin or cytochrome c_6 (5-7). In addition to the core proteins, the cyanobacterial PS I complex contains 9 small subunits (1-3). PsaC binds the terminal electron acceptors F_A and F_B, which are two [4Fe-4S] center (8). PsaD provides an essential ferredoxin-docking site on the reducing side of PS I (9-11) and is required for the stable assembly of PsaC and PsaE into the PS I complex (12, 13). PsaE is involved in ferredoxin-docking (10, 14-16) and in cyclic electron flow around PS I (17, 18). PsaF provides a component of the docking site for plastocyanin in the plant PS I (7, 19, 20), but not in the cyanobacterial PS I (6, 21). PsaL is essential for the formation of PS I trimers in cyanobacteria (22). PsaI and PsaJ are required for the correct organization of PsaL and PsaF, respectively (23, 24). The absence of PsaM in cyanobacterial mutants causes deficiency in growth at high light intensity and affects stable assembly of PsaD.[4] The role of PsaK has not been identified.

During the past few years, major advances in X-ray crystallography (25, 26), electron microscopy (27), molecular genetics (10, 22) and biochemical studies (28, 29) have provided a framework for understanding the overall architecture of PS I. The PS I complex has an elongated shape with a local pseudo-2-fold symmetry. PsaC, PsaD and PsaE are peripheral subunits, located on the n-side (stromal side in chloroplasts and cytoplasmic side in cyanobacteria) of photosynthetic membranes, with PsaC positioned in the center of each monomeric PS I on the axis of symmetry (26, 27). The recent crystal analysis of PS I has indicated the location of [4Fe-4S] clusters F_X, F_A and F_B, 71 chlorophyll a molecules, 31 transmembrane α-helices, and 9 surface and 3 stromal α-helices (26). A monomer of PS I consists of a 'catalytic domain' and a smaller 'connecting domain' that links monomers to form a trimer. The connecting domain contains three transmembrane helices which may belong to PsaL and PsaI (22, 23). The remaining helices belong to the PS I core and other subunits in the catalytic domain. Twenty-two transmembrane and eight peripheral helices in the catalytic domain are arranged in an approximate symmetry (25, 26). Therefore, in agreement with the

---

hydropathy analysis, the PsaA and PsaB cores are proposed to contain eleven transmembrane helices each (30).

Although the X-ray crystallography studies provided information of the PS I core, PsaA and PsaB could not be distinguished at the present resolution (26). Similarly, the interactions between PS I core and small subunits, the surface domains and residues of the PS I core, and positioning of extramembrane loops with respect to the photosynthetic membranes have not been elucidated clearly. Topographical studies provide a valuable tool to understand these unresolved structural features of PS I. In this paper, we describe biochemical studies that used subunit-deficient mutants, limited proteolysis, and domain-specific antibodies. We studied the accessibility of PsaA and PsaB to different proteases, the shielding of PsaA and PsaB by smaller PS I subunits and the position of the N-terminus of PsaA with respect to the membrane plane.

Experimental Procedures

Cyanobacterial Strains and Culture. Strains of *Synechocystis* sp. PCC 6803 that were used in this study are listed in Table 3-1. Cultures of wild type and mutant strains were grown in BG-11 with or without 5 mM Glucose and antibiotics (30 μg/ml chloramphenicol or 40 μg/ml kanamycin) under a light intensity of 21 μmol·m^{-1}·s^{-1}. Cells were harvested at the late exponential growth phase and resuspended in 0.4 M sucrose, 10 mM NaCl, 1 mM PMSF, 2 mM benzamidine and 10 mM MOPS, pH 7.0 for isolation of thylakoids.

Isolation of the Photosynthetic Membranes and Purification of PS I Complexes. Photosynthetic membranes were isolated after cell breakage with a bead beater (Biospec Products) (28). To isolate PS I, the membranes were solubilized with Triton X-100, and subjected to DEAE-cellulose chromatography and sucrose gradient centrifugation (31). Chlorophyll concentrations in the thylakoid membranes and PS I complexes were determined in 80% (v/v) acetone (32).

Preparation of Osmotically Shocked Cells of Synechocystis sp. PCC 6803. Cells were harvested at the late exponential growth phase by centrifugation (7,000 g, 10 min). The pellet was resuspended in 0.4 M sucrose, 5 mM EDTA and 10 mM HEPES, pH 7.0, pelleted again and resuspended in the same buffer with 0.2% (w/v) lysozyme to 1 g cells per 10 ml. Cell wall was digested by incubation at 27°C for 12 hours under illumination (21 μmol·m^{-1}·s^{-1}) with constant shaking. Cells were harvested by centrifugation (7,000 g, 10 min), resuspended in osmotic shock solution (50 mM potassium phosphate, pH 6.8, 30 mM sodium citrate, 0.2 mM CaCl$_2$, 1 mM PMSF and 2 mM benzamidine), incubated on ice for 30 min and harvested by centrifugation (7,000 g, 10 min) again. This osmotic shock treatment was repeated for two

additional times. The cells were pelleted and resuspended twice with 10 mM NaCl, 10 mM HEPES, pH 7.0 and finally resuspended in 0.4 M sucrose, 10 mM NaCl, 10 mM HEPES, pH 7.0 for protease treatment (33).

Treatment of PS I with Proteases and NaI. To study the accessibility of PS I subunits to proteases, purified wild type and mutant PS I complexes, wild type thylakoid membranes and osmotically shocked cells were incubated with protease at a final chlorophyll concentration of 200 μg /ml. The protease reaction conditions are listed in Table 3-2. To remove peripheral subunits from the PS I core, purified wild type PS I complex was incubated with 3 M NaI for 30 minutes on ice (34). The samples were diluted with an excess amount of 10 mM MOPS-HCl (pH 7.0), 0.05% Triton X-100, and desalted by ultrafiltration through a Centricon-100 (Amicon).

Oxygen Uptake Measurements. Purified PS I complexes that had been treated with proteases were used for oxygen uptake measurements. In a total volume of 1 ml, PS I containing 10 μg chlorophyll was used for the reaction. PS II inhibitor, electron donors and electron acceptor were added to a final concentration of: 50 μM 3-(3,4-dichlorophenyl)-1,1-dimethylurea; 1 mM ascorbate; 1 mM 3,6-diamino durene and 2 mM methyl viologen. Oxygen uptake was measured on the Oxygen Monitoring System (Hansatech, England) under the light density of 2430 μmol m^{-2} s^{-1}.

Preparation of Antibodies. Domain-specific antibodies were generated using overexpressed fusion proteins as antigens. DNA fragments coding the appropriate peptides in PsaA and PsaB of *Synechocystis* sp. PCC 6803, PsaA2 for residues A2-TISPPEREAKAKVS VDNNPVPTSFEKWGKPGHFDRTL of PsaA and PsaB450 for residues B450-QILIEPVFA QWIQATSGKALYGFDVLLSNPDSIASTTGAAWLPGWLDAINSGINSLF of PsaB, were amplified by polymerase chain reaction and inserted into expression vector pGEX-KG between *Eco*RI and *Xho*I sites. The expression of fusion proteins was induced by isopropyl β-D-thiogalactopyranoside (IPTG). Cells were harvested by centrifugation and lysed by a probe sonicator. The fusion proteins in inclusion bodies were isolated from membranes by centrifugation through 10% sucrose and applied directly for electrophoresis. The gel was stained by Coomassie Blue. The fusion proteins were excised from the gel and used for raising antibodies at Cocalico Biological. Antibody anti-PsaB718 was raised against the C-terminus of PsaB (35). Antisera were evaluated by Western blotting against both thylakoid membranes and purified PS I complex. All three domain-specific antibodies anti-PsaA2, anti-PsaB450 and anti-PsaB718 recognized only the 66 kDa diffuse band corresponded to the comigrating PsaA and PsaB proteins.

Analytical Gel Electrophoresis, Immunodetection and N-Terminal Amino Acid Sequencing.
Isolated PS I complexes and photosynthetic membranes were solubilized at 37°C for 2 hours
with 1% SDS and 0.1% 2-mercaptoethanol. Proteins were resolved by a modified Tricine-urea
SDS-PAGE for better resolution of the PS I subunits (10). After electrophoresis, gels were
electrotransferred to Immobilon-P polyvinylidene difluoride membranes (Millipore).
Immunodetection was performed using the enhanced chemiluminescence reagents
(Amersham). For sequencing of N-termini of proteolytic cleavage fragments, peptides were
separated by electrophoresis, transferred to Immobilon-P membranes, stained with Coomassie
Blue containing 1% acetic acid for several minutes, destained with 50% methanol, and rinsed
with deionized water. The N-terminal sequences were determined on an Applied Biosystems
477A Sequencer.

Results

Activity of the Protease-treated PS I Complexes. In this study, we used limited proteolysis
to map surface domains in the PsaA-B core of PS I. To examine activity of the protease-treated
complexes, we determined PS I-mediated oxygen consumption rates by Mehler reaction (36,
37). Purified wild type PS I complexes were treated by eight proteases and employed in
oxygen uptake measurements (Table 3-3). The PS I activity of untreated sample was 377.5
μmol O_2 / mg Chl hour. The PS I activities in all eight protease treatments ranged from 99% to
133% of the control activity. An active reaction center and functional electron transfer chain are
required for the PS I activity that is measured by the oxygen uptake. Thus the protease
treatments did not damage the electron transfer chain within the PS I complex. This may imply
that the limited proteolysis could only access extramembrane loops. In most protease-treated
samples, the PS I activity was higher than that in the untreated control. Proteases might have
degraded the extramembrane loops and small subunits, thereby facilitating access of electron
donor or acceptor to the electron transfer centers in the PS I complexes.

Accessibility of PsaA and PsaB to Proteases. Purified PS I complexes from the wild type
strain were treated with proteases to study the accessibility of cleavage sites in PsaA and PsaB.
The PS I complexes were treated with different concentrations of proteases and the resulting
fragments were stained by Coomassie Blue or immunodetected by the three domain-specific
antibodies (Fig. 3-1). The apparent masses of protein fragments were determined from the
migration of prestained protein molecular weight standards (GIBCO-BRL) upon
electrophoresis. The protein fragments that were visible in Coomassie Blue staining were
subjected to N-terminal amino acid sequencing. Three criteria, the N-terminal sequences, the

apparent mass, and the immunoreactivities of proteolytic fragments, were used to identify the proteolytic fragments (Table 3-4).

The ThII, GlIII, and PaIII fragments were deduced accurately from their N-terminal sequence and from their immunodetection by anti-PsaB718 showing that they contain the C-terminus of PsaB. The ThI, ThIII, ThIV, and ChI fragments were recognized by the anti-PsaB450 antibody indicating that they contain the PsaB450 peptide. The ThI fragment also contained the N-terminus of PsaB and showed a similar accumulation pattern as the ThII fragment. The immunodetection pattern and apparent mass imply that these fragments resulted from a single cleavage at Ile-498 of PsaB. The ThIII and ThIV fragments were predicted with the same C-terminus of the ThI fragment and matched the immunodetection and apparent mass. They may have resulted from the further cleavage of the ThI fragment as their accumulation followed that of ThI. The N-terminus of the ChI fragment resulted from the cleavage at Phe-8 of PsaB protein. The immunodetection and apparent mass of the ChI fragment is similar to the ThI fragment, thus the C-terminus of the ChI fragment should result from a cleavage close to Ile-498. The only reasonable site to generate C-terminus of the ChI fragment is Phe-506. When the PS I complexes were treated with trypsin, the signals corresponding to the intact PsaA were decreased significantly when detected by anti-PsaA2. Also, a diffused band that migrated slightly faster than the PsaA-B band was visible in Coomassie Blue staining. This can be explained as a cleavage in the N-terminal sequence of PsaA. The N-terminal sequence of the TrI fragment revealed the cleavage site in the N-terminal extramembranal domain of PsaA. Thus these fragments, grouped as type I fragments, could be identified with accuracy. Similar to many membrane proteins, the electrophoretic behavior of the PS I core proteins was anomalous compared to the migration of soluble proteins. The comigrating PsaA and PsaB formed the 66 kDa diffuse band in PAGE while the deduced mass is more than 80 kDa. The predicted mass was higher than the apparent mass. This was also true for the type I fragments and was considered during the prediction of the other fragments.

Table 3-5 lists the results of Western blotting, the apparent mass, and the predicted proteolysis regions for the protein fragments that could be immunodetected with domain-specific antibodies. The identity of these fragments could be predicted by several ways. The prediction of type 1 fragments was described in the previous paragraph. Type 2 and type 3 fragments contained epitope for N-terminus of PsaA or epitope at the C-terminus of PsaB, as shown by the immunodetection results. Based on their apparent mass, there was only one reasonable cleavage site for the fragments of type 2. For example, the GIV fragment, a 44.5 kDa polypeptide recognized by anti-PsaA2, could result from the proteolysis at Glu-512 in PsaA with a predicted mass of 47.5 kDa. The adjacent Glu-C cleavage sites were Glu-342 or

Glu-695 in PsaA which made the predicted mass of 37.9 kDa or 76.9 kDa unreasonable for GIV. In type 3 fragments, there were several possible cleavage sites located within one extramembrane loop or in a region containing two extramembrane loops. For example, the GIII fragment, a 33.7 kDa peptide immunodetected with anti-PsaA2, could result from four reasonable cleavages between Glu-323 and Glu-342 in PsaA with the predicted mass from 35.8 kDa to 37.9 kDa. These four possible cleavage sites were located in the E loop. The LyI fragment is the only type 4 fragment. It accumulated similar as the TrI fragment, so it was predicted to have the similar cleavage at the N-terminal loop of PsaA. The type 5 fragments contained the peptide PsaB450 but there was not enough data to identify them accurately. Overall, the limited proteolysis of the wild type PS I provided extensive information about the residues that are exposed on the surface of the PS I complex.

Treatment of mutant PS I complexes with proteases. As the components of the multiprotein PS I complex, the PsaA and PsaB core proteins interact with the small subunits. To study these interactions, subunit-deficient mutant PS I complexes (Table 3-1) and NaI-treated PS I complexes were used for limited proteolytic treatments. Different PS I complexes were incubated with proteases, and resulting fragments were detected by Western blotting (Fig. 3-2). When specific small subunits were absent, the proteolytic sites in the core proteins that are shielded by the small subunits were expected to be exposed to proteases. Indeed, additional peptide fragments that reacted with the three domain-specific antibodies were obtained in mutant PS I complexes compared to the protease-treated wild type PS I complexes. The apparent mass and the immunoreactivity were used in prediction of the additional fragments (Table 3-6).

In general, the ADC4, AEK2, and NaI-treated PS I complexes yielded more additional proteolytic fragments than the AFK6 and AIC9 complexes indicating that the peripheral PS I subunits shield more extramembrane proteolytic sites in the core proteins than the integral membrane proteins. When the ADC4 and NaI-treated PS I complexes were incubated with proteases, PsaA and PsaB were digested much more rapidly than the core proteins in the wild type PS I complexes. The AEK2, AFK6, and AIC9 complexes were more resistant to proteolysis than ADC4 and NaI treated PS I complexes. The untreated ADC4 and NaI-treated PS I complexes contained 42 kDa fragments detected by anti-PsaA2 and anti-PsaB450. The natural degradation of PsaA is predicted in the H loop. The degradation fragment of PsaB was similar to the ThI fragment that resulted from the cleavage at Ile-498 in the H loop. Therefore, these results suggest that the natural degradation may occur in the H loops of both core proteins.

Information about the protection of PsaA by small subunits can be obtained from the immunodetection data with the anti-PsaA2 antibody. Additional fragments were not observed in the protease treatments of the AIC9 complexes. Therefore, PsaL and PsaI may not shield protease-recognition sites in PsaA from proteolysis. When the PS I complexes from the AFK6 strain were treated with trypsin, the additional 40 kDa TrA fragment was obtained. The TrA fragment could result from a cleavage in the H loop of PsaA. When the PS I complexes of the ADC4 strain were treated with proteases, the major fragments detected by anti-PsaA2 was the 42 kDa degradation fragments. However, when the PS I complexes of the AEK2 strain were treated with proteases, small additional proteolytic fragments (ThC-F, ChC-F, and ClC) resulted from the cleavages in the N-terminal domain of PsaA. Also, a 44 kDa fragment (ClA) resulted from accessible sites in the C-terminal domain of PsaA. The cleavages in the N-terminal domain of PsaA could be detected only upon protease-treatment of the PsaE-less AEK2 complexes, implying that the N-terminal domain of PsaA may interact with PsaE. The NaI treatment of PS I complexes removed PsaD, PsaE, and PsaC from the core proteins. When the NaI-treated PS I complexes were treated with proteases, the anti-PsaA2 antibody immunoreacted with the 42 kDa degradation product that was similar to the one in the protease-treated ADC4 complex and also with the large proteolytic fragments similar to the ones in the protease-treated AEK2 complex.

When detected with the anti-PsaB450 antibody, the protease-treated PS I complexes of the AEK2, AFK6, and AIC9 strains contained the similar pattern as the protease-treated wild type PS I proteins. For the protease treatments of the ADC4 and NaI-treated PS I complexes, the 28.2 kDa LyC fragment was detected in addition to the 42 kDa degradation fragment. Some diffused fragments between the 42 kDa fragment and the intact PsaA-B protein were also observed, especially in the NaI-treated PS I complexes. When compared with the detection by the anti-PsaB718 antibody, these fragments did not contain the C-terminal epitope. These fragments could result from the cleavages in the I, J, or K loops which are close to the C-terminus of PsaB.

Additional fragments were detected by the anti-PsaB718 antibody in all mutant PS I complexes. The 28.2 kDa LyC fragment that was recognized by the anti-PsaB450 antibody was also immunodetected by the anti-PsaB718 antibody when the ADC4 and NaI-treated PS I complexes were treated with the Lys-C protease. From its apparent mass and the presence of the C-terminal epitope, this fragment was predicted to have N-terminus from one of 5 possible cleavage sites in the G and H loops to the C-terminus of PsaB. Proteolysis at these sites should result in fragments with a predicted mass of 31.0 kDa to 36.8 kDa. When the PS I complexes of AFK6 were treated with trypsin, the 22.7 kDa TrB fragment was detected by the anti-

PsaB718 antibody. This fragment could have resulted from a cleavage at Lys-449 or Lys-467 in the H loop of PsaB. In the ADC4 and NaI-treated PS I complexes, an additional 40.0~45.0 kDa fragment shown as LF in Fig. 3-2 was detected in most protease treatments. This fragment was absent in the untreated PS I complex. The possible cleavage sites may be located in the C, D, and E loops of PsaB with a predicted mass of 45.0 kDa to 63.4 kDa. However, no such fragment was observed in the AEK2, AFK6 and AIC9 PS I complexes. Therefore, the N-terminal domain of PsaB is protected by PsaD, but may not interact with the other subunits.

Previous work has indicated that a 16 kDa proteolytic fragment detected by anti-PsaB718 in thermolysin treated ADC4 PS I complex was resulted from a cleavage at Leu-531 in the I loop of PsaB (28). Similar proteolytic fragments, such as ChB, ClB, LyA, LyB, ThA in different mutant PS I complexes, were detected. These proteolytic fragments could result from cleavages in the I loop of PsaB indicating that the I loop in the C-terminal domain of PsaB may interact with several subunits. In the Lys-C treatments, two close fragments from the cleavages in the I loop of PsaB were obtained in the AFK6, AIC9, and NaI-treated PS I complexes with apparent mass about 15.5 kDa and 16.8 kDa. Only one such fragment was detected in ADC4 and AEK2 each, with a slight difference in their apparent mass. One of the four lysyl residues in the I loop may be involved in the cleavage by the Lys-C endoprotease. The cleavage at Lys-533 may yield a C-terminal fragment with a predicted mass of 22.7 kDa while the cleavage at Lys-542, Lys-547 or Lys-548 would result in the fragment containing C-terminal epitope with a predicted mass of 21.1~21.8 kDa. According to these results, LyB was predicted as the cleavage at Lys-533 in the AEK2, AFK6, AIC9, and NaI-treated PS I complexes while LyA might have resulted from the cleavage at one of the other three lysyl residues in the ADC4, AFK6, AIC9, and NaI-treated PS I complexes.

Apparently, numerous proteolytic fragments resulted from the cleavages in the C-terminal domain of PsaB in the mutant PS I complexes indicating the shielding and protection of this domain by the missing small subunits. These results imply that the C-terminal domain of PsaB may play an important role in the assembly of the PS I complex.

Orientation of the N-terminus of the PsaA protein. The osmotically shocked *Synechocystis* sp. PCC 6803 cells were treated with trypsin and Lys-C and examined by Western blotting. The thylakoid membranes that had been isolated by usual procedure (38) were used as a control. Two antibodies, anti-PsaD and anti-PsbO were used to test the intactness of thylakoid membranes after osmotic treatment and during protease digestions. The domain-specific antibody anti-PsaA2 was used to determine the orientation of PsaA (Fig. 3-3). PsaD, which is located on the *n*-side of photosynthetic membrane, was expected to be exposed to proteases during the treatment. Small fragments in Lys-C and trypsin treatments were recognized by anti-

PsaD indicating the digestion of PsaD in membranes from both control and osmotically shocked cells. Digestion of PsaD in the osmotically shocked cells was not as extensive as in isolated membranes. Due to a large amount of cytoplasmic proteins, protease to protein ratio in the cell treatments was expected to be lower than in the thylakoid treatments. If the thylakoid membranes were intact during the protease treatments, PsbO which is located on the p-side of photosynthetic membrane was expected to remain intact. In membranes, PsbO was not detected after protease treatment. Contrastingly, most PsbO remained intact in the osmotically shocked cells. These results showed that the osmotically shocked thylakoid membranes remain largely intact during the protease treatments. In Lys-C and Trypsin treatments, significant degradation of PsaA was observed when anti-PsaA2 was used for detection. As described before, the degradation of PsaA in Lys-C and trypsin treatments was resulted by the cleavage in the N-terminal loop of PsaA. Therefore N-terminus of PsaA was exposed to proteases in the osmotically shocked cells showing that it is on the n-side of photosynthetic membranes.

Discussion

PS I is a multisubunit protein complex that contains at least 11 polypeptides in cyanobacteria (1). In this study, we used domain-specific antibodies, limited proteolysis, and subunit-deficient PS I complexes to understand the topography of the PsaA and PsaB proteins which form the catalytic hydrophobic core of PS I. Domain-specific antibodies were generated against specific peptides in PsaA and PsaB. Western blotting with thylakoid membranes and purified PS I complexes showed that the antibodies are specific to PsaA or PsaB. N-terminal amino acid sequences of the fragments recognized by antibodies (Table 3-4) demonstrated the domain-specificity of the antibodies to PsaA and PsaB proteins. The GIII fragment with the N-terminus at Lys-449 of PsaB was recognized by the anti-PsaB450 antibodies, while the ThII fragment with the N-terminus at Ile-498 of PsaB was not recognized by anti-PsaB450. These results indicated that the specific binding domain of anti-PsaB450 should be located between Lys-449 and Ile-498 of PsaB protein, the corresponding peptide of anti-PsaB450. N-terminus of the TrI fragment which was not recognized by anti-PsaA2 started at Trp-28 of PsaA. Therefore anti-PsaA2 specifically recognizes the N-terminus of PsaA. Limited proteolysis has been successfully used to probe transmembrane topology of membrane proteins. In these analyses, it is necessary to establish conditions that allow cleavage of the extramembrane loops, but not of the transmembrane regions. We ensured integrity of the hydrophobic core of PS I after proteolysis from measuring PS I activity using artificial electron donor and acceptor (Table 3-3).

The structure of cyanobacterial PS I complex at 4-Å resolution has indicated that PsaA and PsaB have eleven transmembrane helices each. These helices span the lipid bilayer completely (26). Based on the available information and the results in this paper, we proposed a model for transmembrane folding of the PsaA and PsaB core proteins (Fig. 3-4). The homology between PsaA and PsaB proteins implied that they would fold similarly. Therefore, the model in Fig. 3-4 should be applicable to both PsaA and PsaB proteins. In this model, eleven transmembrane helices span the thylakoid membrane completely with the N-termini on the n-side of thylakoid membrane. Consequently, the C-termini are on the p-side of thylakoid membrane (Fig. 3-4). Such orientation is supported by the following observations. The 4-Å crystal structure indicated clearly the complete spanning of the eleven transmembrane helices (26). The Lys-C and trypsin treatments of the osmotically shocked cells in this paper suggested that the N-terminus of PsaA is located on the n-side of the thylakoid membrane. Xu and Chitnis showed that the K loop interacts with PsaD which is located on the n-side of the thylakoid membrane (28). Vallon and Bogorad located the G loop on the n-side and the F and H loops on the p-side by using immunogold labeling (29). The I loop with the F_X binding domain should be located on the n-side of the thylakoid membrane. Also, the six n-side extramembrane loops contain majority of the positive residues, which agrees with the 'positive inside' rule (39, 40). Therefore, now there is sufficient evidence from different sources that collectively demonstrate the transmembrane orientation of the PsaA and PsaB proteins (Fig. 3-4).

Because of the folded structure of the substrate proteins, proteases cannot cleave at every recognition site in the primary sequence. The accessibility of extramembrane loops in PsaA and PsaB to proteases is determined by folding of the loops. Some loops may form loose conformation which will be exposed readily to proteases. In contrast, some loops may have compact conformation, like the helices that are parallel to the membrane plane. Many protease recognition sites in the compact loops may not be accessible to proteases. Also, the protection from other proteins will reduce the surface exposure of the loops. For these reasons, the accessibility of extramembrane loops in PsaA and PsaB differed for each loop (Fig. 3-4). The protease recognition sites in the C, F, and K loops of PsaA and PsaB could not be cleaved, while the H and E loops of PsaB were readily accessible to proteases. The H loop is on the p-side of the thylakoid membrane in the model. It is only one transmembrane helix from the I loop which contains the F_X-binding motif and interacts with PsaC on the n-side (41, 42). From the arrangement of helices in the 4-Å model of PS I, both I and H loops should be located in the center of the PS I core. The extensive accessibility of the H loop to proteases and its p-side-location imply that the H loop of PsaB could be accessible to interaction with plastocyanin or cytochrome c_6, the electron carriers that transfer electrons from cytochrome $b_6 f$ complex to the

P700 reaction center of PS I complex in the p-side of the thylakoid membrane. PsaF is involved in docking of plastocyanin in the plant PS I (7, 19, 20), but not in the cyanobacterial PS I (6, 21). This difference is ascribed to a lysine rich sequence that is present in the N-terminal region of the plant PsaF but not in the cyanobacterial PsaF (43). Besides PsaF, the H and J loops are the only two domains exposed to p-side and located in the center the PS I complex. When the H and J loops sequences of PsaA and PsaB from high plants and cyanobacteria are aligned, there is major difference in a twelve residues sequence in the H loop of PsaB while not in others (4). This information suggests that the H loop of PsaB in cyanobacterial PS I complex may help the docking of plastocyanin or cytochrome c_6 from the p-side of the thylakoid membrane and even contribute to the electron transfer from these two electron donors to the P700 reaction center.

In the 4-Å crystal structure of PS I, the C-terminal domains from both PsaA and PsaB core proteins form a cage where the electron transfer chain is located. This important cage is the catalytic center of PS I complex and is protected by PsaD, PsaC, and PsaE subunits from the n-side and by the surface helices l and l' in the J loop of PsaA and PsaB from the p-side of the thylakoid membrane (26). The protection of the C-terminal domains in PsaA and PsaB is also observed in the protease-treatments of the wild type PS I complex. The only cleavages may occur in the I, J, K, and L loops were the PaVI and PaVII fragments from the papain treatment accompanying with the complete degradation of the small subunits PsaD and PsaF. With intact small subunits, the C-terminal loops I, J, K, and L are well protected from the limited proteolysis. Protection by the small subunits is also shown by the numerous proteolytic fragments from the cleavages in the I loop of PsaB in the mutant PS I complexes (Table 3-6).

The additional fragments in protease treatments of the subunit-deficient PS I complexes provide information about the interactions between the small subunits and the loops of PsaA and PsaB. PsaE is the only missing subunit in the PS I complex from the AEK2 strain. The additional fragments from the protease treatments of AEK2 complexes indicated that the absence of PsaE resulted in possible cleavages in the B, C, D, E, F, G, H, and I loops of PsaA and the I loop of PsaB (Table 3-6). As a n-side subunit, PsaE may interact with the C, E, F, and I loops in the n-side of the thylakoid membrane. The cleavages in the p-side loops may result from further digestion of the degradation products. Therefore, PsaE may interact with the n-side loops in the N-terminal domain of PsaA and the I loops of both PsaA and PsaB (Fig. 3-4). In the protease treatments of the ADC4 PS I complexes, additional cleavages were located in the C, D, E, G, H, and I loops of PsaB (Table 3-6). Thus, PsaD may interact with the n-side loops in the N-terminal domain of PsaB and the I loop of PsaB (Fig. 3-4). Additionally, Xu and Chitnis identified that PsaD may shield the I and K loops of PsaB (28). When the PS I

complexes from the AFK6 and AIC9 strains were treated by proteases, no additional fragments from the N-terminal domains of PsaA and PsaB was observed. The AFK6 and AIC9 mutant PS I complexes do not contain PsaF-PsaJ and PsaI-PsaL, respectively. Therefore, the extramembrane loops in the N-terminal domains of PsaA and PsaB may not interact with these subunits. The trypsin treatment of the AFK6 PS I complex yielded the TrA and TrB fragments. These two fragments resulted from the cleavages in the H loops of PsaA and PsaB (Table 3-6). Between the two subunits absent in the AFK6 complex, PsaJ is mainly a transmembrane helix while PsaF has been proposed to contain a peripheral domain on the p-side of membrane (44). Therefore, the p-side domain of PsaF may interact with the H loops of PsaA and PsaB on the p-side of the thylakoid membrane (Fig. 3-4). In the Lys-C treatments of the AFK6 and AIC9 PS I complexes, additional cleavages were observed in the I loop of PsaB. The missing subunits in these mutant PS I complexes may not directly interact with the I loop of PsaB because the predicted position of these subunits in the 4-Å crystal structure were not close enough to the I loop of PsaB (26). However, chemical crosslinking studies have yielded the following cross-linked products: PsaC-PsaD, PsaC-PsaE, PsaD-PsaL, PsaE-PsaF (44, 45). The interactions between the cross-linked subunits may cause some conformation changes of PsaD, PsaE, or even PsaC in the mutant PS I complexes. Therefore, the I loop of PsaB which was protected by PsaD and PsaE subunits could be exposed to protease in the AFK6 and AIC9 PS I complexes. Correspondingly, the absence of PsaE may cause the conformational change in PsaF and result the exposure of the H loops of PsaA and PsaB which are shielded by PsaF. In the thermolysin treatment of the AEK2 PS I complex, the ThB fragment resulted from the cleavage in the H loop of PsaB (Table 3-6). As described above, PsaF may interact with the H loops of PsaA and PsaB while PsaI, PsaL, and PsaJ may not shield the extramembrane loops of the core proteins (Fig. 3-4).

In the 4-Å crystal structure of PS I, core proteins PsaA and PsaB contribute their C-terminal domain to form the central cage of PS I core while the N-terminal domain of PsaA and PsaB may form the peripheral helices. PsaA and PsaB may crossover in the central cage so both the C-terminal domains of PsaA and PsaB may be protected by a single subunit (26). For this reason, PsaF can interact with both H loops of the core proteins and PsaE can shield both I loops of PsaA and PsaB (Fig. 3-4). However, the peripheral helices in one of the two symmetry region should be donated from one of the core proteins. The absence of PsaE results further cleavages in the N-terminal domain of PsaA while the absence of PsaD results further cleavages in the N-terminal domain of PsaB in the protease treatments of the mutant PS I complexes (Fig. 3-4). This asymmetrical interactions indicated the arrangement of the N-termini of the PsaA and PsaB core proteins related to the PsaD and PsaE subunits. However,

the electron microscopy study has revealed that PsaD and PsaE are located in different sides of the central axis and they do shield different parts of the core proteins (46). Combining these information, we propose a model to distinguish PsaA and PsaB in the 4-Å crystal structure of PS I (Fig. 3-5). In this model, the region partly covered by PsaD and not by PsaE belongs to PsaB while the region only covered by PsaE belongs to PsaA. Therefore, our data indicate that the primed helices in the 4-Å map belong to PsaA while the unprimed helices are assigned to PsaB if the primed and unprimed helices are contributed from each of the core proteins (Fig. 3-5).

To conclude, the topographical analyses of the PsaA and PsaB proteins have allowed us to examine the accessibility of their extramembrane loops to proteases, the shielding and protection of these loops by small subunits, the location of the N-terminus of PsaA and the assignment of the two core proteins relative to small subunits in the 4-Å map. The biochemical techniques are indeed valuable for deciphering structure of membrane proteins and complement of the biophysical techniques which cannot be applied readily to structural analysis of membrane proteins.

Acknowledgments

References

1. Chitnis, P. R., Xu, Q., Chitnis, V. P., and Nechushtai, R. (1995) *Photosynth. Res.* **44**, 23-40.
2. Fromme, P. (1996) *Curr. Opin. Struct. Biol.* **6**, 473-484.
3. Chitnis, P. R. (1996) *Plant Physiol.* **111**, 661-669.
4. Golbeck, J. H. (1994) in *The Molecular Biology of Cyanobacteria* (Bryant, D. A., ed) , pp. 179-220, Kluwer Academic Publishers, Dordrecht, The Netherlands.
5. Kuhn, M., Fromme, P., and Krabben, L. (1994) *Trends Biochem. Sci.* **19**, 401-402.
6. Xu, Q., Yu, L., Chitnis, V. P., and Chitnis, P. R. (1994) *J. Biol. Chem.* **269**, 3205-3211.
7. Haehnel, W., Jansen, T., Gause, K., Klosgen, R. B., Stahl, B., Michl, D., Huvermann, B., Karas, M., and Herrmann, R. G. (1994) *EMBO J.* **13**, 1028-1038.
8. Oh-oka, H., Takahashi, Y., Kuriyama, K., Saeki, K., and Matsubara, H. (1988) *J. Biochem.* **103**, 962-968.

9. Zilber, A., and Malkin, R. (1988) *Plant Physiol.* **88**, 810-814.

10. Xu, Q., Jung, Y. S., Chitnis, V. P., Guikema, J. A., Golbeck, J. H., and Chitnis, P. R. (1994) *J. Biol. Chem.* **269**, 21512-21518.

11. Lelong, C., Setif, P., Lagoutte, B., and Bottin, H. (1994) *J. Biol. Chem.* **269**, 10034-10039.

12. Li, N., Zhao, J. D., Warren, P. V., Warden, J. T., Bryant, D. A., and Golbeck, J. H. (1991) *Biochemistry* **30**, 7863-7872.

13. Chitnis, P. R., and Nelson, N. (1992) *Plant Physiol.* **99**, 239-246.

14. Sonoike, K., Hatanaka, H., and Katoh, S. (1993) *Biochim. Biophys. Acta* **1141**, 52-57.

15. Strotmann, H., and Weber, N. (1993) *Biochim. Biophys. Acta* **1143**, 204-210.

16. Rousseau, F., Setif, P., and Lagoutte, B. (1993) *EMBO J.* **12**, 1755-1765.

17. Yu, L., Zhao, J., Mühlenhoff, U., Bryant, D. A., and Golbeck, J. H. (1993) *Plant Physiol.* **103**, 171-180.

18. Chitnis, P. R., Chitnis, V. P., Xu, Q., Jung, Y.-S., Yu, L., and Golbeck, J. H. (1995) in *Photosynthesis: from Light to Biosphere* (Mathis, P., ed) II, pp. 17-22, Kluwer, Dodrecht.

19. Wynn, R. M., Luong, C., and Malkin, R. (1989) *Plant Physiol.* **91**, 445-449.

20. Hippler, M., Ratajczak, R., and Haehnel, W. (1989) *FEBS Lett.* **250**, 280-284.

21. Chitnis, P. R., Purvis, D., and Nelson, N. (1991) *J. Biol. Chem.* **266**, 20146-20151.

22. Chitnis, V. P., and Chitnis, P. R. (1993) *FEBS Lett.* **336**, 330-334.

23. Xu, Q., Hoppe, D., Chitnis, V. P., Odom, W. R., Guikema, J. A., and Chitnis, P. R. (1995) *J. Biol. Chem.* **270**, 16243-16250.

24. Xu, Q., Odom, W. R., Guikema, J. A., Chitnis, V. P., and Chitnis, P. R. (1994) *Plant Mol. Biol.* **26**, 291-302.

25. Krauß, N., Hinrichs, W., Witt, I., Fromme, P., Pritzkow, W., Dauter, Z., Betzel, C., Wilson, K. S., Witt, H. T., and Saenger, W. (1993) *Nature* **361**, 326-331.

26. Krauß, N., Schubert, W.-D., Klukas, O., Fromme, P., Witt, H. T., and Saenger, W. (1996) *Nature Struct. Biol.* **3**, 965-973.

27. Boekema, E. J., Boonstra, A. F., Dekker, J. P., and Rögner, M. (1994) *J. Bioenerg. Biomemb.* **26**, 17-29.

28. Xu, Q., and Chitnis, P. R. (1995) *Plant Physiol.* **108**, 1067-1075.

29. Vallon, O., and Bogorad, L. (1993) *Eur. J. Biochem.* **214**, 907-915.

30. Fish, L. E., Kuck, U., and Bogorad, L. (1985) *J. Biol. Chem.* **260**, 1413-1421.

31. Reilly, P., Hulmes, J. D., Pan, Y.-C. E., and Nelson, N. (1988) *J. Biol. Chem.* **263**, 17658-17662.

32. Arnon, D. (1949) *Plant Physiol.* **24**, 1-14.

33. Tae, G. S., and Cramer, W. A. (1994) *Biochemistry* **33**, 10060-10068.

34. Xu, Q., Armbrust, T. S., Guikema, J. A., and Chitnis, P. R. (1994) *Plant Physiol.* **106**, 1057-1063.

35. Henry, R. L., Takemoto, L. J., Murphy, J., Gallegos, G. L., and Guikema, J. A. (1992) *Plant Physiol. Biochem.* **30**, 357-364.

36. Mehler, A. H. (1951) *Arch. Biochem. Biophys.* **33**, 65-77.

37. Mehler, A. H. (1951) *Arch. Biochem. Biophys.* **34**, 339-351.

38. Chitnis, V. P., Xu, Q., Yu, L., Golbeck, J. H., Nakamoto, H., Xie, D. L., and Chitnis, P. R. (1993) *J. Biol. Chem.* **268**, 11678-11684.

39. von Heijne, G., and Gavel, Y. (1988) *Eur. J. Biochem.* **174**, 671-674.

40. von Heijne, G. (1988) *Biochim. Biophys. Acta* **947**, 307-333.

41. Smart, L. B., Warren, P. V., Golbeck, J. H., and McIntosh, L. (1993) *Proc. Natl. Acad. Sci. U. S. A.* **90**, 1132-1136.

42. Warren, P. V., Smart, L. B., McIntosh, L., and Golbeck, J. H. (1993) *Biochemistry* **32**, 4411-4419.

43. Hippler, M., Reichert, J., Sutter, M., Zak, E., Altschmied, L., Schröer, U., Herrmann, R. G., and Haehnel, W. (1996) *EMBO J.* **15**, 6374-6384.

44. Armbrust, T. S., Chitnis, P. R., and Guikema, J. A. (1996) *Plant Physiol.* **111**, 1307-1312.

45. Xu, Q., Chitnis, V. P., Ke, A., and Chitnis, P. R. (1995) in *Photosynthesis: from Light to Biosphere* (Mathis, P., ed) II, pp. 87-90, Kluwer, Dodrecht.

46. Kruip, J., Chitnis, P. R., Lagoutte, B., Rogner, M., and Boekema, E. J. (1997) *J. Biol. Chem.* **271**, 17061-17069

47. Cohen, Y., Chitnis, V. P., Nechushtai, R., and Chitnis, P. R. (1993) *Plant Mol. Biol.* **23**, 895-900.

48. Chitnis, P. R., Reilly, P. A., and Nelson, N. (1989) *J. Biol. Chem.* **264**, 18381-18385.

49. Chitnis, P. R., Reilly, P. A., Miedel, M. C., and Nelson, N. (1989) *J. Biol. Chem.* **264**, 18374-18380.

Figure Legends

FIG. 3-1. **Accessibility of the wild type PS I complex to proteases.** Purified wild type PS I complexes were incubated with different concentrations of proteases for the time indicated in Table 3-2. The concentrations 0-3 were 0, 0.4, 2, 10 µg papain/mg chlorophyll in papain treatment and 0, 10, 50, 250 µg protease/mg chlorophyll in other protease treatments.

The samples were resolved by Tricine-urea-SDS-PAGE and transferred to the Immobilon-P polyvinylidene difluoride membranes. The protein fragments were detected by Coomassie Blue (*CB*) staining (25 µg chlorophyll used) and Western blotting (5 µg chlorophyll used) with three domain-specific antibodies. The clostripain and pepsin treatments are not shown here. The molecular masses of protein fragments were determined from migration of the following protein markers: insulin (2.9 kDa), bovine trypsin inhibitor (5.8 kDa), lysozyme (14.7 kDa), β-lactoglobulin (18.5 kDa), carbonic anhydrase (28.9 kDa) and ovalbumin (44.0 kDa).

FIG. 3-2. **Treatment of the subunit-deficient PS I complexes with proteases.** The PS I complexes were incubated with different proteases at the final concentration as described in Table 3-2. The samples equivalent to 5 µg chlorophyll were analyzed by Tricine-urea-SDS-PAGE and Western blotting with three domain-specific antibodies. For treatments: -, control; *Ch*, chymotrypsin; *Cl*, clostripain; *Gl*, Glu-C; *Ly*, Lys-C; *Pa*, papain; *Pe*, pepsin; *Th*, thermolysin; *Tr*, trypsin.

FIG. 3-3. **Transmembrane orientation of the N-terminus of the PsaA protein.** Thylakoid membranes were isolated from osmotically shocked cells treated by Lys-C and trypsin while isolated thylakoid membranes were treated by proteases as control. Samples equivalent to 5 µg chlorophyll were analyzed by Tricine-urea-SDS-PAGE and Western blotting with three antibodies. *O.S.*, osmotically shocked; *Ly*, Lys-C; *Tr*, trypsin.

FIG. 3-4. **A folding model for PS I core proteins PsaA and PsaB.** The putative transmembrane helices are based on the hydropathy analyses of PsaA and PsaB from *Synechocystis* sp. PCC 6803 (30). The 11 transmembrane helices are shown as *dark boxes* for the N-terminal helices and *light boxes* for the C-terminal helices and are *numbered* as *I-XI* followed by *italic letters a-o* corresponding to the helices in the 4-Å crystal structure (26) with the starting and ending sites. Extramembrane loops are named as *italic capital letters A-L* and shown as *light thin lines*. Two α-helices that are parallel to the membrane plane (26) are shown as *boxes* in the J and K loops. The peptides for raising domain-specific antibodies are indicated as *dark bold lines* with starting and ending sites. In the model, the '⇨' and '➡' with amino acid residues indicate the identified cleavage site on PsaA and PsaB, respectively. A pair of '>' or '>' coupled with numbers indicate the possible region of cleavage on PsaA and PsaB, respectively. Information from immunogold labeling which showed orientation of some extramembrane loops of PsaA (29) are marked as *small boxes* in the F, G, and H loops. The *large* 'c' and 'k' with the descriptions indicate the interactions among the small subunits and PsaA and PsaB, respectively. '*' indicates the information from reference (28).

FIG. 3-5. **A topological model for PS I complex.** The model is modified from the 4-Å crystal structure (26). The organization of PS I complex is viewed from the *top*. The PS I subunits are indicated as the regions distinguished by *dotted lines* with the transmembrane helices (26).

Table 3-1. Strains of Synechocystis sp. PCC 6803 that were used in this study

Strains	Description	Characteristics of the purified PSI complexes
Wild type	Glucose-tolerant strain	Eleven subunits resolved upon electrophoresis; capable of light-driven Cyt c6 oxidation and Fd reduction
ADC4	psaD replaced by a chloramphenicol-resistance gene	PsaD and PsaL missing; no Fd-mediated NADP+ photoreduction (10, 34, 47, 48)
AEK2	psaE replaced by a kanamycin-resistance gene	Only PsaE missing; reduced Fd-mediated NADP+ photoreduction (10, 49)
AFK6	psaF replaced by a kanamycin-resistance gene; psaJ transcriptionally inactivated	PsaF and PsaJ missing and level of PsaE decreased; normal rate of P700 reduction by Cyt c6 (6, 10, 21)
AIC9	psaI interrupted by a chloramphenicol-resistance gene; psaL transcripts decreased	PsaI and PsaL missing; small decrease of Fd-mediated NADP+ photoreduction (23)

Table 3-2. Reaction conditions of proteases treatment

Proteases	Thermolysin (EC 3.4.24.4)	Glu-C (EC 3.4.21.19)	Chymotrypsin (EC 3.4.21.1)	Papain (EC 3.4.22.2)	Lys-C (EC 3.4.21.50)	Trypsin (EC 3.4.21.4)	Clostripain (EC 3.4.22.8)	Pepsin (EC 3.4.23.1)
Specificity	^[VILWMF]	[E]^	[YFW]^	[RKILG]^	[K]^	[KR]^	[R]^	[FLYWI]^
Source	*Bacillus thermo- proteolyticus* (Sigma)	*Staphylococcus aureus* (Boehringer Mannheim)	bovine pancreas (Boehringer Mannheim)	*Carica papaya* (Boehringer Mannheim)	*Pseudomonas aeruginosa* (Promega Biotech)	porcine pancreas (Promega Biotech)	*Clostridium histolyticum* (Promega Biotech)	porcine stomach (Boehringer Mannheim)
Final protease concentration	250 µg/mg Chl	250 µg/mg Chl	250 µg/mg Chl	10 µg/mg Chl	250 µg/mg Chl	250 µg/mg Chl	250 µg/mg Chl	250 µg/mg Chl
Proteolysis condition*	10mM MOPS (pH7.0); 5mM CaCl$_2$	50mM NH$_4$HCO$_3$ (pH7.8)	50mM Tris-HCl (pH8.0); 10mM CaCl2	10mM MOPS (pH7.0); 0.5mM EDTA; 1.5mM CySH	25mM Tris-HCl (pH7.5); 1mM EDTA	50mM Tris-HCl (pH8.0); 1mM CaCl2	20mM Tris-HCl (pH7.5); 1mM CaCl2; 2mM DTT	20mM NaH$_2$PO$_4$ (pH4.0)
Incubation	37°C 30min	15°C 30min	25°C 1hour	25°C 1hour	37°C 1hour	37°C 1hour	37°C 1hour	37°C 1hour
Termination	20mM EDTA	20mM PMSF	20mM PMSF	20mM PMSF	20mM PMSF	20mM PMSF	20mM EDTA	20µM pepstatinA

*: 0.05% Triton X-100 was added for purified PS I complexes.

74

Table 3-3. Oxygen measurements of protease-treated PS I complexes

Protease treatment	PS I activity (μmol O_2/mg Chl·hour)
Control	377.5
Chymotrypsin	416.0
Clostripain	371.9
Glu-C	408.8
Lys-C	472.8
Papain	380.9
Pepsin	431.5
Thermolysin	455.9
Trypsin	503.4

Table 3-4. N-terminal amino acid sequence analysis of the proteolytic fragments in Fig. 3-1

The position of the first amino acid was identified after comparison with the deduced amino acid sequence of PsaA and PsaB.

Proteolytic fragments	N-terminal sequence	Position of the first amino acid	Predicted fragment	Apparent mass(kDa)	Predicted mass(kDa)
ThI	ATKFPKF	PsaB: 2	PsaB2-497	45.0	54.7
ThII	INSGINS	PsaB: 498	PsaB498-731	23.8	26.4
ThIII	WGIGHS	PsaB: 295	PsaB295-497	16.2	22.1
ThIV	ILNAHKG	PsaB: 304	PsaB304-497	15.2	21.1
GlIII	KQILIE	PsaB: 449	PsaB449-731	27.6	31.7
ChI	SQDXA	PsaB: 9	PsaB9-506	43.2	54.8
PaIII	QATXGK	PsaB: 462	PsaB462-731	26.2	30.1
TrI	WGXPG	PsaA: 28	PsaA28-?	53.6	?

Table 3-5. Accessibility of PsaA and PsaB to proteases: the predicted proteolysis sites

Proteolytic fragments	Immunodetection	Apparent mass (kDa)	Predicted fragment	Accessible site location*	Predicted mass (kDa)	Prediction type
ThI	Anti-PsaB450	45.0	PsaB: 2-497	PsaB: H	54.7	1
ThII	Anti-PsaB718	23.8	PsaB: 498-731	PsaB: H	26.4	1
ThIII	Anti-PsaB450	16.2	PsaB: 295-497	PsaB: E&H	22.1	1
ThIV	Anti-PsaB450	15.2	PsaB: 304-497	PsaB: E&H	21.1	1
GII	Anti-PsaB450&B718	41.2	PsaB: 304-731	PsaB: E	47.5	2
GIII	Anti-PsaA2	33.7	PsaA: 1-(323~342)	PsaA: E	35.8~37.9	3
GIIII	Anti-PsaB450&B718	27.6	PsaB: 449-731	PsaB: H	31.7	1
GIIV	Anti-PsaA2	21.0	PsaA: 1-(241~251)	PsaA: D	26.7~27.8	3
GIV	Anti-PsaA2	44.5	PsaA: 1-512	PsaA: H	56.7	2
GIVI	Anti-PsaA2	29.1	PsaA: 1-(323~342)	PsaA: E	35.8~37.9	3
GIVII	Anti-PsaA2	12.0	PsaA: 1-101	PsaA: B	11.5	2
GIVIII	Anti-PsaB450&B718	45.9	PsaB: (202~267)-731	PsaB: D	51.7~58.5	3
GIIX	Anti-PsaB450	36.9	PsaB: ?	PsaB: ?	?	5
GIX	Anti-PsaB450	23.4	PsaB: ?	PsaB: ?	?	5
ChI	Anti-PsaB450	43.2	PsaB: 9-506	PsaB: A&H	54.8	1
ChII	Anti-PsaB450&B718	17.3	PsaB: 445-731	PsaB: H	32.1	4
PaI	Anti-PsaA2	40.6	PsaA: 1-(414~433)	PsaA: G	45.8~48.1	3
PaII	Anti-PsaA2	30.3	PsaA: 1-(280~344)	PsaA: DorE	31.1~38.1	3
PaIII	Anti-PsaB450&B718	26.2	PsaB: 462-731	PsaB: H	30.1	1
PaIV	Anti-PsaA2	22.7	PsaA: 1-(223~269)	PsaA: D	24.7~29.8	3
PaV	Anti-PsaA2	13.0	PsaA: 1-(120~151)	PsaA: B	13.6~16.7	3
PaVI	Anti-PsaB718	20.8	PsaB: (477~549)-731	PsaB: HorI	21.1~28.6	3
PaVII	Anti-PsaB718	13.7	PsaB: (595~614)-731	PsaB: J	13.6~15.7	3
PaVIII	Anti-PsaB450	42.6	PsaB: ?	PsaB: ?	?	5
PaIX	Anti-PsaB450	36.4	PsaB: ?	PsaB: ?	?	5
LyI	None	53.4	PsaA: ?	PsaA: A	?	4
TrI	None	53.6	PsaA: 28-?	PsaA: A	?	1
TrII	Anti-PsaB450	39.5	PsaB: ?	PsaB: ?	?	5
TrIII	Anti-PsaB450	16.7	PsaB: ?	PsaB: ?	?	5
PeI	Anti-PsaB450	41.4	PsaB: ?	PsaB: ?	?	5
PeII	Anti-PsaB450	35.9	PsaB: ?	PsaB: ?	?	5
PeIII	Anti-PsaB450	14.6	PsaB: ?	PsaB: ?	?	5
ClI	Anti-PsaB450&B718	43.8	PsaB: 293-731	PsaB: E	48.8	2

*: For nomenclature of loops, see Fig. 3-4.

Table 3-6. Additional proteolytic fragments upon treatment of mutant PS I complexes with proteases

| Proteolytic fragments	Mutant PS I complexes	Immuno-detection	Apparent mass (kDa)	Predicted fragment	Predicted mass (kDa)	Accessible site location*
ChA	NaI	anti-PsaA2	15.1	PsaA: 1-(144~190)	15.9~21.2	PsaA: B,C
ChB	NaI, ADC4	anti-PsaB718	15.9	PsaB: (551~571)-731	18.8~20.8	PsaB: I
ChC	AEK2	anti-PsaA2	30.4	PsaA: 1-(277~341)	30.8~37.7	PsaA: D,E
ChD	AEK2	anti-PsaA2	19.8	PsaA: 1-(189~289)	21.1~32.0	PsaA: C,D
ChE	AEK2	anti-PsaA2	17.6	PsaA: 1-(189~289)	21.1~32.0	PsaA: C,D
ChF	AEK2	anti-PsaA2	11.4	PsaA: 1-(100~156)	11.4~17.3	PsaA: B
ClA	NaI, AEK2	anti-PsaA2	49.1	PsaA: 1-(462~571)	51.5~63.1	PsaA: H,I
ClB	NaI	anti-PsaB718	15.9	PsaB: (540~562)-731	19.7~22.1	PsaB: I
ClC	AEK2	anti-PsaA2	24.0	PsaA: 1-312	34.6	PsaA: E
LyA	NaI, ADC4, AFK6, AIC9	anti-PsaB718	15.5	PsaB: (543~549)-731	21.1-21.8	PsaB: I
LyB	NaI, AEK2, AFK6, AIC9	anti-PsaB718	16.8	PsaB: 534~731	22.7	PasB: I
LyC	NaI, ADC4	anti-PsaB718	28.2	PsaB: (403~450)-731	31.0~36.8	PsaB: G,H
ThA	NaI, ADC4, AEK2	anti-PsaB718	15.5	PsaB: (532~570)-731	19.0~22.9	PsaB: I
ThB	AEK2	anti-PsaB718	26.0	PsaB: (440~498)-731	26.4~32.6	PsaB: H
ThC	AEK2	anti-PsaA2	37.4	PsaA: 1-(380~429)	42.0-47.5	PsaA: F,G
ThD	AEK2	anti-PsaA2	29.0	PsaA: 1-(314-343)	34.8~38.0	PsaA: E
ThE	AEK2	anti-PsaA2	22.8	PsaA: 1-(222-289)	24.6~32.0	PsaA: D
ThF	AEK2	anti-PsaA2	14.3	PsaA: 1-(129~192)	14.4~21.5	PsaA: B,C
TrA	AFK6	anti-PsaA2	40.0	PsaA: 1-(462~519)	51.5~57.4	PsaA: H
TrB	AFK6	anti-PsaB718	22.7	PsaB: (450~468)-731	29.5~31.6	PsaB: H
LF	NaI, ADC4	anti-PsaB718	40.0~45.0	PsaB: (158~327)-731	45.0~63.4	PsaB: C,D,E

*: For nomenclature of loops, see Fig. 3-4.
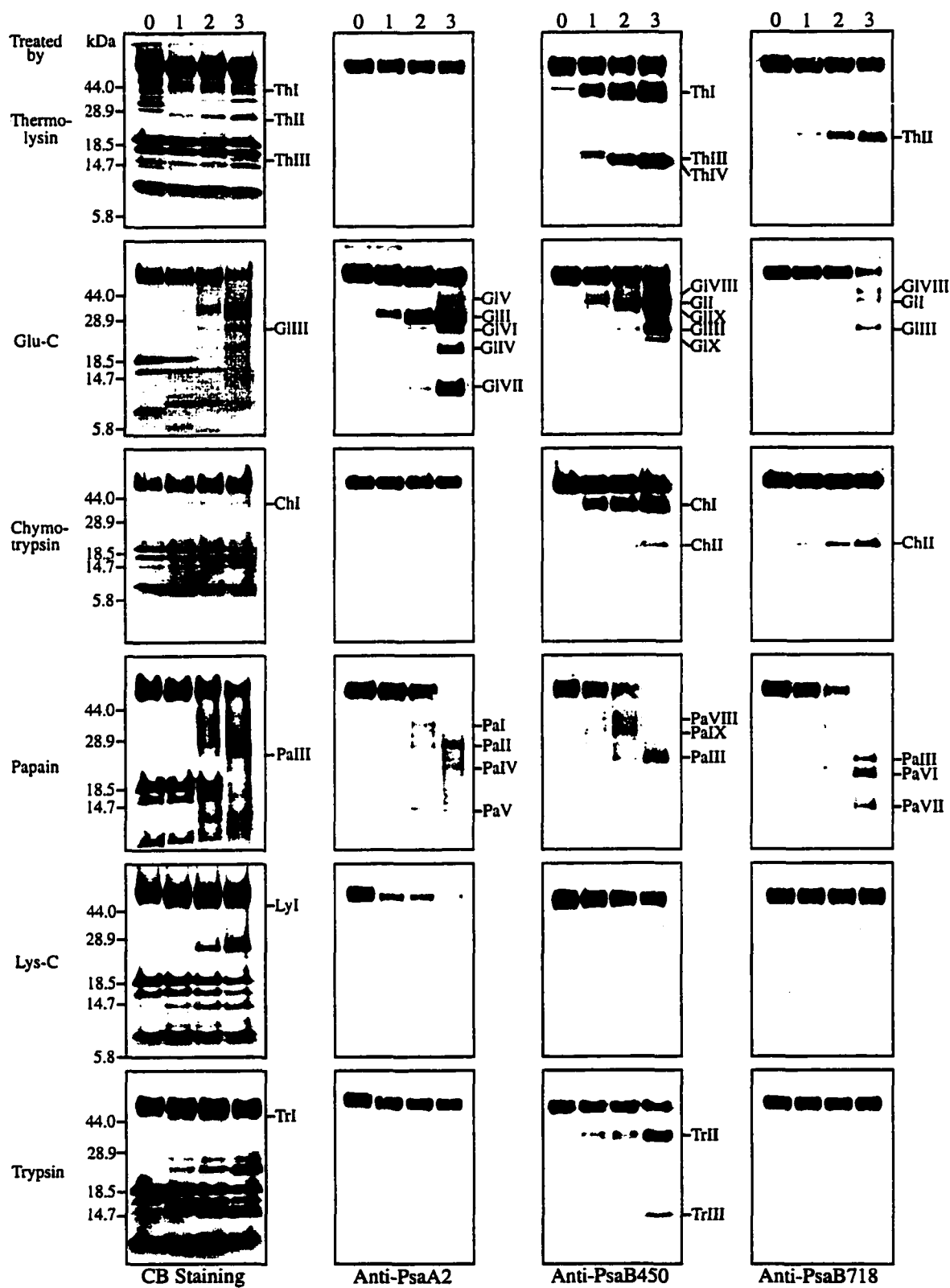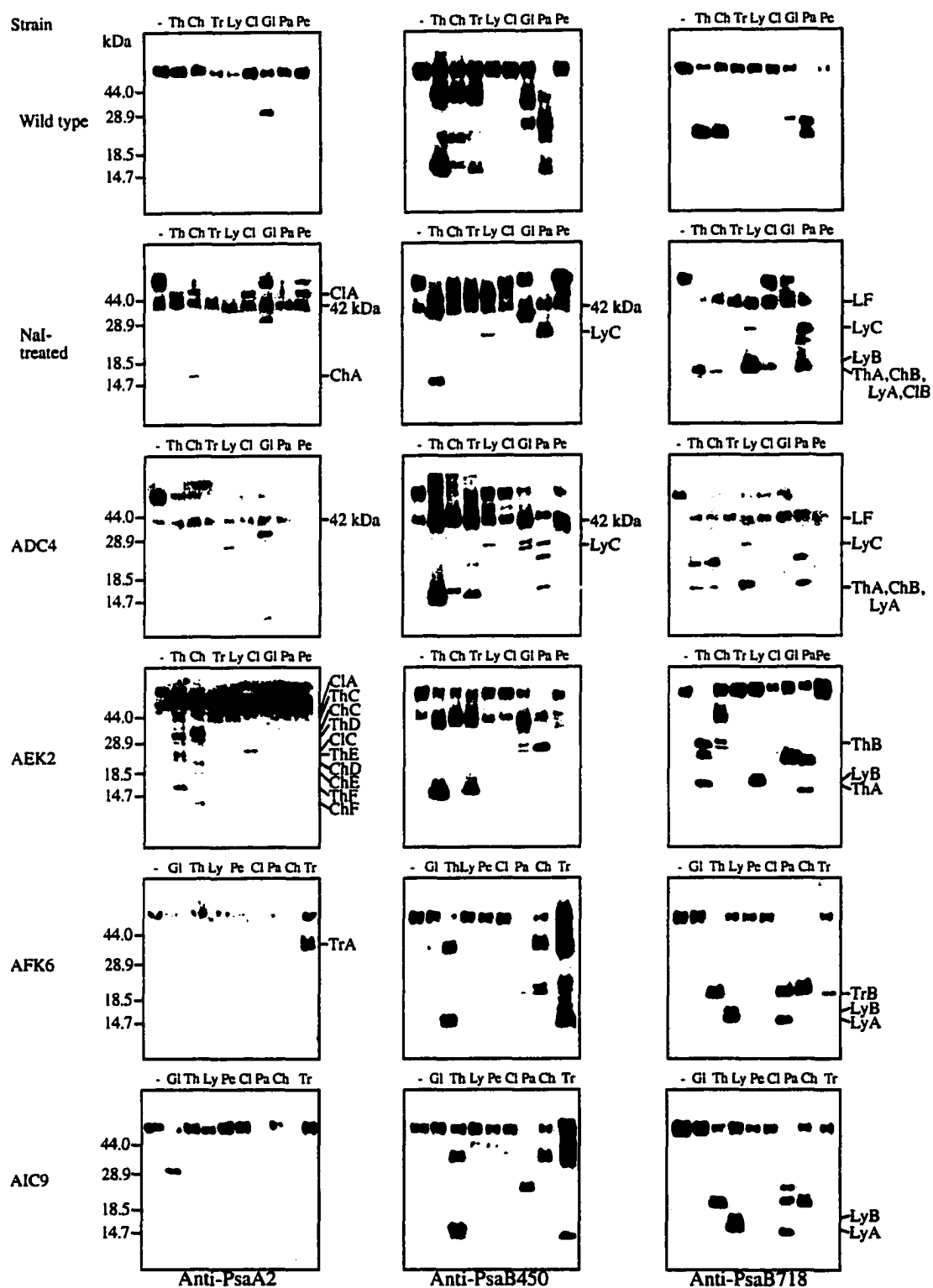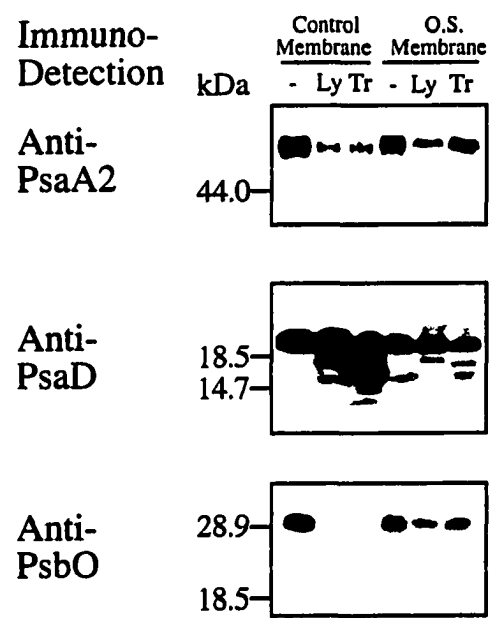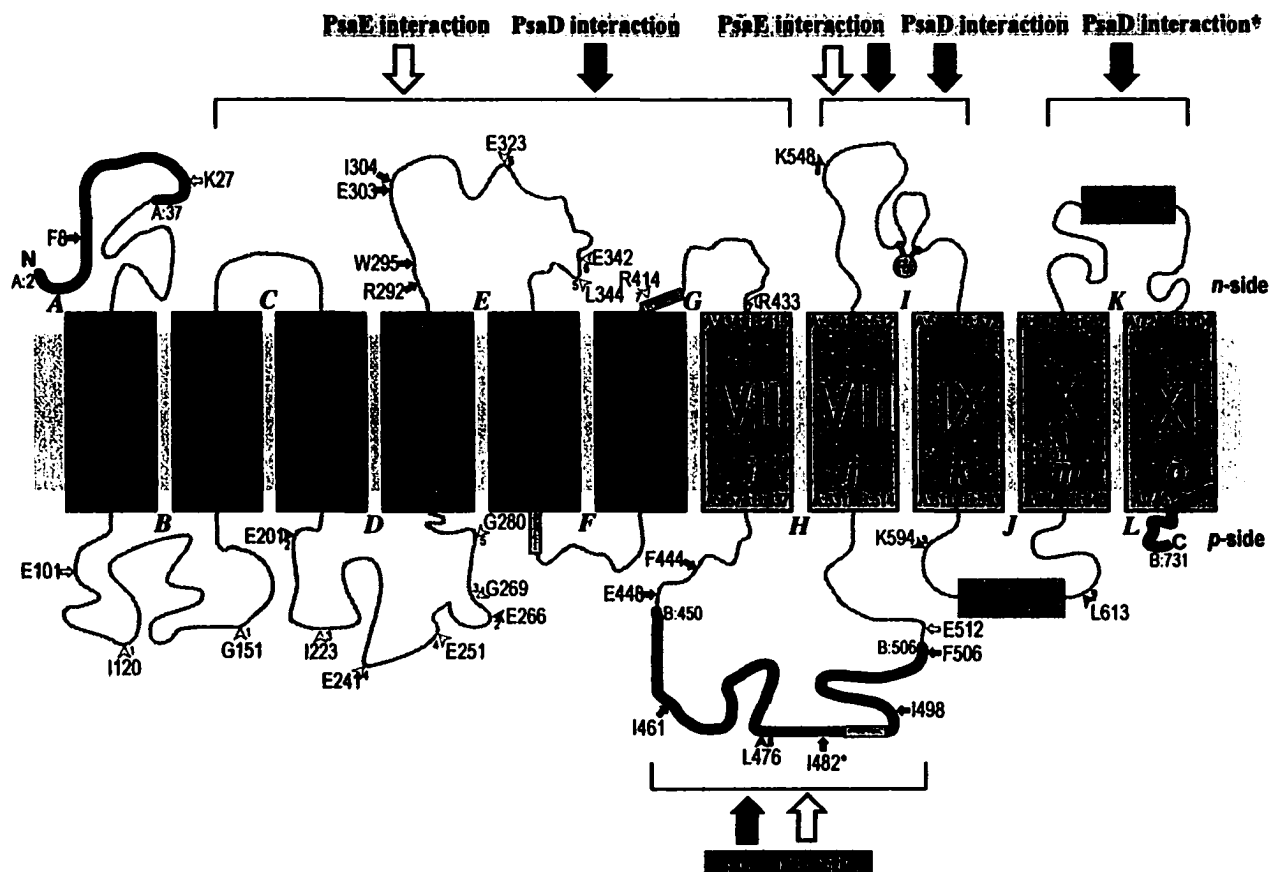
Fig. 3-1

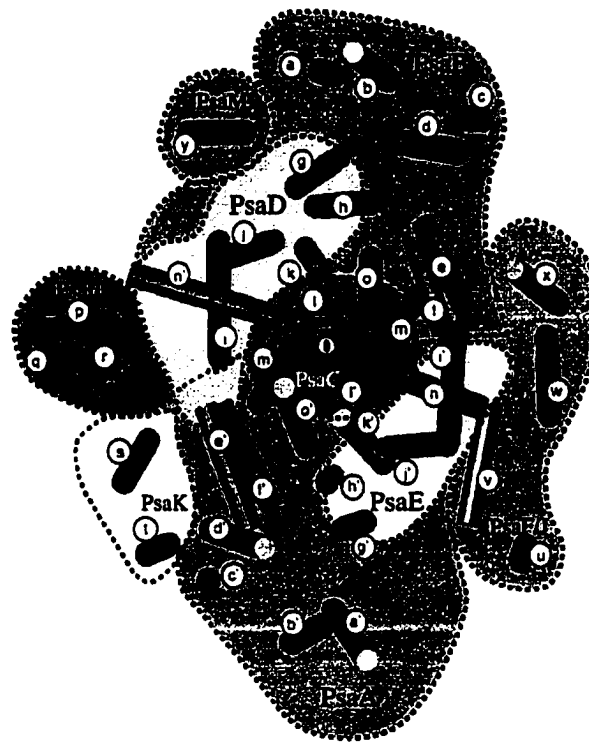Fig. 3-2

Fig. 3-3

Fig. 3-4

Fig. 3-5

CHAPTER 4. OXIDIZING SIDE OF THE CYANOBACTERIAL PHOTOSYSTEM I: EVIDENCE FOR INTERACTION BETWEEN THE ELECTRON DONOR PROTEINS AND A LUMINAL SURFACE HELIX OF THE PSAB SUBUNIT[1]

A paper published in the Journal of Biological Chemistry[2]

Jun Sun, Wu Xu, Manuel Hervás, José A. Navarro, Miguel A. De La Rosa, Parag R. Chitnis

Summary

Photosystem I (PSI) interacts with plastocyanin or cytochrome c_6 on the luminal side. To identify sites of interactions between plastocyanin/cytochrome c_6 and the PSI core, site-directed mutations were generated in the luminal J loop of PsaB protein from *Synechocystis* sp. PCC 6803. The eight mutant strains differed in their photoautotrophic growth. Western blotting with subunit-specific antibodies indicated that the mutations affected the PSI level in the thylakoid membranes. PSI proteins could not be detected in the S600R/G601C/N602I, N609K/S610C/T611I, or M614I/G615C/W616A mutant membranes. The other mutant strains contained different levels of PSI proteins. Among the mutant strains that contained PSI proteins, the H595C/L596I, Q627H/L628C/I629S, and N638C/N639S mutants showed similar levels of PSI-mediated electron transfer activity when either cytochrome c_6 or an artificial electron donor was used. In contrast, cytochrome c_6 could not function as an electron donor to the W622C/A623R mutant, even though the PSI activity mediated by an artificial electron donor was detected in this mutant. Thus, the W622C/A623R mutation affected the interactions of the PSI complex with cytochrome c_6. Biotin-maleimide modification of the mutant PSI complexes indicated that the H595, W622, L628, Y632, and N638 residues in the wild type PsaB maybe exposed on the surface of PSI complex. The results presented here demonstrate the role of an extramembrane loop of a PSI core protein in the interaction with soluble electron donor proteins.

Introduction

PSI[3] is a multisubunit membrane-protein complex that catalyzes electron transfer from the reduced plastocyanin in the thylakoid lumen to the oxidized ferredoxin in the chloroplast stroma or cyanobacterial cytoplasm (1-4). In cyanobacteria and green algae, cytochrome c_6 can substitute plastocyanin depending on the growth conditions (5-7). The crystal structure of PSI at 4 Å resolution is available (8,9). PSI contains 89 chlorophyll a molecules, 83 of which constitute the core antenna system. The PsaA and PsaB subunits form the heterodimeric core that harbors most of the antenna chlorophyll a molecules, β-carotenes, the primary electron donor P700, and a chain of electron acceptors, A_0, A_1, and F_X. In addition to the core proteins, the cyanobacterial PSI complex contains three peripheral proteins (PsaC, PsaD, and PsaE) and six integral membrane proteins (PsaF, PsaI, PsaJ, PsaK, PsaL, and PsaM) (1-3). The PsaC, PsaD, and PsaE subunits constitute the reducing side of the PSI complex. PsaC binds the terminal electron acceptors F_A and F_B, which donate electrons to ferredoxin. PsaD and PsaE facilitate the docking of ferredoxin on PSI (1). Functions of the other subunits have been studied by using subunit-deficient mutants of cyanobacteria and algae (10-17).

On the luminal side of thylakoid membranes, PSI accepts electrons from plastocyanin or cytochrome c_6. The interaction of plastocyanin with plant and algal PSI complexes shows a fast kinetic step, which can be attributed to a multi-step reaction mechanism of electron transfer (18,19). Some cyanobacteria have a simpler one-step bimolecular collision mechanism (20,21). Cross-linking studies have indicated that plastocyanin can be cross-linked to the N-terminal lysine-rich region of chloroplast PsaF, which is not found in the cyanobacterial PsaF (22). Thus, the interactions between plastocyanin and the plant PSI include initial electrostatic interactions between the N-terminal domain of PsaF and the conserved negative patches of plastocyanin. However, the PsaF subunit of PSI is not required in the interactions with plastocyanin in *Synechocystis* sp. PCC 6803 (13,14,23) and in *Synechococcus elongatus* (24). The deletion of PsaF in *Chlamydomonas reinhardtii* did not abolish the electron transfer from plastocyanin to P700 (25). Therefore, plastocyanin and cytochrome c_6 contact the PsaA and PsaB core proteins directly. The luminal extramembrane loops of PsaA and PsaB are likely candidates for interaction with plastocyanin during electron transfer.

---

[3] The abbreviations used are: PS, photosystem; DM, dodecyl-β-D-maltoside; WT, wild type; RWT, recovered wild type; PCR, polymerase chain reaction; OD, optical density; NADP, nicotinamide adenine dinucleotide phosphate; DAD, 3,6-diaminodurene; MV, methyl viologen; SDS, sodium dodecyl sulfate; PAGE, polyacrylamide gel electrophoresis; Tricine, N-[2-hydroxy-1,1-bis(hydroxymethyl)ethyl]glycine.

In the crystal structure of PSI, the luminal side of PSI is flat with a 10 Å protrusion beyond the membrane boundary (8,9). There is a 3-nm deep indentation in the center, perhaps caused by a partial separation between PsaA and PsaB. In the structural modeling, the dimensions of plastocyanin matched well inside this cavity (26,27). Near the luminal indentation, two surface α-helices *l* and *l'* are parallel to the membrane plane and are located near the P700 chlorophyll *a* dimer (8,9). The *l* and *l'* helices are analogous to similar surface helices in the purple bacterial reaction center (26,28). The *l* and *l'* helices are in the J extramembrane loops that are located between the transmembrane helices *k* and *m* of the core proteins (see reference (29) for the topology of PSI core proteins and nomenclature of loops). We postulate that these helices interact with plastocyanin during electron transfer.

To investigate the role of the J loops in the assembly and function of the PSI complex and in the interaction with the electron donors, we generated cysteine-scanning multipoint mutations in conserved amino acids in the J loop of the PsaB protein. A residue was changed to a cysteinyl residue in each of the mutations. Such approach has been used to study the topographical features of membrane proteins (30,31). The mutations were introduced into a *psaB*-deletion strain of *Synechocystis* sp. PCC 6803. Here we present the biochemical characterization of the mutant strains.

Experimental procedures

Cyanobacterial cultures, membrane isolation and PSI purification. Strains of *Synechocystis* sp. PCC 6803 were cultured in BG-11 medium with appropriate antibiotics (30 mg/l chloramphenicol or 40 mg/l kanamycin) at 30°C. For autotrophic growth, cells were grown in BG-11 medium under medium light intensity of 40 $\mu mol \cdot m^{-2} \cdot s^{-1}$. For heterotrophic growth, cells were grown in BG-11 supplemented with 5 mM of glucose under low light intensity of 5 $\mu mol \cdot m^{-2} \cdot s^{-1}$. Cells were harvested at the late exponential growth phase. Previously published methods were used for isolation of thylakoid membranes and purification of trimeric PSI complexes with DM (32). The chlorophyll *a* concentration (33) and the carotene concentration (34) were estimated according to previously published methods.

Generation of mutations in the psaB gene. For mutagenesis in the C-terminal region of the PsaB protein of *Synechocystis* sp. PCC 6803, a PSI-less recipient strain (LKC) was generated by replacing an 1187-bp 3'-coding region of the *psaB* gene (the *Hind*III-*Eco*RI fragment) with a cassette for kanamycin resistance (Fig. 4-1). For this purpose, we constructed a plasmid that contained the kanamycin resistance gene cassette and an 843-bp 3'-flanking region downstream of the *psaB* gene. Upstream from the resistance cartridge, the plasmid contained a 2703-bp *Acc*I-*Hind*III fragment that includes most of the *psaA* gene, the 5'-region of the *psaB* gene,

and the untranslated region between the *psaA* and *psaB* genes. The plasmid was introduced into a PSI-less strain, which has a partial deletion of *psaA* and *psaB* genes and is capable of heterotrophic growth under low light intensity (35,36). The resulting kanamycin-resistant recipient strain is capable of heterotrophic growth under low light intensity. To introduce the WT and mutant *psaB* gene into the recipient strain, we constructed the p3C+ recombinant plasmid. In this plasmid, a 1587-bp *SmaI-EcoRI* fragment of the *psaB* gene (including the 3'-coding region of *psaB*), a chloramphenicol resistance gene, and the 3'-flanking region were cloned into the polylinker of pBluescript II KS (Stratagene, CA) (Fig. 4-1). All PsaB mutants were generated by a PCR-mediated mutation technique (37). The mutagenic oligonucleotide primers contained a *PstI* or *NsiI* restriction endonuclease recognition site. The mutated recombinant plasmids were sequenced completely to ensure the presence of desired changes and the absence of errors by *Taq* DNA polymerase. The DNAs were used to transform the recipient strain LKC. The p3C+ plasmid with the WT gene was introduced back into the LKC strain to yield the recovered wild type (RWT) strain that was used as the positive control in these studies. The transformation was performed at 30°C under heterotrophic growth condition according to reference (38). The chloramphenicol-resistant transformants were selected, segregated for three generations, and replica-plated to confirm the absence of the kanamycin resistance gene.

Characterization of the mutant strains. After segregation, the chloramphenicol-resistant transformants were cultured in liquid BG-11 medium and the genomic DNA was isolated. Integration of the chloramphenicol resistance gene into the genome of the mutant strains was confirmed by PCR amplification of appropriate fragments using genomic DNA. Nucleotide sequence of the corresponding PCR fragments was determined to confirm mutations. Cell counting showed that number of cells per OD at 730 nm is the same (5.5×10^7 cells·OD_{730}^{-1}ml^{-1}) for both the RWT and LKC cultures. OD_{730} was measured using an UV-160U spectrophotometer (Shimadzu, Tokyo, Japan) and was used as a measure of cell count to monitor the growth of the mutant strains and in normalizing other characteristics of the mutant strains. Accumulation of PSI proteins was examined by analytical SDS-PAGE and immunodetection (29). The antibodies that were used for immunodetection have been described previously (32). The P700 content was estimated by the measurement of photoinduced absorbance changes at 820 nm (20,39). The mutant PSI complexes were modified by biotin-maleimide according to a previously published method (32).

The PSII activity of *Synechocystis* cells was measured as light-driven oxygen evolution in which electrons are transferred from water to *p*-benzoquinone via the PSII complex. The PSI activity was monitored by oxygen uptake with the Mehler reaction (40,41) using the artificial

electron carriers DAD and MV (32). In this reaction, ascorbate reduces DAD, which in turn donates electrons to P700. Light-driven PSI electron transfer reduces MV. The oxidation of the reduced MV consumes oxygen. Alternatively, the PSI activity in the membrane can be measured by oxygen uptake with 15 μM cytochrome c_6 replacing DAD as the electron donor. The PSI activity in the membrane was also determined from NADP$^+$ photoreduction assays using cytochrome c_6 and ferredoxin as the electron donor and acceptor of the PSI complex (32). These activities were normalized on equal cell basis.

Results

Mutagenesis of the J loop of the PsaB protein. In the crystal structure of the PSI complex, a pair of surface helices l and l' are present in the J extramembrane loops. The secondary structure prediction using the Garnier algorithm (42) indicated a putative α-helix in the J loop of PsaB from M614 to Y632 (Fig. 4-2). This peptide fragment is highly conserved among the PsaB proteins from higher plants, algae, and cyanobacteria. This region also shows high homology between the PsaA and PsaB proteins. Besides the putative helix, several other amino acid residues in the J loop are also conserved among PsaB from different sources and between the PsaA and PsaB proteins. We targeted these conserved residues in the mutagenesis experiments, and generated eight multipoint mutations in the J loop of the PsaB protein (Fig. 4-2).

Characterization of the mutant cells. The PSI-less LKC cells were more blue than the WT cells due to the reduced level of chlorophyll while retaining phycobilisomes (36). During segregation, the RWT strain as well as the SJ1, SJ2, SJ4, SJ6, and SJ8 mutant strains formed green colonies, whereas the SJ3, SJ5, and SJ7 mutant strains formed bluish colonies that resembled the recipient LKC strain.

The RWT, LKC, and mutant strains were cultured under photoautotrophic and heterotrophic growth conditions and the increase in cell density was measured (Table 4-1). All strains grew heterotrophically with similar doubling time, ranging from 27 to 30 hours, indicating their similar abilities to utilize externally supplied glucose under low light intensity. Therefore, the respiratory system was not affected in the mutant strains. Under photoautotrophic growth conditions, cells of the LKC, SJ3, SJ5, SJ7, and SJ8 strains either died or did not grow. The RWT and SJ6 cells had the fastest growth, whereas the SJ1, SJ2 and SJ4 cells grew slower than the RWT cells. Therefore, all mutations, except for the amino acid replacements in SJ6, affected the autotrophic growth of the mutant strain. These differences in the autotrophic growth rates could result from the effects of mutations on the photosynthetic activity.

The chlorophyll and carotene contents of these strains were measured using the cells that had been grown under heterotrophic conditions (Table 4-1). The LKC cells had the lowest content whereas the RWT cells contained the highest content of these pigments. Among the mutant strains, the bluish SJ3, SJ5, and SJ7 strains had relatively low chlorophyll and carotene content whereas the other strains showed higher chlorophyll to cell and carotene to cell ratios. Therefore, the color of the mutant cells correlates to their pigment content, which in turn may reflect the change of the abundance of the pigment-binding proteins. The strains that were able to grow photoautotrophically were green strains containing relatively high pigment content. Thus, the mutations might affect the photosystem complexes, which are the major pigment-binding proteins.

The impact of mutations on the photosystem activity in the mutant strains was studied by oxygen measurement. The PSII and PSI activities in the intact cells were measured by oxygen evolution and uptake with the artificial electron carriers, respectively (Table 4-1). The photosynthetic activities were normalized on an equal cell basis. The PSII activity of the 10 strains ranged from 576 to 787 nmol $O_2 \cdot OD_{730}^{-1} \cdot h^{-1}$, which were 84% to 114% of the RWT level. Therefore, the PSII activity was not affected substantially by the mutations in the PsaB protein. As expected, the PSI-less LKC strain contained no PSI activity, whereas the RWT cells had an activity of -237 nmol $O_2 \cdot OD_{730}^{-1} \cdot h^{-1}$. The lack of PSI activity in the SJ3, SJ5, and SJ7 mutant strains was consistent with their inability to grow autotrophically. The SJ8 mutant strain contained only 8% of the RWT activity, which might not be sufficient for autotrophic growth. The SJ1, SJ2, SJ4, and SJ6 mutant strains showed different levels of PSI activity with various autotrophic growth rates. The changes of PSI activity in the mutant strains may result from the effect of the mutations on the assembly and/or function of PSI. To test these possibilities, we examined accumulation and function of the PSI complexes in the thylakoid membranes.

Accumulation of PSI proteins in the mutant membranes. PsaB is an integral membrane protein with eleven transmembrane helices. Mutations in the PsaB protein could disturb protein folding and affect the assembly of the PSI complex. We performed Western blotting to estimate the steady-state levels of PSI proteins in the membranes. Thylakoid membranes were isolated from mutant strains and their proteins were resolved by SDS-PAGE. Immunodetection was performed with polyclonal antibodies against PsaA, PsaB, PsaC, PsaF, PsaI, PsaK, or PsaL (Fig. 4-3). The results were consistent in all seven Western blots. As expected, no PSI protein was detected in the LKC membranes whereas the RWT membranes contained PSI proteins. PSI proteins were not detected in SJ3, SJ5, and SJ7 membranes, consistent with the lack of PSI activity in these cells. Therefore, the SJ3, SJ5, and SJ7 mutations abolished the

accumulation of PSI proteins in the membrane. The absence of PSI proteins in the SJ3, SJ5, and SJ7 mutants resulted in their inability to grow autotrophically and the blue color of the cells. PSI proteins were detected in the SJ1, SJ2, SJ4, SJ6, and SJ8 mutants at varying levels that were less than the RWT level. Therefore, the mutations in the SJ1, SJ2, SJ4, SJ6, and SJ8 strains allowed some accumulation of PSI proteins in the membrane. To study the effect of mutations on the photosynthetic function of the accumulated PSI complexes, the SJ1, SJ2, SJ4, SJ6, and SJ8 mutant membranes were subjected for functional analysis.

Photosynthetic characterization of the mutant membranes. The active P700 reaction centers in the intact thylakoid membranes were measured by laser-induced changes in the absorbance at 820 nm and were normalized on equal cell basis (Table 4-2). The active P700 reaction centers in the DM extracts were also measured to investigate the stability of the reaction centers (Table 4-2). The PSI photosynthetic activity was determined with different sets of electron donors and acceptors: DAD-MV, cytochrome c_6-MV, and cytochrome c_6-ferredoxin. The DAD-MV PSI activity, which was measured by oxygen uptake with excess of the artificial electron donor (DAD) and acceptor (MV), excludes the limitation by interprotein recognition and docking on both sides of the membrane and therefore indicates the efficiency of electron transfer within the PSI complex. When cytochrome c_6 replaces DAD as the electron donor of PSI in the oxygen uptake measurements, the cytochrome c_6-MV PSI activity reflects both the electron transfer rate within the PSI complex and the interaction between cytochrome c_6 and the PSI complex. The PSI-mediated $NADP^+$ photoreduction uses cytochrome c_6 and ferredoxin as the electron donor and acceptor, respectively. Thus, the cytochrome c_6-ferredoxin PSI activity includes the electron transfer activity and the interaction between the PSI complex and the soluble proteins on both sides of the membrane. The difference between the DAD-MV PSI activity and the cytochrome c_6-MV PSI activity indicates an impact on the interaction between the PSI complex and cytochrome c_6. Similarly, the difference between the cytochrome c_6-MV PSI activity and the cytochrome c_6-ferredoxin PSI activity indicates the effect on the interaction between the PSI complex and ferredoxin. In all mutant membranes, the cytochrome c_6-MV PSI activity and the cytochrome c_6-ferredoxin PSI activity were at the similar percentage of the RWT level. Thus, the mutations on the luminal loop did not affect the interaction between the PSI complex and ferredoxin on the cytoplasmic side.

The SJ1 and SJ6 mutations were located in the two ends of the J loop. These two mutants contained higher autotrophic growth rates than the other mutants. They both contained active P700 and the cytochrome c_6-MV PSI activity at the same level compared to the RWT level. However, 41% active P700 in the intact membrane of the SJ1 mutant was lost after DM extraction. Therefore, the P700 reaction centers of SJ1 mutant were labile to detergent

extraction, suggesting an impact of the mutation on the packing of helices in the membrane. We reported earlier that proteolysis of the extramembrane loops facilitates the access of the small artificial electron carriers to the electron transfer centers in the PSI complex, resulting in an increase of the DAD-MV PSI activity (29). The SJ1 mutation might change the packing of the transmembrane helix k that is adjacent to the P700 reaction center, which may favor the access of small DAD molecules to the P700 reaction center. Consistent with this postulate, we observed high DAD-MV PSI activity in the SJ1 mutant. Similarly, the SJ6 mutant also lost 22% active P700 reaction centers upon DM extraction. With less loss of active P700, the SJ6 mutant did not show a dramatic increase in the DAD-MV PSI activity as the SJ1 mutant. The SJ6 mutation may have less impact on the packing of transmembrane helices than the SJ1 mutation. In summary, the SJ1 and SJ6 mutations affected the accumulation of PSI proteins in the membrane and the packing of helices around P700, but did not interrupt the interactions between the PSI complex and cytochrome c_6.

The SJ2, SJ4, and SJ8 mutations were located in the middle of the J loop. These mutants grew slowly or did not grow under autotrophic growth condition. Upon extraction by DM, the SJ2, SJ4, and SJ8 extracts maintained a similar level of active P700 reaction centers as in their intact membranes. Therefore, the SJ2, SJ4, and SJ8 mutations did not affect the conformation around the P700 reaction center. Among them, the SJ4 mutant contained similar levels of active P700, DAD-MV PSI activity, and cytochrome c_6-MV PSI activity, which were about a quarter of the RWT level. Therefore, the SJ4 mutation decreased greatly the accumulation of PSI proteins in the membrane, but did not affect the interactions of the PSI complex with cytochrome c_6. In contrast, the SJ2 mutant contained 29% active P700 and 38% DAD-MV PSI activity of the RWT level, but neither cytochrome c_6-MV nor cytochrome c_6-ferredoxin electron transfer activity was detected in the SJ2 mutant membranes. Therefore, SJ2 mutation affected the interactions between the PSI complex and cytochrome c_6. It reduced the accumulation of PSI complexes, but did not affect the conformation around P700. The slow autotrophic growth of SJ2 mutant in the absence of cytochrome c_6-mediated PSI activity may be due to the electron transfer from plastocyanin or a third electron donor as indicated in an earlier study (43). Similar to the SJ2 mutant, the SJ8 mutant membrane contained no cytochrome c_6-MV PSI activity, even though active P700 and the DAD-MV PSI activity were detected in the SJ8 mutant. Therefore, the SJ8 mutation greatly decreased the accumulation of the PSI complexes and might have interrupted the interactions of the PSI complex with cytochrome c_6.

Modification of mutant PSI complexes. The PsaA and PsaB proteins in the WT complexes cannot be modified by biotin maleimide (Fig. 4-4), which specifically reacts with the sulfhydryl group of cysteinyl residues. Therefore, the cysteinyl residues of the WT PsaA and

PsaB proteins are not exposed on the surface of PSI complexes. To study the topology of the J loop, we changed one amino acid to a cysteinyl residue in each of the eight mutations. PSI complexes from the SJ1, SJ2, SJ4, SJ6, SJ8, and RWT strains were purified and treated with biotin-maleimide. The biotin-maleimide treated PSI complexes were resolved by Tricine-urea-SDS-PAGE, probed with peroxidase-conjugated avidin, and then developed with enhanced chemiluminescence reagents (Fig. 4-4). The WT PsaAB cannot be modified by biotin-maleimide. When the WT PSI complexes were incubated with SDS to denature the proteins, we could detect modification of the PsaAB proteins by biotin-maleimide. A small amount of RWT PsaAB proteins was labeled by biotin-maleimide, which might be due to partial unfolding in a small fraction of the PSI complexes during the preparation. The SJ1, SJ2, SJ4, SJ6 and SJ8 PSI complexes were modified by biotin-maleimide. Therefore, the cysteinyl residues introduced in these strains were exposed on the surface, suggesting that the corresponding residues in the WT PsaB (H595, W622, L628, Y632, and N638) may be exposed on the surface of the PSI complex.

To study the effect of the biotin-maleimide modification on PSI function, the cytochrome c_6-ferredoxin PSI activity was measured after the modification and expressed as percentage of the RWT level. The cytochrome c_6-ferredoxin activities of modified PSI complexes from mutant strains were reduced substantially from their activity before modification. SJ1 was reduced from 58% to 34%, SJ4 was reduced from 28% to 11%, and SJ6 was reduced from 56% to 26% of the activity of modified RWT membranes. Therefore, the modification of residues in the J loop by biotin-maleimide may interfere with the interactions of the PSI complex with the electron donor cytochrome c_6, providing further support for an interaction between the exposed surface of the J loop and cytochrome c_6.

Discussion

The PSI complex accepts electrons from plastocyanin or cytochrome c_6 on the luminal side of the thylakoid membrane. Examination of the structures of plastocyanin and cytochrome c_6 reveals the presence of a flat hydrophobic surface around the redox center in both proteins (44,45). These flat hydrophobic surfaces are essential for the electron transfer from plastocyanin or cytochrome c_6 to PSI (12,46). Correct hydrophobic interactions are expected to ensure the accurate orientation of plastocyanin or cytochrome c_6 on the PSI complex. Therefore, the two surface α-helices l and l' and other amino acid residues in the J loops of the core proteins might provide the site for interaction with plastocyanin or cytochrome c_6. We tested this hypothesis by generating mutations in the J loop of PsaB.

Replacement of conserved residues in the J loop affected levels of PSI proteins in the membranes to varying degrees. The decreased accumulation of PSI proteins in the mutant membranes could result from several factors. A mutation might disturb the assembly of the mutated PsaB protein into the thylakoid membrane or cause a rapid turnover of the mutated PsaB protein. The mutation might affect the interaction between PsaB and other PSI subunits and result in fast degradation of PSI complexes. Since the deletion of PsaF, PsaL, PsaI, and PsaJ subunits did not affect the accumulation of PsaA and PsaB proteins (14,16,17,47), the decreased accumulation of PSI proteins in the mutant strains is likely due to the decreased accumulation of the PsaB protein. The SJ3, SJ5, and SJ7 mutants did not allow accumulation of detectable levels of PSI proteins in the membranes. These mutations are located in the region between residues S600 and W616. Therefore, this peptide fragment is important for the stability of the PsaB protein in the membrane. Biotin-maleimide modification of the SJ1, SJ2, SJ4, SJ6, and SJ8 PSI complexes indicated that the residues H595, W622, L628, Y632, and N638 in WT PsaB might be exposed on the surface of the PSI complex. Mutations of the surface-exposed residues had a less destabilizing effect on the PsaB protein than the changes in the buried residues. For this reason, we propose that the l helix is exposed on the surface of the J loop whereas the peptide fragment S600-W616 may fold underneath the helix.

Upon extraction by DM, the SJ1 and SJ6 mutants lost some active P700 reaction centers, suggesting an impact of mutations on the packing of transmembrane helices around P700. Other mutants maintained their active P700 after detergent extraction. The SJ1 and SJ6 mutations are located in the ends of J loop and close to the ends of the k and m transmembrane helices. Therefore, the amino acid residues at the junction of the transmembrane helix and extramembrane loop might be important for the packing of transmembrane helices.

The SJ2, SJ4, and SJ8 mutations were predicted to be located in the l helix. When we viewed the l helix as a wheel diagram, the residues W622, L628, and Y632 were aligned on one side of the helical wheel that is largely hydrophobic. These residues were determined exposed to solvent in the WT PSI complex (Fig. 4-4). This hydrophobic side of l helix, containing residues W622, L628, and Y632, may provide a surface for the hydrophobic interaction with plastocyanin/cytochrome c_6. The SJ2 and SJ8 membranes contained no cytochrome c_6-MV and cytochrome c_6-ferredoxin PSI activity, but maintained DAD-MV PSI activity. Therefore, the SJ2 and SJ8 mutations maintained electron transfer activity but failed in interacting with cytochrome c_6. The SJ2 and SJ8 mutants maintained their active P700 reaction centers upon the detergent extraction, indicating no impact on the conformation around P700 by the mutations. Therefore, the observed interruption of PSI interaction with cytochrome c_6 in the SJ2 and SJ8 mutants is likely due to the amino acid replacement. In each of these two

mutants, a large aromatic residue was replaced with the smaller cysteinyl residue. In contrast, the SJ4 membrane maintained similar levels of PSI proteins, active P700, and PSI activities and did not interrupt the interactions between the PSI complex and cytochrome c_6. In the SJ4 mutation, a leucinyl residue was changed to a cysteinyl residue. However, when the SJ4 PSI complexes were modified by biotin-maleimide with dramatic structural change, the PSI NADP$^+$ photoreduction activity was reduced substantially. The physical structure of the hydrophobic side of the l helix is important for the interactions of the PSI complex with cytochrome c_6. Therefore, our results show that the hydrophobic side of the l helix of the PsaB protein that contains residuesW622, L628, and Y632 provides the site of interaction with cytochrome c_6.

Acknowledgment

References

1. Chitnis, P. R. (1996) *Plant Physiol.* **111**, 661-669
2. Fromme, P. (1996) *Curr. Opin. Struct. Biol.* **6**, 473-484
3. Chitnis, P. R., Xu, Q., Chitnis, V. P., and Nechushtai, R. (1995) *Photosynth. Res.* **44**, 23-40
4. Golbeck, J. H. (1994) in *The Molecular Biology of Cyanobacteria* (Bryant, D. A., ed), pp. 179-220, Kluwer Academic Publishers, Dordrecht, The Netherlands
5. Wood, P. M. (1978) *Eur. J. Biochem.* **87**, 9-19
6. Sandmann, G. (1986) *Arch. Microbiol.* **145**, 76-79
7. Kerfeld, C. A., and Krogmann, D. W. (1998) *Annual Rev. Plant Physiol. Plant Mol. Biol.* **49**, 397-425
8. Krauß, N., Schubert, W.-D., Klukas, O., Fromme, P., Witt, H. T., and Saenger, W. (1996) *Nature Struct. Biol.* **3**, 965-973
9. Schubert, W.-D., Klukas, O., Krauß, N., Saenger, W., Fromme, P., and Witt, H. T. (1997) *J. Mol. Biol.* **272**, 741-769
10. Wynn, R. M., Luong, C., and Malkin, R. (1989) *Plant Physiol.* **91**, 445-449
11. Hippler, M., Ratajczak, R., and Haehnel, W. (1989) *FEBS Lett.* **250**, 280-284
12. Haehnel, W., Jansen, T., Gause, K., Klosgen, R. B., Stahl, B., Michl, D., Huvermann, B., Karas, M., and Herrmann, R. G. (1994) *EMBO J.* **13**, 1028-1038

13. Chitnis, P. R., Purvis, D., and Nelson, N. (1991) *J. Biol. Chem.* **266**, 20146-20151

14. Xu, Q., Yu, L., Chitnis, V. P., and Chitnis, P. R. (1994) *J. Biol. Chem.* **269**, 3205-3211

15. Chitnis, V. P., and Chitnis, P. R. (1993) *FEBS Lett.* **336**, 330-334

16. Xu, Q., Hoppe, D., Chitnis, V. P., Odom, W. R., Guikema, J. A., and Chitnis, P. R. (1995) *J. Biol. Chem.* **270**, 16243-16250

17. Xu, Q., Odom, W. R., Guikema, J. A., Chitnis, V. P., and Chitnis, P. R. (1994) *Plant Mol. Biol.* **26**, 291-302

18. Haehnel, W., Propper, A., and Krause, H. (1980) *Biochim. Biophys. Acta* **593**, 384-399

19. Bottin, H., and Mathis, P. (1985) *Biochemistry* **24**, 6453-6460

20. Hervas, M., Navarro, J. A., Diaz, A., Bottin, H., and De la Rosa, M. A. (1995) *Biochemistry* **34**, 11321-11326

21. Hervas, M., Navarro, J. A., Diaz, A., and De la Rosa, M. A. (1996) *Biochemistry* **35**, 2693-2698

22. Hippler, M., Reichert, J., Sutter, M., Zak, E., Altschmied, L., Schröer, U., Herrmann, R. G., and Haehnel, W. (1996) *EMBO J.* **15**, 6374-6384

23. Xu, Q., Jung, Y. S., Chitnis, V. P., Guikema, J. A., Golbeck, J. H., and Chitnis, P. R. (1994) *J. Biol. Chem.* **269**, 21512-21518

24. Hatanaka, H., Sonoike, K., Hirano, M., and Katoh, S. (1993) *Biochim. Biophys. Acta* **1141**, 45-51

25. Farah, J., Rappaport, F., Choquet, Y., Joliot, P., and Rochaix, J. D. (1995) *EMBO J.* **14**, 4976-4984

26. Fromme, P., Schubert, W.-D., and Krauss, N. (1994) *Biochim. Biophys. Acta* **1187**, 99-105

27. Boekema, E. J., Boonstra, A. F., Dekker, J. P., and Rögner, M. (1994) *J. Bioenerg. Biomemb.* **26**, 17-29

28. Deisenhofer, J., and Michel, H. (1991) *Annual Review of Cell Biology* **7**, 1-23

29. Sun, J., Xu, Q., Chitnis, V. P., Jin, P., and Chitnis, P. R. (1997) *J. Biol. Chem.* **272** (35), 21793-21802

30. Altenbach, C., Flitsch, S. L., Khorana, H. G., and Hubbell, W. L. (1989) *Biochemistry* **28**, 7806-7812

31. He, M. M., Sun, J., and Kaback, H. R. (1996) *Biochemistry* **35**, 12909-12914

32. Sun, J., Ke, A., Jin, P., Chitnis, V. P., and Chitnis, P. R. (1998) *Meth. Enzymol.* **297**, 124-139

33. Arnon, D. (1949) *Plant Physiol.* **24**, 1-14

34. Furr, H. C., Barua, A. B., and Olson, J. A. (1992) in *Modern Chromatographic Analysis of Vitamins*. (Leenheer, A. P. d., Lambert, W. E., and Nelis, H. J., eds), pp. 1-71, Dekker, New York, N. Y.

35. Boussiba, S., and Vermaas, W. F. J. (1992) in *Research in Photosynthesis* (Murata, N., ed) Vol. III, pp. 429-432, Dordrecht: Kluwer

36. Shen, G., Boussiba, S., and Vermaas, W. F. (1993) *Plant Cell* **5**, 1853-63

37. Higuchi, R. (1989) in *PCR Technology* (Erlich, H. A., ed), pp. 61-70, Stockton Press, New York

38. Williams, J. G. K. (1988) *Meth. Enzymol.* **167**, 766-778

39. Mathis, P., and Setif, P. (1981) *Isr. J. Chem.* **21**, 316-320

40. Mehler, A. H. (1951) *Arch. Biochem. Biophys.* **33**, 65-77

41. Mehler, A. H. (1951) *Arch. Biochem. Biophys.* **34**, 339-351

42. Garnier, J., Osguthorpe, D. J., and Robson, B. (1978) *J. Mol. Biol.* **120**, 97-120

43. Zhang, L., Pakrasi, H. B., and Whitmarsh, J. (1994) *J Biol Chem* **269**, 5036-42

44. Navarro, J. A., Hervas, M., and De la Rosa, M. A. (1997) *J. Biol. Inorg. Chem.* **2**, 11-12

45. Frazao, C., Soares, C. M., Carrondo, M. A., Pohl, E., Dauter, Z., Wilson, K. S., Hervas, M., Navarroo, J. A., De la Rosa, M. A., and Sheldrick, G. M. (1995) *Structure* **3**, 1159-1169

46. Sigfridsson, K., Young, S., and Hansson, O. (1996) *Biochemistry* **35**, 1249-1257

47. Chitnis, V. P., Xu, Q., Yu, L., Golbeck, J. H., Nakamoto, H., Xie, D. L., and Chitnis, P. R. (1993) *J. Biol. Chem.* **268**, 11678-11684

Figure legends

FIG. 4-1. **Generation of PsaB mutants.** The restriction map of *Synechocystis* sp. PCC 6803 genomic region around the *psaA* and *psaB* genes is shown on the *top line*. *Arrows* show the location, size and direction of complete or partial *psaA* and *psaB* genes. The *small black boxes* indicate the coding region for the extramembrane J loop (EL-J) of PsaB. The kanamycin resistance gene (Kan-r) and chloramphenicol resistance gene (Cam-r) are shown as the *long boxes*. The *bold lines* in the construction of the p3C+ plasmid represent the pBluescript II KS vector.

FIG. 4-2. **Mutagenesis of the J loop of the PsaB protein.** A. Folding model for the extramembrane J loop of PsaB. Amino acids are indicated and numbered for the PsaB protein of *Synechocystis* sp. PCC 6803. The surface helix is represented as a *box* with the predicted sequence aligned inside. Positions and identities of the mutations are indicated. **B**.

Comparison of primary sequences of J loop of PsaB and PsaA from different sources. The completely conserved residues among species are *shaded*. *Dots* indicate the residues that are conserved between PsaA and PsaB.

FIG. 4-3. **Accumulation of the PSI proteins in the mutant strains.** Membranes were analyzed by Tricine/urea/SDS-PAGE and Western blotting with subunit-specific antibodies. The immunodetection was visualized by enhanced chemiluminescence.

FIG. 4-4. **Modification of the mutant PSI complexes.** Purified PSI complexes containing 5 μg chlorophyll were treated with biotin-maleimide and analyzed by Tricine/urea/SDS-PAGE. The blot was probed with peroxidase-conjugated avidin and visualized by enhanced chemiluminescence reagents.

Table 4-1. Characterization of the mutant cells

Strains	Doubling time (h)		Pigment content ($\mu g \cdot OD_{730}^{-1} \cdot ml^{-1}$)		Photosynthetic activity (nmol $O_2 \cdot OD_{730}^{-1} \cdot h^{-1}$)	
	heterotrophic	autotrophic*	chlorophyll	carotene	PSII	PSI
LKC	30	-	0.73	0.32	576	0
RWT	27	54	1.29	0.83	688	-237
SJ1	27	70	1.19	0.79	685	-260
SJ2	27	81	0.99	0.63	743	-89
SJ3	28	-	0.85	0.45	668	-4
SJ4	27	172	1.02	0.72	787	-62
SJ5	28	-	0.75	0.39	692	0
SJ6	27	54	1.04	0.70	686	-124
SJ7	28	-	0.88	0.44	727	-5
SJ8	28	-	0.89	0.55	730	-19

*: '- ' indicates that the strains died or did not grow.

Table 4-2. Characterization of the mutant photosynthetic membranes

The results were normalized on equal cell basis and expressed as percentage of the RWT level that is shown in parentheses. The level of P700 in DM extract was expressed as percentage of the RWT level in membrane.

Strains	Level of active P700		PSI photosynthetic activity $(nmol \cdot OD_{730}^{-1} \cdot h^{-1})$		
	membrane	DM extract	DAD to MV	cytochrome c_6 to MV	cytochrome c_6 to ferredoxin
RWT	100 (6.91 ×10⁴ P700/cell)	95	100 (-237)	100 (-326)	100 (49)
SJ1	44	26	110	44	58
SJ2	29	29	38	0	0
SJ4	23	26	26	23	28
SJ6	45	35	52	44	56
SJ8	10	8	8	0	0

Fig. 4-1

A

Helix IX (k)

Membrane

SJ3

S600R, G601C, N602I

Lumen

SJ4

Q627H, L628C, I629S

Helix X (m)

SJ5

N609K, S610C, T611I

SJ8

Y632C, N633I

H595C, L596I

SJ1

M614I, G615C, W616A

W622C, A623R

N638C, N639S

SJ7

SJ2

SJ6

Surface Helix (l)

B
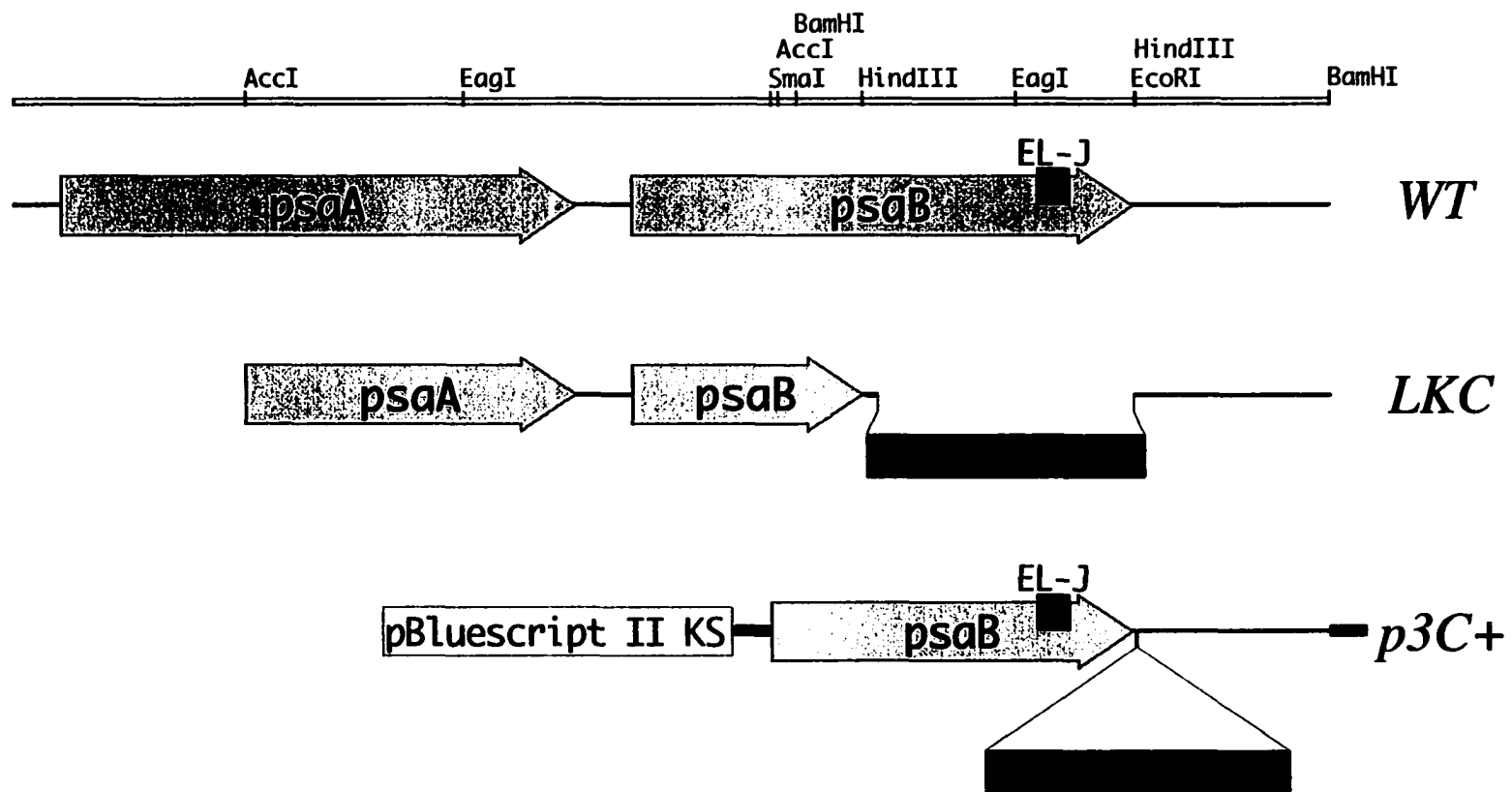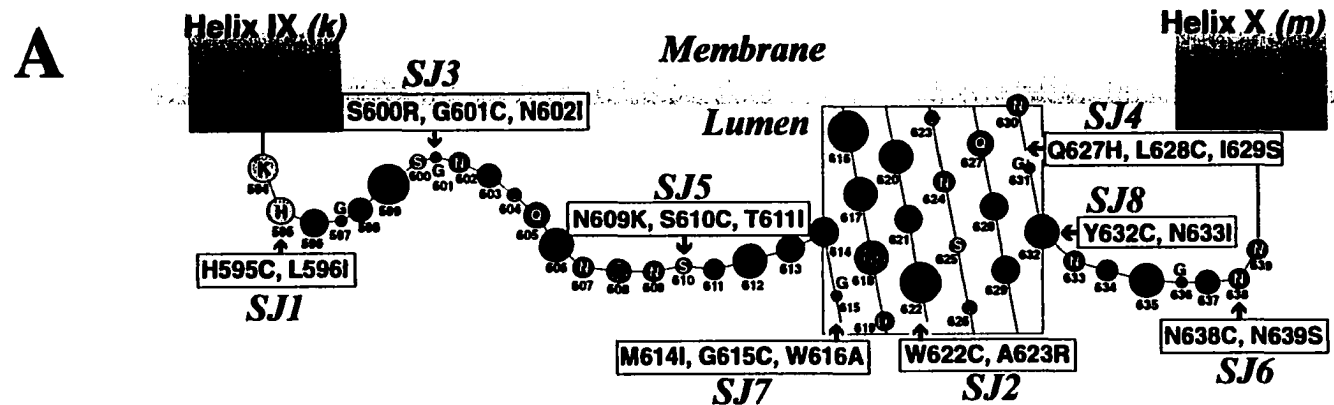
```
                       •        ••      •     •      •• •• ••       •     •
B-Synechocystis        KHLGVWSGNV  AQFNENSTYL  MGWFRDYLWA  NSAQLINGYN  PYGVNN    46
B-S. elongatus         KHLGVWEGNV  AQFNESSTYL  MGWLRDYLWL  NSSQLINGYN  PFGTNN    46
B-Chlamydomonas        KHLTLWQGNV  AQFDESSTYL  MGWLRDYLWL  NSSQLINGYN  PFGMNS    46
B-Spinach              KHITLWQGNV  SQFNESSTYL  MGWLRDYLWL  NSSQLINGYN  PFGMNS    46
B-Maize                KHITLWQGNV  SQFNESSTYL  MGWLRDYLWL  NSSQLINGYN  PFGMNS    46

A-Synechocystis  KMQSDVWGTV  SPDGSVTHVTL  GN    FAQSAITI  NGWLRDFLWA  QAANVINSYG  SA    53
A-S. elongatus   KMQSDVWGTV  APDGTVSHITG  GN    FAQSAITI  NGWLRDFLWA  QASQVIGSYG  SA    53
A-Chlamydomonas  KMQSDVWGTV  TASG-VSHITG  GN    FAQSANTI  NGWLRDFLWA  QSSQVIQSYG  SA    52
A-Spinach        KMQSDVWGSI  SDQGVVTHITG  GN    FAQSSITI  NGWLRDFLWA  QASQVIQSYG  SS    53
A-Maize          KMQSDVWGTI  SDQGIVTHITG  GN    FAQSSITI  NGWLRDFLWA  QASQVIQSYG  SS    53
```

Fig. 4-2

Fig. 4-3

Fig. 4-4

103

CHAPTER 5. OXIDIZING SIDE OF THE CYANOBACTERIAL PHOTOSYSTEM I: MUTATIONAL ANALYSIS OF THE LUMINAL H LOOP OF THE PSAB SUBUNIT[1]

A paper submitted to the Plant Physiology
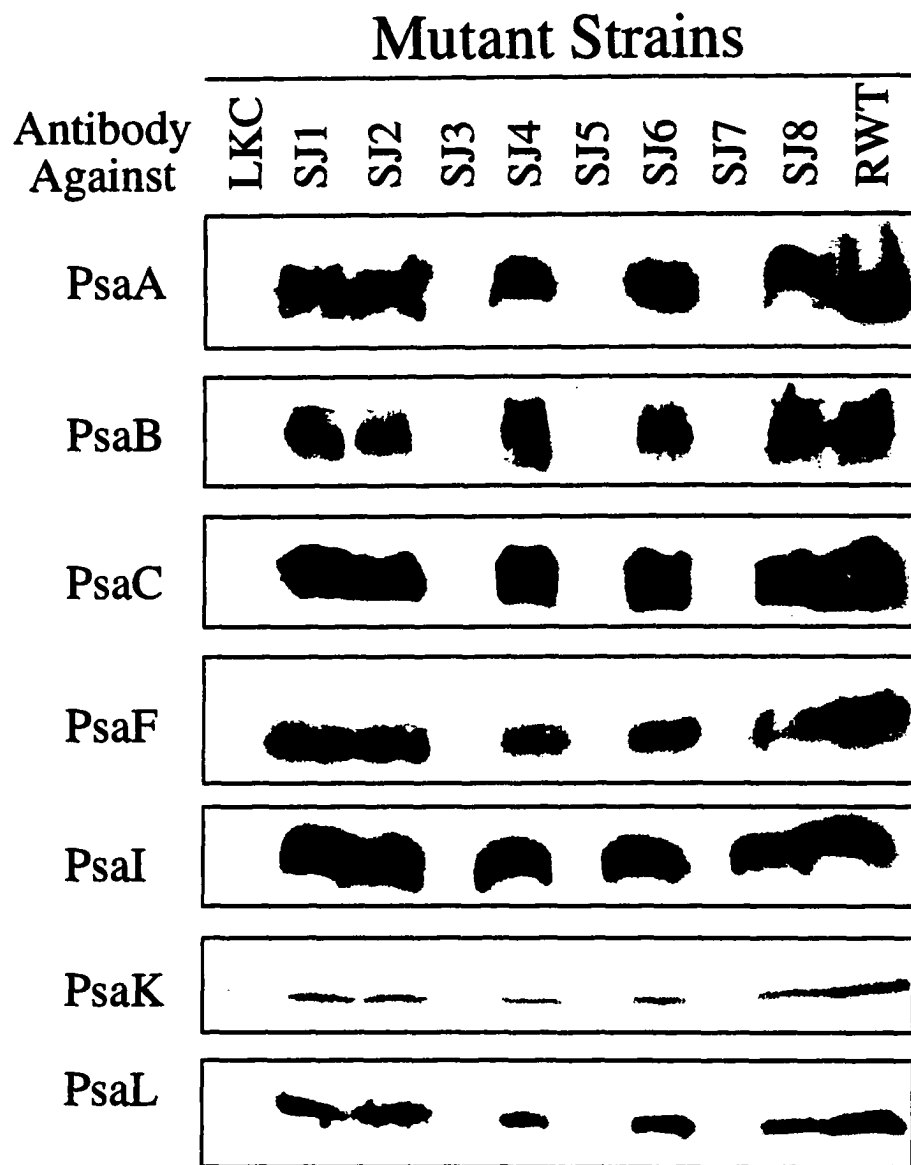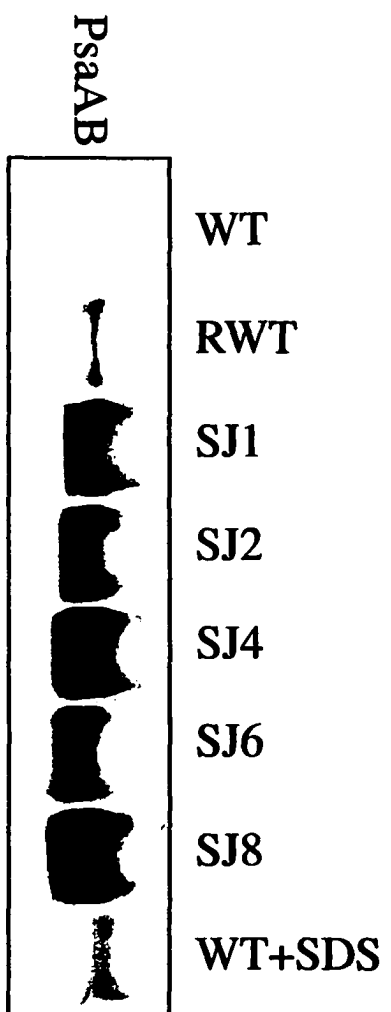
Jun Sun, Manuel Hervás, José A. Navarro, Miguel A. De la Rosa, and Parag R. Chitnis

Abstract

Photosystem I (PSI) core proteins are expected to interact with the electron donor proteins plastocyanin or cytochrome c_6. To investigate the role of the luminal H loop of PsaB in the assembly and function of the PSI complex, we generated fifteen deletion and repetition mutations in the H loop of the PsaB protein from *Synechocystis* sp. PCC 6803. The mutant strains differed in their photoautotrophic growth. The PSI proteins could not be detected in the membranes of mutants in which the N438-E448, I453-T464, or S500-G512 region was deleted from the PsaB protein, indicating the essential role of these segments in proper folding of the PsaB protein. Mutants with partial or complete deletion of the L469-D496 segment could accumulate the PSI proteins. These results indicate that the regions close to the transmembrane helices are more important for the assembly of PsaB than the middle region of the H loop. The L469-D496 segment in the H loop of PsaB is dispensable in the interaction between the PSI complex and the soluble donor proteins. These results suggested that sections of the H loop of PsaB are crucial for the structural integrity of the PsaB protein.

Introduction

PSI[2] is a multisubunit membrane-protein complex that catalyzes the light-driven electron transfer from plastocyanin in the thylakoid lumen to ferredoxin in the chloroplast stroma or cyanobacterial cytoplasm (Golbeck, 1994; Chitnis et al., 1995; Chitnis, 1996; Fromme, 1996).

[2] Abbreviations: DM, dodecyl-β-D-maltoside; DAD, 3,6-diaminodurene; MV, methyl viologen; WT, wild type; RWT, recovered wild type.

Cyanobacteria and green algae contain cytochrome c_6 as an alternative electron carrier protein depending on the relative availability of copper and iron in the culture medium (Wood, 1978; Kerfeld and Krogmann, 1998). The crystal structure of PSI at 4 Å resolution has shown that a monomeric PSI complex from cyanobacteria contains 89 chlorophyll a molecules, 83 of which constitute the core antenna system (Krauß et al., 1996; Schubert et al., 1997). The PsaA and PsaB subunits form the heterodimeric core that harbors the primary electron donor P700. In addition to the core proteins, the cyanobacterial PSI complex contains three peripheral proteins (PsaC, PsaD, and PsaE) and six integral membrane proteins (PsaF, PsaI, PsaJ, PsaK, PsaL, and PsaM) (Chitnis et al., 1995; Chitnis, 1996; Fromme, 1996). The PsaC, PsaD, and PsaE subunits form the reducing side of PSI. PsaC binds the terminal electron acceptors F_A and F_B, which donate electrons to ferredoxin. PsaD and PsaE facilitate docking of ferredoxin on PSI (Chitnis, 1996). Functions of the other subunits have been deciphered from the subunit-deficient mutants of cyanobacteria and algae (Chitnis et al., 1995; Chitnis, 1996).

On the luminal side of thylakoid membranes, plastocyanin or cytochrome c_6 donates electrons to PSI. Plastocyanin interacts with the plant and algal PSI complexes showing a complex electron transfer kinetics, which can be attributed to a multi-step reaction mechanism of electron transfer (Haehnel et al., 1980; Bottin and Mathis, 1985). Some cyanobacteria including *Synechocystis* sp. PCC 6803 have a simpler one-step bimolecular collision mechanism (Hervás et al., 1995; Hervás et al., 1996). The negative region of plastocyanin can be cross-linked to the N-terminal lysine-rich region of chloroplast PsaF, which is not found in the cyanobacterial PsaF (Hippler et al., 1996). Therefore, plastocyanin interacts the plant PSI through initial electrostatic interactions between the N-terminal domain of PsaF and the conserved negative patches of plastocyanin. However, the cyanobacterial PsaF is not required in the interaction of PSI with plastocyanin or cytochrome c_6 (Chitnis et al., 1991; Xu et al., 1994a; Xu et al., 1994b; Hatanaka et al., 1993). The deletion of PsaF in *Chlamydomonas reinhardtii* did not abolish the electron transfer from plastocyanin to PSI (Farah et al., 1995). Therefore, plastocyanin and cytochrome c_6 must be able to contact the PsaA and PsaB core proteins directly. The luminal extramembrane loops of PsaA and PsaB are the most logical candidates for interaction with plastocyanin and cytochrome c_6.

The H loops are the large, luminal, extramembrane loops located between the i and j transmembrane helices of the core proteins (see reference (Sun et al., 1997) for the topology of PSI core proteins and nomenclature of loops). From the crystal structure of PSI, the i and j transmembrane helices appear to contribute to the central cage (Krauß et al., 1996; Schubert et al., 1997). Therefore, the H loops should be located close to the center of PSI. The H loop of PsaB was extensively accessible to protease implying that this loop could interact with

plastocyanin or cytochrome c_6 (Sun et al., 1997). To investigate the role of the H loop in the assembly and function of PSI complex and in the interaction with the electron donors, we generated deletion and repetition mutations in the H loop of the PsaB protein. The mutations were introduced into a psaB-deletion strain of Synechocystis sp. PCC 6803. Here we present the biochemical characterization of the mutant strains and their PSI complexes.

Materials and methods

Cyanobacterial cultures, membrane isolation, and PSI purification. The Synechocystis sp. PCC 6803 strains were cultured in BG-11 medium at 30°C with appropriate antibiotics (40 mg/l kanamycin or 30 mg/l chloramphenicol). For autotrophic growth, cells were grown in BG-11 medium under medium light intensity (40 μmol·m^{-2}·s^{-1}). For heterotrophic growth, cells were grown in BG-11 supplemented with 5 mM of glucose under low (5 μmol·m^{-2}·s^{-1}) or medium light intensity. Cells were harvested at the late exponential growth phase. Previously published methods were used for isolation of thylakoid membranes and purification of trimeric PSI complexes with DM (Sun et al., 1998). Chlorophyll *a* (Arnon, 1949) and carotene concentrations (Furr et al., 1992) were estimated according to the previously published methods.

Generation of deletion and repetition mutations in the psaB gene. The mutagenesis in the C-terminal region of the PsaB protein of Synechocystis sp. PCC 6803 involved a PSI-less LKC recipient strain and the p3C+ recombinant plasmid as described before (Sun et al., 1999). All PsaB mutants were generated by a PCR-mediated mutation technique (Higuchi, 1989). For deletion mutations, the upstream and downstream coding regions were amplified by PCR with mutagenic primers containing PstI restriction endonuclease recognition site. The PCR fragments were ligated into the digested p3C+ plasmid. For repetition mutations, overlapping PCR fragments were amplified. The mutated recombinant plasmids were sequenced completely to ensure the presence of desired changes and the absence of errors by *Taq* DNA polymerase. The recombinant plasmids were used to transform the recipient strain LKC according to reference (Williams, 1988). The chloramphenicol-resistant transformants were selected at 30°C under heterotrophic growth condition, segregated for three generations, and replica-plated to confirm the absence of kanamycin-resistance gene.

Characterization of the mutant strains. The chloramphenicol-resistant transformants were cultured in liquid BG-11 medium after segregation. The genomic DNA was isolated from the mutant strains. PCR amplification of appropriate fragments was used to confirm the mutations and the integration of chloramphenicol resistance gene in genome of the mutant strains. Nucleotide sequence of the corresponding PCR fragments was determined to confirm

mutations. DNA and protein sequence analysis was performed with GeneWorks software (IntelliGenetics, CA). Same number of the RWT and LKC cells yielded same A_{730} (5.5×10^7 cells·A_{730}^{-1}·ml^{-1}) using an UV-160U spectrophotometer (Shimadzu, Tokyo, Japan). A_{730} was used as a measure of cell count to monitor the growth of the mutant strains. Accumulation of PSI proteins was examined by analytical SDS-PAGE and immunodetection (Sun et al., 1997). The antibodies that were used for immunodetection have been described previously (Sun et al., 1998). The P700 content was estimated by the measurement of photoinduced absorbance change at 820 nm (Mathis and Setif, 1981).

The PSI activity was monitored by following the oxygen uptake, according to the Mehler reaction (Mehler, 1951a; Mehler, 1951b), using the artificial electron carriers DAD and MV (Sun et al., 1998). Alternatively, the PSI activity in the membrane can be measured by following oxygen uptake with 15 μM cytochrome c_6 replacing DAD as the electron donor. The PSI activity in the membrane was also determined from NADP$^+$ photoreduction assays using cytochrome c_6 and ferredoxin as the electron donor and acceptor of the PSI complex (Sun et al., 1998). These activities were normalized on equal cell basis.

For laser flash spectroscopy analysis, plastocyanin from *Synechocystis* sp. PCC 6803 was purified as described previously (De la Cerda et al., 1997). Kinetics of flash induced absorbance changes in PSI was followed at 820 nm and the experimental set-up, data collection and kinetic analyses were reported previously (Hervás et al., 1995). For experiments at varying ionic strength, the magnesium salt was omitted and the ionic strength was adjusted at the desired value by adding NaCl.

Results

Mutagenesis of the H loop of the PsaB protein. The H loop of PsaB contains 76 amino acid residues. The secondary structure prediction using Garnier algorithm (Garnier et al., 1978) indicated no major α-helix or β-sheet structure. In the crystal structure, this loop might be packed loosely and was not resolved (Krauß et al., 1996; Schubert et al., 1997). Since the H loop of PsaB protein is large and without clear structural information, we opted to generate 12 deletion and 3 repetition mutations in the H loop of PsaB protein (Fig. 5-1). The p3C+ plasmid with WT gene was introduced back into the LKC strain to yield the RWT strain that was used as a positive control in these studies.

After we obtained the transformants, genomic DNA was isolated from liquid culture of the mutant strains. The integration of chloramphenicol resistance gene in genome of the mutant strains was confirmed by PCR analysis (data not shown). Mutations were confirmed by PCR amplification with the primers GGCCAATAAAGATAACGT and CATCAGGTAGGTGGAG

TTTTCG. A DNA fragment of 645 bp was amplified when the WT genomic DNA was used for PCR amplification (Fig. 5-2). As expected, single PCR fragments larger than 645 bp were amplified from the repetition mutant genomic DNA and single PCR fragments smaller than 645 bp were amplified from the deletion mutant genomic DNA. The fragment sizes corresponded to the changes of residue number. These PCR fragments were sequenced and the DNA sequences matched the desired mutations. Therefore, the mutant strains contained the desired mutations.

Characterization of the mutant cells. The PSI-less LKC cells were more blue than the WT cells due to the reduced level of chlorophyll while retaining phycobilisomes (Shen et al., 1993). During segregation, the RWT strain as well as the ch, ci, df, dh, and di mutant strains formed green colonies, whereas the af, ag, ah, ai, aj, bg, cj, dg, dj, and ej mutant strains formed bluish colonies that resembled the recipient LKC strain.

When the RWT, LKC, and mutant strains were cultured with glucose under low light intensity, all strains could grow with similar doubling time, ranging from 27 to 30 hours (Table 5-1). The mutant strains could utilize the externally supplied glucose under low light intensity, indicating a normal respiratory system in the mutant strains. When the strains were cultured with exogenous glucose under medium light intensity, the LKC recipient strain could not grow. The inability of the PSI-less strains to grow at medium light intensity has been attributed to the reductants produced by the PSII complex (Smart et al., 1991). Excess reducing power could be toxic to the cells. Similar to LKC, the af, ag, ah, ai, aj, and bg mutant strains did not grow under medium light intensity. In contrast, the RWT, ch, ci, cj, df, dg, dh, di, dj, and ej mutant strains could grow with glucose under medium light intensity, but showed different growth rates (Table 5-1). This indicated that the mutant cells differed in their ability to tolerate the excess reductants produced by PSII when the PSI activity was relatively insufficient to use the electron throughput from PSII. The RWT, ch, ci, df, dh, and di mutant strains could grow under photoautotrophic growth condition (Table 5-1). The RWT and ch cells had the fastest growth, the ci, di, and dh cells grew slower than RWT, whereas the df cells had the longest doubling time. Therefore, these mutations affected the ability of the mutant strain to grow autotrophically, indicating their effect on the PS-mediated electron transfer.

The chlorophyll and carotene contents of the mutant strains were measured using the cells that had been grown under heterotrophic conditions (Table 5-1). The LKC cells had the lowest contents whereas the RWT cells contained the highest levels of these pigments. Among the mutant strains, the bluish strains had relatively low pigment content whereas the green strains showed higher pigment content, especially the carotene content. The pigment content of the mutant cells may reflect the change of the abundance of the pigment-binding proteins. The PSI complexes are the major proteins binding these pigments, thus, the mutations might affect the

abundance of the PSI complexes in the membrane. To test the effect of mutations on the assembly of PSI, we examined accumulation of PSI complexes in the thylakoid membranes.

Accumulation of PSI proteins in the mutant membranes. We performed Western blotting to estimate the level of PSI proteins in the membranes. Thylakoid membranes were isolated from mutant strains and the proteins were resolved by SDS-PAGE. Immunodetection was performed with polyclonal antibodies against PsaA, PsaC, PsaF, PsaI, PsaK, or PsaL (Fig. 5-3). The results were consistent in all six Western blots. As expected, the PSI proteins could not be detected in the LKC membranes whereas the RWT membranes contained all PSI proteins. The PSI proteins were not detected in the af, ag, ah, ai, aj, bg, cj, dg, dj, and ej membranes, consistent with the bluish color of the mutant cells. The lowest limit for the immunodetections was 2% of the RWT level (data not shown). Therefore, the af, ag, ah, ai, aj, bg, cj, dg, dj, and ej mutations greatly reduced or abolished accumulation of the PSI proteins in the membranes. The absence of PSI proteins in these mutants resulted in their inability of autotrophic growth. However, the cj, dg, dj, and ej mutant strains could grow with glucose under medium light intensity, whereas the af, ag, ah, ai, aj, and bg mutants did not grow under this condition. Excess reductant produced by PSII has been considered the cause of light sensitivity of the PSI-less mutants (Smart et al., 1991). Trace amount (<2% of RWT level) of PSI complex in the cj, dg, dj, and ej mutant strains might contribute to their ability to tolerate the excess reductants. The PSI proteins were detected in the ch, ci, df, dh, and di mutants. However, their levels were less than in the RWT strain. Therefore, the mutations in the ch, ci, df, dh, and di strains allowed some accumulation of PSI proteins in the membranes. To study the effects of mutations on the photosynthetic function of the accumulated PSI complexes, the ch, ci, df, dh, and di mutant membranes were used to assay PSI activity.

Photosynthetic electron transfer by the mutant membranes. PSI activity was determined with different sets of electron donors and acceptors: DAD-MV, cytochrome c_6-MV, and cytochrome c_6-ferredoxin (Sun et al., 1999). The DAD-MV PSI activity excludes the limitation by interprotein recognition and docking on both sides of the membrane and therefore indicates the efficiency of electron transfer within the PSI complex. The cytochrome c_6-MV PSI activity reflects both the electron transfer rate within the PSI complex and the interaction between cytochrome c_6 and the PSI complex. The cytochrome c_6-ferredoxin PSI activity includes the electron transfer activity and the interaction between the PSI complex and the soluble proteins on both sides of the membrane. The PSI activities in the mutant membranes were less than in the RWT membranes, reflecting the lower accumulation of PSI complexes. When the PSI activities were expressed as percentage of the RWT level, all three PSI activities were at the similar percentage level in each mutant, indicating that the mutant PSI complexes were equally

efficient in accepting electron from artificial or natural electron transfer partners (Table 5-2). Thus, these mutations did not affect the PSI-cytochrome c_6 and PSI-ferredoxin interactions.

Photoreduction of P700⁺ in the mutant PSI complexes by plastocyanin. The PSI complexes were purified from the RWT, ch, ci, di, and dh strains cultured under autotrophic condition (the slow autotrophic growth of df strain did not allow effective purification of PSI complexes). The purified PSI complexes were subjected to plastocyanin photoreduction experiments by laser flash spectroscopy to study the interaction between the PSI complex and plastocyanin. The chlorophyll to P700 molar ratios for the mutant PSI complexes were similar as for the RWT PSI (Table 5-3). With all mutant PSI complexes, the kinetics of plastocyanin oxidation was monophasic, and the observed pseudo-first order rate constant (k_{obs}) yielded linear dependence on donor protein concentration. This finding suggested that the mutant PSI complexes interact with plastocyanin according to the oriented collisional reaction mechanism, as is the case with the RWT PSI (Hervás et al., 1995; Hippler et al., 1996).

The second-order rate constant (k_{bim}) of P700⁺ reduction by plastocyanin can be calculated from the linear dependence of k_{obs} on protein concentration. All the mutant PSI complexes reacted with plastocyanin in a similar extension as the RWT PSI, with a second-order rate constant that was of the same order of magnitude as that of the RWT PSI (Table 5-3). Therefore, the ch, ci, dh, and di mutations in the H loop did not affect significantly the reactivity of PSI with plastocyanin. Similar reactivity was observed when cytochrome c_6 was used as the electron donor protein in the kinetic analysis (data not shown). It has been previously shown that the interaction of the WT PSI with cytochrome c_6 and plastocyanin is electrostatically repulsive in nature (Hervás et al., 1994). Therefore, the rate of PSI reduction increases with increasing ionic strength. The mutant PSI complexes showed a similar ionic strength dependence, from which the bimolecular rate constants extrapolated at infinite ionic strength (k_{inf}) were estimated (Table 5-3). The bimolecular rate constants for the mutants were similar to the wild type value. Thus, the ch, ci, dh, and di mutations in the H loop of PsaB did not affect the interaction between PSI and the donor proteins.

Discussion

Electrons are transferred from plastocyanin or cytochrome c_6 to PSI on the luminal side of thylakoid membranes. To understand the electron transfer between PSI and the donor proteins, it is necessary to identify the elements involved in the molecular recognition. The structures of plastocyanin and cytochrome c_6 are available (Frazao et al., 1995; Navarro et al., 1997). A flat hydrophobic surface is present around the redox centers of both proteins and is essential for the electron transfer from plastocyanin or cytochrome c_6 to PSI (Haehnel et al., 1994; Sigfridsson

et al., 1996). Correct hydrophobic interactions are expected to ensure accurate orientation of plastocyanin or cytochrome c_6 on PSI complex. Previously, we showed that the surface α-helix l in the J loop of the PsaB protein might provide the site for hydrophobic interaction with plastocyanin or cytochrome c_6 (Sun et al., 1999). Here, we examined the role of the H loop in the assembly and function of the PSI complex by mutagenesis analysis.

The deletion and repetition mutations in the H loop affected the accumulation of PSI proteins in the membranes. This might result from a decreased rate of assembly of the mutated PsaB proteins into membrane or from an increased turnover of the mutated PsaB proteins. The N438-E448 region was deleted in the af, ag, ah, ai, and aj mutations, the I453-T464 segment was deleted in the ag, ah, ai, aj, and bg mutations, and the S500-G512 segment was deleted in the cj, dj, and ej mutations. The PSI proteins could not be detected in the membranes of these mutants. The ch, ci, and di mutants contained these protein segments and accumulated the PSI complexes. Therefore, the N438-E448, I453-T464, and S500-G512 regions are essential for the normal accumulation of the PSI complex. The ch, ci, and di mutants contained a partial or complete deletion of the L469-D496 region and could accumulate PSI proteins. Therefore, the L469-D496 region is not essential for maintaining a stable folding of PsaB and the normal level of PSI. When the H loop sequences of the PsaB protein from different sources were aligned, the N438-E448, I453-T464, and S500-G512 sequences are found to be highly conserved whereas the L469-D496 segment contains a major difference in a 12-residue sequence between higher plants and cyanobacteria. The N438-E448, I453-T464, and S500-G512 segments are located close to the transmembrane helices. They may play important roles in maintaining the structure of the H loop and/or packing of the adjacent transmembrane helices. Deletion of these fragments may affect the integration of PsaB protein into membrane and diminish the assembly of other PSI proteins. The L469-D496 segment is located in the central region of the H loop. The ch, ci, and di deletion mutants, which lack L469-D496 segment, contain PSI proteins. Therefore, this segment may not play a structural role in the assembly of PsaB protein and other PSI proteins. Repetition mutants also suggested that the structural role of the H loop in the assembly of the PSI complex. It is interesting that an additional 7-residue peptide and an additional 39-residue peptide did not abolish the accumulation of PSI protein, but an additional 23-residue peptide reduced the PSI proteins to an undetectable level. It seems that the proper folding of additional peptide fragment is necessary to maintain structural integrity of the H loop.

The deletion of the L469-D496 segment did not affect the interaction between the PSI complex and plastocyanin/cytochrome c_6. Thus, the L469-D496 segment is not essential for the interaction between the PSI complex and plastocyanin/cytochrome c_6 during the electron

transfer. The repetition mutants did not interrupt the interaction of the PSI complex with the soluble protein donors. It seems that the middle region of the H loop of PsaB is not essential for the electron transfer function of the PSI complex. However, we could not exclude the possibility that the N438-E448, I453-T464, and S500-G512 regions of PsaB, required for stable assembly of PsaB, are also important for the interaction of PSI with the donor proteins. It is also possible that the H loop of PsaA plays an important role in the interaction between PSI and the donor proteins.

The H loop of PsaB was extensively accessible to proteases, suggesting that this loop should be exposed to the solvent (Sun et al., 1997). However, the L469-D496 segment in the middle of H loop is not essential for the interaction between the PSI complex and plastocyanin/cytochrome c_6 during the electron transfer. In contrast, the surface α-helix l in the J loop of PsaB has been shown to provide the site for hydrophobic interaction with plastocyanin or cytochrome c_6 (Sun et al., 1999). Thus, the J loop should be exposed to the solvent. In the topographical studies, the J loop of PsaB was not accessible to proteases (Sun et al., 1997). Electron microscopic and crystallographic analyses have revealed the presence of a cavity on the luminal side of PSI (Krauß et al., 1996; Schubert et al., 1997). Plastocyanin and cytochrome c_6 are much smaller in size than trypsin or Glu-C proteases. It is likely that the J loop is located in a cavity in which the proteases could not access, but the donor proteins are able to enter and interact with the J loop. Since the H loop of PsaB is exposed to solvent, we propose that the H loop might fold on the surface and form an entrance to the cavity, inside which the J loop folds close to the membrane and provides the interaction site for the donor proteins.

Acknowledgment

Literature Cited

Arnon D (1949) Copper enzyme in isolated chloroplasts. Polyphenol oxidase in *Beta vulgaris*. Plant Physiol **24:** 1-14

Bottin H, Mathis P (1985) Interaction of plastocyanin with the photosystem I reaction center: a kinetic study by flash spectroscopy. Biochemistry **24:** 6453-6460

Chitnis PR (1996) Photosystem I. Plant Physiol **111:** 661-669

Chitnis PR, Purvis D, Nelson N (1991) Molecular cloning and targeted mutagenesis of the gene psaF encoding subunit III of photosystem I from the cyanobacterium *Synechocystis* sp. PCC 6803. J Biol Chem **266:** 20146-20151

Chitnis PR, Xu Q, Chitnis VP, Nechushtai R (1995) Function and organization of photosystem I polypeptides. Photosynth Res **44:** 23-40

De la Cerda B, Navarro JA, Hervás M, De la Rosa MA (1997) Changes in the reaction mechanism of electron transfer from plastocyanin to photosystem I in the cyanobacterium *Synechocystis* sp. PCC 6803 as induced by site-directed mutagenesis of the copper protein. Biochemistry **36:** 10125-10130

Farah J, Rappaport F, Choquet Y, Joliot P, Rochaix JD (1995) Isolation of a *psaF*-deficient mutant of *Chlamydomonas reinhardtii*: efficient interaction of plastocyanin with the photosystem I reaction center is mediated by the PsaF subunit. EMBO J **14:** 4976-4984

Frazao C, Soares CM, Carrondo MA, Pohl E, Dauter Z, Wilson KS, Hervas M, Navarroo JA, De la Rosa MA, Sheldrick GM (1995) *Ab initio* determination of the crystal strucutre of cytochrome c_6 and compariosn with plastocyanin. Structure **3:** 1159-1169

Fromme P (1996) Structure and function of photosystem I. Curr Opin Struct Biol **6:** 473-484

Furr HC, Barua AB, Olson JA (1992) Retinoids and carotenoids. *In* APD Leenheer, WE Lambert, HJ Nelis, (eds.), Modern Chromatographic Analysis of Vitamins. Dekker, New York, N. Y., pp. 1-71

Garnier J, Osguthorpe DJ, Robson B (1978) Analysis of the accuracy and implicaitons of simple methods for predicting the secondary structure of globular proteins. J Mol Biol **120:** 97-120

Golbeck JH (1994) Photosystem I in Cyanobacteria. *In* DA Bryant, (ed.) The Molecular Biology of Cyanobacteria. Kluwer Academic Publishers, Dordrecht, The Netherlands, pp. 179-220

Haehnel W, Jansen T, Gause K, Klosgen RB, Stahl B, Michl D, Huvermann B, Karas M, Herrmann RG (1994) Electron transfer from plastocyanin to photosystem I. EMBO J **13:** 1028-1038

Haehnel W, Propper A, Krause H (1980) Evidence for complexed plastocyanin as the immediate electron donor of P-700. Biochim Biophys Acta **593:** 384-399

Hatanaka H, Sonoike K, Hirano M, Katoh S (1993) Small subunits of photosystem I reaction center complexes from *Synechococcus elongatus*. II. Is the *psaF* gene productrequired for oxidation of cytochrome c_{553}? Biochim Biophys Acta **1141:** 45-51

Hervás M, Navarro JA, Diaz A, Bottin H, De la Rosa MA (1995) Laser-flash kinetic analysis of the fast electron transfer from plastocyanin and cytochrome c_6 to photosystem I. Experimental evidence on the evolution of the reaction mechanism. Biochemistry **34:** 11321-11326

Hervás M, Navarro JA, Diaz A, De la Rosa MA (1996) A comparative thermodynamic analysis by laser-flash absorption spectroscopy of photosystem I reduction by plastocyanin and cytochrome c_6 in *Anabaena* PCC 7119, *Synechocystis* PCC 6803, and spinach. Biochemistry **35**: 2693-2698

Hervás M, Ortega JM, Navarro JA, de la Rosa MA, Bottin H (1994) Laser flash kinetic analysis of *Synechocystis* sp. PCC 6803 cytochrome c6 and plastocyanin oxidation by photosystem I. Biochim Biophys Acta **1184**: 235-241

Higuchi R (1989) Using PCR to engineer DNA. *In* HA Erlich, (ed.) PCR Technology. Stockton Press, New York, pp. 61-70

Hippler M, Reichert J, Sutter M, Zak E, Altschmied L, Schröer U, Herrmann RG, Haehnel W (1996) The plastocyanin binding domain of photosystem I. EMBO J **15**: 6374-6384

Kerfeld CA, Krogmann DW (1998) Photosynthetic cytochromes *c* in cyanobacteria, algae, and plants. Annual Rev Plant Physiol Plant Mol Biol **49**: 397-425

Krauß N, Schubert W-D, Klukas O, Fromme P, Witt HT, Saenger W (1996) Photosystem I at 4 Å resolution represents the first structural model of a joint photosynthetic reaction centre and core antenna system. Nature Struct Biol **3**: 965-973

Mathis P, Setif P (1981) Near-infrared absorption spectra of the chlorophyll a cations and triplet state *in vitro* and *in vivo*. Isr J Chem **21**: 316-320

Mehler AH (1951a) Studies on reactions of illuminated chloroplasts. I Mechanism of the reduction of oxygen and other Hill reagents. Arch Biochem Biophys **33**: 65-77

Mehler AH (1951b) Studies on reactions of illuminated chloroplasts. II Stimulation and inhibition of the reaction with molecular oxygen. Arch Biochem Biophys **34**: 339-351

Navarro JA, Hervas M, De la Rosa MA (1997) Co-evolution of cytochrome c_6 and plastocyanin, mobile proteins transferring electrons from cytochrome b_6f to photosystem I. J Biol Inorg Chem **2**: 11-12

Schubert W-D, Klukas O, Krauß N, Saenger W, Fromme P, Witt HT (1997) Photosystem I of *Synechococcus elongarus* at 4 Å Resolution: Comprehensice Structure Analysis. J Mol Biol **272**: 741-769

Shen G, Boussiba S, Vermaas WF (1993) *Synechocystis* sp PCC 6803 strains lacking photosystem I and phycobilisome function. Plant Cell **5**: 1853-1863

Sigfridsson K, Young S, Hansson O (1996) Structural dynamics in the plastocyanin-photosystem 1 electron-transfer complex as revealed by mutant studies. Biochemistry **35**: 1249-1257

Smart LB, Anderson SL, McIntosh L (1991) Targeted genetic inactivation of the photosystem I reaction center in the cyanobacterium *Synechocystis* sp. PCC 6803. EMBO J **10**: 3289-3296

Sun J, Ke A, Jin P, Chitnis VP, Chitnis PR (1998) Isolation and functional study of photosystem I subunits in the cyanobacterium *Synechocystis* sp. PCC 6803. Meth Enzymol **297**: 124-139

Sun J, Xu Q, Chitnis VP, Jin P, Chitnis PR (1997) Topography of the Photosystem I Core Proteins of the Cyanobacterium *Synechocystis* sp. PCC 6803. J Biol Chem **272**: 21793-21802

Sun J, Xu W, Hervás M, Navarro JA, De La Rosa MA, Chitnis PR (1999) Oxidizing side of the cyanobacterial photosystem I: Evidence for interaction between the electron donor proteins and a luminal surface helix of the PsaB subunit. J Biol Chem **Accepted**

Williams JGK (1988) Construction of specific mutations in photosystem II photosynthetic reaction center by genetic engineering methods in *Synechocystis* 6803. Meth Enzymol **167**: 766-778

Wood PM (1978) Interchangeable copper and iron proteins in algal photosynthesis. Studies on plastocyanin and cytochrome c-552 in *Chlamydomonas*. Eur J Biochem **87**: 9-19

Xu Q, Jung YS, Chitnis VP, Guikema JA, Golbeck JH, Chitnis PR (1994a) Mutational analysis of photosystem I polypeptides in *Synechocystis* sp. PCC 6803. Subunit requirements for reduction of NADP$^+$ mediated by ferredoxin and flavodoxin. J Biol Chem **269**: 21512-21518

Xu Q, Yu L, Chitnis VP, Chitnis PR (1994b) Function and organization of photosystem I in a cyanobacterial mutant strain that lacks PsaF and PsaJ subunits. J Biol Chem **269**: 3205-3211

Figure legends

FIG. 5-1. **Mutagenesis of the H loop of the PsaB protein.** The amino acid sequence of the H loop (N438-D513) of *Synechocystis* sp. PCC 6803 PsaB protein is shown in the top. The deletion and repetition mutations are indicated by lines corresponding to the amino acid sequence of WT protein. The length of deletion or repetition is shown after the lines and the number of charged residues in the mutant H loop is shown in parentheses.

FIG. 5-2. **Confirmation of the mutations by PCR analysis.** The genomic DNA isolated from the mutant strains was used for PCR amplification to confirm the mutations. The

length of deletion or repetition is shown for the mutants. M: pGEM DNA Markers (Promega, WI).

FIG. 5-3. **Accumulation of the PSI proteins in the mutant strains.** Membranes containing 5 μg of chlorophyll were analyzed by Tricine/urea/SDS-PAGE and Western blotting with subunit-specific antibodies. The immunodetection was visualized by enhanced chemiluminescence.

Table 5-1. Characterization of the mutant strains

Strains	Doubling time (h)			Pigment contents ($\mu g \cdot A_{730}^{-1} \cdot ml^{-1}$)	
	with glucose low light	with glucose medium light*	without glucose medium light*	chlorophyll	carotene
LKC	30	-	-	0.72	0.32
RWT	27	13	54	1.44	0.97
af	29	-	-	0.73	0.35
ag	30	-	-	0.76	0.41
ah	30	-	-	0.74	0.39
ai	30	-	-	0.82	0.42
aj	29	-	-	0.85	0.44
bg	28	-	-	0.84	0.45
ch	28	13	52	1.22	1.04
ci	27	15	62	1.34	1.10
cj	28	20	-	0.75	0.38
di	27	14	59	1.32	0.99
dj	27	23	-	0.88	0.53
ej	27	31	-	0.86	0.45
df	28	17	107	1.22	0.85
dg	29	33	-	1.10	0.49
dh	29	16	62	1.30	0.86

*: '- ' indicates that the strains died or did not grow.

Table 5-2. Characterization of the mutant photosynthetic membranes

The results were normalized on equal cell basis and expressed as percentage of RWT level that is shown in parentheses. Level of P700 in DM extract was expressed as percentage of RWT level in membrane.

| Strains | PSI photosynthetic activity (nmol·A_{730}^{-1}·h^{-1}) | | |
	DAD to MV	cytochrome c_6 to MV	cytochrome c_6 to ferredoxin
RWT	100 (-448)	100 (-279)	100 (49)
ch	50	57	56
ci	59	61	48
di	92	89	87
df	45	53	46
dh	60	62	68

Table 5-3. Characterization of the mutant PSI complexes

The chlorophyll to P700 molar ratio and bimolecular rate constants for the mutant PSI complexes reduction by plastocyanin.

PSI complex	Chlorophyll to P700 molar ratio	K_{bim} $(\times 10^{-6} M^{-1} s^{-1})$	K_{inf} $(\times 10^{-6} M^{-1} s^{-1})$
RWT	131	8.6	9.70
ch	123	6.7	7.23
ci	146	6.8	8.31
di	104	7.3	9.49
dh	131	7.1	7.40

Helix-VII   H loop   Helix-VIII

YVH<u>NDVVVAFGTPEKQILIEPVFAQWIQATSGKALYGFDVLLSNPDSIASTTGAAWLPGWLDAINSGTNSLFLTIGPGD</u>FLV
   438   513

RWT ━━ 0 (7-/2+)

af ━   ━━━━━━━━━━━━━━━━━━━━━━━━━━━━━━━━━━━━━ D11 (5-/2+)

ag ━   ━━━━━━━━━━━━━━━━━━━━━━━━━━━━━━━ D27 (4-/1+)

ah ━   ━━━━━━━━━━━━━━━━━━━━━━━━━━ D43 (2-/0+)

ai ━   ━━━━━━━━━━━━━━━━━━━━ D59 (1-/0+)

aj ━   ━━━ D75 (1-/0+)

bg ━━━━━━━━━   ━━━━━━━━━━━━━━━━━━━━━━ D12 (6-/2+)

ch ━━━━━━━━━━━━━   ━━━━━━━━━━━━━━ D12 (5-/2+)

ci ━━━━━━━━━━━━━   ━━━━━━━━ D28 (4-/2+)

cj ━━━━━━━━━━━━━   ━━━ D44 (4-/2+)

di ━━━━━━━━━━━━━━━━━━━━   ━━━━━━━━━━ D11 (6-/2+)

dj ━━━━━━━━━━━━━━━━━━━━   ━━━ D27 (6-/2+)

ej ━━━━━━━━━━━━━━━━━━━━━━━━   ━━ D13 (7-/2+)

df ━   ━━━━━━━━━━━━━━━━━━━━━━━━━━━━━━━━━ R39 (10-/4+)

dg ━━━━━   ━━━━━━━━━━━━━━━━━━━━━━━━━━━━ R23 (9-/3+)

dh ━━━━━━━━━━━━━━━━━   ━━━━━━━━━━━━ R7 (7-/2+)

Fig. 5-1

Fig. 5-2

Mutant Strains

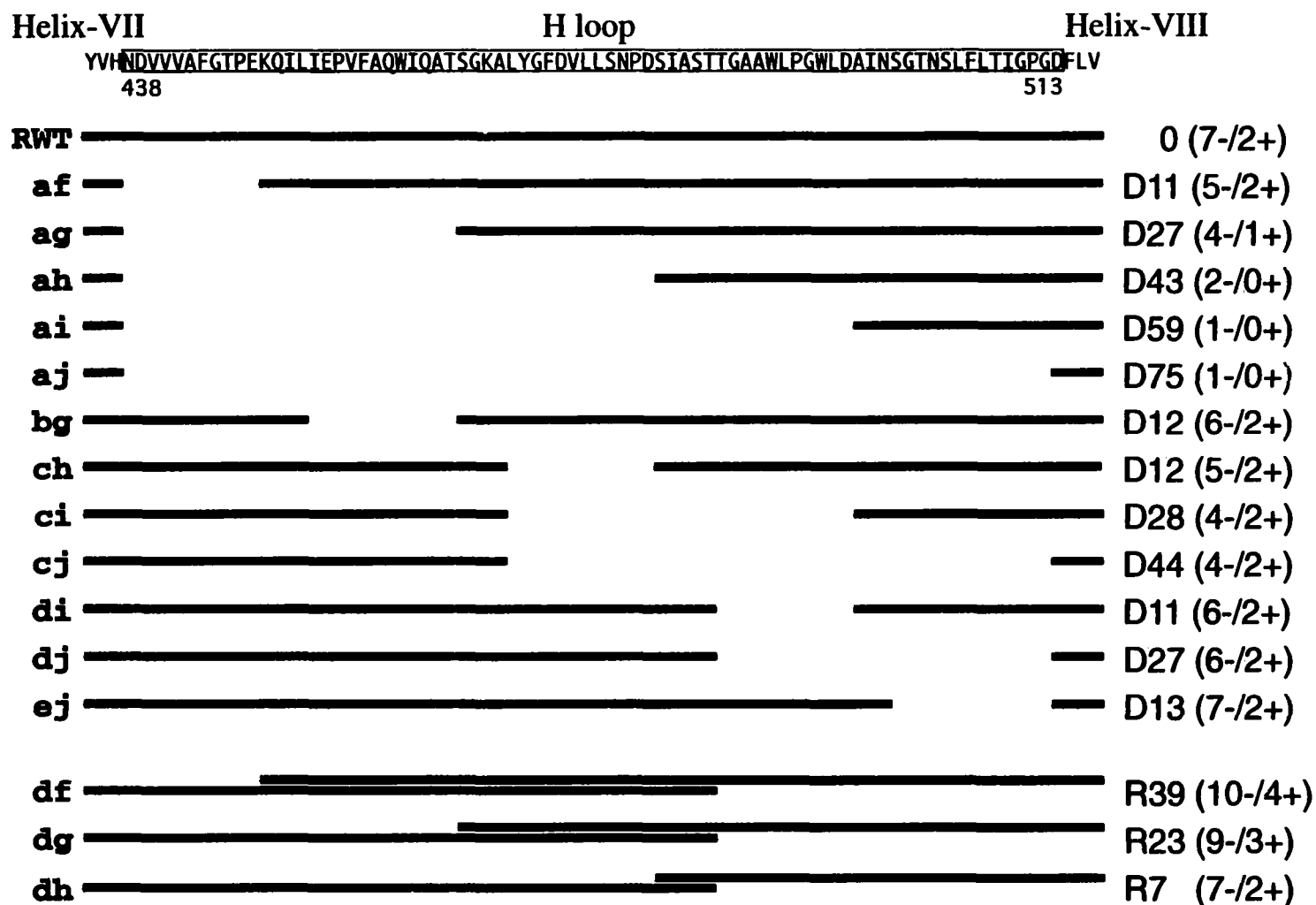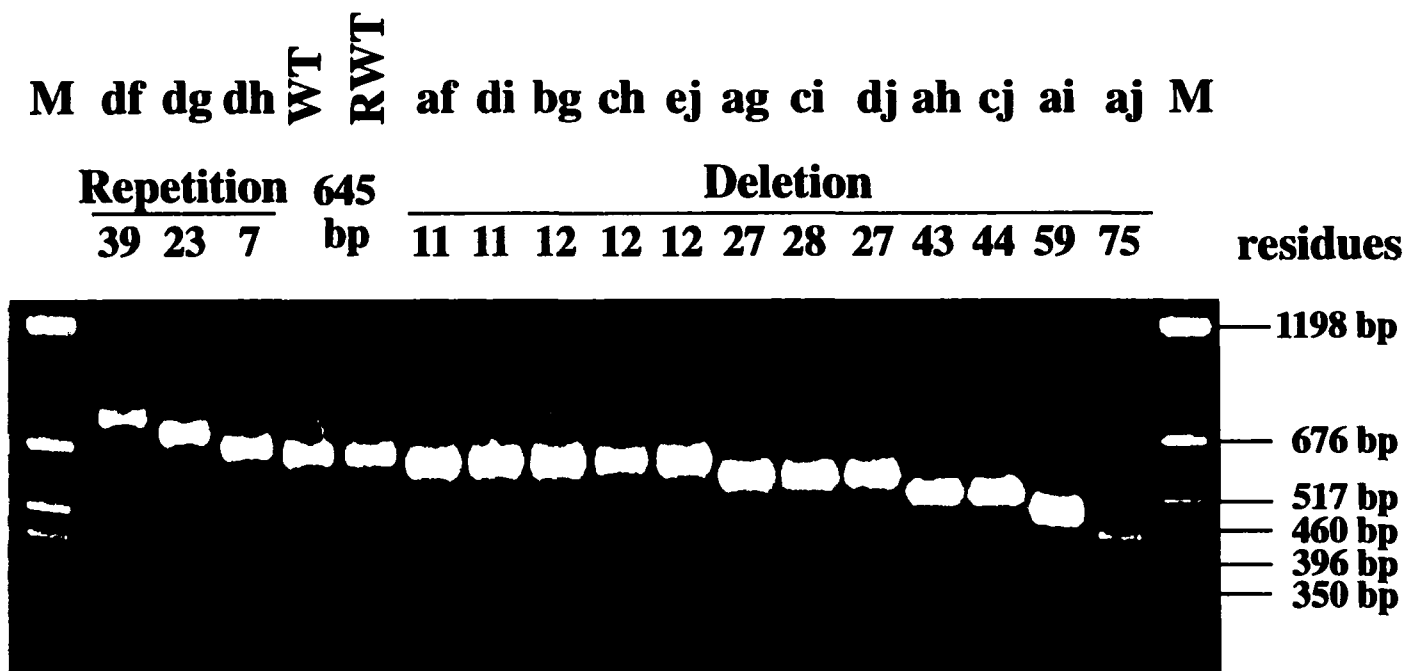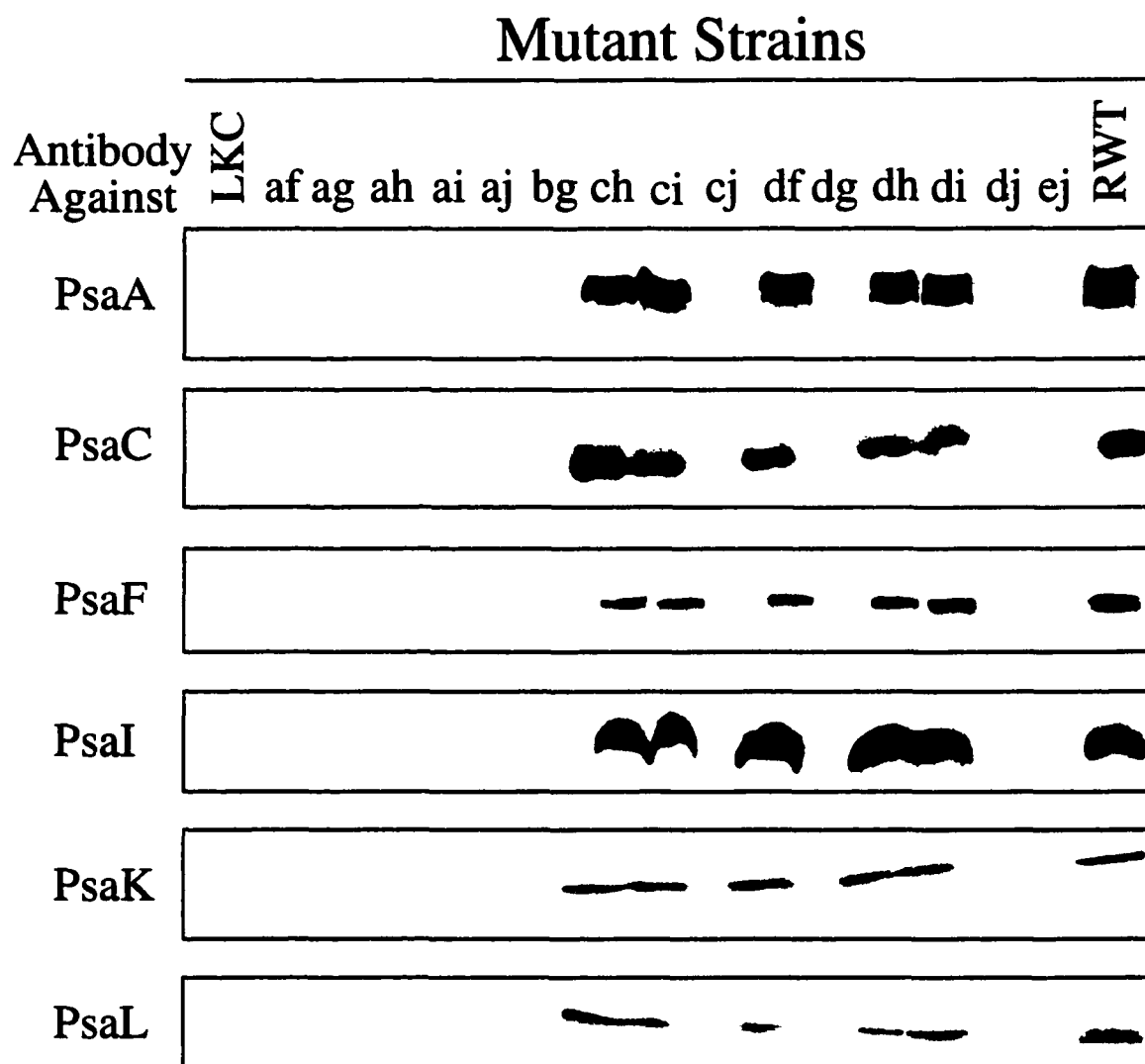| Antibody Against	LKC	af	ag	ah	ai	aj	bg	ch	ci	cj	df	dg	dh	di	dj	ej	RWT

PsaA

PsaC

PsaF

PsaI

PsaK

PsaL

Fig. 5-3

CHAPTER 6. OXIDIZING SIDE OF PHOTOSYSTEM I: THE LYSINE-RICH REGION OF PLANT PSAF IS SUFFICIENT FOR BINDING OF THE DONOR PROTEINS, BUT NOT FOR THE ELECTRON TRANSFER WITHIN THE INTERMOLECULAR COMPLEX[1]

Jun Sun, Huadong Tang, Manuel Hervás, José A. Navarro, Miguel A. De La Rosa,

and Parag R. Chitnis

Summary

The N-terminal lysine-rich region in the PsaF protein of the plant and algal photosystem I (PSI) complexes has been proposed to provide binding site for plastocyanin and cytochrome c_6 during the electron transfer. To test this hypothesis, we generated the CFa, CFb, and CFc mutant strains of *Synechocystis* sp. PCC 6803, containing chimeric *psaF* genes with coding regions for the mature protein, the lysine-rich region, and the first α-helix in the lysine-rich region of spinach PsaF protein, respectively. The CFb and CFc mutant strains accumulated reduced levels of the chimeric PsaF proteins whereas the PsaF protein was not detected in the CFa mutant strain. The chimeric PsaF proteins were associated with the PSI complexes, but were less stable than the wild type PsaF protein. The CFb and CFc chimeric PsaF proteins could be cross-linked to algal plastocyanin or cytochrome c_6. These results indicated that the first α-helix in the lysine-rich region of spinach PsaF protein is sufficient for binding of the donor proteins whereas the helix-turn-helix structure provides stability of the chimeric PsaF protein. However, the fast phase of electron transfer was not observed in the interactions of eukaryotic donor proteins with the chimeric PSI complexes. Our results indicate that the lysine-rich region is sufficient for the binding of the donor proteins, but not for the electron transfer within the intermolecular complex.

Introduction

PSI[2] is a light-driven membrane-bound oxidoreductase that transfers electrons from the reduced plastocyanin in the thylakoid lumen to the oxidized ferredoxin in the chloroplast stroma or cyanobacterial cytoplasm (1,2). A monomer of cyanobacterial PSI contains eleven proteins, about 90 chlorophyll a molecules, 10-12 β carotene molecules, two phylloquinones, and three [4Fe-4S] clusters. The PsaA and PsaB proteins of PSI form the heterodimeric core that harbors most of the chlorophyll a molecules, including the primary electron donor P700. In addition to the core proteins, the cyanobacterial PSI complex contains three peripheral proteins (PsaC, PsaD, and PsaE) and six integral membrane proteins (PsaF, PsaI, PsaJ, PsaK, PsaL, and PsaM) (1,2). Structural organization of PSI components is known from the X-ray crystallographic analysis of PSI at 4 Å (3,4). On the oxidizing side of PSI, the P700 reaction center accepts electrons from plastocyanin, which is present in chloroplasts and cyanobacteria. Some cyanobacteria and green algae contain cytochrome c_6 as an alternative electron carrier to plastocyanin. These proteins are expressed differentially depending on the relative availability of copper and iron in the culture medium (5-7).

The interactions between the plant plastocyanin and PSI shows a fast kinetic step, indicating first-order electron transfer within a complex of plastocyanin and PSI, and a slow phase attributed to the bimolecular reaction between plastocyanin and PSI (8-10). The PSI-mediated oxidation of algal plastocyanin or cytochrome c_6 also takes place with a multi-step kinetic mechanism (11-13). In contrast, kinetic analysis of cytochrome c_6 and plastocyanin oxidation by PSI from some cyanobacteria shows the absence of the fast phase, suggesting a one-step bimolecular collision mechanism (14-16). Examination of the structures of plastocyanin and cytochrome c_6 reveals the presence of a conserved hydrophobic surface and a conserved negative region (17,18). The hydrophobic surface and its flat structure are required for the association and electron transfer to PSI (19,20). The negative region of eukaryotic plastocyanin has a significant role in the binding of plastocyanin to PSI (15,21). Thus, the interactions between eukaryotic plastocyanin and PSI involve the electrostatic interaction through the negative region of plastocyanin for the initial docking and the hydrophobic interaction that is crucial during electron transfer. The surface α-helix l of PsaB is located near

---

[2] The abbreviations used are: PS, photosystem; MOPS, 3-[N-morpho]linepropanesulfonic acid; PCR, polymerase chain reaction; DM, dodecyl-β-D-maltoside; SDS, sodium dodecyl sulfate; DTT, dithiothreitol; EDC, N-ethyl-1,3-[3-(diethylamino)propyl]carbodiimide; Tricine, N-[2-hydroxy-1,1-bis(hydroxymethyl)ethyl]-glycine; PAGE, polyacrylamide gel electrophoresis; AA, amino acid.

the P700 chlorophyll *a* dimer (3,4) and provides the site for hydrophobic interaction with the donor proteins (22).

The PsaF subunit of PSI contains a large luminal N-terminal domain that may provide a docking site for plastocyanin on the oxidizing side of PSI. The deletion of PsaF reduced the electron transfer rate from plastocyanin to PSI in the green alga *Chlamydomonas reinhardtii* (23). However, the PsaF subunit of PSI is not required in the interactions with plastocyanin or cytochrome c_6 in *Synechocystis* sp. PCC 6803 (16,24,25) and in *Synechococcus elongatus* (26). This discrepancy in the function of PsaF is addressed by chemical cross-linking studies. The conserved negative region in plant plastocyanin can be cross-linked with a lysine-rich region in the N-terminal domain of plant PsaF, which could fold into an amphipathic α-helix with the positively charged face interacting with plastocyanin (15). This lysine-rich region is well conserved among plant and algal PsaF proteins, but is not found in the cyanobacterial PsaF (24). Site-directed mutagenesis has indicated that Lys16 and Lys23 play important roles in this recognition site (27). It has been proposed that the lysine-rich region in the N-terminal domain of eukaryotic PsaF is responsible for the complex formation between PSI and plastocyanin or cytochrome c_6 in plant and algae. To test if the lysine-rich domain is sufficient for complex formation and fast electron transfer to P700, we introduced the lysine-rich region of spinach PsaF into the PsaF protein of *Synechocystis* sp. PCC 6803. Here we present the characterization of the PSI complexes containing chimeric PsaF proteins.

Experimental procedures

Cyanobacterial cultures. Strains of *Synechocystis* sp. PCC 6803 were cultured in BG-11 medium with appropriate antibiotics (30 mg/l chloramphenicol or 40 mg/l kanamycin) at 30°C and were aerated by bubbling with air. The growth of the *Synechocystis* cells was monitored from absorption of cultures at 730 nm (A_{730}) using an UV-160U spectrophotometer (Shimadzu, Tokyo, Japan). Cells were harvested at the late exponential growth phase, resuspended in 0.4 M sucrose, 10 mM NaCl, 10 mM MOPS-HCl (pH 7.0), and stored at -20°C for further use.

Site-directed mutagenesis and generation of the mutant strains. The AFK6 strain of *Synechocystis* sp. PCC 6803 contains a deletion of the *psaF* gene (24) and was used as the recipient strain for introduction of the chimeric *psaF* genes into the *Synechocystis* genome (Fig. 6-1). The *Synechocystis psaF* gene has been replaced by the kanamycin-resistance gene in the AFK6 recipient strain (24). The FWT recombinant plasmid was constructed to introduce the chimeric *psaF* genes into the AFK6 recipient strain. In this plasmid, the *Synechocystis psaF-psaJ* operon and its 5'- and 3'-flanking regions were cloned into the polylinker of

pBluescript II KS (Stratagene, CA) and the chloramphenicol-resistance gene was inserted after the *psaJ* gene (Fig. 6-1). The high-fidelity *Vent* DNA Polymerase (New England Biolabs, MA) was used for all PCR amplifications in this study. In addition, the *psaF-psaJ* operon in the FWT plasmid was sequenced completely to ensure the absence of errors during PCR amplification. The PCR-mediated mutation technique (28) was used to introduce an *Hpa*I restriction enzyme site through silent mutation after the codon 5 for the matured PsaF protein and an *Spe*I restriction enzyme site after the stop codon of the *Synechocystis psaF* gene in the FWT plasmid. The mutagenic oligonucleotide primers used for generation of the chimeric *psaF* genes that contain coding regions from the spinach *psaF* cDNA and the *Synechocystis psaF* gene are listed in Table 6-1. These primers contained different restriction endonuclease recognition sites for cloning purposes. The amplified PCR fragments were digested by appropriate restriction endonucleases and were ligated into the modified FWT plasmid that had been digested with the *Hpa*I and *Spe*I restriction enzymes. The chimeric *psaF* genes in the mutated recombinant plasmids were sequenced completely to ensure the presence of desired changes and the absence of errors by PCR amplification. The plasmid DNAs were isolated and used to transform the AFK6 recipient strain. Transformation was performed at 30°C using chloramphenicol for the selection pressure (29). The chloramphenicol-resistant transformants were selected, segregated for three generations, and replica-plated to confirm the absence of the kanamycin-resistance gene. After segregation, the chloramphenicol-resistant transformants were cultured in liquid BG-11 medium and the genomic DNA was isolated. PCR amplification of the *psaF* gene was performed by using genomic DNA templates from the mutant strains and the primer pair FJ05 (GGATCACGGTAACAGGTTGC) and FJ06 (GTACAACCTCTGCCA GAATCC). The nucleotide sequence of these PCR fragments was determined to confirm mutations.

Preparation of thylakoid membranes, PSI complexes, and donor proteins. Thylakoid membranes were isolated from *Synechocystis* cells after cell breakage with a bead beater (Biospec Products) and from spinach leaves after cell breakage with a blender. The trimeric PSI complexes were purified from membranes by extraction with DM and sucrose gradient ultracentrifugation (30). Chlorophyll *a* concentrations in the thylakoid membranes and PS I complexes were determined in 80% (v/v) acetone (31). The P700 content was estimated by the measurement of photoinduced absorbance changes at 820 nm (13,32,33). Spinach plastocyanin and plastocyanin and cytochrome c_6 from *Synechocystis* sp. PCC 6803 and green alga *Monoraphidium braunii* were purified as described previously (13,34).

Analytical gel electrophoresis, immunodetection, and cross-linking. The PS I complexes and photosynthetic membranes were solubilized at 37°C for 2 hours with 1% SDS and 0.1%

DTT. Proteins were then resolved by Tricine/urea/SDS-PAGE and examined by immunodetection (35). We used polyclonal antibodies that were specific for *Synechocystis* PsaB (35), *Synechocystis* PsaF (36) or plant PsaF (37). The apparent mass of protein was determined from the migration of prestained protein molecular weight standards (Life Technologies, MD) upon electrophoresis. The cross-linking experiments were performed using EDC as the cross-linker (15). The cross-linking reaction mixture contained 30 mM HEPES, pH 7.5, 5 mM $MgCl_2$, 1 mM ascorbate, 5 mM EDC, 0.05% DM, and 20 μM donor protein. The concentrations of PSI complexes used in the cross-linking reaction were 0.1 mg chlorophyll/ml for spinach and FWT PSI complexes and 0.3 mg chlorophyll/ml for CFb and CFc PSI complexes.

Laser-flash spectroscopy. Kinetics of flash induced absorbance changes in PSI was followed at 820 nm and the experimental set-up, data collection and kinetic analyses were performed as reported previously (13).

Results

Generation of the mutant strains containing chimeric psaF genes. Alignment of the amino acid sequences of mature PsaF proteins from different sources revealed that the sequences were highly conserved in the C-terminal domain whereas the N-terminal domain contained a major difference between the eukaryotic and prokaryotic PsaF proteins (Fig. 6-2A). This difference is located in a lysine-rich region of Lys9-Leu61 in the N-terminal domain of spinach PsaF (Fig. 6-2A). This lysine-rich region was predicted to form one α-helix in the region of Lys9-Tyr32, a second α-helix in the region of Ala37-Asn55, and a turn-structure connecting these two α-helices in the short stretch of Ala33-Ser36 (15). Cross-linking experiment have indicated that the lysine residues at positions 12, 16, 19, 23, 24, 30 in the first α-helix and Lys43 in the second α-helix are possible sites for cross-linking PsaF with plastocyanin. The lysine residues in the first α-helix can be aligned on one side of the helix to form a positive face that could provide binding site for plastocyanin (15).

To examine if the lysine-rich region is sufficient for the binding of plastocyanin to the PSI complex, we generated three chimeric *psaF* genes (Fig. 6-1). Since the genes would be expressed in *Synechocystis* cells and the protein needed to be targeted properly to the membrane, the CFa, CFb, and CFc *psaF* genes contained the DNA region encoding the signal peptide and the first 4 amino acid residues of the mature *Synechocystis* PsaF protein. The DNA region coding for the remaining mature *Synechocystis* PsaF protein was replaced by the coding region for Gly4-Phe154 of the mature spinach PsaF protein in the CFa *psaF* gene. The DNA region coding for the Gly4-Leu61 lysine-rich domain of spinach PsaF was used to replace the

coding sequence for the corresponding Asn5-Ala42 region of the cyanobacterial PsaF protein in the CFb *psaF* gene. Finally, the coding region for the Gly5-Asp35 first α-helix region of spinach PsaF substituted coding sequence for the corresponding Asn5-Leu23 region of the *Synechocystis* PsaF protein in the CFc *psaF* gene. The three DNA constructs containing the chimeric *psaF* genes and the FWT plasmid containing the wild type *Synechocystis psaF* gene were used to transform the AFK6 recipient strain. Fig. 6-2B shows the alignment of the deduced amino acid sequences of the chimeric PsaF proteins along with the spinach and the wild type *Synechocystis* (FWT) PsaF protein sequences.

After segregation, the resulting transformant strains were cultured in liquid BG-11 medium. The genomic DNA templates were isolated from the transformant strains for PCR amplification. Appropriate PCR fragments containing the chloramphenicol-resistance gene were resolved on an agarose gel and yielded DNA bands as expected (data not shown). Thus, the chloramphenicol-resistance gene was integrated into the genomic DNA at the desired position in the transformant strains. PCR fragments containing the *psaF* genes were amplified with primer pair FJ05 and FJ06. The nucleotide sequences of these PCR fragments matched the desired mutations. These results indicated that the desired transformant strains containing chimeric *psaF* genes were obtained.

Accumulation of chimeric PsaF proteins in the mutant strains. Thylakoid membranes were isolated from mutant strains and resolved by SDS-PAGE. For comparison, we loaded samples of the FWT membranes that contained different amounts of chlorophyll. The CFb, CFc, CFa, and AFK6 membranes containing 5 μg of chlorophyll were loaded in each lane. Immunodetection was performed with polyclonal antibodies against *Synechocystis* PsaB and PsaF (Fig. 6-3A). The PsaB protein accumulated at the same level in the FWT, CFb, CFc, CFa, and AFK6 membranes containing same amount of chlorophyll, indicating similar amounts of PSI complexes accumulated in these mutant membranes. As expected, no PsaF protein was detected in the membranes of the PsaF-less AFK6 strain. The CFb and CFc membranes contained PsaF proteins that migrated more slowly during electrophoresis than the PsaF protein in the FWT membrane. The apparent masses of the FWT, CFb, and CFc PsaF proteins were determined to be 15.8 kDa, 18.2 kDa, and 17.7 kDa, respectively. These masses matched the predicted molecular weights of 15.7 kDa, 18.0 kDa, and 17.2 kDa for the FWT, CFb, and CFc PsaF proteins, respectively. To estimate the level of PsaF in the mutant membrane, different amounts of the FWT PSI preparations were used in immunoblotting and the signals were compared after densitometry. These comparative analyses showed that the CFb mutant contained at least 10% chimeric PsaF proteins and the CFc mutant contained at least 5% chimeric PsaF proteins in their membranes. Since the antibody against *Synechocystis*

PsaF does not bind to the chimeric proteins with the same affinity, our estimates represent the minimum level of these chimeric proteins in the membranes. In the CFb and CFc membranes, the antibody against *Synechocystis* PsaF recognized a protein with an apparent mass of 9.2 kDa. This protein is likely to be a degradation product from the chimeric PsaF proteins, indicating the reduced stability of these two chimeric PsaF proteins. However, the PsaF protein was not detected in the CFa membrane by the antibody against *Synechocystis* PsaF. Since the spinach PsaF did not cross-react with the antibody against *Synechocystis* PsaF, we also used the antibody against plant PsaF for Western blotting. The antibody against plant PsaF did not react with the FWT, CFb, and CFc PsaF proteins, and did not detect PsaF protein in the CFa membranes (data not shown). These results indicated that the CFb and CFc mutant strains accumulated the chimeric PsaF proteins at a reduced level whereas the CFa mutant strain could not accumulate detectable level of the PsaF protein.

To examine if the chimeric PsaF proteins were associated with the PSI complex, the DM extracts of the mutant membranes were subjected to sucrose gradient ultracentrifugation and fractions were collected after the ultracentrifugation. The heavier green band containing trimeric PSI was collected as fraction 4. The lighter green band containing monomeric PSI and PSII was harvested as fraction 3. Fraction 1 contained the top layer in the ultracentrifugation tube. Fraction 2 was collected between fractions 3 and 1. The fractions were resolved by SDS-PAGE and Western blotting was performed using the antibody against *Synechocystis* PsaF (Fig. 6-3B). The PsaF proteins were detected in fractions 3 and 4 from FWT extract whereas chimeric PsaF protein was detected in fraction 4 from CFb extract. Similar results were observed with CFc extract (data not shown). Other fractions did not contain detectable PsaF proteins. Thus all CFb and CFc chimeric PsaF proteins in the membranes were integrated into the PSI complexes.

The PSI complexes were purified by DM extraction and ultracentrifugation. The purified CFb, CFc, CFa, and AFK6 PSI complexes containing 5 µg of chlorophyll and a gradient of FWT PSI complexes were resolved by SDS-PAGE. Western blotting analysis was performed by using antibodies against *Synechocystis* PsaB and PsaF (Fig. 6-3C). The PSI complexes from all 5 strains contained similar levels of the PsaB protein. Compared with the gradient of FWT PsaF proteins, the purified PSI complexes from the CFb and CFc strains contained approximately 10% and 5% chimeric PsaF, respectively. These estimates are similar to the estimated levels in the CFb and CFc membranes indicating that the chimeric PsaF proteins were associated with the PSI complexes. However, the 9.2 kDa protein fragment was largely removed from the purified PSI complexes, indicating that this fragment was not associated with the PSI complexes or can be easily removed from the PSI complexes by DM extraction.

Cross-linking of the chimeric PsaF proteins to plastocyanin and cytochrome c_6. The role of the plant PsaF N-terminal lysine-rich region in the complex formation with donor proteins was proposed from the cross-linking experiments (15). During the interaction on the oxidizing side, this lysine-rich region of PsaF is expected to come close to the negative region of donor proteins through electrostatic interactions, resulting in the complex formation. Thus, the lysine and the aspartate/glutamate residues involved in the interactions should be positioned proximally and could be cross-linked by the zero length cross-linker EDC that forms a covalent bond between primary amine and carboxyl groups. To examine the complex formation between the chimeric PsaF proteins and the donor proteins, we performed cross-linking experiments using EDC as the cross-linker. Because the algal plastocyanin functions similarly as the plant plastocyanin (13) and plants contain no cytochrome c_6 protein, we used plastocyanin and cytochrome c_6 isolated from *Synechocystis* sp. PCC 6803 and green alga *M. braunii* in the cross-linking reactions. After quenching the cross-linking reaction, the proteins were resolved by Tricine/urea/SDS-PAGE and the anti-PsaF antibodies were used to detect the cross-linking products that contained the PsaF proteins (Fig. 6-4). No cross-linked product was formed when the FWT PSI complex was used, indicating that the *Synechocystis* PsaF protein did not form a complex with the donor proteins through electrostatic interactions. Cross-linked products were observed in the reactions of spinach PSI with the algal donor proteins, but not with the *Synechocystis* donor proteins. The cross-linked product of spinach PsaF with algal plastocyanin had a larger apparent mass (33.9 kDa) than that with algal cytochrome c_6 (28.5 kDa), because of the larger molecular weight of plastocyanin than of cytochrome c_6. Thus, the spinach PsaF can form a complex with the algal donor proteins. Similar to the spinach PsaF, the CFb and CFc PsaF could also be cross-linked to the algal donor proteins, but not to the *Synechocystis* donor proteins (Fig. 6-4). Therefore, the chimeric PsaF proteins could interact with algal donor proteins through electrostatic attraction. These results indicated that the first N-terminal α-helix of spinach PsaF is sufficient for enabling the formation of physical complexes between PSI and the algal donor proteins. The introduction of this helix into prokaryotic PsaF enables the electrostatic interaction with the eukaryotic donor proteins, which will bring the PSI complex and the donor proteins together to form the intermolecular complex.

Electron transfer from donor proteins to PSI complexes containing chimeric PsaF proteins. Electron transfer within the intermolecular complex formed by PSI and donor proteins shows the first-order kinetics (8-13). The PSI complexes containing the chimeric PsaF proteins were used for laser-flash spectroscopy studies. However, we failed to observe any first order kinetics in the electron transfer from spinach or algal plastocyanin or algal cytochrome c_6 to the PSI complexes containing chimeric PsaF proteins (Fig. 6-5A). Different concentrations of

electron donor proteins (25 µM to 200 µM) or Mg^{++} (1 mM to 10 mM) were used during the electron transfer assays. The fast phase of electron transfer was not observed under any of the conditions attempted in our studies. The reduced level of chimeric PsaF in the mutant PSI complexes was expected to yield only a small fraction of the PSI complexes to participate in fast electron transfer with eukaryotic plastocyanin. To assess the sensitivity of the spectroscopic analysis, 0.17 µM of spinach PSI complexes were added to the sample cuvette containing 200 µM of plastocyanin and 3.02 µM of *Synechocystis* PSI complexes. A first order electron transfer was evident after addition of the spinach PSI complexes, which constituted only 5.3% of the total PSI complexes. Therefore, our inability to observe a fast phase of electron transfer in the chimeric PSI complexes was not caused by the sensitivity of our detection system. To examine the efficiency of the chimeric PSI complexes in accepting electrons from *Synechocystis* plastocyanin, rate constants were determined using different concentrations of *Synechocystis* plastocyanin (Fig. 6-5B). The rate constants given by the slopes of the linear fit were 6.34×10^{-6} M^{-1} s^{-1} for FWT PSI, 6.21×10^{-6} M^{-1} s^{-1} for CFb PSI, and 6.29×10^{-6} M^{-1} s^{-1} for CFc PSI. The CFb and CFc PSI complexes were as efficient as the FWT PSI complexes. Therefore the lack of functional interaction between eukaryotic plastocyanin and the chimeric PSI complexes was not due to the inability of the PSI in electron transfer, but was due to the lack of recognition between the eukaryotic electron donors and the chimeric PSI complexes. Therefore, the chimeric PSI complexes were able to form physical complexes with eukaryotic electron donors, but these complexes were not functional in electron transfer.

Discussion

The PSI complex accepts electrons from plastocyanin or cytochrome c_6 on the luminal side of the thylakoid membrane. Studies of the interactions on the oxidizing side of PSI have shown that the eukaryotic PSI complexes interact with eukaryotic donor proteins following a multi-step electron transfer mechanism. An initial docking of the donor proteins occurs through electrostatic interactions, followed by rearrangement in many cases (12). In contrast, some cyanobacterial PSI complexes interact with prokaryotic donor proteins following a one-step bimolecular collision mechanism (10,13,15). Comparison of the PsaF protein sequences from eukaryotic and prokaryotic photosynthetic organisms has revealed that the eukaryotic PsaF proteins contain a conserved lysine-rich region, which is not found in prokaryotic PsaF (24). This region may form a helix-turn-helix structure and can be cross-linked with the negative region of plastocyanin (15). The insertion of the N-terminal part of PsaF from *Chlamydomonas reinhardtii* into PSI from *Synechococcus elongatus* enables the binding of

algal plastocyanin and cytochrome c_6 (38). To test if the lysine-rich region is sufficient for complex formation, we introduced coding regions for the lysine-rich region of spinach PsaF into the *psaF* gene of *Synechocystis* and produced the chimeric PsaF proteins. The chimeric PsaF proteins enabled the formation of intermolecular complexes between PSI and donor proteins indicating the sufficient role of this lysine-rich region in the electrostatic interaction.

The CFb and CFc mutant strains accumulated chimeric PsaF proteins whereas the CFa mutant strains did not contain detectable PsaF protein (Fig. 6-3A). The accumulation of PsaF protein could be affected by several factors including transcription, translation, membrane translocation, assembly into the PSI complex, and stability of the chimeric PsaF proteins. The FWT PSI complexes contained similar levels of PsaF and PsaB proteins as compared to the PSI complexes isolated from the wild type strain, suggesting a normal transcription of the *psaF* gene in the FWT strain. The same upstream and downstream DNA sequences in the FWT strain were used in the CFa, CFb, and CFc mutant strains. The CFa, CFb, and CFc strains should contain a normal transcription level of the *psaF* gene.

The chimeric *psaF* genes might be translated inefficiently due to the differences in the codon usage in the spinach and *Synechocystis* genes. To investigate this possibility, we analyzed the codon frequencies in the chimeric and FWT psaF genes (Table 6-2). The codon usage in the wild type *Synechocystis psaF* gene matched well with the codon frequency in the *Synechocystis* genome. Some major codons used in the CFa *psaF* gene were rare codons or were at low frequency in the *Synechocystis* genome, such as AGG and AGA for arginine, GAG for glutamate, GGG and GGA for glycine, AAG for lysine, CCA for proline, and ACA for threonine. The rare codons may have very few corresponding tRNA molecules. The extensive use of the rare codons in the CFa *psaF* gene might have resulted in its greatly reduced translation. Thus, the codon frequency in the CFa *psaF* gene is a likely reason for the undetectable levels of the PsaF protein in the mutant strain. A relatively small number of rare codons is used in the CFb and CFc *psaF* genes. Examples of these codons include AGG for arginine, CCA for proline, and ACA for threonine. The use of these codons might result in reduced translation. The chimeric PsaF proteins and the 9.2-kDa degradation product together were still far less than the normal level of PsaF protein in the thylakoid membranes. Thus, the peculiar codon usage in the CFb and CFc *psaF* genes could result in a reduced biosynthesis of the chimeric PsaF proteins in these mutant strains.

We used the lumen-targeting peptide of the *Synechocystis* PsaF in all mutant strains. Thus, it is unlikely that the translocation of the N-terminal domain affected the accumulation of PsaF protein. The transmembrane helices play an important role in the assembly of membrane protein complex. Protein sequence analysis revealed that the C-terminal domain of the PsaF

proteins contains two transmembrane helices in the regions of Leu65-Leu86 and Val100-Ser127 of *Synechocystis* PsaF protein. The CFb and CFc PsaF proteins contained the *Synechocystis* PsaF C-terminal domain. Also, the chimeric PsaF proteins were associated with the PSI complexes (Fig. 6-3B). Therefore, the CFb and CFc PsaF proteins are likely to have a normal mode of assembly. Since the CFa PsaF protein contains the plant PsaF C-terminal domain, we could not exclude that improper assembly resulting in fast turnover as another reason for its undetectable level in the membranes. Finally, the CFc membranes contained more PsaF degradation product than the CFb membranes (Fig. 6-3A). It is likely that the CFc PsaF protein is more unstable than the CFb PsaF protein. In summary, difficulties in translation and improper assembly might be the reasons for the failure of the CFa protein to accumulate in the membranes, whereas reduced translation and decreased stability of the chimeric PsaF protein could result in the low levels of PsaF proteins in the CFb and CFc mutant strains.

The antibody against the *Synechocystis* PsaF protein recognized the CFb and CFc chimeric PsaF proteins, but did not cross-react with the spinach PsaF protein. The antigen epitope for the antibody against *Synechocystis* PsaF is located possibly in the C-terminal domain. The 9.2 kDa degradation product can be detected by the antibody against *Synechocystis* PsaF and thus should be released from a cleavage after Leu43 of the *Synechocystis* PsaF protein. A cleavage at His60 of *Synechocystis* PsaF protein would yield a 9.2 kDa degradation product containing the C-terminus. Therefore, the cleavage site for the degradation product is located in the region between Leu43 to His60. This region is before the first transmembrane helix and located on the luminal side of the thylakoid membrane. Thus, the degradation site of the chimeric PsaF protein, which might be the same site for degradation of *Synechocystis* PsaF protein, is located on the thylakoid lumen.

The CFb and CFc chimeric PsaF proteins can be cross-linked to the algal donor proteins (Fig. 6-4), indicating that the lysine-rich region is sufficient to provide electrostatic interaction with the negative region of the eukaryotic donor proteins. This lysine-rich region contains a helix-turn-helix structure (Fig. 6-2). The lysine residues in the first helix are likely to be cross-linked with plastocyanin (15) and important for binding of donor proteins (27). In our results, the introduction of the first helix only in the CFc chimeric PsaF protein allowed cross-linking. Therefore, the first helix, which contains 30 amino acid residues, is sufficient for the electrostatic interaction with the eukaryotic donor proteins. However, the CFc membranes contained more degradation product than the CFb membrane (Fig. 6-3A). Therefore, the CFb chimeric PsaF protein containing the helix-turn-helix structure is much more stable than the CFc chimeric PsaF protein containing only the first helix. Our results indicated that the first helix with a positively charged face is sufficient for binding to the donor proteins and the

second helix, which is expected to complete the helix-turn-helix structure, can provide stability to the chimeric protein.

The CFb and CFc PSI complexes contained similar electron transfer rate constants in accepting electrons from *Synechocystis* plastocyanin (Fig. 6-5A), indicating that these chimeric PSI complexes were active and efficient in electron transfer. However, first-order electron transfer was not observed in the electron transfer assays under different conditions (Fig. 6-5B). Therefore, the introduction of the lysine-rich region of spinach PsaF into *Synechocystis* PSI complex enabled the complex formation, but the complex was not functional. It is possible that the chimeric PsaF proteins attract the donor proteins to form the intermolecular complex, but the donor proteins are not orientated optimally within the complex to allow the proper hydrophobic interaction for electron transfer. Alternatively, it has been proposed that a rearrangement step following the complex formation is required for electron transfer from eukaryotic donor protein to PSI (12). It is also possible that the components required by the rearrangement are absent in the CFb and CFc chimeric PSI complexes. The insertion of the N-terminal Asp1-Gly85 region of algal PsaF into *Synechococcus* PSI complex enables the fast first-order electron transfer from algal cytochrome c_6 to the hybrid PSI complex (38). Comparing these two results, it is likely that the Leu62-Gly81 region of spinach PsaF may contain residues that are required for the proper orientation of the donor proteins within the complex or are necessary for the rearrangement of the complex to allow the electron transfer. Therefore, the results presented here demonstrate that the lysine-rich domain of plant PsaF is sufficient for the binding of the donor proteins but not for the electron transfer within the intermolecular complex.

Acknowledgment

References

1. Chitnis, P. R. (1996) *Plant Physiol.* **111**, 661-669

2. Fromme, P. (1996) *Curr. Opin. Struct. Biol.* **6**, 473-484

3. Krauß, N., Schubert, W.-D., Klukas, O., Fromme, P., Witt, H. T., and Saenger, W. (1996) *Nature Struct. Biol.* **3**(11), 965-973

4. Schubert, W.-D., Klukas, O., Krauß, N., Saenger, W., Fromme, P., and Witt, H. T. (1997) *J. Mol. Biol.* **272**, 741-769

5. Wood, P. M. (1978) *Eur. J. Biochem.* **87**(1), 9-19

6. Ho, K. K., and Krogman, D. W. (1984) *Biochim. Biophys. Acta* **766**, 310-316

7. Kerfeld, C. A., and Krogmann, D. W. (1998) *Annual Rev. Plant Physiol. Plant Mol. Biol.* **49**, 397-425

8. Haehnel, W., Propper, A., and Krause, H. (1980) *Biochim. Biophys. Acta* **593**, 384-399

9. Bottin, H., and Mathis, P. (1985) *Biochemistry* **24**, 6453-6460

10. Ratajczak, R., Mitchell, R., and Haehnel, W. (1988) *Biochim. Biophys. Acta* **933**, 306-318

11. Diaz, A., Hervas, M., Navarro, J. A., De La Rosa, M. A., and Tollin, G. (1994) *Eur. J. Biochem.* **222**(3), 1001-7

12. Hervás, M., De la Rosa, M. A., and Tollin, G. (1992) *Eur. J. Biochem.* **203**(1-2), 115-20

13. Hervás, M., Navarro, J. A., Diaz, A., Bottin, H., and De la Rosa, M. A. (1995) *Biochemistry* **34**(36), 11321-11326

14. Hervás, M., Ortega, J. M., Navarro, J. A., de la Rosa, M. A., and Bottin, H. (1994) *Biochim. Biophys. Acta* **1184**, 235-241

15. Hippler, M., Reichert, J., Sutter, M., Zak, E., Altschmied, L., Schröer, U., Herrmann, R. G., and Haehnel, W. (1996) *EMBO J.* **15**, 6374-6384

16. Xu, Q., Yu, L., Chitnis, V. P., and Chitnis, P. R. (1994) *J. Biol. Chem.* **269**(5), 3205-3211

17. Frazao, C., Soares, C. M., Carrondo, M. A., Pohl, E., Dauter, Z., Wilson, K. S., Hervas, M., Navarroo, J. A., De la Rosa, M. A., and Sheldrick, G. M. (1995) *Structure* **3**(11), 1159-1169

18. Navarro, J. A., Hervas, M., and De la Rosa, M. A. (1997) *J. Biol. Inorg. Chem.* **2**, 11-12

19. Nordling, M., Sigfridsson, K., Young, S., Lundberg, L. G., and Hansson, O. (1991) *FEBS Lett.* **291**, 327-330

20. Haehnel, W., Jansen, T., Gause, K., Klosgen, R. B., Stahl, B., Michl, D., Huvermann, B., Karas, M., and Herrmann, R. G. (1994) *EMBO J.* **13**(5), 1028-1038

21. Lee, B. H., Hibino, T., Takabe, T., Weisbeek, P. J., and Takabe, T. (1995) *J. Biochem.* **117**, 1209-1217

22. Sun, J., Xu, W., Hervás, M., Navarro, J. A., De La Rosa, M. A., and Chitnis, P. R. (1999) *J. Biol. Chem.* In press

23. Farah, J., Rappaport, F., Choquet, Y., Joliot, P., and Rochaix, J. D. (1995) *EMBO J.* **14**(20), 4976-4984

24. Chitnis, P. R., Purvis, D., and Nelson, N. (1991) *J. Biol. Chem.* **266**(30), 20146-20151

25. Xu, Q., Jung, Y. S., Chitnis, V. P., Guikema, J. A., Golbeck, J. H., and Chitnis, P. R. (1994) *J. Biol. Chem.* **269**(3424), 21512-21518

26. Hatanaka, H., Sonoike, K., Hirano, M., and Katoh, S. (1993) *Biochim. Biophys. Acta* **1141**, 45-51

27. Hippler, M., Drepper, F., Haehnel, W., and Rochaix, J.-D. (1998) *Proc. Natl. Acad. Sci. USA* **95**, 7339-7344

28. Higuchi, R. (1989) in *PCR Technology* (Erlich, H. A., ed), pp. 61-70, Stockton Press, New York

29. Williams, J. G. K. (1988) *Meth. Enzymol.* **167**, 766-778

30. Sun, J., Ke, A., Jin, P., Chitnis, V. P., and Chitnis, P. R. (1998) *Meth. Enzymol.* **297**, 124-139

31. Arnon, D. (1949) *Plant Physiol.* **24**, 1-14

32. Hervás, M., Navarro, J. A., Diaz, A., and De la Rosa, M. A. (1996) *Biochemistry* **35**, 2693-2698

33. Mathis, P., and Setif, P. (1981) *Isr. J. Chem.* **21**, 316-320

34. Hervás, M., Navarro, F., Navarro, J. A., Chavez, S., Diaz, A., Florencio, F. J., and De la Rosa, M. A. (1993) *FEBS Lett* **319**(3), 257-60

35. Sun, J., Xu, Q., Chitnis, V. P., Jin, P., and Chitnis, P. R. (1997) *J. Biol. Chem.* **272**(35), 21793-21802

36. Xu, Q., Odom, W. R., Guikema, J. A., Chitnis, V. P., and Chitnis, P. R. (1994) *Plant Mol. Biol.* **26**(1250), 291-302

37. Nelson, N. (1986) *Methods Enzymol.* **118**, 352-369

38. Hippler, M., Drepper, F., Rochaix, J.-D., and Mühlenhoff, U. (1999) *J. Biol. Chem.* **274**, 4180-4188

Figure legends

Fig. 6-1. **Generation of the chimeric *psaF* genes.** The *Synechocystis* sp. PCC 6803 genomic region around the *psaF-psaJ* operon is shown as *dark lines* and the spinach cDNA clone is shown as *light lines*. *Arrows* show the location, size and direction of genes. The kanamycin resistance and chloramphenicol resistance genes are shown as *long boxes*. The precursor domains of both *Synechocystis* and spinach PsaF are shown as *boxes* with labels. PCR-based mutagenesis techniques were used to generate the chimeric *psaF* genes.

Fig. 6-2. **Amino acid sequence alignments of the PsaF proteins.** A, The PsaF protein sequences from spinach, barley, *Chlamydomonas reinhardtii* (Ch.r.), *Synechococcus elongatus* (Sy.e.), and *Synechocystis* sp. PCC 6803 (Sy.6803) were aligned using

GeneWorks software (IntelliGenetics, CA). The lysine-rich region is *underlined*. The two N-terminal α-helices and the predicted transmembrane helices are marked by *bold lines*. Lysine residues that might be cross-linked to plastocyanin are labeled by *asterisks*. The conserved amino acid residues are *shaded*. B, protein sequence alignment of the deduced chimeric PsaF proteins with spinach and *Synechocystis* PsaF proteins. The replacements in the chimeric PsaF proteins are *underlined*.

FIG. 6-3. **Western blotting analysis of the membranes and PSI complexes from the mutant strains.** The proteins were resolved by Tricine/urea/SDS-PAGE. The antibodies against *Synechocystis* PsaB and PsaF were used and the immunodetection was visualized by enhanced chemiluminescence. A, membranes were isolated from the mutant strains and samples containing the indicated chlorophyll amount were loaded in each lane. B, fractions were collected as described in 'Results'. Fractions 3 and 4 containing 5 μg of chlorophyll were loaded, whereas fractions 1 and 2 were loaded in a volume three times of the volume of fraction 4. C, PSI complexes were purified from the membranes by DM extraction and were loaded with the indicated chlorophyll amount.

FIG. 6-4. **Western blotting analysis of the cross-linked PSI complexes with the donor proteins.** Spinach and FWT PSI complexes containing 5 μg of chlorophyll and CFb and CFc PSI complexes containing 30 μg of chlorophyll were loaded for Tricine/urea/SDS-PAGE. The donor proteins used were plastocyanin (Pc) and cytochrome c_6 (Cyt) from *Synechocystis* sp. PCC 6803 (Sy.6803) and green alga *Monoraphidium braunii* (Mo.b.). The antibody against *Synechocystis* PsaF was used for immunodetections with FWT, CFb, and CFc PSI complexes and the antibody against plant PsaF was used for immunodetection with spinach PSI complexes. The immunodetection was visualized by enhanced chemiluminescence.

FIG. 6-5. **Electron transfer from donor proteins to the chimeric PSI complexes.** A, laser-flash spectroscopy of purified PSI complexes with spinach and algal plastocyanin. *Trace a* represents kinetic traces recorded using FWT, CFb, and CFc PSI complexes and reduced spinach and algal plastocyanin (25 μM to 200 μM) in presence of Mg^{++} (1 mM to 10 mM). *Trace b* was recorded with a mixture of 5.3% spinach PSI and 94.7% *Synechocystis* PSI complexes interacting with 200 μM of plastocyanin. B, electron transfer rate constants of the FWT, CFb, and CFc PSI complexes were measured using different concentrations of *Synechocystis* plastocyanin.

Table 6-1. Mutagenic oligonucleotide primers used for generation of the chimeric psaF genes

Chimeric *psaF* gene	Template	5'-Primer	3'-Primer
CFa	Spinach cDNA	FJ17 (*HpaI*) ACATTGCAGGGTTAACACCATGC	FJ18 (*SpeI*) GGACTAGTTAAAAGTTGTTGTCAACAAGCTCACC
CFb	Spinach cDNA	FJ17 (*HpaI*) ACATTGCAGGGTTAACACCATGC	FJ16 (*BamHI*) CCATCGGATCCACAAAGCAAACCATAC
	FWT plasmid	FJ11 (*BamHI*) CGCGGATCCGAAGGTTATCCCCACCTG	FJ12 (*SpeI*) GCCCAACTAGTTAGCGGGG
CFc	Spinach cDNA	FJ17 (*HpaI*) ACATTGCAGGGTTAACACCATGC	FJ14 (*SalI*) AATGGTCGACTGCGTACAGCTTCAACG
	FWT plasmid	FJ09 (*SalI*) ACGCGTCGACAATACCACCAACGATCCC	FJ12 (*SpeI*) GCCCAACTAGTTAGCGGGG

Table 6-2. Codon frequency in the chimeric psaF genes and the genomic DNA

AA	Codon	CFa	CFb	CFc	FWT	6803*
Arg	CGG	0—0.00	1—0.17	2—0.29	2—0.33	0.32
	CGA	0—0.00	0—0.00	0—0.00	0—0.00	0.07
	CGT	0—0.00	2—0.33	3—0.43	3—0.50	0.26
	CGC	0—0.00	1—0.17	1—0.14	1—0.17	0.25
	AGG	4—0.57	2—0.33	1—0.14	0—0.00	0.05
	AGA	3—0.43	0—0.00	0—0.00	0—0.00	0.04
Glu	GAG	7—0.88	2—0.20	1—0.10	0—0.00	0.24
	GAA	1—0.12	8—0.80	9—0.90	9—1.00	0.76
Gly	GGG	5—0.38	1—0.07	1—0.08	0—0.00	0.19
	GGA	3—0.23	2—0.14	0—0.00	0—0.00	0.12
	GGT	4—0.31	9—0.64	9—0.69	9—0.75	0.38
	GGC	1—0.08	2—0.14	3—0.23	3—0.25	0.31
Lys	AAG	14—0.88	13—0.73	8—0.57	2—0.22	0.31
	AAA	2—0.12	5—0.28	6—0.43	7—0.78	0.69
Pro	CCG	0—0.00	0—0.00	0—0.00	0—0.00	0.16
	CCA	3—0.38	2—0.20	1—0.09	0—0.00	0.08
	CCT	4—0.50	2—0.20	2—0.18	2—0.17	0.18
	CCC	1—0.12	6—0.60	8—0.73	10—0.83	0.58
Thr	ACG	0—0.00	0—0.00	0—0.00	0—0.00	0.11
	ACA	4—0.67	3—0.43	2—0.29	1—0.14	0.08
	ACT	1—0.17	1—0.14	1—0.14	1—0.14	0.21
	ACC	1—0.17	3—0.43	4—0.57	5—0.71	0.60

*. Codon frequencies were summarized from more than 140 genes related to photosynthesis and respiration containing a total of 36087 codons and were used to represent the codon frequencies in the *Synechocystis* sp. PCC 6803 genome.
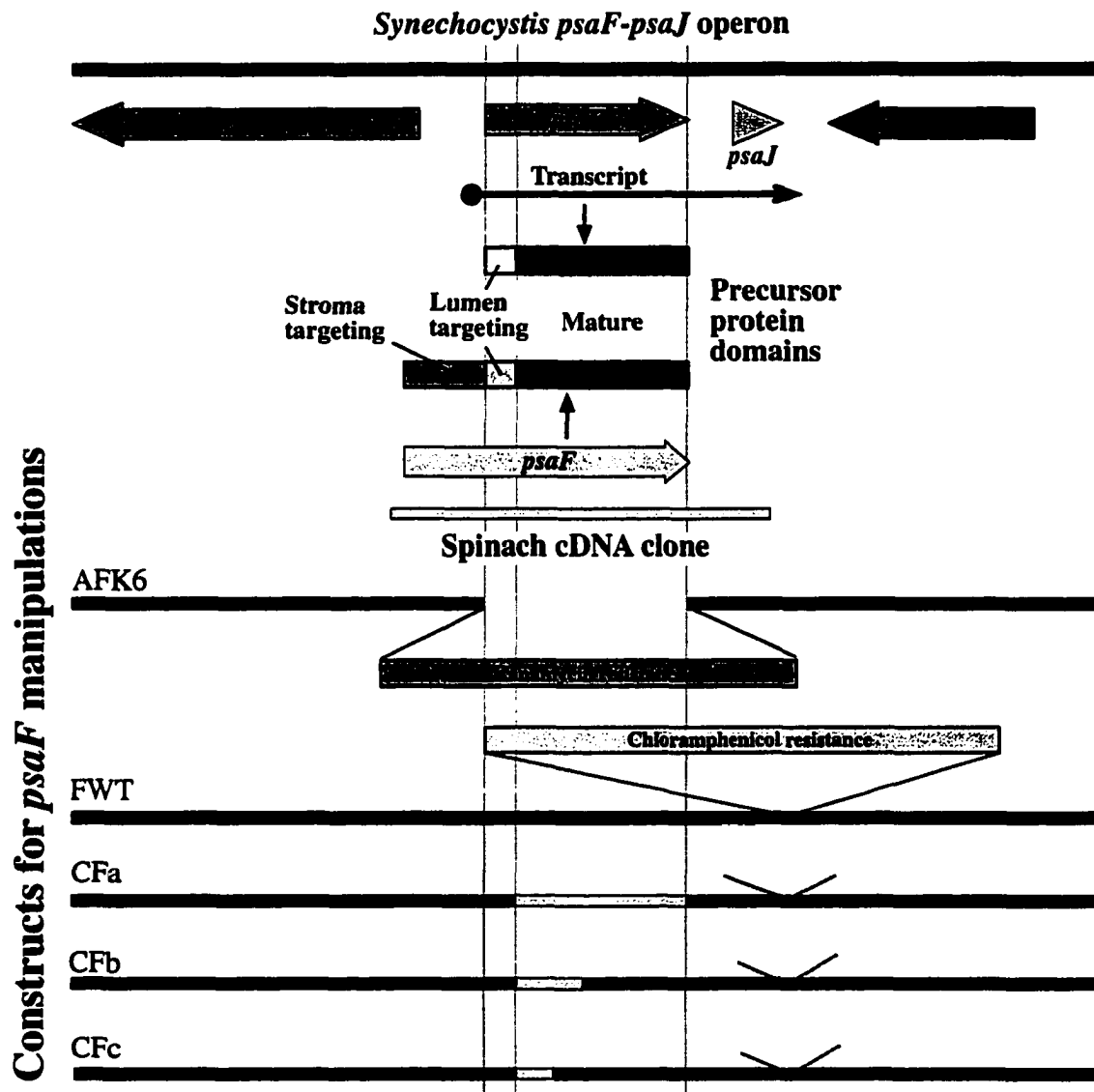
Synechocystis psaF-psaJ operon

Fig. 6-1

A

N-terminal α-helix 1   N-terminal α-helix 2

```
                  *   *  *    **      *          *
spinach   D-IAGLTPCK ESKQFAKREK QALKKLQASL KLYADDSAPA LAIKATMEKT KKRFDNYGKY GLLCGSDGLP HLIV-SG-DQ R--HWG   81
barley    D-IAGLTPCK ESKAFAKREK QSVKKLNSSL KKYAPDSAPA LAIQATIDKT KRRFENYGKF GLLCGSDGLP HLIV-SG-DQ R--HWG   81
Ch.r.     D-IAGLTPCS ESKAYAKLEK KELKTLEKRL KQYEADSAPA VALKATMERT KARFANYAKA GLLCGNDGLP HLIADPGLAL KYGHAG   85
Sy.e.     D-VAGLVPCK DSPAFQKRAA AAVNT----- ---TADPASG ---------- QKRFERYSQA --LCGEDGLP HLVVDG---- RLSRAG   61
Sy.6803   DDFANLTPCS ENPAYLAKSK NFLNT----- ---TNDPNSG ---------- KIRAERYASA --LCGPEGYP HLIVDG---- RFTHAG   62
```

Transmembrane helix 1   Transmembrane helix 2

```
spinach   EFIT PGILFLYIAG WIGWVGRSYL IAIRDEKKPT QKEIIIDVPL ASSLLFRGFS WPVAAYRELL NGELVDNNF- ------   154
barley    EFIT PGVLFLYIAG WIGWVGRSYL IAVSGEKKPA MREIIIDVEL AARIIPRGFI WPVAAYRELI NGDLVVDDAD IGY---   158
Ch.r.     EVFI PTFGFLYVAG YIGYVGRQYL IAVKGEAKPT DKEIIIDVPL ATKLAWQGAG WPLAAVQELQ RGTLLEKEEN ITVSPR   165
Sy.e.     DFLI PSVLFLYIAG WIGWVGRAYL IAVRNSGEAN EKEIIIDVPL AIKCMLTGFA WPLAALKELA SGELTAKDNE ITVSPR   141
Sy.6803   DFLI PSILFLYIAG WIGWVGRSYL IEIRESKNPE MQEVVINVPL AIKKMLGGFL WPLAAVGEYT SGKLVMKDSE IPTSPR   142
```

B

```
spinach   D-IAGLTPCK ESKQFAKREK QALKKLQASL KLYADDSAPA LAIKATMEKT KKRFDNYGKY GLLCGSDGLP HLIVSGDQRH WG    81
CFa       DDFAGLTPCK ESKQFAKREK QALKKLQASL KLYADDSAPA LAIKATMEKT KKRFDNYGKY GLLCGSDGLP HLIVSGDQRH WG    82
CFb       DDFAGLTPCK ESKQFAKREK QALKKLQASL KLYADDSAPA LAIKATMEKT KKRFDNYGKY GLLCGSEGYP HLIVDGRFTH AG    82
CFc       DDFAGLTPCK ESKQFAKREK QALKKLQASL KLYAVDNTTN -----DPNSG KIRAERYA-- SALCGPEGYP HLIVDGRFTH AG    75
FWT       DDFANLTPCS ENPAYLAKSK NFL------- ------NTTN -----DPNSG KIRAERYA-- SALCGPEGYP HLIVDGRFTH AG    62
```

```
spinach   EFITPGIL FLYIAGWIGW VGRSYLIAIR DEKKPTQKEI IIDVPLASSL LFRGFSWPVA AYRELLNGEL V--DNNF--- --   154
CFa       EFITPGIL FLYIAGWIGW VGRSYLIAIR DEKKPTQKEI IIDVPLASSL LFRGFSWPVA AYRELLNGEL V--DNNF--- --   155
CFb       DFLIPSIL FLYIAGWIGW VGRSYLIEIR ESKNPEMQEV VINVPLAIKK MLGGFLWPLA AVGEYTSGKL VMKDSEIPTS PR   162
CFc       DFLIPSIL FLYIAGWIGW VGRSYLIEIR ESKNPEMQEV VINVPLAIKK MLGGFLWPLA AVGEYTSGKL VMKDSEIPTS PR   155
FWT       DFLIPSIL FLYIAGWIGW VGRSYLIEIR ESKNPEMQEV VINVPLAIKK MLGGFLWPLA AVGEYTSGKL VMKDSEIPTS PR   142
```
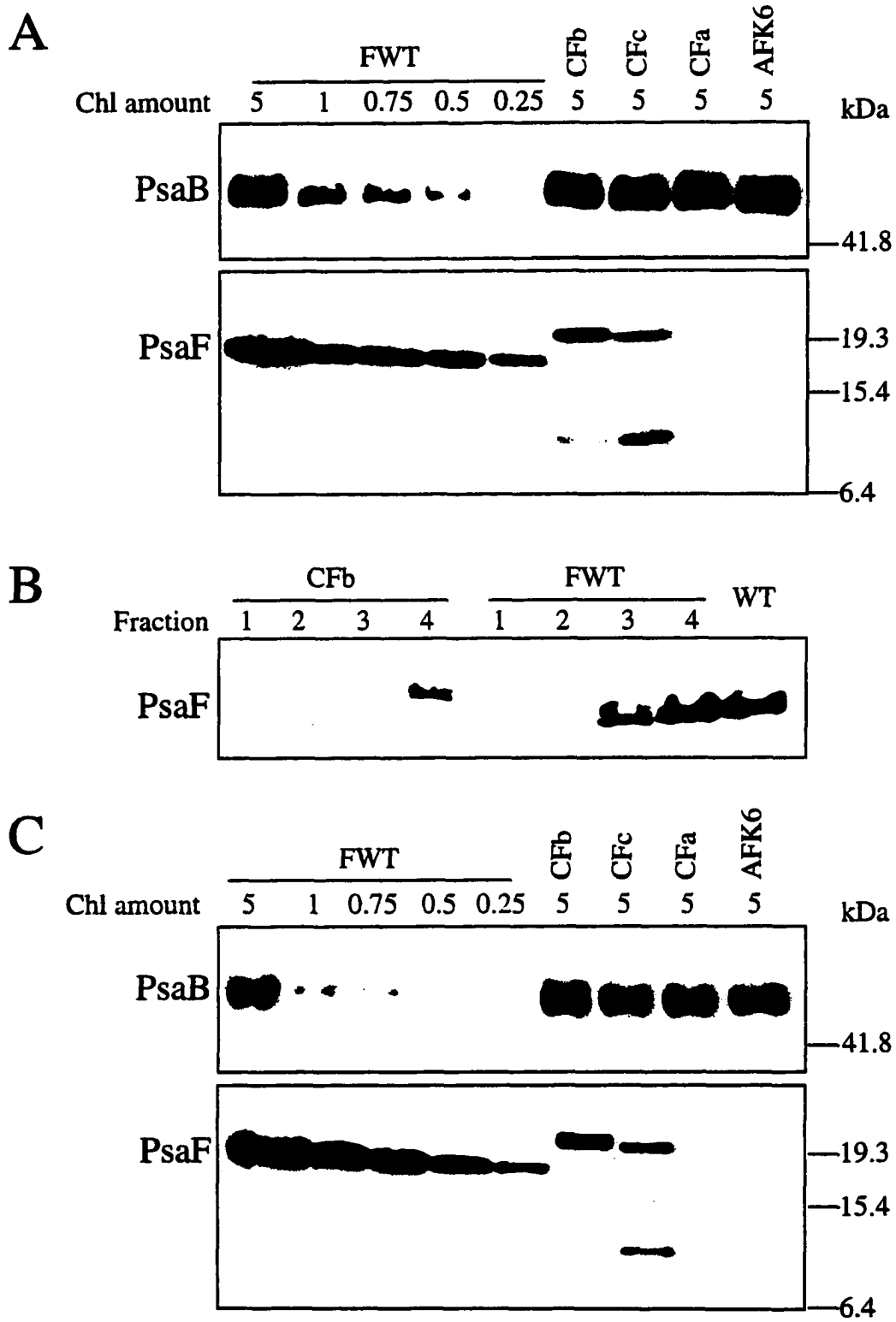
Fig. 6-2

Fig. 6-3

Fig. 6-4

A

B
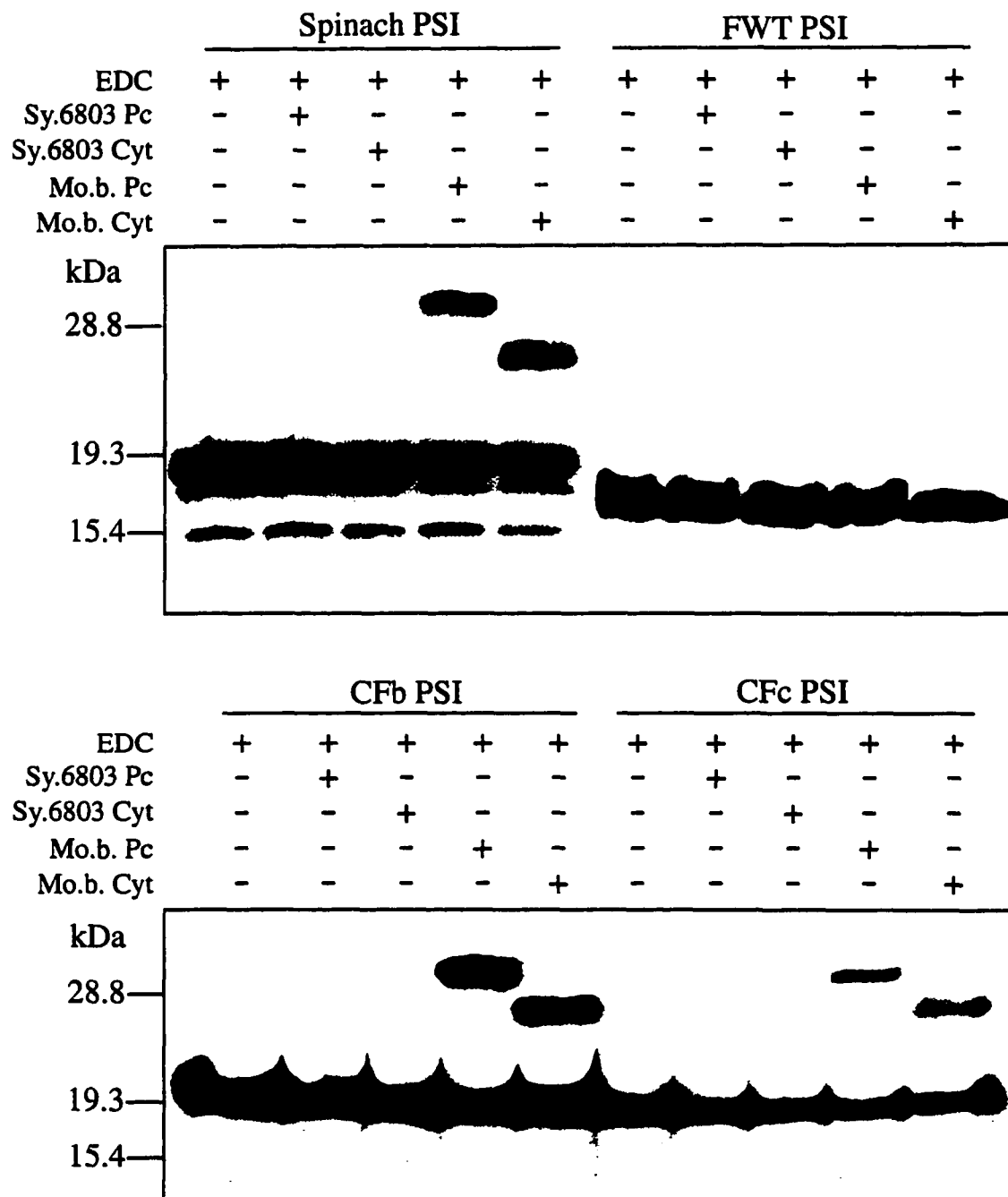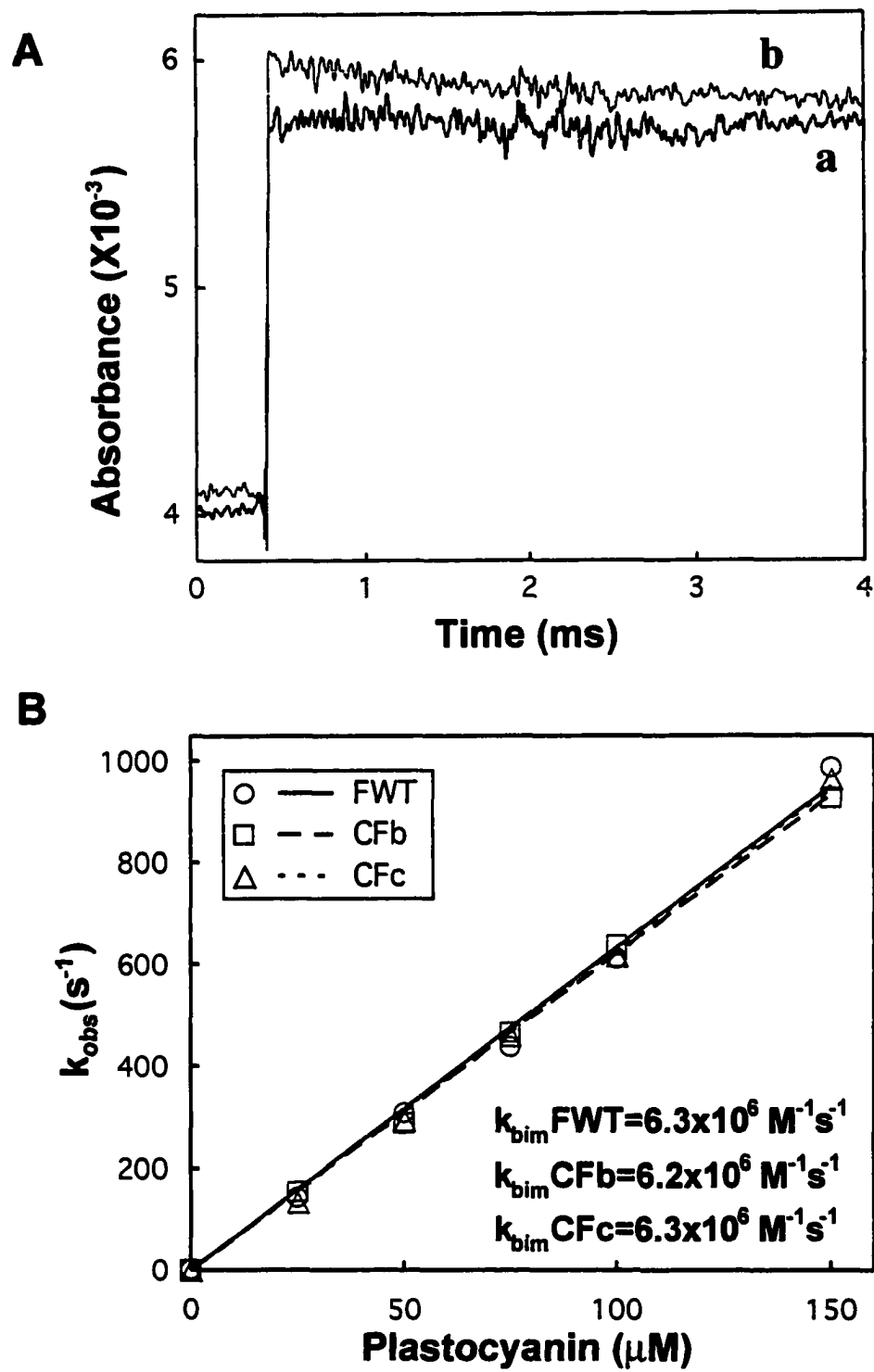

Fig. 6-5

CHAPTER 7. GENERAL CONCLUSIONS

Electron transfers between two proteins constitute many important biological reactions that are involved in different biological functions. These reactions include the electron transfers from cytochrome b_6f complex to plastocyanin/cytochrome c_6 to PSI in oxygenic photosynthesis, from Complex III to cytochrome c to Complex IV in respiration, from electron-transfer flavoprotein to acyl-CoA dehydrogenase in fatty acid oxidation, and cytochrome b_5 to desaturase in fatty acid desaturation, etc. Since the rate of electron transfer is related exponentially to the distance between the redox centers of the two proteins, the interactions between the two proteins play a crucial role for the electron transfer reactions. In this dissertation, we studied the interactions between plastocyanin/cytochrome c_6 and the PSI complex.

On the oxidizing side of photosystem I (PSI), the donor proteins interact with the PSI complex with a multi-step kinetic mechanism in chloroplasts and a one-step kinetic mechanism in some cyanobacteria. The multi-step kinetic mechanism includes initial electrostatic interactions leading to the formation of an intermolecular complex and hydrophobic interactions for the fast electron transfer within the intermolecular complex. The one-step kinetic mechanism involves only hydrophobic interactions for the electron transfer through bimolecular collision. The structural basis on the donor proteins for the electrostatic and hydrophobic interactions has been proposed from their structures based on X-ray crystallography and has been confirmed by site-directed mutagenesis. These regions include the conserved negative and hydrophobic regions of plastocyanin and cytochrome c_6. In the research leading to this dissertation, the structural basis on the PSI complex for the interactions was studied by biochemical and molecular genetic analyses in the model system *Synechocystis* sp. PCC 6803. Specifically, site-directed mutagenesis was used to identify the roles of the N-terminal lysine-rich region of plant PsaF and the luminal loops of PsaB in the molecular recognition with plastocyanin and cytochrome c_6.

The N-terminal domain of chloroplast PsaF contains a lysine-rich region, which is not present in the cyanobacterial PsaF. This lysine-rich region has been predicted to form a helix-turn-helix structure. Chimeric *psaF* proteins containing the lysine-rich region of spinach PsaF were generated in *Synechocystis* sp. PCC 6803 cells and the *Synechocystis* chimeric PsaF proteins could be cross-linked to algal plastocyanin and cytochrome c_6. However, the fast electron transfer was not observed in the interactions of eukaryotic donor proteins to the

chimeric PSI complexes. Thus, the lysine-rich region is sufficient for the binding of the donor proteins, but not for the electron transfer within the intermolecular complex.

The PSI core proteins are expected to interact with the donor proteins directly. Topography of the PSI core proteins was examined to identify the best candidate luminal loops of PsaA and PsaB for interactions with the donor proteins. These studies distinguished PsaA and PsaB in the structural model of PSI and identified the luminal J and H loops of the core protein for mutational studies. Studies on the site-directed mutations in the J loop of PsaB provided evidence for interactions between the electron donor proteins and the luminal surface helix *l* in the J loop of PsaB. The H loop of PsaB was extensively accessible to protease. Studies on the deletion and repetition mutations in the H loop of PsaB suggested that sections of the H loop of PsaB might play an important role in the structural integrity of the PsaB protein. The H loop of PsaB might fold on the surface and form an entrance to the interaction site for the donor proteins.

Based on these results, plastocyanin recognizes the PSI complex in plants through ionic interactions that involve the acidic residues in the negative region of chloroplast plastocyanin and the basic residues in the lysine-rich region of plant PsaF protein. The electrostatic interactions lead to the formation of intermolecular complex. Other components are required for the proper orientation of plastocyanin to the PSI complex, which is crucial for the hydrophobic interaction to allow the electron transfer. The H loop of the PsaB protein forms an entrance to a cavity, inside which the *l* helix of the J loop folds close to the membrane and provides the hydrophobic interaction site for the donor proteins. The H and J loops of PsaA and PsaB may function cooperatively. With the proper hydrophobic interactions, the donor proteins donate electron to the P700 reaction center of the PSI complex.

APPENDIX A. ISOLATION AND FUNCTIONAL STUDY OF PHOTOSYSTEM I SUBUNITS IN THE CYANOBACTERIUM SYNECHOCYSTIS SP. PCC 6803

A paper published in Methods in Enzymology[1]

Jun Sun, An Ke, Ping Jin, Vaishali P. Chitnis, Parag R. Chitnis

Introduction

Photosystem I (PS I) is a multiheteromeric pigment-protein complex in thylakoid membranes of cyanobacteria.[1-3] PS I catalyzes the photooxidation of plastocyanin or cytochrome c_6 in thylakoid lumen and the photoreduction of ferredoxin or flavodoxin in cyanobacterial cytoplasm. The PS I complex contains the photosynthetic pigments (chlorophyll a and β carotene) and five electron transfer centers (A_0, A_1, F_X, F_A, and F_B) that are bound to the PsaA, PsaB, and PsaC proteins. In addition, PS I complex contains at least eight other polypeptides that are accessory in their functions. Recent x-ray crystallographic analysis of cyanobacterial PS I at 4 Å resolution[4] has revealed its structure and overall organization. Application of molecular genetics has now become indispensable to determine the role of individual amino acids that provide precise environment for the cofactors to function in efficient transfer of energy and electrons.

In recent years, cyanobacteria have been used increasingly to study structure-function relations in photosynthetic proteins, including PS I. The mesophilic cyanobacterium, *Synechocystis* sp. PCC 6803 is a model system for using molecular genetic approaches to study functions of PS I proteins. Its genome is completely sequenced[5] and the protein components of its photosystems are identified.[1] Targeted mutations in all genes for PS I proteins are available. Here we describe biochemical and molecular genetic methods and resources to study PS I of *Synechocystis* sp. PCC 6803.

Isolation of Photosystem I Complexes

Rapid Preparation of Photosystem I Trimers

Cyanobacterial PS I can exist in trimeric quaternary structure in the membranes.[6] The PS I trimers can be purified rapidly by sucrose gradient ultracentrifugation.[7] The yield of PS I trimers is influenced by several factors: the choice of detergent that is used for solubilization of membranes, the ratio of detergent to membranes, and ionic conditions and pH during solubilization. Among a dozen different detergents tested, dodecyl-β-D-maltoside has been shown to be the most suitable detergent to dissolve membranes with minimum disturbance to the quaternary structure of PS I. The optimal ratio of chlorophyll to detergent for the photosynthetic membranes of *Synechocystis* sp. PCC 6803 is 1:15. The presence of high concentrations of monovalent cations or acidic pH shifts the monomer-trimer balance towards monomers while calcium stimulates trimerization. A typical procedure for isolation of PS I trimers is given below.

Cells are harvested at the late exponential stage of growth, and suspended in SMN solution (0.4 mM sucrose, 10 mM NaCl, 50 mM MOPS, pH 7.0) with the protease inhibitors phenylmethyl sulfonylfluoride (0.2 mM) and benzamidine (5 mM). The cells are broken in a bead beater and thylakoids are isolated by centrifugation at 50,000 × g for 60 minutes. Typically, three liters of cells (1.0 OD at 730 nm) yield thylakoids containing about 5 mg chlorophyll.

The membranes (1 mg chlorophyll/ml) are incubated for 30 minutes at room temperature with 1 mM $CaCl_2$ in SMN. They are solubilized by addition of dodecyl β-D-maltoside to a final concentration of 1.5% and incubating for 15 minutes on ice.

Insoluble material is pelleted by centrifugation at 20,000 × g for 15 minutes and the supernatant is layered on a 10-30% step gradient of sucrose in 10 mM MOPS, pH 7.0, 0.05% dodecyl β-D-maltoside. Ultracentrifugation at 160,000 × g for 16 hours resolves the pigmented complexes of the photosynthetic membranes into distinct bands (Fig. A-1A). Samples containing 200 µg chlorophyll can be used in 13 ml tubes of SW41 rotor. The heavier green band contains PS I trimers without any significant impurity (Fig. A-1B). Typically, 60% chlorophyll in thylakoid can be recovered as PS I trimers by this procedure.

Purification of Photosystem I by Ion-Exchange Chromatography and Ultracentrifugation

The 'Nelson' method for purification of plant PS I[8] can be used for purifying active PS I from *Synechocystis* sp. PCC 6803 membranes. The isolated thylakoid membranes are adjusted to 500 µg chlorophyll/ml with SMN buffer and Triton X-100 is added at a ratio of 1:10

(chlorophyll : Triton X-100, w/w). The membranes containing 5-10 mg chlorophyll are solubilized for 15-20 minutes on ice and centrifuged at 20,000 x g for 10 minutes at 4°C. After centrifugation, the supernatant is applied to a 2.5 cm x 10 cm DEAE-cellulose column equilibrated with the MOPS-Triton buffer (10 mM MOPS, pH 7.0, 0.05% Triton X-100). The unbound and loosely bound proteins are removed by washing the column with 50 mM NaCl in MOPS-Triton buffer. The bound proteins are eluted with a 50 to 200 mM NaCl gradient in MOPS-Triton buffer. The green fraction, containing the PS I complexes, is eluted by ~100 mM NaCl. To concentrate PS I complexes further, this chromatography step can be repeated by diluting the green fraction four times with MOPS-Triton buffer without NaCl and loading this diluted green fraction on a second DEAE-cellulose colume. After washing, PS I complexes can be eluted with 200 mM NaCl in MOPS-Triton buffer and collected as a dark green fractions. Chromatography is performed at 4°C.

The dark green fractions are combined for sucrose gradient ultracentrifugation. The fractions are applied to a 5% to 30% sucrose step-gradient in MOPS-Triton buffer and ultracentrifuge at 160,000 x g for 16-18 hours at 4°C. Purified PS I complexes form a distinct green layer in the centrifuge tube and can be collected by puncturing bottom of the tube or by using a glass Pasteur pipette. If necessary, PS I complexes can be concentrated with a 50K Macrosep centrifugal concentrator (Amicon, Beverly, CA). Purified PS I is stored at -20°C or -80°C for further use. Typical yield of PS I using this method is approximately 7 mg chlorophyll in PS I from thylakoids containing 10 mg chlorophyll. The PS I purified by this method is suitable for biochemical and spectroscopic studies. These preparations contain approximately 100 chlorophyll molecules per P700.

Alternative Methods

In addition to the methods described above, several other methods have been successfully used to purify PS I complexes from cyanobacterial membranes. Digitonin-solubilization, sucrose gradient ultracentrifugation, and preparative PAGE can be used to isolate different types of PS I reaction centers from cyanobacterial thylakoids.[9] Homogeneous PS I complexes can also be purified by preparative HPLC purification: anion exchange chromatography step followed by hydroxyapatite chromatography and gel-filtration chromatography steps.[10]

Purification of Photosystem I subunits

Purified individual PS I subunits are useful in structural, cross-linking, and topographical studies. They are also used in resolution-reconstitution experiments to understand function of PS I proteins. In addition, they have been used as antigens to raise subunit-specific antibodies.

For purpose of raising subunit-specific antibodies, individual PS I subunits can be separated by Tricine-urea-SDS-PAGE[11] and stained with Coomassie Blue. The gel slices can be excised and used directly as antigens for subunit-specific antibodies.

From isolated complexes

PsaC, PsaD, and PsaE are peripheral subunits on the reducing side of PS I complex. They can be separated and purified from the PS I complexes. To extract these subunits from the PS I core, solid ultrapure urea is added to a final concentration of 7.5 M. The final PS I concentration is adjusted to 200 μg chlorophyll/ml and 1 M Tris-HCl buffer (pH 7.5) is added to make a final concentration of 20 mM. Urea is dissolved by slow shaking at room temperature for about 30 minutes. Most of the PsaC, PsaD and PsaE subunits should dissociate from the PS I core by urea treatment. Extracted proteins are separated by ultrafiltration with 100K Microsep centrifugal concentrator at 3,000 × g for 2 hours at 10-15°C. The eluted fraction contains PsaC, PsaD and PsaE and can be concentrated by ultrafiltration with a 3K Microsep centrifugal concentrator.

The individual subunits from the mixture of PsaC, PsaD and PsaE can be separated by ion-exchange chromatography. An Econo-Pac high S cartridge (Bio-Rad Laboratories, Hercules, CA) is equilibrated with 20 mM Tris-HCl (pH 7.5) buffer, the urea extracted peripheral proteins are loaded and the column is washed with 2 ml of 20 mM Tris-HCl (pH 7.5) buffer. The unbound fraction contains the PsaC and PsaE subunits while the PsaD subunit binds to the column and can be eluted with a 0 to 500 mM NaCl gradient. To separate PsaC and PsaE subunits, the concentrated unbound fraction from the Econo-Pac high S cartridge is applied on an Econo-Pac high Q cartridge (Bio-Rad Laboratories, Hercules, CA) equilibrated with 20 mM Tris-HCl (pH 7.5) buffer, and the column is washed with 2 ml of 20 mM Tris-HCl (pH 7.5) buffer. The unbound fraction contains PsaE subunit. PsaC subunit can be eluted with a 0 to 500 mM NaCl gradient. The purity of the separated proteins is examined by Tricine-urea-SDS-PAGE and Western blotting.

From overexpressed proteins

The peripheral PS I subunits (as PsaD and PsaE) can also be purified after overexpression in *Escherichia coli* cells. The genes (*psaD* and *psaE*) are cloned in pET-21a and the transformed *E. coli* cells are used for overexpression. Typically, a fermentor container with 10 liters LB is prewarmed to 37°C and inoculated with 400 ml overnight culture. Cells are aerobically grown at 37°C for 2-3 hours till the OD_{600} of the culture reaches 0.6-1.0. 1 mM of isopropylthiol-β-D-galactoside (IPTG) is used to induce the protein overexpression. Cells are harvested at 3 hours

after induction and suspended in minimal TS buffer (20 mM Tris-HCl, pH 7.0) containing 5 mM PMSF and 5 mM benzamidine.

To extract proteins, the cells are broken by sonication and centrifuged at 20,000 × g for 30 minutes to pellet inclusion bodies and membranes. The pellets are resuspended in 5 volumes of wash buffer (100 mM Tris-HCl, pH 7.0; 5 mM EDTA; 5 mM DTT; 2 M urea; and 2% Triton X-100) and centrifuged. This step is repeated until the supernatant is clear. The pellets are resuspended in 5 volumes of wash buffer without Triton X-100 and urea and centrifuged again. Finally, the pellets are homogenized in extraction buffer (50 mM Tris-HCl, pH 7.0; 5 mM EDTA; 8 M guanidine-HCl and 5 mM DTT) at the ratio of 1 ml buffer per gram of original wet cells and centrifuged at 120,000 × g for 1 hour. The supernatant containing overexpressed protein is filtered through a 0.45-μm filter. PsaE can be purified by DEAE-cellulose chromatography as unbound fraction while impurities remain bound to DEAE-cellulose with 10 mM Tris-HCl buffer (pH 7.5). Purification of PsaD can be performed on an Econo-Pac high S cartridge as described before. Purified proteins can be desalted by dialysis against 10 mM Tris-HCl (pH 8.0) at 4°C for 16 hours and concentrated by ultrafiltration with 3K Microsep centrifugal concentrator. Protein concentrations are measured from deduced extinction coefficiency 1 A_{280}=0.97 mg/ml for PsaD and 1 A_{280}=1.38 mg/ml for PsaE.

The PsaD and PsaE subunits can be overexpressed as fusion proteins with polyhistidine tag at C-terminus and purified by affinity chromatography. The *psaD* gene is inserted into pET-21b (+) vector between *Xho*I and *Nde*I sites. Plasmid containing *psaD* gene is introduced into BL21 (DE3) strain of *Escherichia coli*. The gene is induced by incubating with 1 mM IPTG at 37°C for 3 hours. Induced cells are broken by sonication. Most overexpressed PsaD is in the soluble fraction. The soluble overexpressed tagged PsaD protein is purified by His•Bind Resin and Buffer kit (Novagen, Madison, WI). 2.5 ml His•Bind Resin is prepared in a small polypropylene column and washed by 3 volumes of sterile deionized water. The affinity material Ni^{+2} is immobilized on resin by 5 volumes of Charge Buffer (50 mM $NiSO_4$). After the column is equilibrated by 3 volumes of Binding Buffer (5 mM imidazole, 0.5 M NaCl, 20 mM Tris-HCl, pH 7.9), samples are loaded on column. The column is then washed by 10 volumes of Binding Buffer and 6 volumes of Wash Buffer (60 mM imidazole, 0.5 M NaCl, 20 mM Tris-HCl, pH 7.9). Bound proteins are finally eluted in Elute Buffer (1 M imidazole, 0.5 M NaCl, 20 mM Tris-HCl, pH 7.9), and desalted twice using Econo-Pac 10DG column (Bio-Rad Laboratories, Hercules, CA) to remove the imidazole completely. Purified PsaD proteins are stored in -20°C for further use.

Topographical characterization of Photosystem I

During the past few years, major advances in x-ray crystallography[4,12] have provided a framework for understanding the overall architecture of PS I. However, due to the lower resolution of these studies, more detailed information about the structure of PS I is not available. Topographical studies using biochemical techniques reveal exposed domains or exposed amino acid residues, the interactions among PS I subunits or between PS I and its electron donor or acceptor, and the roles of individual residues in the interactions. Topographical studies on complex assemblies like PS I are the most convenient means for correlating defects in function due to mutations with perturbations in structural organization. It is prudent to generate information beyond crystallographic studies for a complete and rapid understanding of structure.

Limited proteolysis

Limited proteolysis coupled with domain-specific antibodies and N-terminal amino acid sequencing provides a powerful tool to understand details of the organization of PS I.[13-15] To study the accessibility of PS I subunits to proteases, purified PS I complexes, thylakoid membranes or osmotically shocked cells[16] are incubated with proteases at a final chlorophyll concentration of 200 µg /ml. The proteolysis reaction conditions for eight proteases are listed in Table A-1.[15]

The PS I complexes are incubated with different concentrations of proteases, denatured with SDS and separated by modified Tricine-urea-SDS-PAGE. After electro-transfer, polyvinylidene difluoride (PVDF) membranes are stained by Coomassie Blue or immunodetected by three domain-specific antibodies: anti-PsaA2 against the N-terminus of PsaA, anti-PsaB450 against a extramembrane loop between transmembrane helix VII and VIII, and anti-PsaB718 against the C-terminus of PsaB (Fig. A-2). The apparent mass of a protein fragment can be determined from the migration of protein molecular weight standards upon electrophoresis. The protein fragments that are visible in CB staining and recognized by immunodetection, can be subjected to N-terminal amino acid sequencing. Exposed proteolysis sites can be located from the N-terminal sequences of proteolysis fragments, their apparent mass and reactivity to antibodies.

Modification of surface-exposed residues

To study the topography of PS I, it is important to probe the exposed protein surface by modification of specific residues. Two biotin derivatives can be used to modify surface-exposed residues. N-hydroxysuccinimidobiotin (NHS-biotin) specifically reacts with the N-

terminus and the ε-amino group of lysyl residues[17] while biotin-maleimide (M-biotin) modifies the sulfhydryl groups of cysteinyl residues. Both reagents are used to study surface-exposed residues in the PS I complex. Purified PS I complex or PS I subunits are biotinylated at a final protein concentration of 0.5 to 1.5 mg/ml under the modification conditions listed in Table A-2.

Biotin-labeled PS I can be further used in protease treatments. The labeled PS I subunits are separated by Tricine-urea-SDS-PAGE and electroblotted to Immobilon-P membranes.[18] The blot is probed with peroxidase-conjugated Avidin (Cooper Biomedical, Malvern, PA) and then developed with hydrogen peroxide and 4-chloro-1-naphthol[19] or with enhanced chemiluminescence reagents (Amersham, Arlington Heights, IL).

Chemical cross-linking

Chemical cross-linking can be used to investigate the interactions of PS I subunits. It can reveal the physical relationship between the PS I subunits. Glutaraldehyde is a bifunctional cross-linking reagent which reacts principally with amino group of lysyl residues,[20] and is stored at -20°C prior to use. Purified PS I complexes at a concentration of 150 μg chlorophyll/ml are treated with 15 mM glutaraldehyde (Sigma, St. Louis, MO) in the presence of 10 mM MOPS-HCl (pH 7.0) and 0.05% Triton X-100 for 30 minutes on ice with continuous shaking. The cross-linking reactions are quenched by the addition of glycine to a final concentration of 100 mM. Subsequently, the samples are diluted with an excess of 10 mM MOPS-HCl (pH 7.0), filtered using Centricon-100 (Amicon, Beverly, CA) ultrafiltration, and then applied for analytical gel electrophoresis, Western Blotting, and other analysis. Nonspecific cross-linking effects may occur at higher concentration of glutaraldehyde. The following cross-linked products can be found[21,22]: PsaC-PsaD, PsaC-PsaE, PsaD-PsaL, PsaE-PsaF.

N-ethyl-1,3-[3-(diethylamino)propyl]carbodiimide (EDC), a zero length crosslinker that forms a covalent bond between primary amines and carboxyls,[23] can also be used for the studies on the physical relationship between the PS I subunits. Purified PS I at a final concentration of 200 μg chlorophyll/ml is mixed well with 80 mM fresh-prepared EDC (Sigma, St. Louis, MO) in the presence of 20 mM HEPES, pH 7.0 and 0.05% Triton X-100. After incubation at room temperature for 60 minutes, the reaction is quenched by the addition of 1 M Tris-HCl, pH 7.0 to a final concentration of 200 mM at room temperature for 15 minutes. The following cross-linked products have been detected by Western blotting[21]: PsaE-PsaF and PsaC-PsaD. EDC can also be used to crosslink the PsaD of *Synechocystis* sp. PCC 6803 PS I with ferredoxin.[24]

Biochemical assays for Photosystem I function

Oxygen evolution and uptake

Photosynthetic electron transport activities are determined by the rates of oxygen evolution or uptake. Oxygen measurements are made on the Oxygen Monitoring System (Hansatech, England) at 25°C under the light density of 2430 μmol m^{-2} s^{-1}. Total photosynthetic activity is measured as oxygen evolution using whole cells (10 μg chlorophyll/ml) suspended in 40 mM HEPES, pH 7.0 after adding the final electron acceptor $NaHCO_3$ to the reaction mixture to a final concentration of 10 mM. PS I activity can be measured as the rate of oxygen uptake via the Mehler reaction[25,26] using whole cells (in 40 mM HEPES, pH 7.0) or thylakoid membranes (in 10 mM MOPS) or isolated PS I complexes in (10 mM MOPS, pH 7.0, 0.05% Triton X-100) containing 10 μg chlorophyll in the presence of 50 μM 3-(3,4-dichlorophenyl)-1,1-dimethylurea (DCMU), 1 mM ascorbic acid, 1 mM 3,6-diamino durene, and 2 mM methyl viologen.[27] In this reaction, PS II activity is inhibited by DCMU while ascorbate donates electrons to PS I via 3,6-diamino durene. Methyl viologen accepts electrons from PS I and donates them in turn to oxygen, thereby reducing oxygen concentration in the reaction mixture. After calculating the slopes of lines, the oxygen evolution or uptake rates are calibrated by measuring the oxygen consumption of air saturated water by sodium dithionite.

NADP+ photoreduction

The reductase activity of PS I can be estimated in a coupled enzyme assay that monitors flavodoxin-mediated or ferredoxin-mediated $NADP^+$ photoreduction with ferredoxin:$NADP^+$ oxidoreductase. Isolated photosynthetic membranes at a concentration of 5 μg chlorophyll/ml are used for the measurement. Rates of flavodoxin-mediated $NADP^+$ photoreduction are measured in a 3-ml volume using 15 μM flavodoxin in 50 mM Tricine, pH 8.0, 10 mM $MgCl_2$ 15 μM cytochrome c_6, 6 mM sodium ascorbate, 0.05% n-dodecyl β-maltoside with 0.5 mM $NADP^+$ and 0.8 μM ferredoxin: $NADP^+$ oxidoreductase. Rates of ferredoxin-mediated $NADP^+$ photoreduction are measured under the same conditions except for the substitution of 5 μM ferredoxin for 15 μM flavodoxin. Both measurements are made by monitoring the rate of change in the absorption of NADPH at 340 nm (the extinction coefficient is 6.22 mM^{-1} cm^{-1}). The rates are determined using a Cary 219 or a Shimadzu 160A spectrophotometer fitted with appropriate narrow band and interference filters attached to the surface of the photomultiplier. The samples are illuminated using banks of high intensity, red light-emitting diodes (LS1, Hansatech Ltd.). The light intensity is saturating at the chlorophyll concentration used. In wild-

type membranes, the rates of ferredoxin- and flavodoxin-mediated $NADP^+$ photoreduction are 460 and 480 μmol/mg chlorophyll per hour, respectively.[18]

P700 estimation

The estimation of P700 involves the measurement of absorption changes at 700 nm or 430 nm induced by chemical oxidation and reduction.[28,29] A Cary 219 or a Shimadzu 160A spectrophotometer is used to measure the oxidized minus reduced spectra. Purified PS I complexes and thylakoid membranes in 10 mM MOPS, pH 7.0, 0.05% Triton X-100 are adjusted to 25 μg of chlorophyll/ml (giving an absorbency of about 2 at 680 nm). Two samples in identical cuvettes are used to record the baseline. Then, one sample is oxidized with ferricyanide (1 mM) and the other is reduced with ascorbic acid (2 mM). After equilibration, a difference spectrum is recorded and the P700 concentration is determined using the extinction coefficients: 64 mM^{-1} cm^{-1} at 700 nm or 44 mM^{-1} cm^{-1} at 430 nm.

In addition to producing an absorbance change at 700 nm, the oxidation of P700 also results in an absorbance increase around 820 nm.[30] This absorbance increase around 820 nm can also be produced by the oxidation of P680. The slower P700 reduction and the faster P680 reduction allow discrimination of the absorbance changes by using a system with time resolution less than 1 microsecond. The Hansatech P700$^+$ Accessory Kit can be used for P700 estimation in isolated membranes or purified complexes by monitoring the absorbance changes at 820 nm by light induced P700 oxidation.

Molecular Genetic and Biochemical Resources

Due to its simplicity and similarity to higher plants, *Synechocystis* sp. PCC 6803 has been extensively used as a model system to study photosynthetic proteins. These studies make a rich resource for further studies. Many subunit-deficient PS I mutants have been developed and many subunit-specific even domain-specific antibodies have been raised in recent years (Table A-3). Finally, the completely sequenced genome of *Synechocystis* sp. PCC 6803 makes another great resource for the studies on this cyanobacterium. This achievement will great benefit the molecular genetics researches. The information of the genome can be easily obtained from the web page: http://pka3.kazusa.or.jp/cyano/cyano.html.

Recipient strains that lack specific photosystem I subunits

Subunit-deficient PS I mutants are made by partially or completely replacing the target gene with antibiotics resistance gene, or by inserting antibiotics resistance gene into the target gene to interrupt the target subunit (Table A-3). Traditionally, the genes were cloned by construction of the genomic DNA libraries and its screening using heterologous probes or labeled

oligonucleotides. Now, with the completely sequenced genome of *Synechocystis* sp. PCC 6803, the required genes can be easily cloned by amplification with PCR. For gene replacement, target gene is deleted by digestion and the upstream and downstream sequences are ligated with the antibiotics resistance gene replacing the gene under study. For gene interruption, the antibiotics resistance gene is introduced into a site in the target gene. Constructions are introduced back into *Synechocystis* sp. PCC 6803 genome through natural transformation and homologous recombination. Recipient strains are tested by PCR, southern blotting, northern blotting, and/or western blotting to ensure that the gene is inactivated and the protein is absent in the mutant strain.

Antibodies

Subunit-specific rabbit polyclonal antibodies have been raised using native proteins from polyacrylamide gel or overproduced proteins in *Escherichia coli*. Several domain-specific rabbit polyclonal antibodies in PsaA and PsaB have also been generated using overexpressed fusion proteins as antigens. The specificity of the antibodies is tested by western blotting using both isolated thylakoid membranes and purified PS I complex resoluted by electrophoresis.

Acknowledgments

Reference

[1] P. R. Chitnis, Q. Xu, V. P. Chitnis and R. Nechushtai, *Photosynthesis Res.* **44**, 23 (1995).

[2] P. R. Chitnis, *Plant Physiol.* **111**, 661 (1996).

[3] P. Fromme, *Current Opinion in Structural Biology* **6**, 473 (1996).

[4] N. Krauß, W.-D. Schubert, O. Klukas, P. Fromme, H. T. Witt and W. Saenger, *Nature Structural Biology* **3**, 965 (1996).

[5] T. Kaneko, S. Sato, H. Kotani, A. Tanaka, E. Asamizu, Y. Nakamura, N. Miyajima, M. Hirosawa, M. Sugiura, S. Sasamoto, T. Kimura, T. Hosouchi, A. Matsuno, A. Muraki, N. Nakazaki, K. Naruo, S. Okumura, S. Shimpo, C. Takeuchi, T. Wada, A. Watanabe, M. Yamada, M. Yasuda and S. Tabata, *DNA Res.* **3**, 109 (1996).

[6] J. Kruip, D. Bald, E. Boekema and M. Rogner, *Photosynth. Res.* **40**, 279 (1994).

[7] V. P. Chitnis and P. R. Chitnis, *FEBS Lett* **336**, 330 (1993).

[8] C. Bengis and N. Nelson, *J. Biol. Chem.* **250**, 2783 (1975).

[9] S. Katoh, *Meth. Enzymol.* **167**, 263 (1988).

[10] M. Rogner, P. J. Nixon and B. A. Diner, *J. Biol. Chem.* **265**, 6189 (1990).

[11] Q. Xu, L. Yu, V. P. Chitnis and P. R. Chitnis, *J Biol Chem* **269**, 3205 (1994).

[12] N. Krauß, W. Hinrichs, I. Witt, P. Fromme, W. Pritzkow, Z. Dauter, C. Betzel, K. S. Wilson, H. T. Witt and W. Saenger, *Nature* **361**, 326 (1993).

[13] Q. Xu and P. R. Chitnis, *Plant Physiol* **108**, 1067 (1995).

[14] Q. Xu, J. A. Guikema and P. R. Chitnis, *Plant Physiol* **106**, 617 (1994).

[15] J. Sun, Q. Xu, V. P. Chitnis, P. Jin and P. R. Chitnis, *J. Biol. Chem.* **272**, 21793 (1997).

[16] G. S. Tae and W. A. Cramer, *Biochemistry* **33**, 10060 (1994).

[17] E. A. Bayer and M. Wilchek, *Meth. Enzymol.* **184**, 138 (1990).

[18] Q. Xu, Y. S. Jung, V. P. Chitnis, J. A. Guikema, J. H. Golbeck and P. R. Chitnis, *J Biol Chem* **269**, 21512 (1994).

[19] L. K. Frankel and T. M. Bricker, *Biochemistry* **31**, 11059 (1992).

[20] K. Peters and F. M. Richards, *Ann. Rev. Biochem.* **46**, 523 (1977).

[21] T. S. Armbrust, P. R. Chitnis and J. A. Guikema, *Plant Physiology* **111**, 1307 (1996).

[22] Q. Xu, V. P. Chitnis, A. Ke and P. R. Chitnis, in "Photosynthesis: from Light to Biosphere" (P. Mathis, eds.), p. 87. Kluwer, Dodrecht, 1995.

[23] S. Bauminger and M. Wilchek, *Methods Enzymol.* **70**, 151 (1980).

[24] C. Lelong, P. Setif, B. Lagoutte and H. Bottin, *J Biol Chem* **269**, 10034 (1994).

[25] A. H. Mehler, *Arch. Biochem. Biophys.* **34**, 339 (1951).

[26] A. H. Mehler, *Arch. Biochem. Biophys.* **33**, 65 (1951).

[27] V. P. Chitnis, Q. Xu, L. Yu, J. H. Golbeck, H. Nakamoto, D. L. Xie and P. R. Chitnis, *J Biol Chem* **268**, 11678 (1993).

[28] B. Kok, *Biochim. Biophys. Acta* **48**, 527 (1961).

[29] T. V. Marsho and B. Kok, *Methods Enzymol.* **69**, 280 (1980).

[30] B. Kok, *Nature* **179**, 583 (1957).

Figure Legends

Fig. A-1. **Resolution of photosystem I.** Monomeric and trimeric forms of PS I are resolved by sucrose-gradient ultracentrifugation (A) and the PS I subunits are separated by Tricine-urea-SDS-PAGE (B). PsaK2 can not be detected in the wild type PS I preparation.

Fig. A-2. **Limited proteolysis of photosystem I proteins.** Purified PS I complexes are partially digested by different proteases and resolved by Tricine-urea-SDS-PAGE. After electrotransfer to PVDF membranes, protein fragments are detected by Coomassie Blue Staining (CB) or by immunodetection with three domain-specific antibodies against different regions in PsaA or PsaB.

Table A-1. Reaction conditions of proteases treatment[a]

Proteases	Thermolysin	Glu-C	Chymotrypsin	Papain	Lys-C	Trypsin	Clostripain	Pepsin
Specificity	^[VILWMF]	[E]^	[YFW]^	[RKILG]^	[K]^	[KR]^	[R]^	[FLYWI]^
Final protease concentration	250 μg/mg chlorophyll	250 μg/mg chlorophyll	250 μg/mg chlorophyll	10 μg/mg chlorophyll	250 μg/mg chlorophyll	250 μg/mg chlorophyll	250 μg/mg chlorophyll	250 μg/mg chlorophyll
Proteolysis condition[b]	10 mM MOPS (pH 7.0); 5 mM CaCl₂	50 mM NH₄HCO₃ (pH 7.8)	50 mM Tris-HCl (pH 8.0); 10 mM CaCl2	10 mM MOPS (pH 7.0); 0.5 mM EDTA; 1.5 mM CySH	25 mM Tris-HCl (pH 7.5); 1 mM EDTA	50 mM Tris-HCl (pH 8.0); 1 mM CaCl₂	20 mM Tris-HCl (pH 7.5); 1 mM CaCl₂; 2 mM DTT	20 mM NaH₂PO₄ (pH 4.0)
Incubation	37°C 30 min	15°C 30 min	25°C 1 hr	25°C 1 hr	37°C 1 hr	37°C 1 hr	37°C 1 hr	37°C 1 hr
Termination	20 mM EDTA	20 mM PMSF	20 mM PMSF	20 mM PMSF	20 mM PMSF	20 mM PMSF	20 mM EDTA	20 mM pepstatinA

[a] The sources of these eight proteases are: Sequencing Grade Endoproteinase Lys-C (from *Pseudomonas aeruginosa*; EC 3.4.21.50), Clostripain (Endoproteinase Arg-C from *Clostridium histolyticum*; EC 3.4.22.8) and Modified Trypsin (from porcine pancreas; EC 3.4.21.4) are purchased from Promega Biotech, Madison, WI. Papain (from *Carica papaya*; EC 3.4.22.2), Pepsin (from porcine stomach; EC 3.4.23.1), Sequencing Grade Endoproteinase Glu-C (protease V8 from *Staphylococcus aureus*; EC 3.4.21.19) and Chymotrypsin (from bovine pancreas; EC 3.4.21.1) are obtained from Boehringer Mannheim, Indianapolis, IN. Thermolysin (protease type X from *Bacillus thermoproteolyticus*; EC 3.4.24.4) is purchased from Sigma, St. Louis, MO.

[b] 0.05% Triton X-100 is added for purified PS I complexes.

Table A-2. Reaction conditions for biotinylation treatment

Modification reagent	N-hydroxysuccinimidobiotin (NHS-biotin)	Biotin-maleimide (M-biotin)
Specificity	ε-amino group of lysine	sulfhydryl group of cysteine
Final concentration	60 μM	60 μM
Modification condition	10 mM MOPS (pH 7.0); 0.05% Triton X-100	10 mM MOPS (pH 7.0); 0.05% Triton X-100
Incubation	Room temperature 60 min in dark	Room temperature 60 min in dark
Termination	100 mM Glycine	10 mM DTT
Labeled proteins in PS I	PsaAB, PsaD, PsaF, PsaL, PsaE	PsaC

Table A-3. Subunit-deficient photosystem I mutants and subunit-specific antibodies in *Synechocystis* sp. PCC 6803

Subunit /gene	Gene Features			Subunit-specific Antibodies		Subunit-deficient Mutants			
	Size (bp)	Expre-ssion	Location in genome	Rabbit polyclonal antibody against	Ref.	Mutant Strain	Genotype	Phenotype	Ref.
PsaA /psaA	2256	with psaB	941686-943941	overproduced fusion protein containing N-terminal sequence	a	PS I-Less	3' end of psaA and 5' end of psaB replaced by Cam^r	PS I missing; no photoautotrophic growth	b
PsaB /psaB	2196	with psaA	944187-946382	overproduced fusion protein containing an extramembrane sequence	a	BDK8	psaB gene partially replaced by Kan^r;	PS I missing; no photoautotrophic growth	c
						ΔB-RCPT	psaB gene partially replaced by Kan^r	PS I missing; no photoautotrophic growth	d
						JUN1	psaB region correspond-ing to C-terminal domain replaced by Kan^r	PS I missing; no photoautotrophic growth	e
PsaC /psaC	246	Mono-cistronic	2287579-2287334	overproduced protein	f	CDK25	psaC interrupted by Kan^r	PsaC, PsaD, PsaE missing; no photoautotrophic growth	g
PsaD /psaD	426	Mono-cistronic	126639-127064	overproduced protein	f	ADC4	psaD replaced by Cam^r	no Fd-mediated electron transfer	h-k
PsaE /psaE	225	Mono-cistronic	1982049-1982273	overproduced protein	f	AEK2	psaE replaced by Kan^r	reduced Fd-mediated NADP$^+$ photoreduction	k,l
PsaF /psaF	498	With psaJ	1688053-1687556	native protein from polyacrylamide gel	m	AFK6	psaF replaced by Kan^r; psaJ transcriptionally inactivated	PsaF, PsaJ missing; PsaE decreased; normal rate of P700 reduction by Cyt c_6	f,k,n
PsaI /psaI	123	with psaL	3458023-3458145	overproduced fusion protein	o	AIC9	psaI interrupted by Cam^r	PsaI, PsaL missing; small decrease in Fd-mediated NADP$^+$ photoreduction	o
PsaJ /psaJ	123	with psaF	1687448-1687326	not available		AJC8	psaJ replaced by Cam^r	PsaF easily lost during detergent treatment	m

161

Table A-3. (continued)

Subunit /gene	Gene Features			Subunit-specific Antibodies		Subunit-deficient Mutants			
	Size (bp)	Expre- ssion	Location in genome	Rabbit polyclonal antibody against	Ref.	Mutant Strain	Genotype	Phenotype	Ref.
PsaK1 /psaK1	261	ND	156391- 156651	native protein from polyacrylamide gel	p	AK1C	psaK1 interrupted by Cam^r		P
PsaK2 /psaK2	387	ND	3322763- 3322377			AK2S	psaK2 replaced by Spec^r		p
PsaL /psaL	474	with psaI	3457459- 3457932	native protein from polyacrylamide gel	j	ALC7	psaL interrupted by Cam^r	No PS I trimers formed	k,q,r
PsaM /psaM	96	ND	467201- 467296	not available		AMS	psaM interrupted by Strep^r	Less PS I activity, reduced growth at high light intensity	p

[a] J. Sun, Q. Xu, V. P. Chitnis, P. Jin and P. R. Chitnis, *J. Biol. Chem.* **272**, 21793 (1997).

[b] S. Boussiba and W. F. J. Vermaas, in "Research in Photosynthesis" (N. Murata, eds.), p. 429. Dordrecht: Kluwer, 1992.

[c] L. B. Smart and L. McIntosh, *Plant Mol. Biol.* **21**, 177 (1993).

[d] L. B. Smart, P. V. Warren, J. H. Golbeck and L. McIntosh, *Proc. Natl. Acad. Sci. USA* **90**, 1132 (1993).

[e] J. Sun and P. R. Chitnis, unpublished results.

[f] Q. Xu, L. Yu, V. P. Chitnis and P. R. Chitnis, *J Biol Chem* **269**, 3205 (1994).

[g] L. Yu, L. B. Smart, Y. S. Jung, J. Golbeck and L. McIntosh, *Plant Mol Biol* **29**, 331 (1995).

[h] P. R. Chitnis, P. A. Reilly and N. Nelson, *J Biol Chem* **264**, 18381 (1989).

[i] Y. Cohen, V. P. Chitnis, R. Nechushtai and P. R. Chitnis, *Plant Mol Biol* **23**, 895 (1993).

[j] Q. Xu, T. S. Armbrust, J. A. Guikema and P. R. Chitnis, *Plant Physiol* **106**, 1057 (1994).

[k] Q. Xu, Y. S. Jung, V. P. Chitnis, J. A. Guikema, J. H. Golbeck and P. R. Chitnis, *J Biol Chem* **269**, 21512 (1994).

[l] P. R. Chitnis, P. A. Reilly, M. C. Miedel and N. Nelson, *J. Biol. Chem.* **264**, 18374 (1989).

[m] Q. Xu, W. R. Odom, J. A. Guikema, V. P. Chitnis and P. R. Chitnis, *Plant Mol Biol* **262**, 291 (1994).

[n] P. R. Chitnis, D. Purvis and N. Nelson, *J Biol Chem* **266**, 20146 (1991).

[o] Q. Xu, D. Hoppe, V. P. Chitnis, W. R. Odom, J. A. Guikema and P. R. Chitnis, *J Biol Chem* **270**, 16243 (1995).

[p] P. Manna and P. R. Chitnis, unpublished results.

[q] V. P. Chitnis, Q. Xu, L. Yu, J. H. Golbeck, H. Nakamoto, D. L. Xie and P. R. Chitnis, *J Biol Chem* **268**, 11678 (1993).

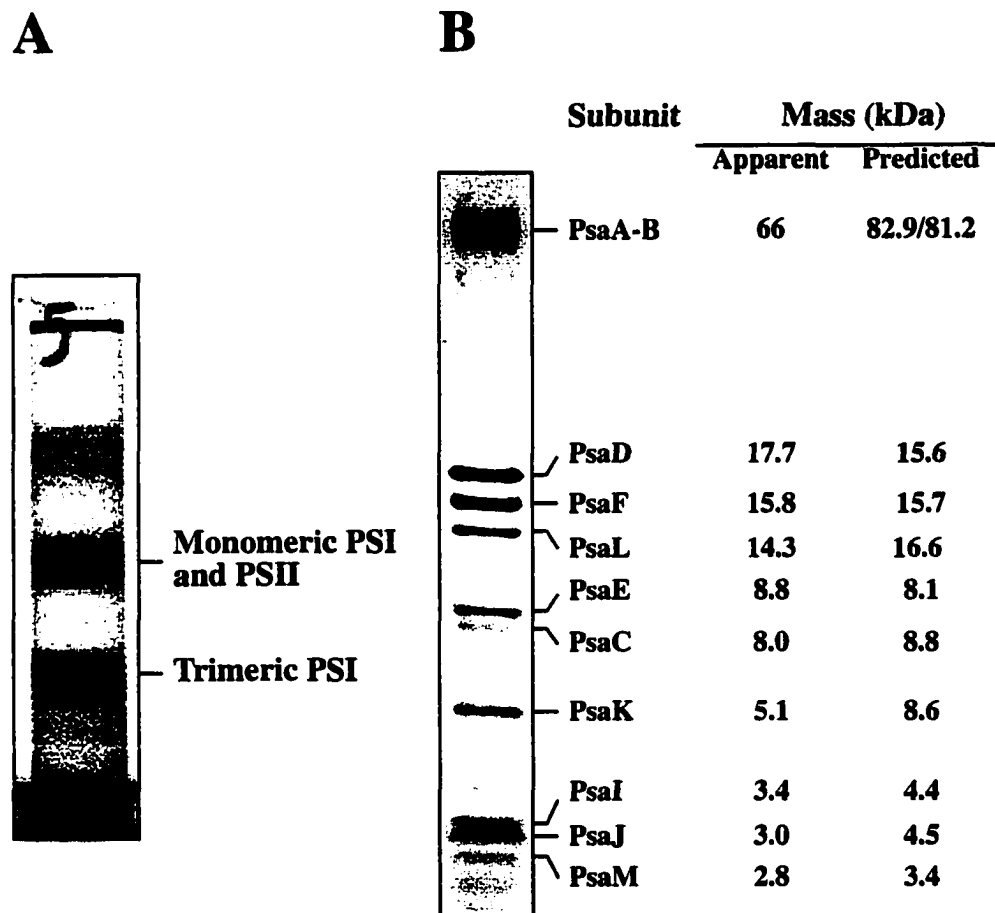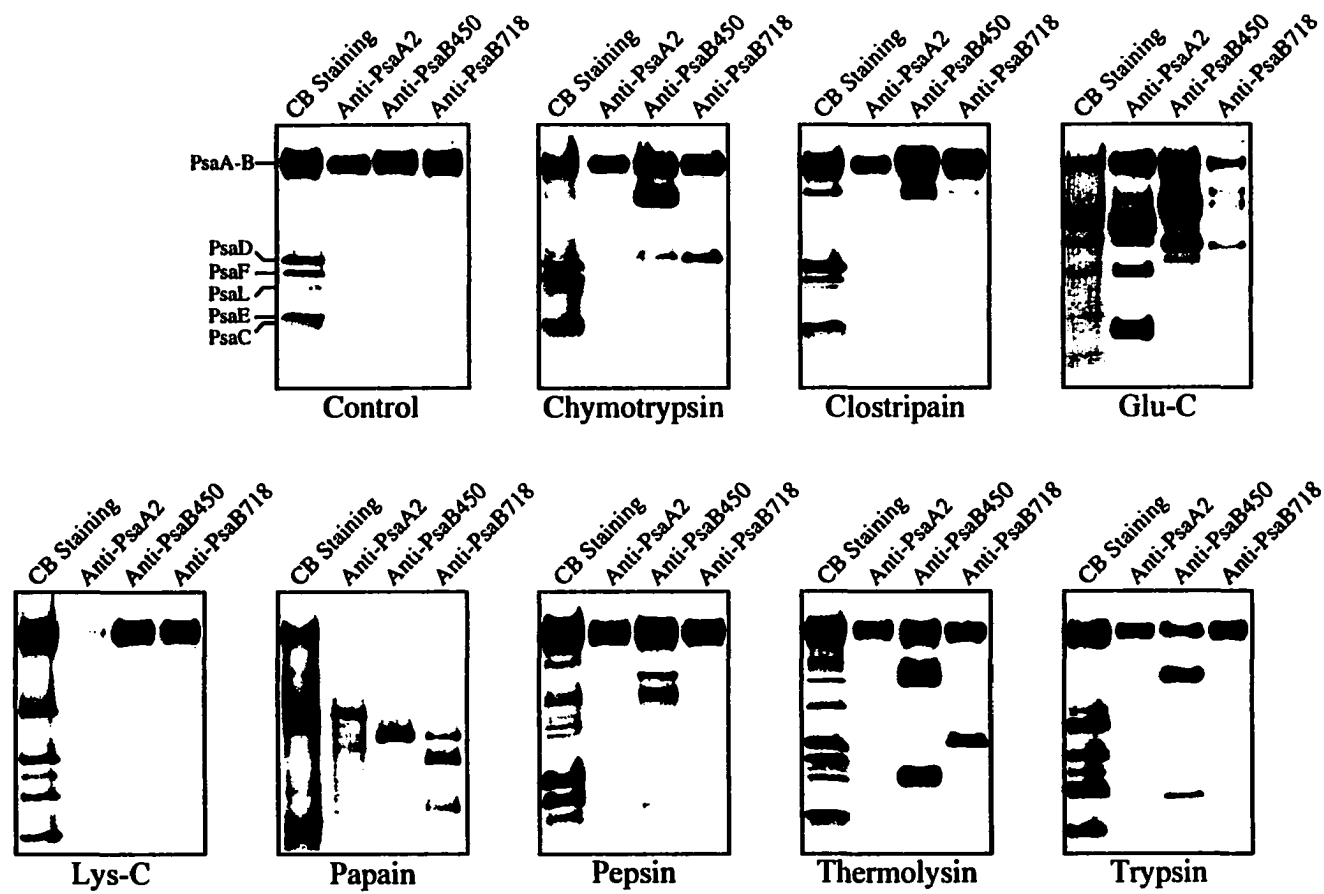[r] V. P. Chitnis and P. R. Chitnis, *FEBS Lett* **336**, 330 (1993).

A

B

Subunit	Mass (kDa)	
	Apparent	Predicted
PsaA-B	66	82.9/81.2
PsaD	17.7	15.6
PsaF	15.8	15.7
PsaL	14.3	16.6
PsaE	8.8	8.1
PsaC	8.0	8.8
PsaK	5.1	8.6
PsaI	3.4	4.4
PsaJ	3.0	4.5
PsaM	2.8	3.4

Monomeric PSI
and PSII

Trimeric PSI

Fig. A-1

Fig. A-2

APPENDIX B. STRUCTURAL FEATURES AND ASSEMBLY OF THE SOLUBLE OVEREXPRESSED PSAD SUBUNIT OF PHOTOSYSTEM I

Jun Sun, Ping Jin, and Parag R. Chitnis

Summary

PsaD is a peripheral protein on the reducing side of photosystem I (PS I). We expressed the *psaD* gene from the thermophilic cyanobacterium *Mastigocladus laminosus* in *Escherichia coli* and obtained a soluble protein with a polyhistidine tag at the carboxyl terminus. The soluble PsaD protein was purified by Ni-affinity chromatography and had a mass of 16716 Da by MALDI-TOF. The N-terminal amino acid sequence of the overexpressed PsaD matched the N-terminal sequence of the native PsaD from *M. laminosus*. The soluble PsaD could assemble into the PsaD-less PS I. As determined by isothermal titration calorimetry, PsaD bound to PS I with 1.0 binding site per PS I, the binding constant of 7.7×10^6 M^{-1}, and the enthalpy change of -93.6 kJ/mol. This is the first time that the binding constant and binding heat have been determined in the assembly of any photosynthetic membrane protein. To identify the surface-exposed domains, purified PS I complexes and overexpressed PsaD were treated with N-hydroxysuccinimidobiotin (NHS-biotin) and biotin-maleimide, and the biotinylated residues were mapped. The Cys^{66}, Lys^{21}, Arg^{118}, and Arg^{119} residues were exposed on the surface of soluble PsaD whereas the Lys^{129} and Lys^{131} residues were not exposed on the surface. Consistent with the X-ray crystallographic studies on PS I, circular dichroism spectroscopy revealed that PsaD contains a small proportion of α-helical conformation.

APPENDIX C. ACCUMULATION OF THE PHOTOSYSTEM I COMPLEX IN *SYNECHOCYSTIS* SP. PCC 6803

A paper to be submitted to the Plant Molecular Biology

Jun Sun and Parag R. Chitnis

Summary

We investigated some factors that regulate the abundance of the photosystem I (PSI) complex in the cyanobacterium *Synechocystis* sp. PCC 6803. We generated recombinant DNA constructs containing the *psaB* gene and its 3'-untranslated region with or without insertion of a chloramphenicol-resistance cassette. These constructs were introduced into the wild type and two PSI-less recipient strains that contained deletion of the *psaB* gene. These D and L PSI-less strains were generated and maintained under dark or low-light heterotrophic growth conditions, respectively. Characterization of the resulting transformant strains indicated that the insertion of the chloramphenicol-resistance cassette immediately after the stop codon of the *psaB* gene decreased the level of PSI in the membranes by reducing the level of *psaB* transcripts. Transformants from various recipient strains contained different levels of PSI proteins. The PSI proteins degraded faster in the transformant strains from the D and L recipient background than those from the wild type background, suggesting changes in the mechanism or machinery of protein degradation in the PSI-less recipient strains. The light intensity also affected the accumulation of PSI possibly through changes in chlorophyll biosynthesis. These results demonstrated that the steady state level of PSI in cyanobacterial membranes is regulated by multiple factors.

ACKNOWLEDGMENTS

It is a great honor to earn a doctorate. For me, this once-in-a-lifetime journey was full of challenges and difficulties as well as help from numerous people. I owe my success to all these people. Thank you all! The honor is mine, it is also yours.

As an advisor, Dr. Parag R. Chitnis is one of the best. His assistance was always available for 24-hours-a-day-and-7-days-a-week. When I first came in the lab, he taught me the way to work scientifically and efficiently. When I was writing my first English paper, he was so patient in helping me with my spelling, grammar, formatting, in addition to the organization and contents of the manuscript. Eventually, he guided me to work and think independently. He encouraged me to work on the ideas that I came up with. He always stood behind me to show his support. As one professor pointed out, "You are lucky to have him as your advisor!" Thank you, Parag, you are just wonderful!

The rest of my advisory committee was also important to my success. I sincerely enjoyed talking with Dr. Donald J. Graves. He always had all the encouraging words for my confidence. I really appreciated Dr. Basil J. Nikolau's suggestions about possible scientific careers. I owe my developing skill as a critical thinker to Dr. David J. Oliver and Dr. Walter S. Struve's inspiring advice. Thank you, my advisory committee, for all your advice and support!

People in the Chitnis' group were such good colleagues. Wu Xu was a solid alliance for my research. Dr. Donald A. Heck was always there for all kinds of my questions, from the use of a single word to the financial world. Huadong Tang, Yingchun Wang, and many others, who worked with me, you gave me so much help. We were a great team! I really enjoyed all the conservation with T. Wade Johnson and Michael Hitchler that allows me to understand American cultures. Thank you, my dear colleagues, for your friendship! I will miss you all!

I could not have gone through this without the support of my family. Ping, my beautiful and lovely wife, not only is my lifelong companion, but also is a great colleague. She helped me with several projects in my dissertation. She has the ability to do the best experiments. Most importantly, her love and support was my source of power to go through this journey. I will also give a lot of credits to Mom, Dad, mother-in-law, father-in-law, Wei, and Xiaohua, for all their love and support. Finally, Kevin, my son, he is the spark of my life. He gives me all the joys of a father. Thank you, my family, this one is for you!